Distribution Agreement

In presenting this thesis or dissertation as a partial fulfillment of the requirements for an advanced degree from Emory University, I hereby grant to Emory University and its agents the non-exclusive license to archive, make accessible, and display my thesis or dissertation in whole or in part in all forms of media, now or hereafter known, including display on the world wide web. I understand that I may select some access restrictions as part of the online submission of this thesis or dissertation. I retain all ownership rights to the copyright of the thesis or dissertation. I also retain the right to use in future works (such as articles or books) all or part of this thesis or dissertation.

Signature:

_____ _____

Katherine Morgan Bricker Date

Investigation of Immune Interventions in SIV-Infected, ART-Treated Infant Rhesus Macaques

By

Katherine Morgan Bricker
Doctor of Philosophy

Graduate Division of Biological and Biomedical Science
Immunology and Molecular Pathogenesis

_____
Ann Chahroudi, M.D., Ph.D.
Advisor

_____
Rama Amara, Ph.D.
Committee Member

_____
Cynthia Derdeyn, Ph.D.
Committee Member

_____
Mirko Paiardini, Ph.D.
Committee Member

_____
Jens Wrammert, Ph.D.
Committee Member

Accepted:

_____
Kimberly Jacob Arriola, Ph.D., M.P.H.
Dean of the James T. Laney School of Graduate Studies

_____
Date

Investigation of Immune Interventions in SIV-Infected, ART-Treated Infant Rhesus Macaques

By

Katherine Morgan Bricker
B.S., University of New Orleans, 2016

Advisor: Ann Chahroudi, M.D., Ph.D.

An abstract of
A dissertation submitted to the Faculty of the
James T. Laney School of Graduate Studies at Emory University
In partial fulfillment of the requirements for the degree of
Doctor of Philosophy

Program in Immunology and Molecular Pathogenesis
Graduate Division of Biological and Biomedical Sciences

2021

Abstract

Investigation of Immune Interventions in SIV-Infected, ART-Treated Infant Rhesus Macaques

By Katherine M. Bricker

The latent viral reservoir is composed of a small subset of infected CD4+ T cells that persist during antiretroviral therapy (ART) and constitute the major barrier to HIV-1 cure. Strategies to reduce or eliminate this reservoir would be highly beneficial to the 1.7 million children living with HIV-1. Here, we used a non-human primate (NHP) model of postnatal oral SIVmac251 transmission and ART suppression to investigate potential cure interventions in a preclinical pediatric model of HIV-1 infection.

First, we evaluated safety and immunogenicity of the toll-like receptor (TLR)-7 agonist, GS-986, in 2 SIV-infected, ART-treated infant rhesus macaques (RMs). We found that oral administration of GS-986 at both tested concentrations was tolerable and resulted in a dose-dependent pharmacodynamic response detectable through increased concentrations of plasma cytokines and chemokines, such as IFN-γ and increased circulating nonclassical monocytes (CD14+CD16+) and circulating macrophages (CD14+CD169+) at 24 hours post-administration.

We next combined GS-986 with an Ad48-prime, MVA-boost therapeutic vaccine in 8 SIV-infected, ART-treated infant RMs. Immunized infants had augmented anti-SIV cellular and humoral immunity. Repeated oral GS-986 induced the expected pharmacodynamic response with activation of monocytes and T cells in the periphery 24-hours post-dose. Despite the vaccine-induced immune responses, vaccination did not result in reductions to the viral reservoir through cell-associated SIV DNA or rebound kinetics following the removal of ART.

Finally, we examined the effect of a newly identified latency reversing agent (LRA), the mimetic of second mitochondrial activator of caspases (SMACm) AZD5582, in 8 SIV-infected, ART-suppressed infant RMs. Latency reversal, measured by on-ART viremia, was observed in 63% of infants. Immunogenicity of AZD5582 was demonstrated through T cell activation and increased transcription of ncNF-kB genes, such as *BIRC3*. Quantification of plasma AZD5582 revealed a lower Cmax in infants compared to adult RMs which may, in part, explain the dampened viremia.

Taken together, these findings hold promise for pediatric HIV-1 cure strategies and inform future pediatric clinical trials. Additionally, these studies highlight the importance of studying HIV-1 cure in a pediatric setting as unique features of the pediatric reservoir and/or the developing immune system may influence the efficacy of HIV-1 cure interventions.

Investigation of Immune Interventions in SIV-Infected, ART-Treated Infant Rhesus Macaques

By

Katherine Morgan Bricker
B.S., University of New Orleans, 2016

Advisor: Ann Chahroudi, M.D., Ph.D.

A dissertation submitted to the Faculty of the
James T. Laney School of Graduate Studies at Emory University
In partial fulfillment of the requirements for the degree of
Doctor of Philosophy

Program in Immunology and Molecular Pathogenesis
Graduate Division of Biological and Biomedical Sciences

2021

Acknowledgements

I would first like to thank my mentor, Ann Chahroudi, for giving me the opportunity to be the first graduate student in her lab. I am absolutely grateful for her support, guidance, and encouragement. I truly appreciate the freedom that I have been given to pursue my own ideas and own my project. Not only have you taught me how to be a better scientist, but you have also taught me how to be a strong female role model in the science world and I will take that with me wherever I go. I would also like to thank all current and former members of the Chahroudi lab for their support, encouragement, and friendship over the years. I would like to especially acknowledge Dr. Maud Mavigner, for helping me to get started as I was joining the lab and teaching me the basics; Ferzan Uddin, Brianna Williams, and Danielle Oliver for technical assistance with my *in vivo* project; and Dr. Veronica Obregon-Perko for being not only a constant source of advice, guidance, and support whenever I needed it, but also an amazing friend. In addition, I would like to thank the Yerkes veterinary and research services staff, especially Sherrie Jean and Stephanie Ehnert, as well as the monkeys that made this work possible.

I also must thank my family. My parents (Jean Rogers-Berry, Stephen Schnell, Laura Schnell, and Frank Hasty) who have raised me to be an independent, strong willed human and encouraged me to pursue whatever my dreams may be no matter how ridiculous. My siblings (Aaron Schnell, Spencer Schnell, Emily Peterson, Lauren Peterson, Mark Hasty, and Sebastian Schnell) who are always my biggest supporters and never fail to make me laugh, even if I am usually the butt of the joke.

Finally, I would like to thank Amy Testa, Becky Catherina, and Lacey Young – the three best friends a woman could ask for. Y'all have provided me with many escapes and a reminder that there is life outside of grad school. Lastly, I would like to thank my cohort and the friends that I have made in the IMP program, it has been nice to know that I am not alone in the ups and the downs that come with graduate school. Specifically, Logan Melot, my IMPerson, I am positive I would not have made it through quals season without you.

Thank you all.

Table of Contents

Table Index

Figure Index

Chapter One: Introduction

Discovery and Origins of HIV-1/AIDS

Acquired immune deficiency syndrome (AIDS) was first officially reported in 1981 when a group of five previously healthy, homosexual men in Los Angeles succumbed to opportunistic infections and rare malignancies (1). By the close of that year, over 100 individuals had died from this unknown disease and nearly 300 cases had been reported (2). The causative agent of AIDS, Human Immunodeficiency Virus (HIV), was isolated and identified shortly following in 1983 by Luc Montagnier and Francoise Barre-Sinoussi who were awarded the Nobel Prize in physiology or medicine for their efforts in 2008 (3). Since its discovery, HIV has infected over 77.5 million individuals and led to around 34.7 million deaths (4). As of 2020 there are nearly 37.5 million people living with HIV globally, 1.7 million of which are children under the age of 14, and around 4,000 new infections daily (5).

There are two closely related, but distinct types of HIV: HIV-1 and HIV-2. HIV-1 is the most prevalent cause of AIDS worldwide and originated from the closely related Simian Immunodeficiency Virus (SIV) SIVcpz, likely transmitted through the common practice of eating bushmeat (6-10). It is believed that zoonotic transmission from chimpanzees to humans has occurred on at least four separate occasions, each corresponding to the four major variants of HIV-1: group M, group N, group O, and group P (11, 12). Sequence analysis of patients' samples

preserved from 1960 reveal diverse HIV-1 subtypes indicating that virus had evolved prior to that time likely due to subclinical endemic spread in West Central Africa (13).

Group M is by far the most predominant of the different subtypes and accounts for approximately 99% of global HIV-1 infections. As it spread globally, population bottlenecks led to several different M lineage subtypes with distinct geographical distribution. Currently there are nine group M subtypes: A – D, F – H, J, and K (14). The A and D subtypes are dominant in eastern Africa an while subtype C dominates Sub-Saharan Africa. Subtype B is the predominant subtype in Europe and the Americas and is believed to have originated in Haiti in the 1960s (15). In addition to the nine subtypes there are also over 40 circulating recombinant forms (CRFs) (14). CRF01 is the most common strain in southeast Asia. The biological properties of these subtypes vary, for instance, subtype D has been associated with faster CD4+ T cell decline and disease progression despite similar viral loads (16, 17).

The significantly less common HIV-2 originated from zoonotic transmission of SIVsm (9, 18). HIV-2 infection is endemic to West Africa and is rarely found outside of that area. HIV-2 infected individuals tend to have lower viral loads and lower transmission rates than those infected with HIV-1 (19, 20).

Virology and HIV-1 Life Cycle

HIV-1 is an enveloped RNA retrovirus belonging to the lentivirus group. The retroviral genome is composed of a positive-sense, single stranded RNA that must be reverse-transcribed to a double-stranded intermediate during replication, a unique feature to retroviruses made possible by the viral protein reverse transcriptase. Other viruses of the *Lentiviridae* genus infect animals such as cats and cattle and also cause immunodeficiency (21, 22).

The 9.2 kb viral RNA genome encodes nine genes, three major genes: Gag, Pol, and Env and six regulatory genes: Tat, Rev, Nef, Vif, Vpr, Vpu. The *gag* gene encodes capsid and matrix proteins necessary for the nucleocapsid of the virion. Pol encodes important enzymes reverse transcriptase, protease, and integrase necessary for viral replication. Env encodes two glycoproteins, gp120 and gp41, that form trimers on the surface of the virion and facilitate entry into target cells. The regulatory proteins are necessary for replication life cycle and virus production. The viral protein Nef has evolved to downregulate expression of MHC class I and class II reducing the likelihood that an actively infected cell will be detected and killed by cytotoxic CD8+ T cells (23-25). Within each virion are two copies of the RNA genome and viral enzymes reverse transcriptase, integrase, and protease.

To enter a target cell, gp120 binds with high affinity to its primary receptor, CD4, causing a conformational change that exposes the binding site for a secondary co-receptor (26). Once gp120 has bound to both CD4 and its obligatory co-receptor (CCR5 or CXCR4) (27-29), gp41 mediates fusion of the viral envelope to the cell's plasma membrane, allowing the virus to enter the target cell (26). Once the virus has entered a target cell, the viral RNA must be transcribed into

a DNA intermediate (cDNA) by the enzyme reverse transcriptase. Due to the error prone nature of reverse transcriptase, HIV-1 evolves around 1 million times faster than mammalian DNA (30).

The intermediate cDNA is converted to dsDNA provirus that is then integrated into the host genome by viral integrase to form provirus. HIV-1 provirus integration is dependent on several host factors and preferentially occurs in transcriptionally active chromatin (31, 32). Integrase recognizes and partially cleaves long terminal repeats (LTRs) located at each end of the viral genome that allows integration of the viral DNA into the host genome. These LTRs contain motifs that are recognized by host transcription factors, NFκB or NFAT, that control expression of viral genes from the integrated provirus. The viral protein Tat serves as a positive feedback circuit for viral replication by forming an RNA polymerase phosphorylation complex that enhances the generation of full-length viral transcripts. Another viral protein, Rev, shuttles full length and singly spliced viral mRNA out of the cell's nucleus. Viral mRNA is translated and processed into proteins the cytoplasm through host cell machinery. Viral particles containing genomic RNA are then assembled and released from the plasma membrane to infect new susceptible cells (33).

Due to the rapid replication of HIV-1 and the error prone nature of reverse transcriptase, numerous variants of HIV-1 develop within an infected individual resulting in a quasi-species. The viral diversity within one infected individual after 6 years of infection is thought to be greater than that of influenza type A that circulates globally throughout a single season (34). Additionally, infected individuals remain at risk for superinfection with multiple strains of HIV-1, indicating

that the HIV-1 immune response is only partially protective against non-autologous strains (35). These are among some of the reasons that HIV-1 has been difficult to prevent and cure.

Transmission and Pathogenesis of HIV-1

HIV-1 infection occurs through the transfer of body fluids such as blood, semen or vaginal fluids, and breastmilk (36). Globally, nearly 70% of infections are due to heterosexual transmission (4). Other transmission routes include same sex transmission and intravenous drug use. Prior to routine screenings of blood banks for HIV-1 blood transfusions were a major source of infection (37), but through policy changes and screening processes this transmission route has largely been eliminated. In the case of pediatric infections, described below, mother-to-child transmission is the primary mode of new infections.

Through most transmission routes risk of infection following exposure is very low, with only 1 transmission per 200-2000 exposures in male-to-female heterosexual transmission and 1 transmission per 700-3000 exposures in female-to-male heterosexual transmission (36). The virus can be transmitted either as free virus or via HIV-1-infected cells and the majority of transmission events occur at mucosal surfaces (38, 39). Primary infection of HIV-1 is most often established by a single viral variant, referred to as the transmitted founder virus (36). The transmitted founder virus has a strong preference for the CCR5 co-receptor and it has also been shown that the newly transmitted virus have more compact, less glycosylated envelope that perhaps interact more efficiently with relevant target mucosal cells (40). The transmitted virus undergoes rapid expansion

shortly after infection and disseminates widely throughout lymphatic tissue to establish systemic infection. In macaques, systemic infection with SIV has been demonstrated within one week of infection (41, 42).

HIV-1 primarily infects and depletes CD4+ T cells, a critical component of the adaptive immune system, but has also been identified to infect myeloid cells such as macrophages (43, 44). The cellular tropism of HIV-1 is influenced, in part, by the preferred chemokine receptor of the virus, CCR5 or CXCR5 (27-29). A virus that utilizes CCR5 as a coreceptor is termed 'R5'-tropic, while a virus that uses CXCR4 is termed 'X4'-tropic and, as stated above, it has been shown that HIV-1 strains from acute and early infection have a strong preference for the coreceptor CCR5 which is expressed primarily by memory CD4+ T cells (45). Virus isolated from individuals during acute infection is nearly always R5-tropic (46, 47), but in most subtypes the dominant viral type switches to X4-tropic variants late in infection in around 50% of infected individuals that progress to AIDS (48). About 1% of Caucasians are homozygous for a mutation in in their CCR5 gene, CCR5Δ32, that results in resistance to HIV-1 infection due to non-functional CCR5 protein (49). It appears that a heterozygous deficiency is partially protective and contributes to a reduction in disease progression (50). Other genetic factors can play an important role in HIV-1 control. For example, different alleles of the human leukocyte antigen (HLA) molecule such as HLA-B57, HLA-B27 and HLA-B13 have been associated with better prognosis in HIV-1 infected individuals (51-53).

Acute infection is accompanied by high levels of HIV-1 RNA in the plasma that peaks in the first few weeks of infection. During this time, there is a profound loss of CCR5+ CD4+ memory T cells in the gut (41, 54). Additionally, there is some evidence of preferential depletion of HIV-1-specific memory CD4+ T cells systemically (55). Loss of helper CD4+ T cells impairs other essential arms of the immune system resulting in disruption of CD8+ T cells and antibody production. High-level viremia typically diminishes to a set point within weeks to months of infection (56, 57). Cytotoxic CD8+ T cells aid in the establishment of this early control as detailed below, and the decline of vRNA copies is typically negatively correlated to HIV-1-specific CD8+ T cell counts. HIV-1-infected individuals can remain asymptomatic for years during this chronic phase, but despite lacking symptoms, most infected individuals will continue to experience CD4+ T cell depletion from circulation and lymph nodes throughout chronic infection resulting in AIDS (58).

Th17 cells secrete cytokines, such as IL-21, that are critical to intestinal barrier maintenance and prevention of microbial translocation. However, these cells are preferentially depleted during early infection, leading to disruption of the mucosal barrier, dysregulation of the microbiome, and microbial translocation into systemic circulation (59). Bacteroides, important for maintenance of the mucosal anti-inflammatory state through IL-10 induction, are depleted and replaced by pathogenic species such as Prevotella, inducers of immune activation, and mucosal adherent Proteobacteria, associated with microbial translocation (60-63). Symbiotic bacteria in a healthy gastrointestinal tract (GI) ferment dietary fibers to produce short-chain fatty acids (SCFA), such as butyrate, essential for epithelial barrier maintenance and mucosal immunity (64-66).

Infection alters production of these SCFAs and is associated with dysfunctional immunity. These gut microbiota changes are evident within the first weeks of HIV-1 infection, are not corrected during ART, and are thought to drive disease progression to AIDS (60, 67-71).

The antiviral immune system exerts strong selective pressure on the virus during HIV-1 infection resulting in escape mutants, which are variants of the virus no longer detectable by the infected individuals CD8+ T cells and antibodies (72-74). Viral escape mutants can be detected as early as 30 days post infection (75). Eventually, viral escape leads to a rapid decline in CD4+ T cell count and progression of AIDS, clinically defined as a CD4+ T cell count of less than 200 cells per uL of blood (76). At this point, the patient's adaptive immune system is no longer capable of mounting an immune response and the individual becomes susceptible to opportunistic infections. Some of the most common opportunistic infections include pneumonia caused by *P. jirovecii*, Kaposi's sarcoma, and cytomegalovirus retinitis (77).

The Immune Response to HIV-1

Acute HIV-1 infection is often associated with fever, sore throat, lymphadenopathy, and rash (78-80). These symptoms, although severe, are nonspecific, short-lived, and self-limiting. Even in individuals that seek medical attention, they are often attributed to nonspecific viral infection and HIV-1-testing is not performed (80). HIV-1-specific cytotoxic CD8+ T cells typically develop early in infection and are critical in the establishment of early viral control and reduction in plasma viremia (56, 81). CD8+ T cells also secrete chemokines such as CCL5, CCL3,

and CCL4 that bind to CCR5 and inhibit viral spread. In HIV-1 infected individuals that do not progress to AIDS, termed nonprogressors, HIV-specific CD8+ T cells remain highly functional longer in infection than HIV-1+ individuals that do progress to AIDS further implicating these cells in viral control (82).

HIV-1-specific antibodies are generated early in infection and are detectable within 6 to 9 weeks after infection but, like CD8+ T cells, are also not able to completely clear infection (83). Both neutralizing and non-neutralizing anti-HIV-1 antibodies are generated throughout the course of infection. Although non-neutralizing antibodies are not effective in blocking transmission of virus to susceptible cells, they do assist in an Fc-dependent antiviral effector functions such as antibody dependent cellular cytotoxicity (ADCC) that may be critical in control (84). Surprisingly, in the only prophylactic vaccine trial to show any efficacy, the RV144 Thai trial, non-neutralizing antibodies capable of mediating ADCC were shown to be correlated with protection (85).

In a rare subset of HIV-1 infected individuals develop broadly neutralizing antibodies (bnAbs) capable of neutralizing the HIV-1 Env spike of multiple viral strains (86). Generation of these bnAbs typically occurs during chronic infection and requires extensive somatic hypermutation (SHM) (86). Development of bnAbs has been correlated to early CD4+ T cell lost, high early viral load, and reduced presence of circulating regulatory CD4+ T cells (Tregs) (84). The most well-characterized target sights are the CD4-binding site, the glycan-associated epitopes at the base of the V3 loop, the V1/V2 trimer apex, and the membrane proximal external region

(MPER) on gp41 (87). Several bnAbs have been isolated and characterized to be used in clinical trials for HIV-1 prevention and treatment (88).

Finally, humans have several restriction factors that inhibit the HIV-1 viral life cycle. These include APOBEC, TRIM5α, and tetherin (89). APOBEC is a cytidine deaminase that catalyzes the conversion of deoxycytidine to deoxyuridine in reverse-transcribed viral cDNA (90). TRIM5α targets viral nucleocapsids to prevent uncoating and release of viral RNA into new target cells (91). Tetherin inhibits budding of new virions from the plasma membrane of infected host cells and can be overcome by the viral protein Vpu (92).

As has been reported with other chronic infections, HIV-1 leads to cellular immune exhaustion (93). The HIV-1-specific CD4+ T cell response is severely impaired during chronic infection (94). Additionally, during chronic infection, CD8+ T cells become functionally impaired resulting in less effective killing of HIV-1-infected cells. Expression of so called "exhaustion markers" such the co-inhibitory receptor PD-1 are upregulated on HIV-1-specific CD8+ T cells. The use of immune checkpoint blockade (ICI) antibodies to restore CD8+ T cell function have been extensively tested in humans living with HIV-1 and animal models (95-97).

Non-human Primate Models

SIVcpz, the ancestor of HIV-1, is endemic in wild chimpanzees (*P. troglodytes*). During the search for an HIV-1 animal model, much early research focused on experimental infection of chimpanzees. SIVcpz transmission rates and mode of transmission are similar to what is observed in HIV-1, but disease occurrence is rare in the natural host limiting its potential as a true model for HIV-1 (98-101). Sooty mangabeys (SM, *C. atys*) are the natural host of SIVsm, the of HIV-2, and also experience a non-pathogenic version of infection. SM maintain high CD4+ T cell counts despite persistent viremia and do not progress to AIDS (102). SMs have lower levels of CCR5 expression on their CD4+ T cells, most pronounced in the central memory compartment (103), and genome-wide comparative analyses of transcript assemblies of several immune-related SM genes revealed substantial sequence divergence in hosts that do progress to AIDS (104). Further understanding these virologic or immunological differences in the natural host that account for the lack of disease progression could provide insight into HIV-1 cure strategies.

SIV infections of asian macaques, rhesus (*M. mulatta*) (RM), pigtailed (*M. nemestrina*), and cynomolgus (*M. fascicaluris*), have become the most used and widely accepted animal models for HIV-1 infection (105, 106). RM are readily infected with many variants of SIV, experience progressive CD4+ T cell depletion, and progress to AIDS. Our group and several others have successfully demonstrated consistent suppression of viremia below detectable limits in SIV-infected ART-treated RM with viral dynamics that recapitulate what is seen in HIV-1 infected individuals treated with ART (107-111). Chimeric viral constructs consisting of the HIV-1 *env* gene spliced into an SIV backbone have generated simian-human immunodeficiency viruses (SHIVs) that allow testing of HIV-1 Env-based vaccines or antibodies in the NHP setting, further

expanding the potential of this model (112-114). More recently, a barcoded virus, SIVmac239M, has been generated containing a 34-base genetic barcode insert between the *vpx* and *vpr* accessory genes of the well-characterized molecular clone SIVmac239 (115). The virus stock includes approximately 10,000 individual barcoded viral variants that can be used to infect RM and track viral variants throughout infection, therapeutic intervention, and analytical treatment interruption (ATI).

The RM model of HIV-1/AIDS provides powerful experimental advantages. The timing, concentration, and infection route can all be controlled during viral challenge. Animals can be infected with a well characterized SIV stock, as described above. ART initiation and adherence can be tightly regulated, and analytical treatment interruption (ATI) can be performed in the NHP without the ethical concerns involved in a human clinical trial. Novel therapeutic interventions can be tested for safety and efficacy in a relevant pre-clinical setting. Additionally, the reservoir can be analyzed to a depth not possible in humans through elective necropsy.

Antiretroviral Therapy

HIV-1 targets the immune system's CD4+ T cells and disseminates throughout the body early in acute infection (116, 117). Adherence to daily administration of ART can sustain HIV-1 suppression, prevent new transmission events, and result in survival rates similar to uninfected individuals. Antiviral drugs have been designed to target all nearly stages of the viral life cycle preventing spread of infection to uninfected cells (**Fig 1**). The three primary targets for drug

intervention are the viral proteins reverse transcriptase, integrase, and protease (118). Nucleoside analogs (nucleoside reverse transcriptase inhibitors, NRTIs), such as Tenofovir (TDF) or the more recent tenofovir alafenamide fumerate (TAF) and non-nucleoside analogs (non-nucleoside reverse transcriptase inhibitors, nNRTIs), such as Efavirenz, are used to inhibit reverse transcriptase and prevent synthesis of provirus. Integrase inhibitors (integrase strand transfer inhibitors, InSTI) such as Dolutegravir (DTG) prevent integration of HIV-1 DNA into the host cell genome (119, 120). Protease inhibitors (PIs) prevents late-stage processing of budding viral particles and are generally typically only used in second- or third-line regimens. Some newer classes of anti-HIV-1 medication target inhibition of viral attachment and entry by blocking CCR5 co-receptor binding or other mechanisms (121).

The first anti-HIV-1 drug licensed in the United States in 1987, zidovudine (AZT), is a NRTI (122). It is no longer used in resource rich settings due to several associated complications but is still used as a second-line regimen in resource limited countries. The introduction of highly active antiretroviral therapy (HAART) dramatically altered patient outcomes reducing morbidity and mortality in HIV-1 infected individuals. New transmissions have continued to decline since their peak in 1997 largely due to the implementation of these regimens (123). Treatment with antiviral drug cocktails leads to a rapid decline in viremia resulting in plasma HIV-1 RNA at or below the limit of detection by standard assays. During ART suppression, CD4+ T cells are partially reconstituted, but not to pre-infection levels. Currently, it is recommended that all HIV-1 infected adults with detectable viral loads begin ART regardless of CD4+ T cell count with the standard initial regimen of 2 NRTIs and one integrase strand transfer inhibitor (InSTI) (124). The

development of long-acting drug delivery strategies would be of great benefit, especially to HIV-1-infected individuals living in resource limited countries. Strategies in development include long-acting slow effective release (LASER) ART, implants, microbicides, and transdermal therapies (125). In recent years, daily TDF and a second NRTI, emtricitabine (ETC), have been implemented as a pre-exposure prophylaxis (PrEP) to prevent HIV-1 infection in high-risk individuals. This regimen has been associated with reductions in the frequency of HIV-1 infection in participants with good adherence by up to 92% (126).

Although ART has dramatically reduced AIDS-related deaths and improved the quality of life in HIV-1-infected individuals, long-term therapy is associated with persistent inflammation and comorbidities. The most common toxicities associated with ART are hematological dysfunction, mitochondrial dysfunction, and metabolic abnormalities (127). Other major barriers to universal ART include drug cost and availability, this is especially a concern in resource limited countries where the majority of HIV-1-infected individuals reside. Even in high-resource areas, there is stigmatization associated with HIV-1 that leads many individuals to resist HIV-1 testing and delay ART. Poor adherence to drugs can lead to the emergence of ART-resistant viral variants that require second and even third-line regimens which may be associated with higher toxicity and adverse effects.

The Viral Reservoir

A unique feature of the HIV-1 virus is its ability to establish a state of latency in which integrated provirus shuts down active transcription, enabling the virus to go undetected by the host immune system for extended periods of time. The reservoir is primarily composed of resting CD4+ memory T cells that reside in lymphoid tissue (117, 128), but myeloid derived cells and naïve CD4+ T cells have also been implicated as components of the viral reservoir (128-132). The stable latent reservoir is established early in acute infection (116, 117, 133). NHP studies using SIV infection? indicate that this reservoir is established as early as 3 days after infection (111), but the majority of the persistent reservoir during ART is formed immediately prior to initiation of therapy (134-136). The viral reservoir forms the major barrier to HIV-1 cure as it serves as the source of viral rebound after treatment failure or interruption.

The SIV-infected RM model has allowed extensive evaluation of the anatomical distribution of the latent viral reservoir. Viral DNA and RNA levels in SIV- or SHIV-infected, ART-treated RM are highest in lymphoid tissues including the spleen, lymph nodes, and GI tract (137-139). The central nervous system has also been implicated as a site of viral persistence in SIV-infected RM model potentially due to poor ART penetrance (140). Quiescent, infected cells are able to escape immune surveillance and therefore persist even in the setting of long-term ART. Much work has been put into identifying phenotypic markers to identify the infected cells that constitute the reservoir. Identification of such markers would provide insight into targeted strategies to therapeutically reduce the reservoir, but thus far no true marker of the reservoir has been identified (141-144).

The mechanism behind the establishment and maintenance of the latent viral reservoir is an active area of investigation. Through recent advances in experimental methodologies, it has become clear that multiple factors contribute to the maintenance of the reservoir (144). Homeostatic proliferation is a large contributor to maintenance of the reservoir as a large portion of replication competent and defective provirus appears to be clonal (145-147). Some argue that low levels of viral replication continue within sanctuary sites, such as lymphatic tissue and the CNS, due to poor drug penetrance to these areas (148, 149). Such replication would result in continued viral evolution during ART but evidence for this phenomenon is mixed (150). Additionally, microbial leakage, a major driver of the immune activation that persists throughout ART, is associated with virus persistence, potentially replenishing the viral reservoir through CD4+ T cell activation and proliferation (68-71, 151, 152).

Resting memory CD4+ T cells that comprise the majority of the latent reservoir are estimated to have a mean half-life of around 44 months (117). Therefore, complete clearance of the reservoir would require over 70 years of adherence to ART. As such, ART alone cannot cure HIV-1 and infected individuals must remain on daily ART indefinitely to prevent progression to AIDS. Alternative strategies to eliminate the viral reservoir and provide a cure continues to remain as major research priorities in the HIV-1 field.

Strategies for HIV-1 Cure

Due to the complexity of the viral reservoir, complete elimination of the virus, or a sterilizing cure, appears difficult if not impossible. A more feasible HIV-1 cure may be obtained through reducing the reservoir enough to allow long-term remission in the absence of daily ART, referred to as a functional cure. With a functional cure, although small numbers of virally infected cells persist in the body, an individual is still able to cease ART without symptoms, transmitting the disease, or progression to AIDS. In a rare subset of HIV-1-infected individuals, patients naturally control viral infection leading to undetectable viral loads without ART (153). These elite controllers maintain normal CD4+ T cell counts and do not progress to AIDS demonstrating the possibility of functional cure.

In one famous case, referred to as the Berlin patient, Timothy Ray Brown, an HIV-1-infected individual, underwent hematopoietic stem-cell transplantation for leukemia treatment from a stem-cell donor homozygous for CCR5Δ32 mutation (154). This genetic mutation makes the HIV-1 coreceptor CCR5 defective and protects the individual from infection by R5-tropic HIV-1, as described above. After immune reconstitution, CD4+ T cell counts rebounded, and the patient remained free from viremia for the remainder of his life, thirteen years, following ART cessation. A second patient, referred to as the London patient, underwent the same treatment strategy and has remained aviremic in the absence of ART for 30 months as of May 2020 (155). While this is not a feasible intervention strategy globally due to the risk associated with stem-cell transplant and scarcity of HLA-matched CCR5Δ32 donors, the outcome does validate the possibility of functional HIV-1 cure. In vivo, ablation of CCR5 hematopoietic stem cells (HSCs) through clustered regulatory interspaced short palindromic repeats (CRISPR) and CRISPR-associated

protein 9 nuclease (Cas9) technology confers resistance to HIV-1 infection potentially making similar cure strategies targeting this genetic advantage more feasible (156).

Administration of ART early in infection is linked to a reduction in the size of the viral reservoir, as described above, and can rescue CD4+ T cell function (157). Early ART also helps to prevent the development of viral escape mutants. Protection is strongest when ART is initiated in the first few weeks post-infection, but the beneficial effects of early ART have been observed up to 6 months post-infection (158-161). Initiation of early ART has demonstrated mixed results in the prevention or delay of viral rebound SIV-infected NHPs (111, 162, 163). In clinical trials, administration of ART in early infection has resulted in better viral control following ATI, but is not curative (164-167). Additionally, the narrow window for early ART administration is often missed due to the lack of distinct symptoms during acute infection and late diagnosis.

A therapeutic vaccine in HIV-1-infected patients could help the individual to overcome immune dysregulation associated with HIV-1 and enhance the anti-HIV-1 immune response allowing control of replication in the absence of ART. Many recent NHP therapeutic vaccination studies have shown significant success. Therapeutic vaccination aimed at generating a broad antibody response has had limited success. As discussed above, generation of bnAbs in adults requires extensive SHM, which is difficult if not impossible to induce through vaccination. In HIV-1-infected patients that initiate ART after the acute infection phase, the majority of the viral reservoir is dominated by CTL escape mutants that are no longer recognized by the host immune system so a vaccine aimed to reshape the CD8+ T response towards more effective epitopes such

as the well conserved *gag* and *pol* genes could help to effectively eliminate virally infected cells (168). NHP studies utilizing recombinant adenovirus serotype 26 (Ad26) prime, modified vaccinia Ankara (MVA) boost therapeutic vaccination in combination with TLR7 stimulation resulted in decreased levels of viral DNA and delayed viral rebound positively correlated to breadth of the cellular immune responses (169).

Immune checkpoint blockade to restore functionally "exhausted" CD8+ T cells, such as the therapeutic anti-PD-1 antibody Keytruda, has shown much success in cancer immunotherapy (170). In the animal model, therapeutic strategies aimed at restoring functionally exhausted CD8+ T cells have enhanced T-cell immunity during chronic SIV infection (171). Other investigators have focused on adoptive T cell transfer in which an HIV-1-infected patient's CD8+ T cells are activated and expanded *ex vivo* then reintroduced to the patient. Passive administration of bnAb cocktails in patients that have not generated a bnAb anti-HIV-1 response may also provide a quick, efficient way to provide this boost the immune system (172-175) and this strategy has been investigated in numerous clinical trials.

Since the major barrier to HIV-1 cure is the persistence of the invisible, latent reservoir, one research strategy is to use small molecules, termed latency reversing agents (LRAs), to reactivate latent provirus. Reactivation of virally infected cells while the patient remains on ART could allow the host immune system to detect and eliminate these cells without risk of productive infection in new susceptible cells. First generation LRAs included protein kinase C (PKC) agonists, histone deacetylase inhibitors (HDACi), and proteasome inhibitors (176). While no LRA

to date has shown strong viral reactivation in ART-suppressed, HIV-1-infected individuals, the majority of completed clinical trials were done with early identified LRAs (177). Clinical trials with the toll-like receptor (TLR)-7 agonist GS-9620 (Vesatolimod) are underway, but Phase Ib results indicate that treatment with GS-9620 does not impact on ART viremia compared to placebo treated individuals (178).

Additional LRAs have been tested in the RM model that have not yet moved to clinical trials. ICIs, described above as an intervention to improve CD8+ T cell exhaustion, may also play a role in reactivating the viral reservoir as they can bind to cell surface markers on latently infected $CD4^+$ T cells, preventing the inhibitory signals and ultimately triggering viral transcription (179). The potential of ICIs as LRAs was demonstrated in vivo through the RM model (180). Mimetics of the second mitochondrial-derived activator of caspases (SMACm) activate the noncanonical NF-κB pathway, representing a potentially selective approach to activate the viral reservoir in SIV-infected, ART-treated RM (181). As stated above, CD8+ T cells are critical for immune mediated control of HIV-1. Depletion of CD8+ T cells through CD8α or CD8β depleting antibodies results in on-ART viremia in ART-suppressed RM (108, 182, 183). While CD8+ T cell depletion may not move forward in human clinical trials, future studies both *in vivo* with NHPs and *ex vivo* may provide insight into the mechanisms of latency that will allow future development of targeted LRAs. Recent NHP studies have shown that latency reversal can be augmented further when multiple LRAs are used in combination (184, 185).

Realistically, an effective cure strategy will probably require combination of the many strategies described here. Due to the diversity of HIV-1, cure may require distinct strategies for different individuals. One example of a combinatorial strategy is the "shock and kill" method in which an LRA, the "shock", is combined with an intervention, such as therapeutic vaccination in combination with LRA administration, aimed at boosting the immune system, the "kill". Other examples include early ART plus bnAbs or therapeutic vaccination plus checkpoint blockade (186, 187).

Pediatric HIV-1

Mother-to-Child Transmission

Pediatric AIDS was first described in 1982, shortly after the first adult cases were reported (188). Of the estimated 37.5 million people currently living with HIV-1 as of 2020, 1.7 million of those individuals are children (189). While heterosexual transmission is the major transmission mode in adults, the majority of pediatric infections occur through mother-to-child transmission (MTCT). Risk of MTCT transmission is influenced by geography, maternal viral load, co-infection with other sexually transmitted infections, delivery mode, and breast-feeding (190). In the absence of ART, the risk of vertical transmission ranges from around 15% to 45%; however, ART is very effective at reducing transmission and in resource rich countries MTCT is highly preventable. Demographically, over 80% of new pediatric infections occur in Sub-Saharan Africa (191).

Transmission can occur during fetal development *in uteru*, during the peripartum phase of pregnancy and delivery, or post-partum through breast milk transmission (190). Prior to preventative interventions, transmission rates ranged from 15% to 25% and 25% to 45% in mothers that formula-fed and breast-fed, respectively (192). Interestingly, while breastfeeding increases the risk of transmission, infants that receive mixed feeding of both breast milk and formula are over two-times more likely to become infected than infants that are strictly formula fed (193, 194).

Maternal viral load is the strongest correlate of protection. This was first supported by the 076 trial which showed that administration of zidovudine (AZT) during pregnancy, delivery, and to the newborn for the first 6 months of life reduced transmission by nearly 70% in HIV-1 infected women who did not breast-feed (195). Subsequent studies have indicated that transmission is reduced even further with triple-drug regimens (196). The "Option B+" program has become the standard of care and recommends that all HIV-1-infected pregnant women begin ART at the time of diagnosis and remain on ART for the duration of their lifetime (197). In resource rich countries, such as the United States, transmission rates are below 1%, demonstrating that MTCT is highly preventable (198). As of 2020, 95% and 56% of pregnant women with known HIV-1 infection in eastern/southern and western Africa, respectively, reportedly had access to daily ART (199). These increased efforts to prevent mother-to-child transmission of HIV-1 have dramatically reduced *in utero* and intrapartum infections. Presently over half of new infections occur postnatally through breast milk (200).

The uniqueness of the *in utero* transmission window allows for rapid detection and treatment of newly infected infants, since children born to HIV-1 positive women can be screened at birth, before release from the hospital. Such early detection is not generally feasible in adult transmissions. Infants that are HIV-1 positive at birth via rapid point-of-care testing can begin ART within the first few hours of life (201). Infections arising from intra- or post-partum transmission will not be detected at the time of birth so follow-up care and repeated testing are required to monitor these transmission modes. In these instances, early ART initiation is not as practical.

The World Health Organization (WHO) recommends that infants exposed to HIV-1 undergo virological testing at birth and again at 4-6 weeks of age, with a final serological test around 9 months of age (202). As of 2017, 63% of HIV-1 exposed infants in eastern and southern African countries received testing by 8 weeks of age. However, countries in western African lag, with only 21% of HIV-1-exposed infants tested by the same age. This highlights a considerable gap in the implementation of this policy (199, 203, 204). In resource limited settings, early diagnosis of infants can be challenging due to factors such as limited training of health workers, unreliable transportation to often distant regional laboratories, and poor follow-up from the infant's caregivers. While the WHO recommendations state that positive test results should be delivered within 4 weeks, turnaround time in Zambia, for instance, averages 6.2 weeks (202, 205-207).

In the MTCT pair, the infant may be disadvantaged in that the transmitted virus has already adapted to evade a genetically similar immune system. Anti-HIV-1 antibodies and T cells

transferred to the child either *in uteru* or through the breastmilk have pre-adapted to the transmitted virus and are ineffective. Additionally, because of shared HLA alleles, the transmitted virus may be preadapted to CD8+ T cell epitopes restricted by HLA alleles inherited from their mother, further complicating pediatric HIV-1 infection (208, 209). HIV-1 susceptible CCR5+CD4+ T cells are nearly absent in the blood and lymph nodes of infants, but previous studies have identified an abundant population of memory CD4+CCR5+ T cells in the GI tract mucosa of neonatal RM that serve as the primary target cells for MTCT (210-212). As such, these cells are rapidly depleted during acute infection (210).

The Pediatric Immune Response

HIV-1 infected infants experience more rapid disease progression as compared to infected adults, but the mechanisms behind this difference are unclear. While the median survival for ART-naïve HIV-1-positive adults is 11 years, over 50% of HIV-1-infected children die before the age of two without ART treatment (58). Infected infants experience rapid rates of viral production and CD4+ T cell turnover, higher peak viremia, a slower decline to set point, which is generally 1 log higher than in HIV-1 infected adults (190).

To survive to term, the developing fetus must avoid generating an inflammatory response to the many foreign maternal antigens to which it is exposed during development, resulting in a predominantly tolerogenic immune system at birth (213). This tolerogenic environment is facilitated by high levels of anti-inflammatory cytokines such as TGFβ and IL-10 (214). TGFβ

directs naïve CD4+ T cell to differentiate into regulatory T cells (Tregs) resulting in 15% of fetal blood T cells compared to 5% of adult blood T cells. Thes Tregs are long-lived and have been detected in children up to 17 years old (214, 215). Many of these regulatory cells reside in intestinal tissue and are critical for mucosal immune homeostasis. Studies in neonatal RM have indicated that Tregs are rapidly depleted during acute SIV infection, which may contribute to intestinal disorders and disease progression (216). In addition to higher levels of Tregs, the CD4+ effector cells of HIV-infected infants are predominantly of the Th17 and Th2 phenotype (217, 218). As discussed above, Th17 cells are critical to maintaining the integrity of the intestinal mucosal barrier, so loss of Th17 cells during pediatric infection may have an exaggerated impact on pediatric disease progression.

HIV-1 also alters normal innate immune development. Even in HIV-1-exposed, uninfected (HEU) infants, myeloid cells are prone to a higher pro-inflammatory response following stimulation (219). Monocyte turnover, a predictor for disease progression, is elevated in uninfected, healthy infant RMs compared to adults. Turnover is further increased with SIV infection and remains elevated throughout AIDS progression (220). These innate differences may influence pediatric disease progression and help to explain the more rapid development of AIDS observed in HIV-1 infected children.

HIV-1-specific CD8+ T cells that help to control viremia are detected at a much lower frequency during acute infection in infants than what is observed in adults (221). CD8+ T cells in HIV-1-infected infants fail to contain viral replication, resulting in a slower decline to viral set

point. This occurs despite higher expression of activation surface markers, such as HLA-DR and CD95, on infant CD8+ T cells, suggesting that cytolytic function is not impaired (222). Defects in memory B cells have also been reported in HIV-1 infected children. In neonatal RM, SIV infection severely impairs germinal center formation (223). Germinal center follicular T helper cells (Tfh) are reduced throughout infection and correspond to high viremia. In HIV-1-infected infants with high viremia, reduced percentages of memory B cells have also been correlated with lower levels of circulating Tfh (224). These findings likely contribute to ineffective antibody response seen in children.

Despite impaired B cell responses, HIV-1 infected infants sometimes develop bnAbs earlier in infection compared to adults (86, 225, 226). These bnAbs do not show evidence of high SHM, which is common in bnAbs generated in adults as discussed above but target conserved epitopes of the HIV-1 Env trimer. How infants develop these bnAbs is unclear but understanding this mechanism may provide a template to elicit bnAbs in a vaccine setting without the requirement for a long-term maturation pathway and somatic hypermutation.

Antiretroviral Therapy and the Viral Reservoir in Children

The WHO recommendations state that all infants and children under two years of age with confirmed HIV-1 infection begin ART immediately at the time of diagnosis irrespective of CD4+ T cell counts (202). Despite this recommendation, HIV-1-infected children are one third less likely to receive ART than infected adults (204). Reasons for this include fewer drugs available for use

by children, higher treatment cost, and dependence on a caregiver to provide ART (203). Side effects related to ART may contribute to morbidities such as cardiovascular disease and osteoporosis. Although ART dramatically improves patient outcomes, quality of life may not be equal to that of uninfected peers. These adverse manifestations may be amplified in children who must adhere to ART throughout critical developmental windows and the effect of cumulative life-long ART (227).

While the latent reservoir has been well-characterized in HIV-1 infected adults, less is known about its cellular and anatomical distribution in HIV-1-infected children. Resting memory CD4+ T cells, the primary latent cell in adult infection, are present at much lower frequencies in children. Our lab recently reported that replication competent SIV/SHIV DNA from naïve CD4+ T cells significantly contributes to the viral reservoir in orally infected, ART-suppressed infant RM. This finding suggests a previously unrecognized naïve CD4+ T cell reservoir in infants that could contribute to described differences between children and adults (114, 149). Adult elite controllers who maintain normal CD4+ T cell counts and successfully suppress viremia in the absence of ART have a strong HIV-1-specific cytotoxic CD8+ T cell response linked to protective MHC class I polymorphisms such as HLA-B27 (228-230). In contrast, ART-naïve non-progressing HIV-1 infected children maintain normal CD4+ T cell counts and low immune activation despite detectable viremia (231). The mechanisms behind control in these children is unclear, but the phenotype observed in elite controlling children resembles what is observed in natural SIV infection such as in the SM (232).

There have been several unique pediatric cases that have inspired hope in the field of cure research, such as the Mississippi baby. This child, born to an HIV-1-infected mother, had detectable viremia at birth and was immediately prescribed ART. When ART was discontinued after 18 months due to loss of follow-up, the child maintained undetectable viral loads for over 2 years (233). Although the virus did eventually rebound and this child had to resume daily ART, the length of time that the child remained off therapy without rebound was significant. Due to the success observed with the Mississippi baby, early ART has been a major focus of clinical trials; however, early ART alone does not appear to guarantee successfully control of viremia (234-236).

While multiple intervention strategies have been tested in HIV-1-infected adults, fewer studies have included HIV-1-infected children besides the very early ART administration as described above. There have been only ten clinical trials focused on reducing the HIV-1 reservoir in the pediatric population compared to over eighty clinical trials in adults (237). Lack of safety and efficacy information in a pediatric population has been a large roadblock in the advancement of pediatric treatment, and the use of a relevant animal model can provide insight and help to advance more therapeutics to this critical population. Previous work using the SIV-infected RM as a model for pediatric HIV-1 infection has established rapid dissemination of virus following oral challenge, leading to dramatic CD4+ T cell depletion as is seen in HIV-1-infected children (211, 216, 238, 239). The infant RM model has also been used previously to test prophylactic vaccination efficacy (240, 241).

Recently, the Chahroudi lab has established a model of oral SIV infection in the infant RM that effectively simulates postnatal HIV-1 infection through breastfeeding with ART-mediated suppression of viremia (149). In this model, infants were infected with SIVmac251 for 5 weeks before initiating a preformulated ART cocktail. A decline in plasma viral loads to undetectable levels simulated the viremia pattern found in perinatally-infected infants following ART initiation and plasma viral loads remained suppressed on this regimen until animals were euthanized for comprehensive assessment of cellular and anatomic reservoirs (242). This model demonstrated that ART can be safely administered to infant RM for prolonged periods of time, efficiently controls viral replication, and provides an opportunity to test important hypotheses regarding viral reservoirs, infant immunity, and novel remission strategies in the pediatric setting.

Chapter 1 Summary

Since its discovery, HIV-1 has infected over 77 million individuals and led to around 35.4 million deaths (4). While the advent of ART has dramatically improved the lives of infected individuals, it is by no means a cure due to its inability to clear the viral reservoir. With the exception of rare cases, such as the Berlin and London patients detailed above, interruption of ART results in reactivation of the reservoir leading to rapid viral rebound and resumed disease progression. As such, infected individuals must rely on lifelong adherence to prevent AIDS. Intervention strategies that reduce or eliminate the viral reservoir could reduce the international burden of ART and provide viable therapeutic strategies in resource poor countries where the majority of infected individuals reside.

Although children represent almost 2 million of those infected with HIV-1 globally, they have been historically neglected in terms of research and clinical trials. Understanding HIV-1 infection in the unique environment of the developing pediatric immune system is of critical importance. Much of what is understood about pediatric infection stems from studies with low sample sizes resulting in many conflicting reports and inconsistencies. There are many gaps in our knowledge especially regarding the source of the pediatric reservoir, cause of accelerated disease progression, and safety and efficacy of potential therapeutic interventions that have only been tested in the adult setting. It is important to expand our knowledge of the virus in the pediatric setting and the NHP SIV/AIDS model provides a valuable resource to explore these questions.

In this dissertation, we provide novel insight into potential clinical interventions to reduce the viral reservoir and promote viral remission using a model of oral post-natal SIV infection and ART suppression in infant RM. We demonstrate that the use of oral GS-986 is safe and efficacious (Chapter Two), evaluate the immunological and virologic effect of a therapeutic Ad48 prime, MVA boost vaccination with oral TLR-7 stimulation by GS-986 (Chapter Three), and evaluate the impact of the LRA AZD5582, a mimetic of the second mitochondrial-derived activator of caspases (SMACm), (Chapter Four) in SIVmac251-infected, ART-treated infant rhesus macaques. The findings described in this dissertation illustrate advances into therapeutic interventions against pediatric HIV-1 and will inform future pediatric clinical trials.

Chapter 1 Figures

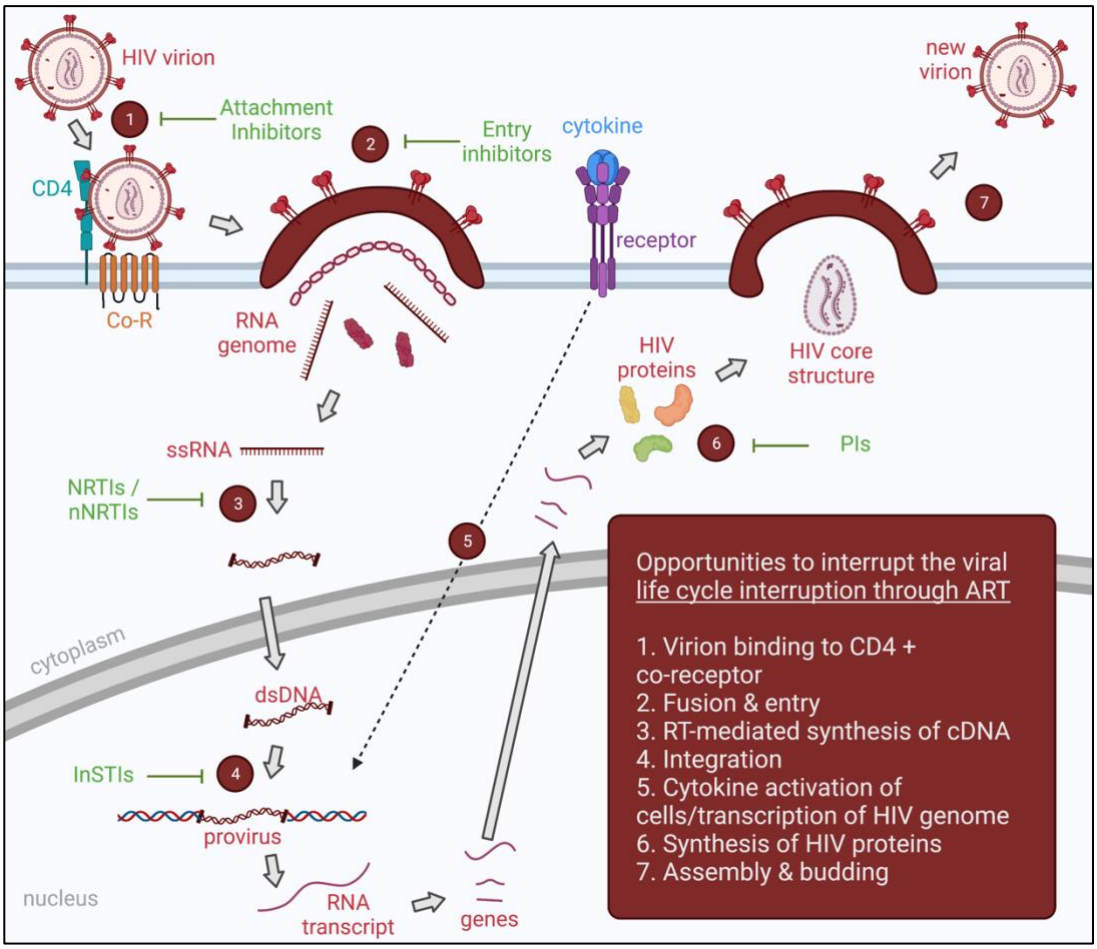

Fig. 1.1. HIV-1 viral life cycle and opportunity for ART Intervention. Stages of the HIV-1 lifecycle that present opportunity for interruption through ART are shown in red. Current HIV-1 medications that inhibit the viral lifecycle are shown in green. Created with BioRender.

Chapter Two: Oral TLR-7 agonist administration induces an immunostimulatory response in SIV-infected ART-suppressed infant rhesus macaques

Katherine M. Bricker[1], Veronica Obregon-Perko[1], Joseph Hesselgesser[2], Ann Chahroudi[1,3,4]

[1]Department of Pediatrics, Emory University School of Medicine, Atlanta, GA; [2]Gilead Sciences Inc., Foster City, CA; [3]Yerkes National Primate Research Center, Emory University, Atlanta, GA; [4]Center for Childhood Infections and Vaccines of Children's Healthcare of Atlanta and Emory University, Atlanta, GA

Oral Presentation at 10th IAS Conference on HIV Science. July 21 – 24, 2019, Mexico City, Mexico.

Abstract

The major obstacle to HIV/AIDS cure is the presence of a reservoir of latently infected cells that persists even under ART treatment. There is some evidence that a toll-like receptor 7 (TLR-7) agonist may reverse viral latency and alone or with use of a therapeutic CD8-inducing vaccine may facilitate reduction of the viral reservoir, but the use of a TLR-7 agonist has not yet been evaluated in a pediatric setting. Here, we sought to evaluate the tolerability and pharmacodynamic responses to this potential therapeutic in a pediatric setting using our infant rhesus macaque model of postnatal oral SIV-infection and ART-suppression. For this study, two dose levels of an orally delivered TLR-7 agonist (GS-986) were administered to SIV-infected ART-suppressed 7-month old rhesus macaques (RMs). RMs received 0.1 mg/kg GS-986 via oral gavage (o.g.) and a second dose of 0.3 mg/kg (o.g.) following 4 weeks of rest. Blood was collected prior to administration, 24 hours, and 1-week post administration to monitor complete blood count (CBC), serum chemistry, plasma viral loads, plasma cytokine concentrations, and immune cell activation. GS-986 was well tolerated at both administered doses with no adverse clinical observations and normal CBC and chemistry at 24 h and 7 d post administration. Both RMs maintained undetectable viremia following administration. Concentrations of plasma cytokines and chemokines such as IFN-γ, IL-1RA, IL-6, IP-10, and I-TAC were elevated in the plasma at 24 h post-administration and returned to pre-dosing levels by 7 d post-administration. Increases in monocytes ($CD3^{-}CD4^{int}\,CD14^{+}\,CD16^{+}$) and circulating ($CD169^{+}$) macrophages was observed 24 h following GS-986 administration with a return to baseline by day 7. Collectively, these findings demonstrate that oral administration of GS-986 is tolerated in infant RMs, with induction of expected immune parameters.

Author Summary

Antiretroviral therapy has improved HIV-1 disease outcome and reduced transmission, but on its own is not curative as it does not eliminate the persistent latent reservoir. Interventions to induce HIV-1 remission in the absence of ART would be highly beneficial to the 1.7 million children living with HIV-1 globally. Here, we used our previously established model of oral SIV infection and ART suppression of viremia in infant rhesus macaques to evaluate the safety and efficacy of the oral TLR-7 stimulant, GS-986 at two dose concentrations. Our study demonstrates that oral GS-986 is safe and induces a dose-dependent pharmacodynamic response, measured through monocyte activation and elevation of plasma cytokines and chemokines, at both dose concentrations evaluated. The efficacy of TLR-7 stimulants as a latency reversing agent has shown conflicting results. In this study, we did not observe on-ART plasma viremia above the limit of detection following either dose concentration of GS-986; however, transient on-ART viremia has only previously been reported following at least 4 consecutive doses. These results are the first to demonstrate that oral TLR-7 stimulation is safe and induces a proinflammatory immune response in a pediatric nonhuman primate setting, which could inform future preclinical and clinical HIV-1 cure trials.

Introduction

Currently, 1.7 million children are living with HIV-1 including 160,000 new pediatric infections annually (191). Increased understanding of transmission and interventions to prevent mother-to-child-transmission (MTCT) has reduced in utero and intrapartum infections, and presently over half of new vertical infections occur postnatally through breast milk (200). While the advent of antiretroviral therapy (ART) has improved disease outcome and reduced mortality, interruption leads to rapid viral rebound due to reactivation of the latent reservoir. Therefore, to prevent disease progression and AIDS, HIV-1 infected children must follow lifelong adherence to ART. Challenges exist, such as availability of ART formulations for children and side effects related to long-term ART. Residual immune activation persists under ART and has been linked with bone, cardiovascular, neurologic, and other complications. The discovery of therapeutics to induce viral remission would help to relieve the lifelong burden of ART and could contribute to a reduction in non-AIDS comorbidities.

While multiple cure strategies have been tested in HIV-infected adults, there has been less emphasis on HIV-infected children. Only ten clinical trials focused on targeting HIV reservoirs have been initiated in the pediatric population compared to over eighty in adults (237). Reluctance to bring experimental therapeutics into this critical population is in part due to a lack of safety and efficacy information. The use of a relevant animal model should help to reduce this apprehension. Recently, our lab has established a model of oral SIV infection in the infant rhesus macaque that effectively simulates postnatal HIV-1 infection through breastfeeding with ART-mediated

suppression of viremia (149). This model provides an opportunity to test important hypotheses regarding viral reservoirs, infant immunity, and remission strategies.

GS-9620 and its tool compound analog GS-986 are small molecule agonists of toll-like receptor (TLR)-7 that activate plasmacytoid dendritic cells (pDCs) upon oral administration. TLR-7 stimulation initiates the MyD88-dependent signaling pathway in pDCs that leads to activation of transcription factors including NF-kB and interferon regulatory factors (IRFs) ultimately leading to activation of the adaptive immune system through secretion of proinflammatory cytokines and chemokines (Fig 2.1) (243, 244). Originally developed for treating hepatitis C (HCV) and hepatitis B (HBV) virus, they have also been shown to be effective in the setting of HIV-1. Whitney *et al*. first reported transient viremia following repeated administration of a TLR-7 agonist that led to prolonged delay of viral rebound following removal of ART (245). Follow up studies combining a TLR-7 agonist with a cure agent have not replicated on-ART viremia, but did result in delayed viral rebound and lower rebound set point (169, 185, 246). Oral TLR-7 agonists have yet to be tested in the pediatric setting.

For this study, we aimed to investigate the safety and pharmacodynamic effect of an oral TLR-7 agonist, GS-986, in the pediatric setting of SIV infection and ART treatment. As a TLR-7 agonist had not yet been investigated in the pediatric setting, we performed a small dose escalation (0.1 mg/kg and 0.3 mg/kg) in two durably ART-suppressed, SIV-infected 7-month infant rhesus macaques. We demonstrate that GS-986 is safe in SIV-infected, ART-suppressed infant rhesus macaques with no adverse clinical reactions and complete blood count (CBC) and serum chemistry remaining in normal parameters throughout the intervention. Additionally, we show that TLR-7

stimulation induces the expected pharmacodynamic response in a transient, dose-dependent manner with activated monocytes and elevated plasma cytokines and chemokines observed in the blood at 24-hours post dose and return to baseline at the next measured time point (2 weeks post-dose). These results are the first to show safety and immunostimulatory potential of an oral TLR-7 stimulant in a pediatric setting and inform future pediatric preclinical and clinical HIV-1 cure trials.

Results

SIV infection and Dose Escalation Strategy

Two female Indian origin RMs were selected for this study. RMs were confirmed negative for the Mamu-B*08 and -B*17 MHC class I alleles associated with natural control of SIV replication. The time course of the experimental design and interventions used are shown in Fig 2.2. RMs were exposed to two consecutive doses of 10^5 50% tissue culture infective doses ($TCID_{50}$) SIV_{mac251} by oral administration at approximately 5 weeks of age (RYi19: 3.9 w; RFj19 5.4 w). As breastfeeding acquisition of HIV-1 is unlikely to be compatible with very early ART initiation, here we started daily ART in all RMs at 4 weeks after SIV infection to approximate this clinical scenario. The ART regimen consisted of two reverse transcriptase inhibitors (tenofovir [TDF] at 5.1 mg/kg of body weight/day and emtricitabine [FTC] at 40 mg/kg/day) and one integrase inhibitor (dolutegravir [DTG] at 2.5 mg/kg/day), co-formulated into a single dose administered once daily by subcutaneous injection for 15 months (as indicated by gray shading in Fig 3.1A). ART was effective at suppressing SIV RNA in plasma below the limit of detection (LOD) of the assay (60 copies/ml) as both RM achieved durable viral suppression following 4 to 8 weeks of daily ART.

At 26 weeks post infection, animals were given one dose of the TLR-7 agonist GS-986 (0.1 mg/kg, o.g.). Blood was collected pre-administration, 24 hours, and 1 week post-administration to monitor safety parameters and measure the immunological response to GS-986. Following 4 weeks

of rest, animals received a second dose of GS-986 (0.3 mg/kg, o.g.) at 30 weeks post infection. This experimental design is detailed in Fig. 2.2.

GS-986 is well tolerated in infant RMs

Oral GS-986 was well tolerated in the infant RMs at both administered doses. No adverse clinical observations were reported. Both infants continued to gain weight throughout study time frame (Fig 2.3A). Complete blood count (CBC) and serum chemistry were monitored at all time points. CBC values indicate that white blood cells, hemoglobin, and platelet counts all remained within expected parameters for the duration of the study (Fig. 2.3B). Additional, serum chemistry showed normal kidney function, measured through blood urea nitrogen (BUN) and creatine, and liver function, measured through alanine aminotransferase (ALT) and gamma-glutamyl transferase (GGT) (Fig 2.3C).

Increase of plasma cytokines and chemokines is observed following oral GS-986

We next assessed the effect of oral GS-986 on plasma cytokines and chemokines using the MSD U-Plex assay (Fig 2.4). GS-986 has been shown to induce activation of plasmacytoid dendritic cells (pDCs) that then release cytokines and chemokines including IFN-γ systemically to recruited activated immune cells. Following the 0.1 mg/kg dose, an average of 2.5 log2 fold change was observed in plasma IP-10, a proinflammatory chemokine found to activate various cell types including Th1 $CD4^+$ T cells, NK cells, and macrophages (247). Plasma concentrations of IP-10 at this time point were 14,357 pg/ml for RYi19 and 6813 pg/ml for RFj19. Additionally, a 5.2 and

4.3 log2 fold change in plasma IL-1RA and I-TAC, respectively. Both IFN-γ and IFN-α2 were detectable above the limit of detection at baseline but did not measurably increase following the 0.1 mg/kg dose of GS-986.

Induction of these pro-inflammatory cytokines and chemokines were even higher following the 0.3 mg/kg dose with a 3.8, 6.7, and 4.3 log2 fold change observed for IP-10, IL-1RA, and I-TAC, respectively. Plasma IFN-α2 increased by a 4.8 log2 fold change was observed at 24 hours following the 0.3 mg/kg dose with concentration reaching an average of 284 pg/ml. Although there was no increase in plasma IFN-γ concentration following the 0.1 mg/kg dose, a 2.9 log2 fold change was observed at 24 hours following 0.3 mg/kg dosing with concentrations reaching 395 pg/ml and 581 pg/ml in RYi19 and RFj19, respectively. Both IL-8 and IL-6 remained below the limit of detection for the assay following the 0.1 mg/kg dose. In RYi19 only, low levels of IL-8 were detected (47 pg/ml) at 24 hours following the 0.3 mg/kg dose. IL-6 was also detected in low levels following the 0.3 mg/kg dose in both animals (mean = 101 pg/ml). We also measured IL-1β, IL-2, and IL-10 which did not reach concentrations higher than the limit of detection for the assay at any time point evaluated. These results indicate that the measurable plasma cytokine and chemokine response to oral GS-986 is dose dependent with a stronger induction of proinflammatory markers following the 0.3 mg/kg dose than the 0.1 mg/kg dose.

Immunological effect of Oral GS-986

To evaluate the immunological impact of oral GS-986 administration, flow cytometry was performed on whole blood. CD169, or Siglec-1, is upregulated on monocytes and macrophages

following TLR-7 stimulation or exposure to IFN-γ produced by pDCs. This CD169 expression then promotes monocytes to travel to the tissue, differentiate and induce adaptive immune responses to pathogens (248). For analysis, monocytes were classified as Live $CD3^-$ $CD4^{int}$ $CD14^+$ cells. A transient increase in nonclassical monocytes, distinguished by CD16, was observed within the monocyte population at 24 hours post-GS-986 administration following both the 0.1 mg/kg and 0.3 mg/kg dose (mean = 66.6±3.2% & 66.5±3.1%, respectively). By 7-days post administration, $CD16^+$ monocytes returned to baseline values (Fig. 2.5A). Similarly, baseline values of circulating macrophages, indicated by CD169 expression, averaged 5.1±4.4%. By 24 hours post-dose a dramatic increase was observed in this cell population after both the 0.1 mg/kg and 0.3 mg/kg dose (mean = 87.7±10.1% and 90.3±6.2%, respectively) (Fig. 2.5B). A representative flow plot of these results is displayed in Fig 2.5C.

T cells were also monitored following oral GS-986 through expression of CD69. No observed increase of CD69 was observed at time points analyzed, however, previous studies performed in adult RMs indicate that CD69 expression peaks 2 days following GS-986 (169, 245). Due to blood volume limits and the small size of infant RMs, collection at this time point was not possible. Despite lack of observed $CD4^+$ or $CD8^+$ T cell activation, a transient increase in peripheral $CD4^+$ T cells was observed at the 24 hour time point following both dose administrations with a return to baseline by 7 days post GS-986 (Fig. 2.6). Previous studies in adult animals have observed a decrease in peripheral $CD4^+$ T cell frequency 4-6 hours following oral TLR-7 stimulation (Joe Hesselgesser, oral communication). The increase observed in our study at 24 hours is likely due to a rebound of $CD4^+$ T cells to the periphery after activated $CD4^+$ T cells have migrated to tissues.

No plasma viremia was detected during TLR7 agonist administration

One main approach to HIV cure strategies, commonly referred to as "kick and kill," aims to push virally infected cells out of a state of latency with the use of a latency reversing agent (LRA) in the setting of ART allowing the immune system to detect and eliminate these cells that compose the viral reservoir. The ability of an oral TLR-7 agonist to act as an LRA is a subject of debate in the field. Lim *et al.* first reported that repeated dosing with the investigational tool? compound, GS-986, and its clinical analog, GS-9620, led to transient viremia on ART and reduced the viral reservoir in SIV-infected RMs (245). Importantly, in that study, plasma viremia was only observed after multiple 0.3 mg/kg doses. However, other studies involving oral TLR-7 stimulation have not observed incidences of plasma viremia (169, 246). In our study, plasma viral loads were evaluated prior to GS-986 administration, 24 hours, and 7 days post dosing. No viremia above the limit of detection (60 copies/mL) was observed in either animal following either the 0.1 mg/kg or the 0.3 mg/kg dose. As stated above, when plasma viremia was observed it was after multiple administrations of GS-9620 at 0.3 mg/kg. In our study, infants only received one 0.3 mg/kg dose, so induction of transient plasma viremia was not an expected outcome as the study was designed.

Discussion

This study provides insight into the first use of an oral TLR-7 agonist in a pediatric setting and provides critical preclinical data for its use in future HIV-1 combination cure interventions. We demonstrate that GS-986 is safe and induces expected pharmacodynamic responses at a dose concentration of both 0.1 mg/kg and 0.3 mg/kg in SIV-infected, ART-treated infant RMs.

TLR-7 is predominantly expressed in the endosome of plasmacytoid dendritic cells and upon stimulation leads to secretion of IFN-γ and type I IFNs that are then released systemically in the plasma to activate peripheral immune cells. Following oral administration of GS-986 in SIV-infected, ART-treated infant RMs, we have demonstrated a dose dependent increase in these pro-inflammatory plasma cytokines and chemokines as expected. In addition to IFN-ɣ, we also saw an increase in IP-10, IL-1RA, I-TAC, IFN-α2, and IL-6.

In addition to increased pro-inflammatory cytokines and chemokines in the plasma, robust activation of nonclassical monocytes and circulating macrophages in the periphery was evident in the periphery at 24-hours post-GS-986 following both dose concentrations tested with a return to baseline by the next sample timepoint at 7 days post-administration. Additionally, a transient increase in peripheral CD4+ T cell frequency was observed at 24 hours post-dose with a return to baseline by 7 days post-dose. In the present study, no activation of CD4+ or CD8+ T cells was observed; however, we believe this was due to the timing of blood draws as T cell activation in previous adult studies was not evident until 36 – 48 hours after TLR-7 stimulation.

There are conflicting reports in the literature as to the latency reversing potential of oral TLR-7 stimulants, such as GS-986, in adult SIV-infected, ART-suppressed macaques (169, 185, 245, 246). In our present study, we did not observe plasma viremia above the limit of detection following either 0.1 mg/kg or 0.3 mg/kg of GS-986. However, these results are not surprising as when transient viremia was reported in adult RMs it was only observed following at least three doses of GS-9620 at 0.3 mg/kg. Future studies administering repeated oral TLR-7 agonists will reveal the latency reversing potential of GS-986 in the pediatric setting.

As this was a pilot study evaluating an oral TLR-7 stimulant in the pediatric setting, our sample size was limited. This prohibited us from performing a robust statistical analysis on our results. Further investigation with more animals will be required to draw meaningful conclusions as to the pharmacodynamic effects of GS-986 in SIV infected, ART treated infant RMs. Additionally, the small physical size of the infant RMs prohibits intensive blood sampling. Post-GS-986 sample frequency was therefore limited to only 24-hours after administration. Despite these limitations, we believe this study presents critical safety information for future trials.

In conclusion, we have demonstrated that an oral TLR-7 agonist is safe and induces the expected pharmacodynamic response in SIV-infected, ART-treated infant RMs. These results inform future clinical and preclinical trials and show potential for the use of TLR-7 stimulation in pediatric combination cure approaches. Future studies, including larger sample sizes, with more frequent dosing and sampling, will provide further insight into the full potential of GS-986 and similar compounds.

Materials and Methods

Animals and SIV infection

Two infant Indian RMs (*Macaca mulatta*), with exclusion of Mamu B*08 and B*17 positive animals, were enrolled in this study. The animals were born at the Yerkes National Primate Research Center (YNPRC) to dams housed in indoor/outdoor group housing. The infants were removed from the dams when they were approximately 2 weeks old and transferred to a nursery, where they were housed in social pairs with either full contact or protected contact for the duration of the study. The infants were fed in accordance with the YNPRC standard operating procedures (SOPs) for NHP feeding and had continual access to water. After being removed from the dam, infants were fed center approved milk replacer (Similac Advance, OptiGro Infant Formula with Iron and/or Similac Soy Isomil OptiGro Infant Formula with Iron; Abbott Nutrition, Columbus, OH) until 14 weeks of age. Infants were provided softened standard primate jumbo chow biscuits (Jumbo Monkey Diet 5037; Purina Mills, St. Louis, MO) and a portion of orange starting between 2 – 4 weeks of age. As animals aged additional enrichment of various fresh produce items were provided daily. Cages also contained additional sources of animal enrichment including objects such as perching and other manipulanda. Animal welfare was monitored daily. Appropriate procedures were performed to ensure that potential distress, pain, or discomfort was alleviated. The sedatives Ketamine (10 mg/kg) or Telazol (4 mg/kg) were used for blood draws and biopsies. Euthanasia of RMs, using Pentobarbital (100 mg/kg) under anesthesia, was performed only when deemed clinically necessary by veterinary medical staff and according to IACUC endpoint guidelines. The animals were orally infected at 4 to 5 weeks of age with two consecutive doses of

10^5 $TCID_{50}$ of SIV_{mac251}. All of the animals were treated in accordance with Emory University and Yerkes National Primate Research Center Institutional Animal Care and Use Committee regulations.

Antiretroviral therapy

The two RM infants were treated with a three-drug ART regimen initiated at 4 weeks post infection. The preformulation ART cocktail contained two reverse transcriptase inhibitors, 5.1 mg/kg Tenofovir Disoproxil Fumarate (TDF) and 40 mg/kg Emtricitabine (FTC), plus 2.5 mg/kg of the integrase inhibitor Dolutegravir (DTG). This ART cocktail was administered once daily at 1 mg/kg via the subcutaneous route.

GS-986 Dose Escalation

Both monkeys were virologically suppressed for over 3 months prior to administration of GS-986. At 7 months of age, RMs received 0.1 mg/kg GS-986 (Gilead Sciences) by oral gavage (o.g.). Following 4 weeks of rest, animals received a second dose of 0.3 mg/kg (o.g.) and analyses were repeated.

Sample collection and processing

EDTA-anticoagulated blood samples were collected regularly and used for a complete blood count, routine chemical analysis and immunostaining, with plasma separated by centrifugation within 1 h of phlebotomy. PBMCs were prepared by density gradient centrifugation.

Plasma RNA

Plasma viral quantification was performed as described previously (179). Frozen cell pellet was lysed with proteinase K (100 μg/ml in 10 mM Tris-HCl pH 8) for 1 h at 56oC. Quantification of SIVmac gag DNA was performed by quantitative PCR using the 5' nuclease (TaqMan) assay with an ABI7500 system (PerkinElmer Life Sciences). The sequence of the forward primer for SIVmac gag was *5′-GCAGAGGAGGAAATTACCCAGTAC-3′*, the reverse primer sequence was *5′-CAATTTTACCCAGGCATTTAATGTT-3′*, and the probe sequence was *5′-6-carboxyfluorescein (FAM)-TGTCCACCTGCCATTAAGCCCGA-6*-carboxytetramethylrhodamine (TAMRA)-*3′.* 7.5 μL of cell lysate were mixed in a 50 μL reaction containing 1x Platinum Buffer, 3.5 mM MgCl2, 0.2 mM dNTP, primers 200 nM, probe 150 nM, and 2 U Platinum Taq. For cell number quantification, quantitative PCR was performed simultaneously for monkey albumin gene copy number. The sequence of the forward primer for albumin was *5'-TGCATGAGAAAACGCCAGTAA-3';* the reverse primer sequence was 5'-*ATGGTCGCCTGTTCACCAA-3'* and the probe sequence was *5'-AGAAAGTCACCAAATGCTGCACGGAATC-3' (249).* The reactions were performed on a 7500 real-time PCR system (Applied Biosystems) with the following thermal program: 5 min at 95ºC, followed by 40 cycles of denaturation at 95oC for 15 s and annealing at 60ºC for 1 min.

Immunophenotyping by flow cytometry

Multicolor flow cytometric analysis was performed on whole blood or cell suspensions using predetermined optimal concentrations of the following fluorescently conjugated monoclonal antibodies (MAbs). For whole blood (WB) T cell analysis the following MAbs were used: CD3-allophycocyanin (APC)-Cy7 (clone SP34-2), CD95-phycoerythrin (PE)-Cy5 (clone DX2), Ki67-AF700 (clone B56), HLA-DR-peridinin chlorophyll protein (PerCP)-Cy5.5 (clone G46-6), CCR7-fluorescein isothiocyanate (FITC) (clone 150503), CCR5-APC (clone 3A9), and CD45-RA-PE-Cy7 (clone L45) from BD Biosciences; CD8-BV711 (clone RPA-T8), CD4-BV650 (clone OKT4), and PD-1-BV421 (clone EH12.2H7) from BioLegend; and CD28-ECD (clone CD28-2) from Beckman-Coulter. For WB activation analysis the following MAbs were used: CD3-allophycocyanin (APC)-Cy7 (clone SP34-2) and CD69-phycoerythrin (PE)-CF594 (clone FN50) from BD Biosciences; CD8-BV711 (clone RPA-T8), CD4-BV650 (clone OKT4), CD16-BV421 (clone 3G8), CD14-phycoerythrin (PE)-Cy7 (clone M5E2), and CD169-phycoerythrin (PE) (clone 7-239) from BioLegend; and CD38-allophycocyanin (APC) (clone OK10) from the NHP Reagent Resource. Flow cytometric acquisition and analysis of samples were performed on at least 100,000 events on an LSR II flow cytometer driven by the FACSDiva software package (BD Biosciences). Analyses of the acquired data were performed using FlowJo version 10.0.4 software (TreeStar). For analysis, T cells were gated as live CD3+ cells and monocytes were gated as live CD3-CD4int cells positive for either CD14 or CD16.

Plasma Cytokines

Using stored plasma, the concentration of IFN-α2a, IFN-γ, IL-1B, IL-1RA, IL-2, IL-6, IL-8, IL-10, IP-10, and I-TAC were assessed using a multiplex array according to the manufacturer's

instructions (Meso Scale Diagnostics, Maryland, USA). For each plate, 200 uL of each biotinylated antibody was incubated with 300 uL of each linker for 30 min at room temp. Each reaction was stopped by incubating with 200 uL of stop solution for min at RT. The linker-coupled capture reagents were then combined and diluted before adding to U-PLEX plates for 1h. Samples, standards, and QCs were diluted and transferred to U-PLEX plates after the plates were washed three times. Samples were incubated for 1 hour at RT, shaking. Sulfo-tag labeled detection antibody was then added to the plates and incubated for 1 h. The plates were washed another three times and read buffer was added after the final wash. Plates were read immediately with the MSD instrument and analyzed on Discover Workbench 4.0.

Chapter Two Figures

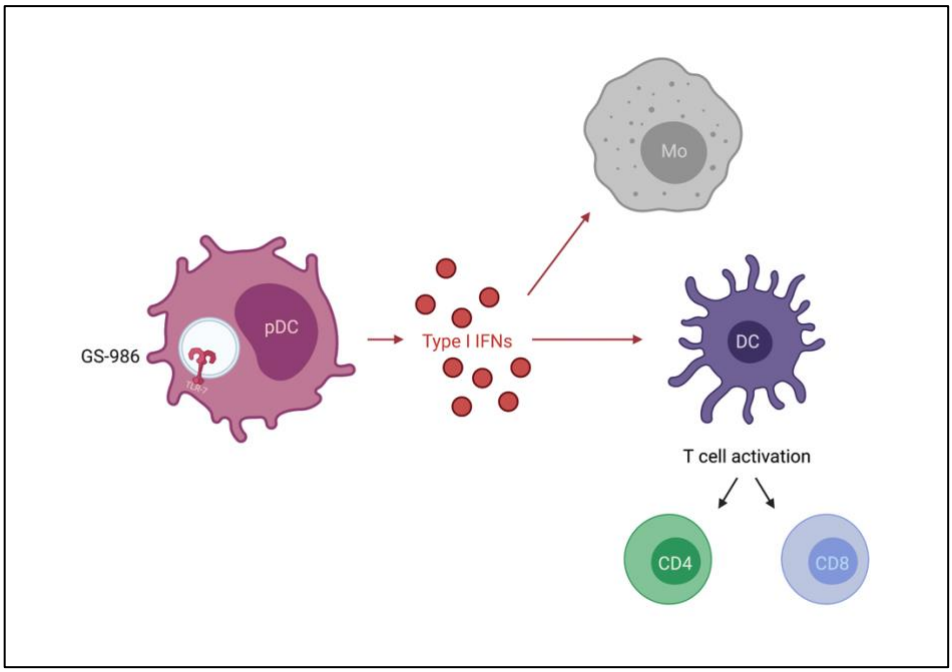

Figure 2.1. Schematic representation of mechanisms of activation following oral GS-986. Oral GS-986 antagonizes TLR-7 in the endosome of plasmacytoid dendritic cells (pDCs) which leads to secretion of type I IFNs that activate macrophages, monocytes (Mo), and dendritic cells (DC). Activated dendritic cells then go on to activate CD4+ and CD8+ T cells.

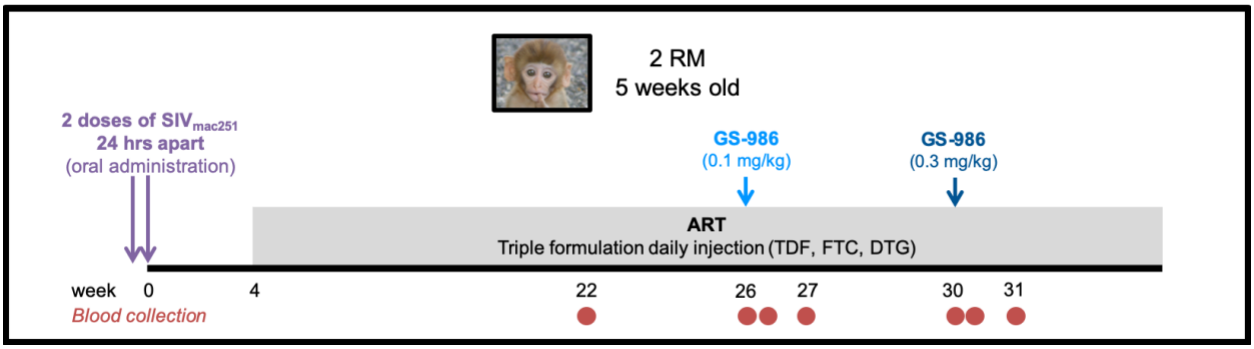

Figure 2.2. Experimental design of oral GS-986 dose escalation in SIV-infected, ART-treated infant RMs. Schematic of the study design. Two infant RMs were infected orally with 10^5 TCID50 SIV_{mac251} (day 0), and starting on 4 weeks p.i. treated with combination ART (TDF, FTC, DTG) for 7 months. Animals received one dose of GS-986 (0.1 mg/kg, o.g.) followed by a second dose of GS-986 (0.3 mg/kg, o.g.) at time points indicated. Blood was collected at the indicated time points.

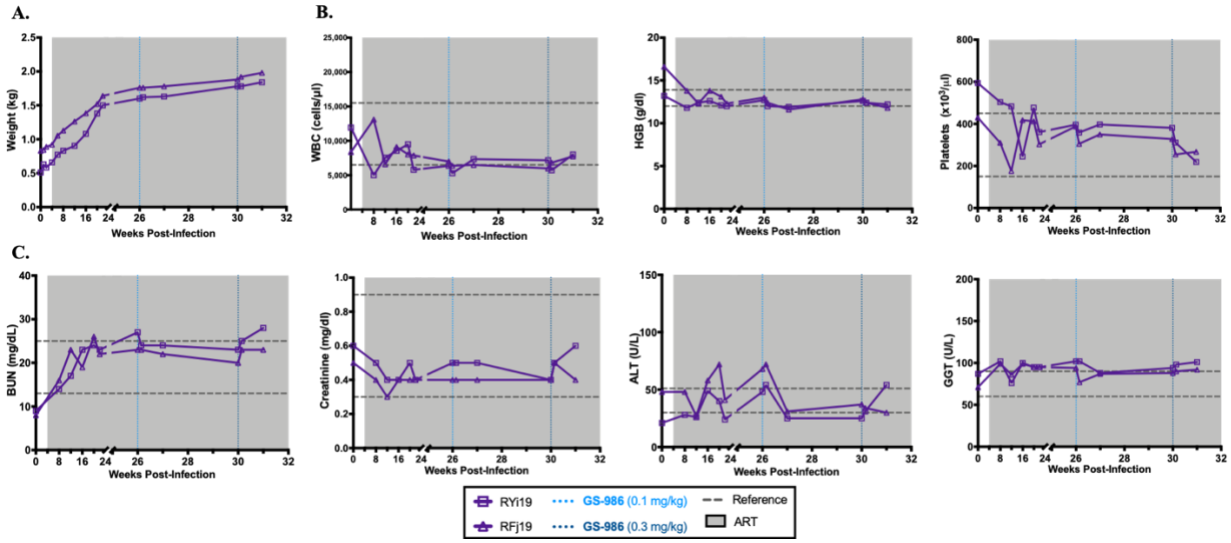

Figure 2.3. Oral GS-986 is safe at both doses evaluated in SIV-infected, ART-treated infant RMs. Longitudinal assessment of complete blood counts, serum chemistries, and body weight. Dotted lines represent normal ranges and values. Each curve represents one animal (*n*=2).

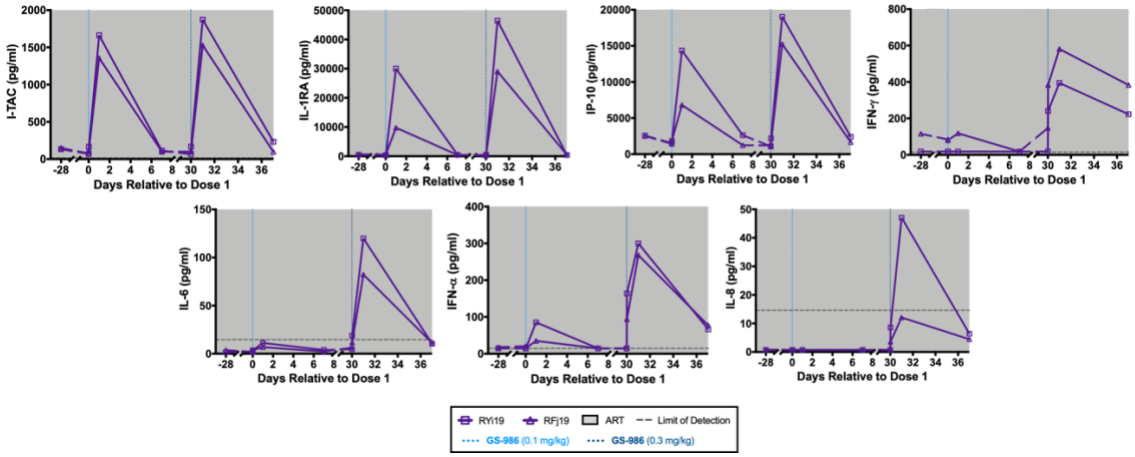

Figure 2.4. Oral GS-986 results in transient increase of plasma cytokine and chemokine concentrations in SIV-infected, ART-treated infant RMs. Plasma concentrations of cytokines were quantified using a multiplex array according to the manufacturer's instructions (Meso Scale Diagnosis, Maryland, USA). Each curve represents one animal (*n*=2).

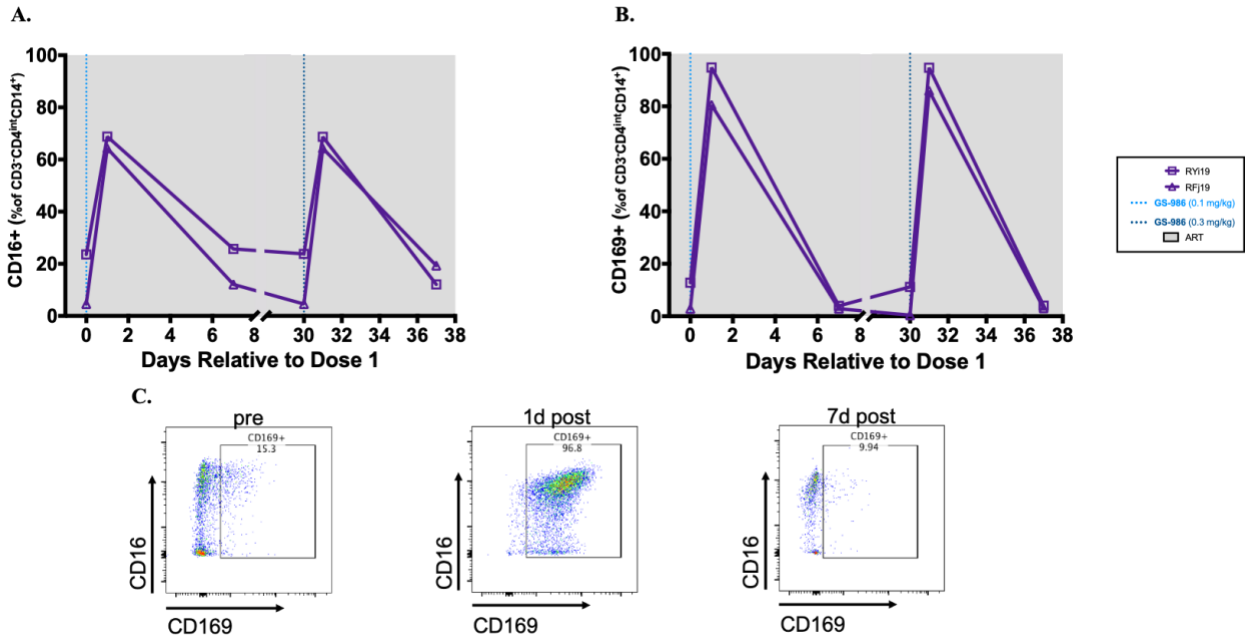

Figure 2.5. Oral GS-986 results in activation of peripheral monocytes and macrophages at 24 hours post dose in SIV-infected, ART-treated infant RMs. Flow cytometry was performed on whole blood at indicated time points. Data shows frequency of (a) CD16-positive activated monocytes and (b) CD169-positive circulating macrophages cells within total blood monocytes. Each curve represents one animal (*n*=2). (c) Representative staining for CD16 and CD69 within monocytes before, 1 day after, and 7 days after GS-986.

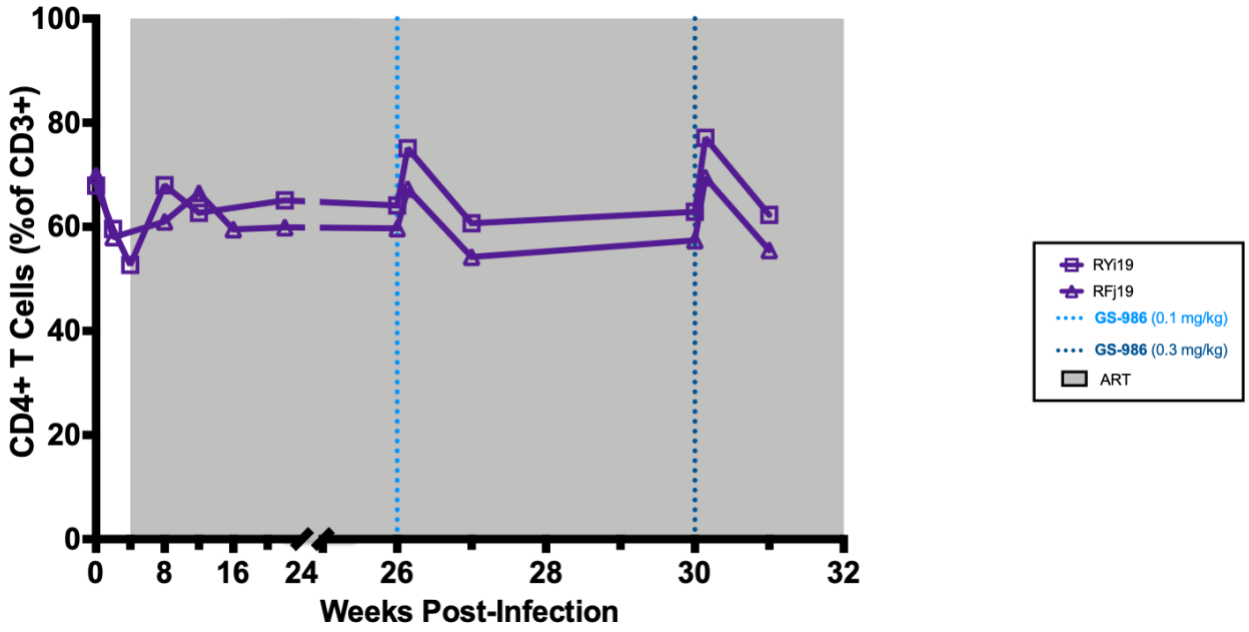

Figure 2.6. Peripheral T cell frequency transiently increases following oral GS-986 in SIV-infected, ART-treated infant RMs. Flow cytometry was performed on whole blood at indicated time points. Data shows frequency of CD4+ T cells within total T cells. Each curve represents one animal (*n*=2).

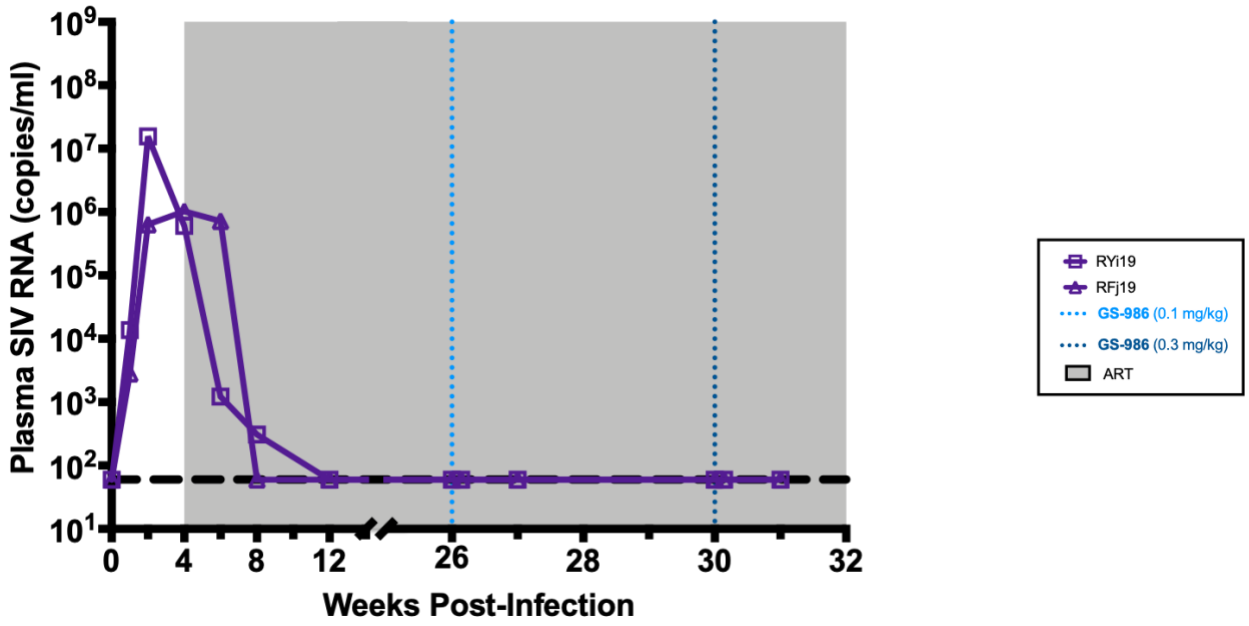

Figure 2.7. Oral GS-986 does not result in plasma viremia on ART in SIV-infected, ART-treated infant RMs. Plasma viral loads were quantified by real-time RT-PCR. Each curve represents one animal (n = 2).

Chapter Three: Therapeutic vaccination of SIV-infected, ART-treated infant rhesus macaques using Ad48/MVA in combination with TLR-7 stimulation

Katherine M. Bricker[1], Veronica Obregon-Perko[1], Ferzan Uddin[1], Brianna Williams[1], Emilie A. Uffman[2], Carolina Garrido[2], Genevieve G. Fouda[2,3], Romas Geleziunas[4], Merlin Robb[5], Nelson Michael[5], Dan H. Barouch[6,7], and Ann Chahroudi[1,8,9]

[1]Department of Pediatrics, Emory University School of Medicine, Atlanta, GA; [2]Duke Human Vaccine Institute, Duke University Medical Center, Durham, NC; [3]Departments of Molecular Genetics and Microbiology and Pediatrics, Duke University School of Medicine, Durham, NC; [4]Gilead Sciences, Inc., Foster City, CA; [5]US Military HIV Research Program, Walter Reed Army Institute of Research, Silver Spring, MD; [6]Center for Virology and Vaccine Research, Beth Israel Deaconess Medical Center, Harvard Medical School, Boston, MA; [7]Ragon Institute of MGH, MIT, and Harvard, Cambridge, MA; [8]Yerkes National Primate Research Center, Emory University, Atlanta, GA; [9]Center for Childhood Infections and Vaccines of Children's Healthcare of Atlanta and Emory University, Atlanta, GA

Published in PLoS Pathogens, 2020, 16(10), PMID: 33104758

Abstract

Globally, 1.7 million children are living with HIV-1. While antiretroviral therapy (ART) has improved disease outcomes, it does not eliminate the latent HIV-1 reservoir. Interventions to delay or prevent viral rebound in the absence of ART would be highly beneficial for HIV-1-infected children who now must remain on daily ART throughout their lifespan. Here, we evaluated therapeutic Ad48-SIV prime, MVA-SIV boost immunization in combination with the TLR-7 agonist GS-986 in rhesus macaque (RM) infants orally infected with SIV_{mac251} at 4 weeks of age and treated with a triple ART regimen beginning 4 weeks after infection. We hypothesized immunization would enhance SIV-specific T cell responses during ART-mediated suppression of viremia. Compared to controls, vaccinated infants had greater magnitude SIV-specific T cell responses (mean of 3475 vs 69 IFN-γ spot forming cells (SFC) per 10^6 PBMCs, respectively, P=0.01) with enhanced breadth of epitope recognition and increased $CD8^+$ and $CD4^+$ T cell polyfunctionality (P = 0.004 and P = 0.005, respectively). Additionally, SIV-specific gp120 antibodies against challenge and vaccine virus strains were significantly elevated following MVA boost (P = 0.02 and P < 0.001, respectively). GS-986 led to expected immune stimulation demonstrated by activation of monocytes and T cells 24 hours post-dose. Despite the vaccine-induced immune responses, levels of SIV DNA in peripheral and lymph node $CD4^+$ T cells were not significantly different from controls and a similar time to viral rebound and viral load set point were observed following ART interruption in both groups. We demonstrate infant RMs mount a robust immunological response to this immunization, but vaccination alone was not sufficient to impact viral reservoir size or modulate rebound dynamics following ART release. Our findings hold promise for therapeutic vaccination as a part of a combination cure approach in children and

highlight the importance of a pediatric model to evaluate HIV-1 cure interventions in this unique setting of immune development.

Author summary

While antiretroviral therapy (ART) has improved disease outcome and reduced HIV-1 transmission, it is not a cure, as interruption of ART results in rapid viral rebound due to the persistent latent reservoir. Interventions to induce HIV-1 remission in the absence of ART would be highly beneficial to children living with HIV-1, sparing them from the associated adherence requirements, side effects, and cost of ART. Here, we used our previously established pediatric model of oral SIV infection and ART suppression of viremia in infant rhesus macaques (RMs) to evaluate the safety and efficacy of an Ad48-SIV prime, MVA-SIV boost therapeutic vaccine approach plus TLR-7 stimulation. Our study demonstrates this vaccination strategy is immunogenic in infants; however, unlike previously reported results in adult RMs using a similar approach, vaccination did not result in a difference in the level of $CD4^+$ T cell-associated SIV DNA or viral rebound dynamics after ART interruption when compared to control infant RMs. These results highlight the importance of pre-clinical studies using pediatric models and indicate potential HIV-1 cure strategies may differentially impact adults and children.

Introduction

Globally, 1.7 million children are living with HIV-1 and there are 150,000 new pediatric infections annually (204). In utero and intrapartum HIV-1 infections have declined with increased understanding of transmission risks and interventions to prevent mother-to-child transmission (MTCT) implemented during pregnancy and delivery. Presently, the majority of new infections occur postnatally through breastmilk transmission (200). While the global roll-out of antiretroviral therapy (ART) has improved disease outcomes and reduced mortality, ART interruption leads to rapid viral rebound due to reactivation of the persistent latent viral reservoir (128, 250, 251). Therefore, to prevent disease progression and AIDS, HIV-1 infected children must follow lifelong adherence to ART.

HIV-1-infected infants experience rapid progression of disease compared to infected adults. While the median survival for ART-naïve HIV-1-infected adults is 11 years, over 50% of HIV-1-infected children die before the age of two in the absence of ART (58). Infected infants experience rapid rates of viral production and $CD4^+$ T cell turnover, higher peak viremia, a slower decline to viral set point, and set points on the order of 1 log higher than what is observed in HIV-1 infected adults (190). The mechanisms behind these differences have not been fully elucidated, but are thought to reflect a more immature immune system and inadequate HIV-1-specific immune responses.

While multiple cure strategies have been tested in HIV-1-infected adults, there has been less emphasis on HIV-1-infected children. Only twelve clinical trials focused on targeting HIV

reservoirs have been initiated in the pediatric population compared to over eighty in adults (252). In the first therapeutic vaccine pediatric clinical trial, PEDVAC, DNA vaccination of vertically HIV-1-infected, ART-suppressed children was well tolerated and resulted in a transient increase in the HIV-1-specific cellular immune response (253). This study was limited by a small sample size, an unboosted vaccine strategy, and the exclusion of an adjuvant. Further trials are necessary to advance this field.

The use of a relevant pediatric animal model may help to provide important safety and efficacy information necessary to bring experimental therapeutics to children. Simian immunodeficiency virus (SIV) infection in the rhesus macaque (RM) has been established as a robust animal model that possesses many similarities to HIV-1 infection including transmission routes, acute infection events, $CD4^+$ T cell dynamics, disease progression, and ART-mediated suppression of plasma viral loads (111, 254, 255). This model has been used extensively to inform HIV-1 cure strategies (106, 181, 182, 256, 257); for example, Borducchi et al recently identified a promising therapeutic vaccine regimen that resulted in robust anti-SIV T cell responses leading to a delay in time to viral rebound and reduced set point viremia following ART interruption in vaccinated adult RM compared to ART-only controls (169). To test hypotheses regarding the viral reservoir, immunity, and remission strategies in a pediatric setting, our laboratory has previously established a model of oral SIV infection in infant RM that effectively simulates postnatal HIV-1 infection through breastfeeding with ART-mediated suppression of viremia (149).

In the present study, we sought to evaluate the immunological and virologic effects of a therapeutic Ad48-SIV prime, MVA-SIV boost immunization strategy in combination with the

TLR-7 agonist GS-986 (TV+TLR7) in our model of SIV-infected ART-treated RM infants. We show therapeutic vaccination is safe in a pediatric setting of SIV infection and ART treatment and generates a high-magnitude, broad, and polyfunctional anti-SIV immune response. These results inform our understanding of lentiviral infection and immune responses in a pediatric model and support the inclusion of therapeutic vaccination as a part of a combination cure approach to be tested in children.

Results

SIV infection and virologic response to ART

Sixteen Indian origin RMs (eight males and eight females) were selected for this study. RMs were confirmed negative for the Mamu-B*08 and -B*17 MHC class I alleles associated with natural control of SIV replication. The time course of the experimental design and interventions used are shown in Fig 1A. All RMs were exposed to two consecutive doses of 10^5 50% tissue culture infective doses ($TCID_{50}$) SIV_{mac251} by oral administration at approximately 5 weeks of age (range: 3.7 w – 10 w, mean: 5.3 w). Once infection was confirmed by SIV RNA in plasma, no significant difference was noted in pre-ART viral kinetics of infants that required multiple challenges compared to infants successfully infected following first challenge (Fig. S3.1). As breastfeeding acquisition of HIV-1 is unlikely to be compatible with very early ART initiation, here we started daily ART in all RMs at 4 weeks after SIV infection to approximate this clinical scenario. The ART regimen consisted of two reverse transcriptase inhibitors (tenofovir [TDF] at 5.1 mg/kg of body weight/day and emtricitabine [FTC] at 40 mg/kg/day) and one integrase inhibitor (dolutegravir [DTG] at 2.5 mg/kg/day), co-formulated into a single dose administered once daily by subcutaneous injection for 15 months (as indicated by gray shading in Fig 3.1A). ART was effective at suppressing SIV RNA in plasma below the limit of detection (LOD) of the assay (60 copies/ml) (Fig 3.1B and 3.1C). As also seen in HIV-1-infected children (258-260), time to suppression was variable, ranging from 4 to 52 weeks (median = 15 w) with some infants showing transient blips of viremia (Fig S3.2). Two RMs (one each allocated to the vaccine (RBe19) and control (RGc19) groups) sustained significantly higher plasma viral loads on ART

than the remainder of the animals (area under the curve [AUC] $1.19x10^5 \pm 5.6x10^4$ vs. $7.58x10 \pm 2.8x10^5$; P = 0.0333; Fig 3.1B and 3.1C insert); however, both animals did achieve levels of plasma SIV RNA below the LOD after 52 weeks of daily ART. In these two RMs, the experimental design was slightly modified to allow at least 3 months of viral load suppression prior to analytical treatment interruption (ATI).

Experimental groups and immunization strategy

Prior to the vaccination phase of the experiment, two groups of eight RMs were balanced for sex, age at infection, peak viral load, $CD4^+$ T cell frequency at ART initiation, and AUC of pre-ART viremia (Table 3.1). One group of eight RMs served as ART-only controls. The remaining eight RMs (referred to as TV+TLR7 group) received two immunizations of Ad48 vectors expressing $3x10^{10}$ viral particles of SIV_{smE543} *gag-pol-env* through the intramuscular (i.m.) route at 22 and 30 weeks post infection (green arrows in Fig 3.1A). Ad48, like the Ad26-vector used in a prior adult macaque study with a similar immunization strategy (169), is a species D adenovirus associated with gastrointestinal infection and previous studies indicate that both Ad26- and Ad48-vectors induce potent polyfunctional IFN-γ^+, TNF-α^+, and IL-2^+ T cell responses along with a strong antiviral, pro-inflammatory cytokine and chemokine response (261-263). Infants were further boosted by two immunizations of MVA vectors expressing 10^8 plaque forming units of SIV_{smE543} *gag-pol-env* i.m. at 38 and 50 weeks post infection (blue arrows in Fig 3.1A). Ten doses of the TLR-7 agonist GS-986 were given by orogastric (o.g.) administration at 0.3 mg/kg biweekly at 40, 42, 44, 46, 48, 52, 54, 56, 58, and 60 weeks post infection (orange arrows in Fig 3.1A). Before administering GS-986 to TV+TLR7 infants, a small dose escalation study was

performed in two RMs to monitor for tolerability, safety, and anticipated immune stimulation (Fig S3.3), with favorable results found at the 0.3 mg/kg dose. In this dose escalation study and in the 8 TV+TLR7 RMs, we did not observe virus reactivation (measured as on-ART viremia that differed from controls) with GS-986 administration. Overall, ART, Ad48- and MVA-vectors, and GS-986 were well-tolerated, without clinical adverse events throughout the study (Fig S3.4).

Cellular immune response to therapeutic vaccination

To evaluate the immunogenicity of the Ad48/MVA vaccine approach we performed IFN-γ ELISPOT assays at week 22 prior to vaccination, week 34 after priming with Ad48, week 52 after boosting with MVA, and 2 weeks prior to ATI. Representative data showing the increase in Gag-, Pol-, and Env-specific spot forming cells over this time course are shown in Fig 3.2A. Vaccinated RMs demonstrated a robust increase in the magnitude of Gag-, Pol-, and Env-specific cellular immune responses against SIV_{mac239} peptides after Ad48 prime that were boosted following MVA ($P = 0.0003$, Fig 3.2B, n=8). In ART-only controls, the SIV-specific immune response remained low throughout ART treatment (Fig 3.2B, n=4) with a decline in spot forming cells observed during ART (Fig S3.5). Variability in the magnitude of responses in the TV+TLR7 group was observed (Fig 3.2C) and, interestingly, 3 RMs (RCc19, RMm19, RAq19) had evidence of increasing SIV-specific immunity from 2 to 10 weeks after the final MVA dose during the period of GS-986 administration.

When cell availability permitted, SIV-specific T cell responses were further interrogated through intracellular cytokine staining (ICS) following stimulation with SIV Gag peptide pools at the timepoints described above. Boolean gating was used to examine Gag-specific T cells for polyfunctional responses associated with enhanced HIV-1 control (82, 264). The frequency of memory $CD8^+$ T cells (gated as $CD95^+$) with 2 or more functions significantly increased after MVA boost (week 52, P = 0.004) and remained significant prior to ATI (week 62, P = 0.0004) compared to the pre-vaccination timepoint (Fig 3.3A). The largest increase was observed in cells double positive for IFN-γ and TNF-α (P = 0.007). In memory $CD4^+$ T cells the most dramatic increase in Gag-specific cells was observed after MVA boost (P = 0.005) with a significant increase observed in TNF-α and IL-2 double positive memory $CD4^+$ T cells (P = 0.03). The frequency of Gag-specific cytokine positive memory $CD4^+$ T cells remained significant prior to ATI (P = 0.04) with the IFN-γ and TNF-α double positive memory $CD4^+$ T cells subset significantly elevated when compared to week 22 (P = 0.005) (Fig 3.3B). A representative flow plot of memory $CD8^+$ T cells expressing IFN-γ, TNF-α, and IL-2 at each described timepoint is shown in Fig 3.3C.

Breadth of SIV-specific immune responses

To estimate cellular breadth, 10-mer peptides were divided into subpools of 20 peptides spanning the entire Gag (7 subpools), Pol (13 subpools), or Env (11 subpools) proteins from SIV_{mac239}. Vaccinated RMs demonstrated a significantly higher magnitude of cellular responses to Gag, Pol, and Env viral subpools when compared to ART-only controls (P = 0.046, 0.046, and 0.02, respectively; Fig 3.4A). Responses varied by RM and subpool (Fig S3.6A). Although not

significant, the total number of positive subpools was higher in TV+TLR7 RMs than ART-only controls (median = 9.5 and 4.5, respectively) (Fig 3.4B). This finding held true for subpools for each viral protein (Fig S3.6B). These analyses were performed using a subset of control RMs with sufficient cells and, surprisingly, one control RM (RJc19) had the highest observed breadth overall. If RJc19 is excluded from comparison in Fig 4B, the results do reach significance (P = 0.04) with a greater number of positive subpools in the TV+TLR7 group.

Humoral immune response to therapeutic vaccination

To further explore the immunological impact of TV+TLR7 we performed ELISAs at week 4 after infection and prior to ART initiation, week 22 prior to vaccination, week 34 after priming with Ad48, week 52 after boosting with MVA, and 2 weeks prior to ATI. The presence of SIV-specific gp120 antibodies was assessed against the vaccine strain virus, SIV_{smE543}, and challenge strain virus, SIV_{mac251} (Fig 3.5A and B, respectively). Vaccinated RMs demonstrated a significant increase in binding antibodies against SIV_{smE543} gp120 following Ad26-prime ($P < 0.001$ compared to week 4 in the TV+TLR7 group and $P = 0.001$ compared to controls at week 34). The gp120 reactivity peaked at week 52 following the MVA boost ($P = 0.001$ compared to week 4 in the TV+TLR7 group and $P < 0.001$ compared to controls at week 52) and remained significantly higher in TV+TLR7 RMs versus controls at week 62 (2 weeks prior to ATI; $P = 0.004$; Fig 3.5A). Antibodies directed against SIV_{mac251} gp120 also peaked at week 52 in TV+TLR7 RMs ($P = 0.02$ compared to controls at the same timepoint), but declined to a level similar to control RMs by week 62 (Fig 3.5B). Two RMs (RBe19 in the TV+TLR7 group and RGc19 in the control group) were excluded from these analyses since they remained viremic on ART for a prolonged period

(Fig 1C insert) and antibody responses could not be reliably attributed to antigen exposure through vaccination.

To evaluate the heterogeneity of the antibody response, we additionally performed a Binding Antibody Multiplex Assay (BAMA) at the above described timepoints against SIV_{mac239} gp120, p27, and Nef. We did not find an increase in SIV_{mac239}-specific antibodies in TV+TLR7 RMs following immunization compared to week 4, although at week 52 after MVA boost gp120-specific antibodies were significantly higher ($P = 0.02$) and p27-specific antibodies trended higher ($P = 0.07$) compared to controls (Fig 3.5C). Binding antibodies against the Nef protein, which was not included in the vaccine insert, were elevated in some RMs from both groups prior to ART initiation but then remained low throughout the subsequent timepoints.

Cellular kinetics following GS-986

To investigate the immunological response to repeated oral GS-986 administration, blood was collected pre-, 24 hours post-, and 2 weeks post-GS-986 doses 1, 5, and 10. These timepoints were selected to allow longitudinal evaluation while remaining within limited blood availability constraints due to the size of the infants. Whole blood flow cytometry was performed to evaluate peripheral immune cell activation and kinetics. The frequency of CD38 expression on $CD4^+$ and $CD8^+$ T cells was high at baseline with a mean of 93% for each in TV+TLR7 RMs, then transiently increased to a mean of 96% and 97% at the 24-hour post-dose timepoint in TV+TLR7 macaques ($P = 0.0003$ and $P < 0.0001$, respectively, Fig 3.6A and Fig S3.7A). CD38 expression on both $CD4^+$ and $CD8^+$ T cells was significantly higher in TV+TLR7 than control RMs at the 24-hour

timepoint (P = 0.0001 and P = 0.0004, respectively) and no significant increase from baseline was observed in control RMs. CD38 expression on both $CD4^+$ and $CD8^+$ T cells returned to baseline levels by 2 weeks post GS-986 in the TV+TLR7 group. Similarly, CD69 expression significantly increased from a mean of 0.17% to a mean of 0.44% in $CD4^+$ T cells and from a mean of 0.65% to 1.2% in $CD8^+$ T cells (P < 0.0001 and P = 0.0002, respectively, Fig 3.6B and Fig S3.7B). For both $CD4^+$ and $CD8^+$ T cells, CD69 expression was significantly higher in TV+TLR7 RMs than control RMs measured at the 24-hour timepoint (P < 0.0001 and P = 0.007, respectively). Overall, responses were similar after doses 1, 5, or 10.

CD169, or Siglec-1, is upregulated on monocytes and macrophages following stimulation of TLR-7 or exposure to type 1 interferons produced by plasmacytoid dendritic cells (248). $CD169^+$ monocytes then travel to the tissue, differentiate, and act to promote adaptive immune responses to pathogens through antigen presentation and secretion of cytokines. For this reason, we sought to evaluate the expression of CD169 on monocytes in the periphery to further validate the immune stimulatory effect of oral GS-986 in RM infants. For this analysis, monocytes were divided into classical ($CD14^+CD16^-$), intermediate ($CD16^+CD14^+$), and non-classical ($CD16^+CD14^-$) subsets. The frequency of CD169 expression on classical, intermediate, and non-classical monocyte subsets was low at baseline with a mean of 11.4, 22.4, and 8.7%, respectively, then transiently increased to a mean of 68, 89, and 54% (P < 0.0001 for each comparison) at the 24-hour post GS-986 timepoint in TV+TLR7 macaques (Fig 3.6C and S3.7C). In control RMs, CD169 expression remained mostly stable over the same time period, although some non-statistically significant fluctuations were observed. As with T cell activation, monocyte stimulation was similar after doses 1, 5, or 10 in the TV+TLR7 group.

TV+TLR7 impact on persistent SIV

To evaluate the impact of the therapeutic vaccine regimen on SIV persistence on ART, the level of total cell-associated SIV DNA was measured longitudinally in $CD4^+$ T cells isolated from whole blood, lymph nodes, and colorectal mucosa. In TV+TLR7 RMs, we observed a significant reduction of 0.8 log in SIV DNA in peripheral $CD4^+$ T cells from week 12 prior to vaccine regimen and week 62 after completion of the vaccine regimen ($P = 0.02$, Fig 3.7A). A trend towards reduced levels of SIV DNA in $CD4^+$ T cells isolated from lymph nodes was also observed over the same time course ($P = 0.08$, Fig 3.7B). We note, however, that neither the frequency of $CD4^+$ T cells with SIV DNA prior to ATI or log change over the observed time course significantly differed in TV+TLR7 infants compared to ART-only controls. Levels of SIV DNA in rectal $CD4^+$ T cells in TV+TLR7 and control RMs remained stable from week 12 to week 62 (Fig 3.7C). Despite these similar findings between groups, we demonstrate that the log reduction in $CD4^+$ T cell-associated SIV DNA in the periphery was significantly positively correlated with the magnitude of the SIV-specific T cell response in TV+TLR7 infants prior to ATI at week 62 ($r = 0.76$, $P = 0.04$, Fig 3.7D). The significance of this correlation was lost when values for ART-only control RMs were added to the analysis ($r = 0.37$, $P = 0.24$) or when compared in ART-only controls alone ($r = -0.2$, $P = 0.92$).

Viral rebound dynamics

To evaluate the impact of TV+TLR7 on the replication competent viral reservoir that contributes to viral rebound upon discontinuation of ART, RMs underwent ATI following 60-67 weeks of daily ART. Plasma viral loads were monitored at days 6, 9, 13, 21, and 28 after ART interruption to determine time to viral rebound and RMs were followed for 16 weeks off ART to trend viral set points. The time to viral rebound was defined as the first of two consecutive timepoints with viremia greater than 500 copies/mL. All RMs rebounded by 28 days post-ATI with no significant difference in time to rebound between TV+TLR7 and control groups (median = 9 days for both groups; P = 0.6) (Fig 3.8A). Similarly, no differences were detected in post-rebound AUC or set point viremia (defined as the mean of the final three plasma viral loads prior to experimental end point) in animals that received the vaccine regimen compared to ART-only controls (median = 4.37 and 3.66 log SIV RNA copies/ml of plasma, respectively, P = 0.38) (Figs 3.8B and C, Fig 3.S8).

Strong and weak responders within the TV+TLR7 group

As mentioned, there was variability in the immune response induced by TV+TLR7 in RM infants. We explored potential correlates of this variability by dividing the TV+TLR7 infants into "strong" (RPd19, RCc19, RUl19, & RMm19) and "weak" (RNd19, RBe19, RPq19, RAq19) cellular responders based on the magnitude of their anti-SIV T cell responses at week 62 prior to ATI, with significantly more IFN-γ-producing T cells in the four best responders compared to the four poorest responders (mean= 5033 vs. 1917 SFC per 10^6 PBMC, P = 0.03, Fig 3.9A). In the subset of 5 TV+TLR7 RMs for which ICS data is available, $CD8^+$ and $CD4^+$ T cells triple positive for IFN-γ, IL-2, and TNF-α were only observed in the strong responders as defined above

following the final MVA boost. Moreover, memory $CD4^+$ T cells with 2 or 3 functions were significantly increased in strong vs. weak responders (P = 0.03, Fig 3.9B).

We then sought to explore immunological or virologic factors that could explain these differential vaccine responses. A distinct immunological activation signature was present in memory $CD8^+$ T cells between strong and weak vaccine responders (Fig 3.9C). Longitudinal HLA-DR expression, measured as AUC, on effector memory $CD8^+$ T cells was significantly higher in strong vaccine responders compared to weak responders (P = 0.03). A correlation was observed between HLA-DR expression on effector memory $CD8^+$ T cells during ART and the magnitude of the anti-SIV T cell response at week 62 (r = 0.71, P = 0.06), (Fig 3.9D). Although not significant, area under-the-curve of longitudinal PD-1 expression in the strong vaccine responders in both effector and central memory $CD8^+$ T cells also tended to be higher than weak vaccine responders (P = 0.09 and 0.07, respectively). Furthermore, PD-1 expression was positively associated with SIV-specific T cell responses at week 62 (Figs 3.9E and F). Despite these described differences, there were no significant differences between strong and weak responders in the levels of $CD4^+$ T cell-associated SIV DNA prior to ATI or in the log reduction in cell-associated SIV DNA after vaccination (S9 Fig). Additionally, time to viral rebound, post-rebound viremia AUC, and viral set point were similar between the strong and weak responder groups (Figs 3.9 G – I). Finally, across all animals in both the TV+TLR7 and ART-only control groups no associations between any of the measured immunological parameters and viral rebound kinetics were identified.

Discussion

This study provides the first insight into the use of a viral vectored therapeutic vaccine approach as a potential cure intervention in a pediatric model of oral HIV-1 infection and long-term ART suppression. We demonstrate safety and immunogenicity of an Ad48 prime, MVA boost immunization in combination with repeated oral TLR-7 stimulant GS-986 in SIV-infected, ART-treated infant RMs.

HIV/SIV-specific $CD8^+$ T cell responses are low during ART (265) and prior to the results presented here, it was unclear how much they could be boosted through therapeutic vaccination of infants. As ART was started 4 weeks after SIV infection in this study, a de novo $CD8^+$ T cell response to the infecting viral strain was likely elicited with sufficient time for viral escape mutations to develop, which could potentially impair the vaccine response. Based on the strong cellular immune response evident in vaccinated animals following completion of the Ad48/MVA regimen that was significantly increased above their pre-vaccine levels and in comparison to unvaccinated controls, we conclude that this vaccine regimen was immunogenic. The vaccine strain SIV_{smE543} shares sequence identity to SIV_{mac239} of 91, 93, and 85%, for Gag, Pol, or Env, respectively, so it is possible we did not fully capture the extent of vaccine elicited responses, especially to Env, with the SIVmac239 peptide pools. However, SIV_{mac239} shares sequence identity of 97% to the infecting virus (SIV_{mac251}) which we anticipated would be the most relevant to target.

In addition to enhanced cellular immunity, we have demonstrated that therapeutic vaccination with TLR-7 stimulation also enhances the humoral immune response. Binding

antibodies against gp120 from SIV_{smE543}, SIV_{mac251}, and SIV_{mac239} peaked at week 52 following the MVA boost. Antibodies directed against SIV_{mac239} p27 were also significantly higher than those measured in control RMs at the week 52 timepoint. A decline in gp120 reactivity in TV+TLR7 RMs was observed following the end of the vaccine regimen and prior to ATI such that immunized animals did not differ from controls in response to gp120 from the challenge (and therefore rebounding) strain, although immunized animals did retain a higher response to the vaccine strain gp120. Incorporating a protein boost to this vaccination approach may maintain humoral immune responses for a longer period and therefore have a greater impact on viral rebound kinetics. A more in-depth investigation of the impact of therapeutic vaccination on the humoral immune response, including functional assays, will likely provide additional insight into the role of vaccine induced antibodies to control viral rebound after ART interruption.

Repeated oral TLR-7 stimulation by GS-986 resulted in transient immune activation, as previously demonstrated in studies with adult RMs (169, 245). CD38 and CD69 expression was significantly elevated at 24 hours post-doses 1, 5, and 10 when compared to baseline in $CD4^+$ and $CD8^+$ T cells. Monocyte activation was also evident at this timepoint, with CD169 expression significantly increased on classical, intermediate, and non-classical monocytes. This study is the first reported use of an oral TLR-7 agonist in infants and provides critical safety and immunogenicity data for future pediatric trials. In our hands, GS-986 was not an effective latency reversal agent. We did observe several blips of viremia in treated RMs, but similar viral blips were also seen in the control group around the same timepoints indicating that this transient viremia was likely unrelated to GS-986 treatment (Fig 3.1B, C). Our findings conflict with Lim *et al.* (245), but are consistent with reports by Del Prete *et al,* and Borducchi *et al,* and Bekerman *et al.* (169, 246,

266). Based on the safe induction of innate immune activation we observed in infants, TLR-7 agonists remain promising for use as vaccine adjuvants or perhaps could be explored in combination with other agents to stimulate virus reactivation from latency.

The impact of therapeutic vaccination on the viral reservoir prior to ATI was estimated through quantification of total SIV DNA in peripheral and lymph node $CD4^+$ T cells. No significant difference was found in the frequency of SIV^+ $CD4^+$ T cells prior to ATI or the reduction of SIV^+ $CD4^+$ T cells during ART regimen between vaccinated and ART-only control RMs. However, an association was observed between the magnitude of the vaccine response prior to ATI and the reduction in the frequency of SIV^+ $CD4^+$ T cells in TV+TLR7 infants that was not present in control RMs. These results imply that in the immunized infants, the observed decline in infected cells may be attributed, in part, to the vaccine-induced immune response. We acknowledge measurement of total SIV DNA represents an overestimate of the viral reservoir that includes cells containing defective virus (267). While quantitative virus outgrowth assays could not be performed here due to limited blood volumes, the newly described Intact Proviral DNA Assay (IPDA) (268) could prove useful for pediatric studies. Interestingly, though, work from the Siliciano and Keele groups suggests that in nonhuman primates total cell-associated SIV DNA may more closely approximate the intact reservoir than in humans (268, 269). A recent study by Garcia-Broncano *et al.* detailed novel molecular single-genome sequencing techniques allowing an in-depth analysis of the viral reservoir composition in HIV-1-infected infants using small blood volumes (270). It is possible that, by using such techniques, we may have uncovered specific viral reservoir parameters impacted by TV+TLR7 and these methodologies should be incorporated into future studies. Nevertheless, ART interruption is still considered to be the most robust readout

(and highest bar) to measure the outcome of a cure-directed intervention. Following analytical treatment interruption in this study, all infants rebounded with detectable viremia within 6 to 28 days and achieved viral set point with no detectable difference between experimental groups. These data suggest that although the infants demonstrate the capability to mount an immune response following vaccination that is detectable at ART interruption, this response was not sufficient to reduce viral reservoirs or set-point viremia following rebound.

Notably, although all vaccinated infants demonstrated an increase in the antiviral cellular immune response, the magnitude and breadth of the individual responses were variable between infants. When vaccinated infants were subdivided into strong and weak responders based on their SIV-specific T cell responses at the time of ATI measured by ELISPOT, cells triple positive for IFN-γ, TNF-α, and IL-2 quantified through ICS following MVA boost was only observed in strong responders. Through the comparison of strong and weak vaccine responders we have also identified a distinct immunological activation signature associated with the magnitude of vaccine response in our infants. Infants with a strong vaccine response show significantly higher HLA-DR expression on effector memory $CD8^+$ T cells and a trend towards higher PD-1 expression in both central and effector memory $CD8^+$ T cell subsets. Despite these described differences and consistent with the rest of our reported results, no difference in time to rebound or viral set point was observed between strong and weak vaccine responders. Although it is difficult to draw meaningful conclusions given the limited sample size, these results suggest that infants with a more activated memory $CD8^+$ T cell repertoire may be more responsive to therapeutic vaccination strategies.

The results presented in this study are distinct from previously published data in adult RMs in which a similar vaccine regimen resulted in delayed viral rebound and reduced viral set point following ATI (169). We note that the magnitude of IFN-γ response in infants after the final immunization was just over 50% of that observed in adults RMs in this prior work and the breadth of responses was also more restricted in infants compared to adults (169), perhaps accounting for some of the differences we observed in viral dynamics after ATI. Other experimental factors such as route of infection (oral vs. intrarectal), timing of ART initiation (4 weeks vs. 1 week post infection), and the use of different Ad vectors (Ad48 vs. Ad26) may also have influenced the different outcomes in infant vs. adult RMs. We hypothesize that the exponential increase in the size of the viral reservoir when ART is initiated at 4 weeks compared to 1 week after infection may have had the most significant impact on our results, although experimental evidence will be needed for confirmation. Additionally, distinct features of pediatric immunity during development or variance in composition of the viral reservoir between these age groups may be key (149, 190, 271-275). Our findings highlight the importance of a pediatric model to evaluate HIV-1 cure interventions in this unique setting of immune development.

As this study was the first of its kind performed in infant RMs, there were several limitations. The small size of infant RMs and collection limitations restricted blood volumes and biopsy frequencies thereby reducing our capacity to perform extensive evaluative assays. Additionally, we are limited by small sample size when drawing comparisons between strong and weak vaccine responders within the TV+TLR7 RMs. However, we believe that studies such as the one presented here are critically important given the scarcity of HIV-1 cure and remission clinical

trials in infants and children. Additionally, these findings provide key preclinical safety data on cure interventions in a pediatric HIV-1 animal model.

In conclusion, we have demonstrated that an Ad-prime, MVA-boost therapeutic immunization and repeated oral TLR-7 stimulation is safe and immunogenic in SIV-infected, ART-treated infant RMs. This finding represents a promising step forward in testing cure-directed interventions for pediatric HIV-1 using a model of breastmilk acquisition in which very early ART is not likely to be possible. Although we did not observe an effect on reservoir size or rebound dynamics, the immune response generated here may serve to eliminate infected cells if elicited contemporaneously with virus reactivation induced by an effective latency reversal agent. Future studies exploring therapeutic vaccination combined with latency reversal to clear virally infected cells may reveal the full potential of this cure approach.

Materials and Methods

Ethics Statement

This study was conducted in strict accordance with USDA regulations and the recommendations in the Guide for the Care and Use of Laboratory Animals of the National Institutes of Health, and were approved by the Emory University Institutional Animal Care and Use Committee (Protocol # YER-3000510-ELMNTS-A).

Animals and SIV infection

Sixteen infant Indian RMs (*Macaca mulatta*), with exclusion of Mamu B*08 and B*17 positive animals, were enrolled in this study. The animals were born at the Yerkes National Primate Research Center (YNPRC) to dams housed in indoor/outdoor group housing. The infants were removed from the dams when they were approximately 2 weeks old and transferred to a nursery, where they were housed in social pairs with either full contact or protected contact for the duration of the study. The infants were fed in accordance with the YNPRC standard operating procedures (SOPs) for NHP feeding and had continual access to water. After being removed from the dam, infants were fed center approved milk replacer (Similac Advance, OptiGro Infant Formula with Iron and/or Similac Soy Isomil OptiGro Infant Formula with Iron; Abbott Nutrition, Columbus, OH) until 14 weeks of age. Infants were provided softened standard primate jumbo chow biscuits (Jumbo Monkey Diet 5037; Purina Mills, St. Louis, MO) and a portion of orange starting between 2 – 4 weeks of age. As animals aged additional enrichment of various fresh produce items were

provided daily. Cages also contained additional sources of animal enrichment including objects such as perching and other manipulanda. Animal welfare was monitored daily. Appropriate procedures were performed to ensure that potential distress, pain, or discomfort was alleviated. The sedatives Ketamine (10 mg/kg) or Telazol (4 mg/kg) were used for blood draws and biopsies. Euthanasia of RMs, using Pentobarbital (100 mg/kg) under anesthesia, was performed only when deemed clinically necessary by veterinary medical staff and according to IACUC endpoint guidelines. The animals were orally infected at 4 to 5 weeks of age with two consecutive doses of 10^5 $TCID_{50}$ of SIV_{mac251}. Four infants required multiple weekly 2-dose challenges prior to successful infection (range two to five challenges). Two of these RMs (one each allocated to the vaccine [RCc19] and control [RGc19] groups) were orally challenged with two consecutive doses of 10^5 $TCID_{50}$ SIV_{mac239} after three and four unsuccessful challenges with SIV_{mac251}, respectively.

Antiretroviral therapy

The sixteen RM infants were treated with a three-drug ART regimen initiated at 4 weeks post infection. The preformulation ART cocktail contained two reverse transcriptase inhibitors, 5.1 mg/kg Tenofovir Disoproxil Fumarate (TDF) and 40 mg/kg Emtricitabine (FTC), plus 2.5 mg/kg of the integrase inhibitor Dolutegravir (DTG). This ART cocktail was administered once daily at 1 mg/kg via the subcutaneous route.

Vaccine regimen

Monkeys assigned to the TV+TLR7 group were primed by the intramuscular route with 3 x 10^{10} viral particles of Ad48 vectors (261) expressing SIV_{smE543} *gag-pol-env* at weeks 22 and 30 post infection and were boosted with 10^8 plaque-forming units of MVA vectors (276) expressing SIV_{smE543} *gag-pol-env* at weeks 38 and 50 post infection. TV+TLR7 animals also received 10 administrations of 0.3 mg/kg GS-986 (Gilead Sciences) by oral gavage every two weeks from week 40 – 48 and 52 – 60 post infection.

Sample collection and processing

EDTA-anticoagulated blood samples were collected regularly and used for a complete blood count, routine chemical analysis and immunostaining, with plasma separated by centrifugation within 1 h of phlebotomy. PBMCs were prepared by density gradient centrifugation. Lymph node and rectal biopsy tissue samples were collected at indicated timepoints (Fig 1). Lymph nodes were ground using a 70-μm cell strainer. Rectal biopsy mucosal mononuclear cells were isolated by digestion with collagenase and DNase I for 2 h at 37 °C and then passed through a 70-μm cell strainer. The cell suspensions obtained were washed and immediately used for immunostaining or cryopreserved at -80 °C until use.

Immunophenotype by flow cytometry

Multicolor flow cytometric analysis was performed on whole blood or cell suspensions using predetermined optimal concentrations of the following fluorescently conjugated monoclonal antibodies (MAbs). For whole blood (WB) T cell analysis the following MAbs were used: CD3-

allophycocyanin (APC)-Cy7 (clone SP34-2), CD95-phycoerythrin (PE)-Cy5 (clone DX2), Ki67-AF700 (clone B56), HLA-DR-peridinin chlorophyll protein (PerCP)-Cy5.5 (clone G46-6), CCR7-fluorescein isothiocyanate (FITC) (clone 150503), CCR5-APC (clone 3A9), and CD45-RA-PE-Cy7 (clone L45) from BD Biosciences; CD8-BV711 (clone RPA-T8), CD4-BV650 (clone OKT4), and PD-1-BV421 (clone EH12.2H7) from BioLegend; and CD28-ECD (clone CD28-2) from Beckman-Coulter. For WB activation analysis the following MAbs were used: CD3-allophycocyanin (APC)-Cy7 (clone SP34-2) and CD69-phycoerythrin (PE)-CF594 (clone FN50) from BD Biosciences; CD8-BV711 (clone RPA-T8), CD4-BV650 (clone OKT4), CD16-BV421 (clone 3G8), CD14-phycoerythrin (PE)-Cy7 (clone M5E2), and CD169-phycoerythrin (PE) (clone 7-239) from BioLegend; and CD38-allophycocyanin (APC) (clone OK10) from the NHP Reagent Resource. Flow cytometric acquisition and analysis of samples were performed on at least 100,000 events on an LSR II flow cytometer driven by the FACSDiva software package (BD Biosciences) or an AURORA flow cytometer driven by the SpectroFlo software package (Cytek). Analyses of the acquired data were performed using FlowJo version 10.0.4 software (TreeStar). For analysis, T cells were gated as live $CD3^+$ cells and monocytes were gated as live $CD3^-CD4^{int}$ cells positive for either CD14 or CD16.

IFN-γ ELISPOT

SIV-specific cellular immune responses were assessed by IFN-γ ELISPOT assays. Cryopreserved cells from selected timepoints pre- and post-immunization were thawed and rested overnight prior to assay. Test and control wells were performed with 200,000 cells per well in duplicate. Briefly,

a 96-well MultiScreen-IP Filter Plate (Millipore) was activated with 70% EtOH for 1 min and washed twice with PBS. Plate was then incubated overnight at 4º with 5 μg/mL anti-human IFN-γ (MabTech). 200,000 PBMC were used per well and incubated with SIV_{mac239} peptide pools (NHP AIDS Reagent Program) at 10 μg/ml for 28 h at 37º in 5% CO_2. SIV_{mac239} peptide pools were selected due to shared sequence identity of 97% with the challenge virus (SIV_{mac251}) (277). Due to limited cell availability, ELISPOTs were not performed using vaccine strain (SIV_{smE543}) peptides; Gag, Pol, and Env from SIV_{smE543} share sequence identity with SIV_{mac239} of 91, 93, and 85%, respectively (278, 279). As a positive control 5 μg/ml of concanavalin A (Millipore) was added to the cells, and a negative control of no peptide was also included on each plate. To estimate cellular breadth, cryopreserved cells from weeks 67 and 72 (weeks 3 and 8 post ATI) were utilized. This analysis was not possible after vaccination but before ATI due to limited cell availability. We note that the AUC of viremia during this time period was not different between TV+TLR7 and control groups (P = 0.46), permitting some inferences about the vaccine strategy to be considered. 10-mer peptides were divided into subpools of 20 peptides per subpool spanning the entire Gag, Pol, or Env SIV_{mac239} viral protein. All tests were performed in duplicate. Plates were scanned using an automated ELISPOT counter (CTL, Cellular Technologies), and verified through manual counting. Background (the mean of wells without peptide stimulation) levels were subtracted from each well on the plate. A response was considered positive if the mean number of spot-forming cells (SFC) from duplicate sample wells exceeded background plus 2 standard deviations. Assay results are shown as SFC per 1 x 10^6 cells. Responses of <50 SFC per 1 x 10^6 cells were not considered positive.

Intracellular cytokine staining (ICS)

ICS was performed using fresh or cryopreserved PBMCs. Cryopreserved PBMCs were rested over night after thaw prior to assay. Briefly, 1-2 x 10^6 cells were incubated in the presence of Brefeldin A (Sigma Aldrich), BD Golgi Stop (BD BioSciences), and SIV_{mac239} Gag peptide pool (NHP AIDS Reagent Program) for 6 hours at 37º. PMA/Ionomycin (Sigma Aldrich) was used as a positive control and no peptide stimulation was used as the negative control. After incubation, the cells were washed twice with PBS and stained for 20 minutes at 37º with LIVE/DEAD then for 30 minutes at RT with predetermined optimal concentrations of the following fluorescently conjugated MAbs: CD3-APC-Cy7 (clone SP34-2), CD4-BV421 (clone OKT4), CD8-PE-CF594 (clone RPA-T8), and CD95-PE-Cy5 (Clone DX2). After the incubation, cells were fixed and permeabilized and then incubated with the following MAbs: IL-17A-AF488 (clone eBio64DEC17), IFN-γ-PE (clone B27), TNFα-AF700 (clone Mab11), IL-2-BV605 (clone MQ1-17H12), IL-22-APC (clone IL22JOP). Flow cytometric acquisition and analysis of samples were performed on at least 100,000 events on an LSR II flow cytometer driven by the FACSDiva software package (BD Biosciences). Analyses of the acquired data were performed using FlowJo version 10.0.4 software (TreeStar) and simplified presentation of incredibly complex evaluations (SPICE, v.6.0) software.

ELISA and Binding Antibody Multiplex Assay (BAMA)

Enzyme-linked immunosorbent assays were conducted to assess IgG binding to SIV antigens. High-binding 384-well plates (Corning Life Sciences) were coated overnight at 4°C at 2 ug/ml with gp120 from SIV_{mac251} (Creative Biolabs), SIV_{smE543}, or gp140 from SIV_{smE543} (Immune Technology Corps, New York, NY). Plates were blocked with assay diluent (PBS containing 4% whey protein, 15% goat serum, 0.5% Tween 20) for 1 h at 20°C. Plasma dilutions were added to the plate and incubated for 1 h at 20°C. IgG was detected by a horse radish peroxidase (HRP)-conjugated mouse anti-monkey IgG polyclonal antibody (Southern Biotech). ELISA plates were developed with SureBlue Reserve TMB substrate and stop solution (KPL). Plates were read immediately after addition of stop solution at 450 nm, 0.1 s/well on a SpectraMax Plus 384 microplate reader (Molecular Devices). Area under the curve was calculated using the GraphPad Prism Software. An anti-SIV_{mac251} polyclonal IgG made from pooled sera from six SIV_{mac251} challenged RMs (AIDS Reagent Program) was used as positive control. Binding Antibody Multiplex Assays (BAMAs) were performed as previously described (280). Briefly, SIV antigens were first coupled to carboxylated fluorescent beads (Bio-Rad Laboratories, Inc.). The antigen panel included SIV_{mac239} gp120, Nef (Immune Technology Corps), and p27 (AIDS Reagent Program). The coupled beads were incubated with diluted plasma (1:50 or 1:2500) for 30 min at 20°C and then IgG binding was detected with streptavidin-conjugated mouse anti-monkey IgG at 0.5 μg/ml. Beads were washed and read on a Bio-Plex 200 instrument (Bio-Rad Laboratories, Inc.). IgG levels were expressed as mean fluorescent intensity (MFI) and all mean fluorescent intensity (MFI) values were blank bead and well subtracted. Consistency between assays was ensured by tracking the maximum MFI and AUC of the positive control (anti-SIV_{mac251} polyclonal IgG) by Levy-Jennings charts.

Plasma RNA and cell-associated DNA viral quantification

Plasma viral quantification was performed as described previously (181). Frozen cell pellet was lysed with proteinase K (100 μg/ml in 10 mM Tris-HCl pH 8) for 1 h at 56ºC. Quantification of SIV_{mac} *gag* DNA was performed by quantitative PCR using the 5' nuclease (TaqMan) assay with an ABI7500 system (PerkinElmer Life Sciences). The sequence of the forward primer for SIV_{mac} *gag* was 5′-GCAGAGGAGGAAATTACCCAGTAC-3′, the reverse primer sequence was 5′-CAATTTTACCCAGGCATTTAATGTT-3′, and the probe sequence was 5′-6-carboxyfluorescein (FAM)-TGTCCACCTGCCATTAAGCCCGA-6-carboxytetramethylrhodamine (TAMRA)-3′. 7.5 μL of cell lysate were mixed in a 50 μL reaction containing 1x Platinum Buffer, 3.5 mM $MgCl_2$, 0.2 mM dNTP, primers 200 nM, probe 150 nM, and 2 U Platinum Taq. For cell number quantification, quantitative PCR was performed simultaneously for monkey albumin gene copy number. The sequence of the forward primer for albumin was 5'-TGCATGAGAAAACGCCAGTAA-3'; the reverse primer sequence was 5'-ATGGTCGCCTGTTCACCAA-3' and the probe sequence was 5'-AGAAAGTCACCAAATGCTGCACGGAATC-3' (249). The reactions were performed on a 7500 real-time PCR system (Applied Biosystems) with the following thermal program: 5 min at 95ºC, followed by 40 cycles of denaturation at 95ºC for 15 s and annealing at 60ºC for 1 min.

Statistical analyses

Statistical analyses were performed using GraphPad Prism Software (v.7 or v.8). $P \leq 0.05$ was considered statistically significant. To test the statistical significance observed in magnitude of T

cell response in Fig 2B and humoral response Fig 5 within groups, the non-parametric Friedman test with Dunn's correction for multiple comparisons was used. To compare memory $CD4^+$ and $CD8^+$ polyfunctionality in Fig 3 and SIV DNA levels in Fig 7A and 7B a two-sided Wilcoxon rank-sum test was used. To compare the magnitude of T cell responses to viral subpools in Fig 4A and to compare the frequency of CD38 and CD69 expression on $CD4^+$ and $CD8^+$ T cells and CD169 expression on monocyte subsets in Fig 6 and S7 a Wilcoxon matched-pairs signed rank test was performed. A two-sided Spearman Rank correlation test was used to determine statistical significance of associations in Fig 7C and 9D-F. In Fig 8A survival curves were compared through a Log-rank (Mantel-Cox) test. To compare differences between groups in pre-ART VL and $CD4^+$ T cell frequency in Fig S2B, S2C, positive subpools in Fig 4B, and S6B, humoral response between groups in Fig 5, VL set point in Fig 8C, magnitude of the anti-SIV ELISPOT response in Fig 9A, AUC between groups in Fig 9C, and rebound kinetics in Fig 9I a two-sided Mann-Whitney was used.

Acknowledgments

We thank Gilead for provision of the antiretroviral drugs and Francois Villinger for providing SIV_{mac251}. The authors also thank Joseph Hesselgesser for his expertise and feedback. The content is solely the responsibility of the authors and does not necessarily represent the official views of the National Institutes of Health. We would also like to thank the Emory CFAR Virology Core, CFAR Immunology core, and Research Services at the Yerkes NPRC for coordinating and performing the NHP studies.

Chapter 3 Figures

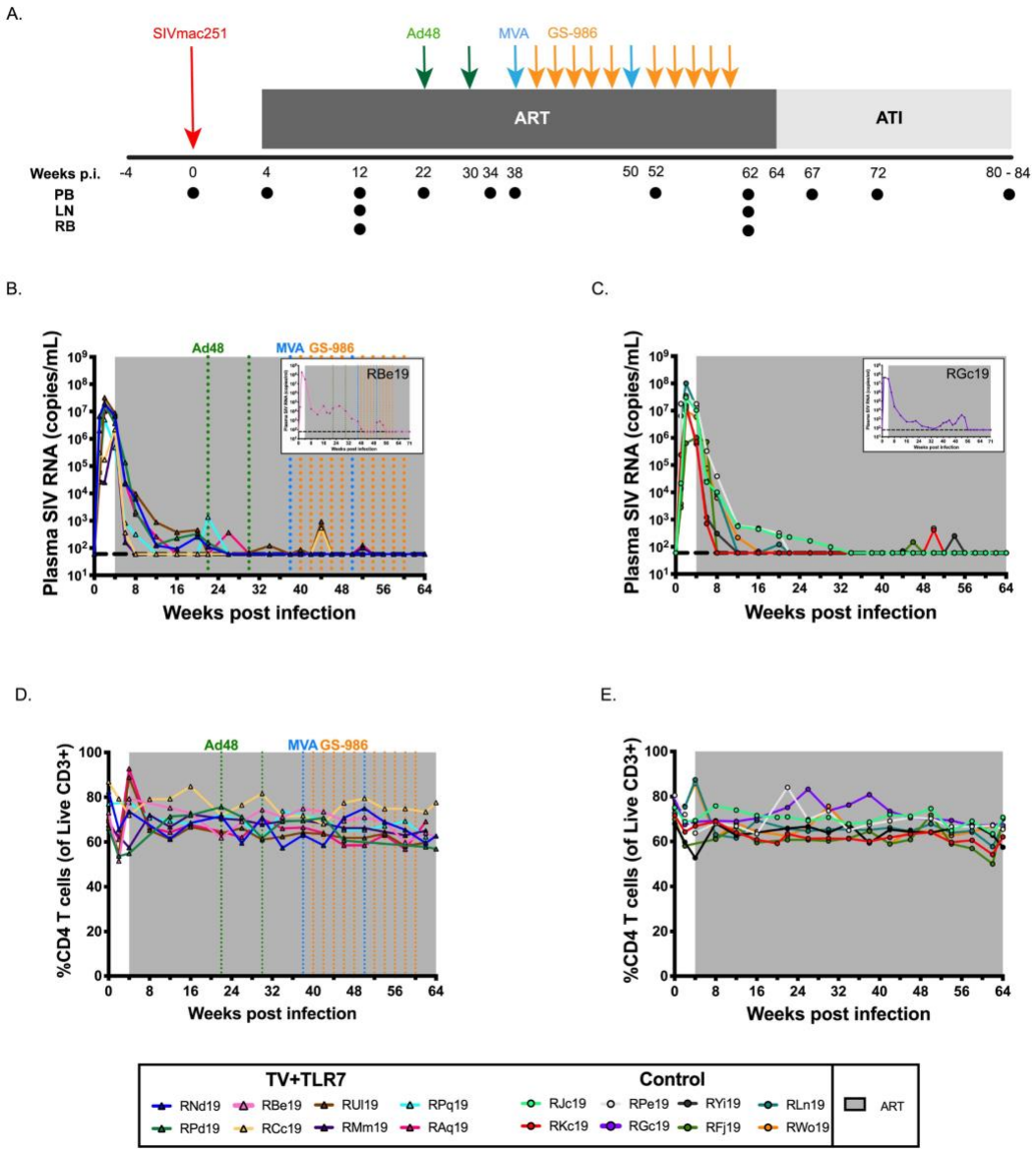

Fig 3.1. Experimental design and response to ART in SIV-infected infant RMs. (A) Schematic of the study design. Sixteen infant RMs were infected orally with 10^5 $TCID_{50}$ SIV_{mac251} (day 0), and starting on 4 weeks post infection (p.i.) treated with combination ART (TDF, FTC, DTG) for

15 months. Eight animals received 2 doses of Ad48-SIV$_{smE543}$ *gag-pol-env* ($3x10^{10}$ viral particles, i.m.), 2 doses of MVA-SIV$_{smE543}$ *gag-pol-env* ($1x10^{8}$ PFU, i.m.), and 10 doses of GS-986 (0.3 mg/kg, o.g.), at the timepoints indicated (TV+TLR7). The remaining 8 animals served as ART-treated controls. At 64-71 weeks p.i. RMs underwent analytical treatment interruption (ATI) and all the animals were monitored for 4 to 6 months. PB, RB, and LN biopsies were collected at the indicated timepoints. Longitudinal analysis of plasma SIV RNA levels in (B) TV+TLR7 and (C) control RMs. The shaded area represents the period of ART treatment. The dashed line represents the limit of detection of the assay. Longitudinal analysis of peripheral $CD4^{+}$ T cell frequency in (D) TV+TLR7 and (E) control RMs. The shaded area represents the period of ART treatment.

Table 3.1. Experimental division of SIV-infected, ART-treated infant macaques.

Group	ID	Sex	A01 Status	Age at infection, weeks	Virus	CD4 Freq, baseline	CD4 Freq, ART initiation	Peak PVL, pre-ART	AUC PVL, pre-ART
ART-only controls	RJc19	M	+	4.4	SIV_{mac251}	73.5%	68.5%	3.05E+07	5.61E+07
	RKc19	F	+	4.1	SIV_{mac251}	70.6%	67.1%	1.27E+07	2.00E+07
	RPe19	M	-	4.3	SIV_{mac251}	73.0%	65.1%	3.51E+07	8.81E+07
	RGc19	M	-	9.6	SIV_{mac239}	76.3%	68.3%	4.32E+07	1.39E+08
	RYi19	F	-	3.9	SIV_{mac251}	50.6%	53.8%	1.56E+07	2.40E+07
	RFj19	F	-	5.4	SIV_{mac251}	69.6%	n/a	1.03E+06	1.99E+06
	RLn19	M	-	4.4	SIV_{mac251}	72.7%	62.7%	1.01E+08	1.71E+08
	RWo19	F	-	3.7	SIV_{mac251}	74.5%	62.4%	9.84E+06	2.07E+07
TV+TLR7[a]	RNd19	M	-	5.4	SIV_{mac251}	65.2%	56.8%	1.98E+07	4.32E+07
	RPd19	F	-	5.3	SIV_{mac251}	81.9%	74.1%	1.78E+07	3.24E+07
	RBe19	F	-	5	SIV_{mac251}	80.1%	80.2%	1.98E+08	3.30E+08
	RCc19	M	+	10	SIV_{mac239}	85.7%	70.4%	2.16E+06	2.73E+06
	RUl19	M	-	4.9	SIV_{mac251}	67.5%	62.7%	3.20E+07	5.68E+07
	RMm19	M	-	5.9	SIV_{mac251}	70.5%	62.9%	1.85E+06	1.92E+06
	RPq19	F	+	3.3	SIV_{mac251}	76.9%	73.7%	5.01E+06	8.07E+06
	RAq19	M	+	4.9	SIV_{mac251}	69.7%	64.1%	1.03E+07	2.31E+07

[a]TV+TLR7, therapeutic vaccination with Ad48/MVA+GS-986.

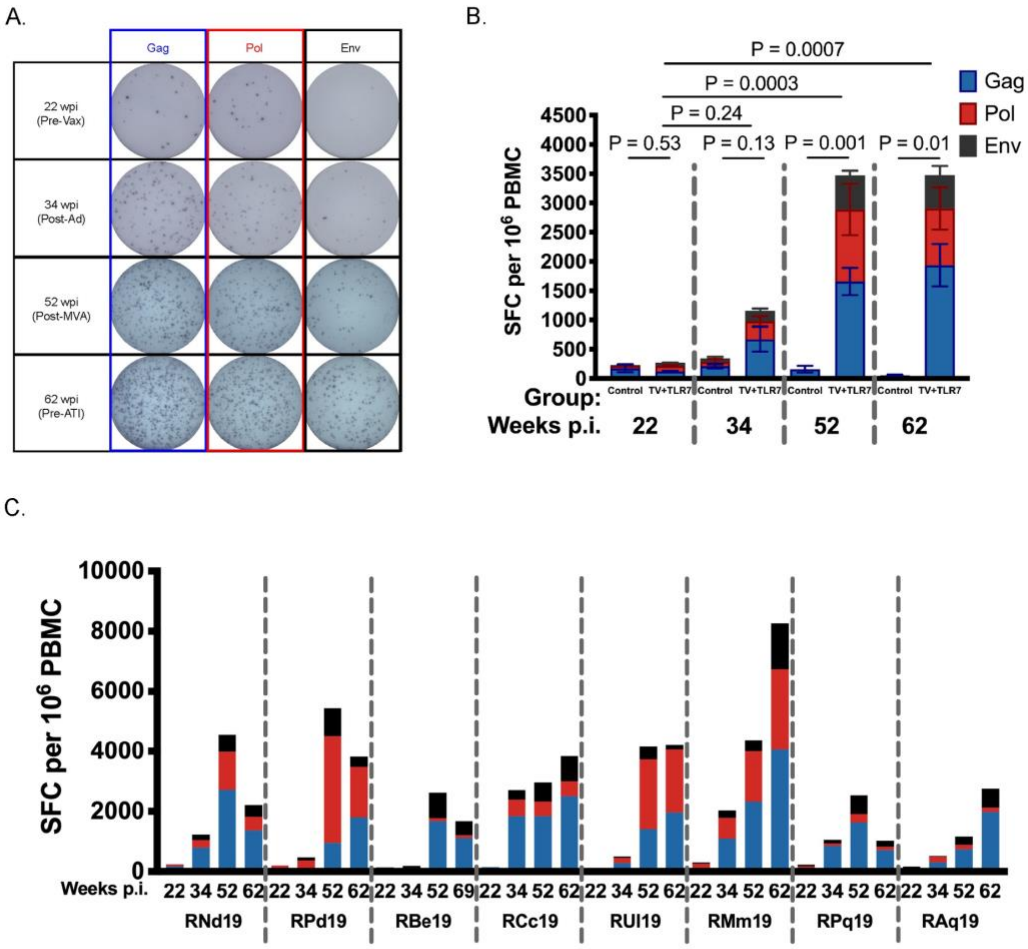

Fig 3.2. Cellular response measured by ELISPOT to therapeutic vaccination in SIV-infected, ART-treated infant RMs. (A) Representative images of spot forming cells (SFC) in response to Gag, Pol, and Env at timepoints indicated above. Wpi, weeks post infection. (B) IFN-γ ELISPOT responses to Gag, Pol, and Env peptide pools from SIV_{mac239} were measured at week 22 prior to vaccination, week 34 after priming with two doses of Ad48, week 52 after boosting with two doses of MVA, and week 62 prior to analytical treatment interruption in control RMs (n = 4) and

TV+TLR7 (n = 8) RMs. Bars represent mean ± SEM. Statistical analysis was performed to compare with week 22 using the non-parametric Friedman test with Dunn's multiple comparison test to correct for multiple comparisons. (C) Individual IFN-γ ELISPOT responses of TV+TLR7 RMs.

	IFN-γ+, TNF-α+, IL-2+	IFN-γ+, TNF-α-, IL-2+	IFN-γ+, TNF-α+, IL-2-	IFN-γ+, TNF-α-, IL-2-	IFN-γ-, TNF-α+, IL-2+	IFN-γ-, TNF-α-, IL-2+	IFN-γ-, TNF-α+, IL-2-
34 wpi	0.36	0.65	0.06	0.58	n.a.	0.27	0.36
52 wpi	0.54	n.a.	0.01	0.01	n.a.	0.81	0.14
62 wpi	0.22	n.a.	0.007	0.14	n.a.	0.14	0.94

	IFN-γ+, TNF-α+, IL-2+	IFN-γ+, TNF-α-, IL-2+	IFN-γ+, TNF-α+, IL-2-	IFN-γ+, TNF-α-, IL-2-	IFN-γ-, TNF-α+, IL-2+	IFN-γ-, TNF-α-, IL-2+	IFN-γ-, TNF-α+, IL-2-
34 wpi	0.17	0.07	0.08	0.41	0.04	0.86	0.36
52 wpi	0.22	n.a.	0.11	0.05	0.03	0.01	0.01
62 wpi	0.42	0.68	0.005	0.74	0.06	0.22	0.81

Fig 3.3. Immunological response measured by ICS to therapeutic vaccination in SIV-infected, ART-treated infant RMs. Pie charts depicting the ability of (A) memory CD8$^+$ and (B) memory CD4$^+$ T cells isolated from TV+TLR7 RMs to produce IFN-γ, IL-2 and/or TNF-α in

response to stimulation with SIV_{mac239} Gag peptide pool at 22 (n=5), 34 (n = 6), 52 (n = 4), and 62 (n = 7) weeks post infection (wpi). Total cytokine positive cells were compared to week 22 through permutation test. Cytokine positive subsets were compared to week 22 using a Wilcoxon Rank Sum Test, table representing P values is shown. (C) Representative flow plot of IFN-γ, TNF-α, and IL-2 expression in $CD95^{+}CD8^{+}$ T cells.

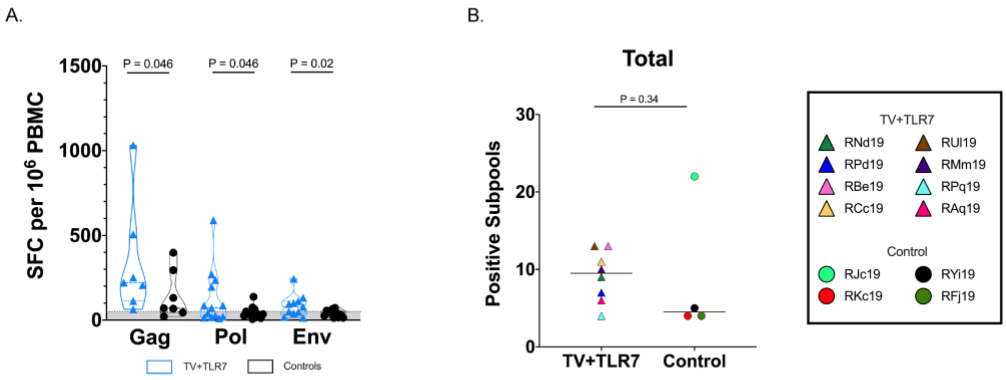

Fig 3.4. Cellular breadth of immunological response following analytical treatment interruption (ATI) measured by ELISPOT to therapeutic vaccination in SIV-infected, ART-treated infant RMs. (A) IFN-γ ELISPOT responses to 10-mer peptide subpools spanning the Gag, Pol, and Env proteins from SIV_{mac239} following ATI in TV+TLR7 RMs and control RMs. Bars represent median ± quartiles and the gray shading bordered by the horizontal dashed line represents the limit of detection. Statistical analysis was performed using Wilcoxon matched-pairs signed rank tests. SFC, spot forming cells. (B) Cellular immune breadth in TV+TLR7 RMs and control RMs as measured by total positive subpools of 10 peptides spanning the SIV_{mac239} Gag, Pol, and Env proteins following ATI. Black bar represents median. Groups were compared using a two-sided Mann-Whitney test ($P < 0.05$ was considered significant).

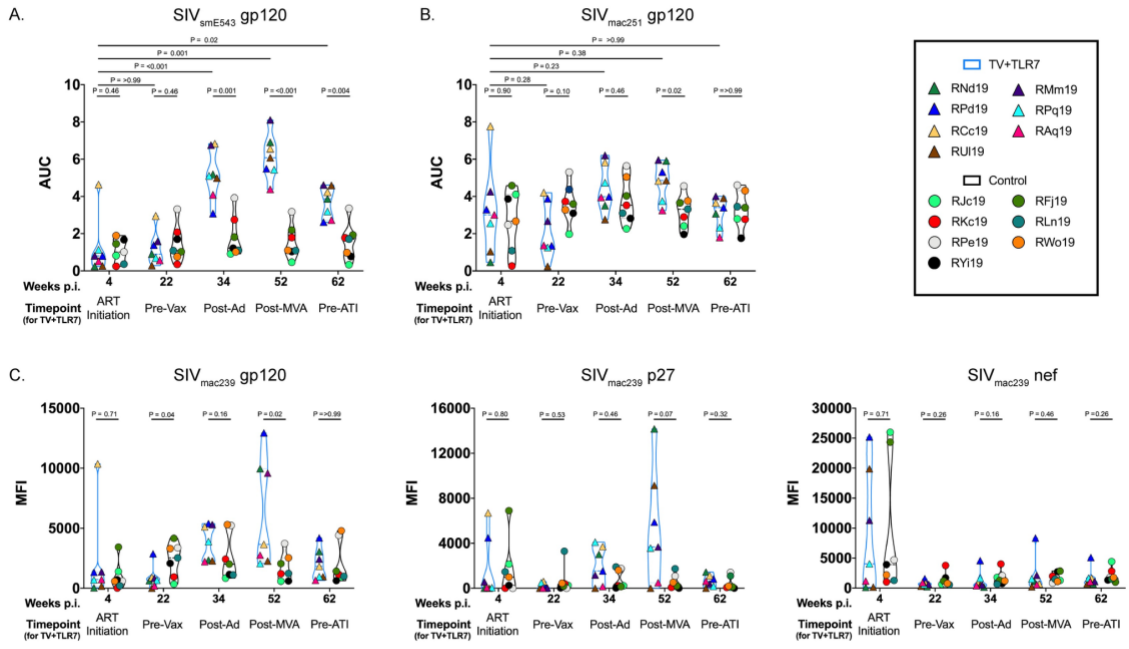

Fig 3.5. Humoral response measured by ELISA and BAMA to therapeutic vaccination in SIV-infected, ART-treated infant RMs. SIV-specific antibodies directed against gp120 from (A) vaccine strain, SIV_{smE543}, and (B) challenge strain, SIV_{mac251}, were quantified by binding ELISA area under the curve (AUC) at week 4 prior to ART initiation, week 22 prior to vaccination, week 34 after priming with two doses of Ad48, week 52 after boosting with two doses of MVA, and week 62 prior to analytical treatment interruption (ATI) in TV+TLR7 RMs and equivalent time points for controls. (C) SIV-specific antibodies directed against SIV_{mac239} gp120, p27, and Nef were measured by Binding Antibody Multiplex Assay (BAMA) at same time points described above. Experimental groups were compared using a two-sided Mann-Whitney test and timepoints within groups were compared using the non-parametric Friedman test with Dunn's multiple comparison test to correct for multiple comparisons ($P < 0.05$ was considered significant).

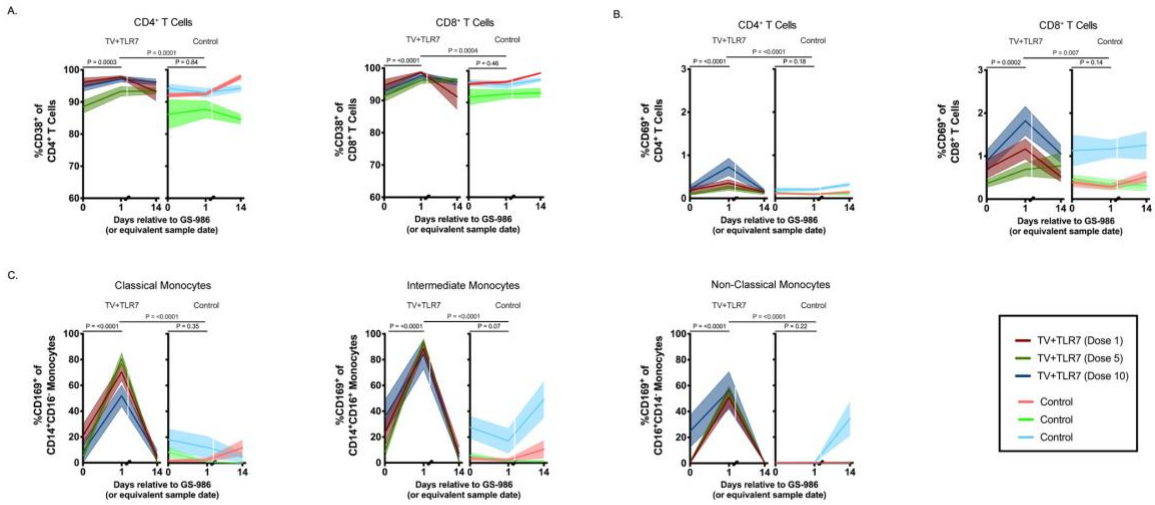

Fig 3.6. Immunological response to repeated oral GS-986 administration in SIV-infected, ART-treated infant RMs. Frequency of (A) $CD38^+$ and (B) $CD69^+$ peripheral $CD4^+$ and $CD8^+$ T cells immediately prior to, 1 day post, and 14 days post oral GS-986 dose 1, 5, and 10 in TV+TLR7 or equivalent sample day in control RMs. (C) Frequency of $CD169^+$ classical, intermediate, and nonclassical monocytes in TV+TLR7 and control RMs. Dose number is indicated by color. Bars represent mean ± SEM. Statistical analysis was performed using a Wilcoxon matched-pairs signed rank test.

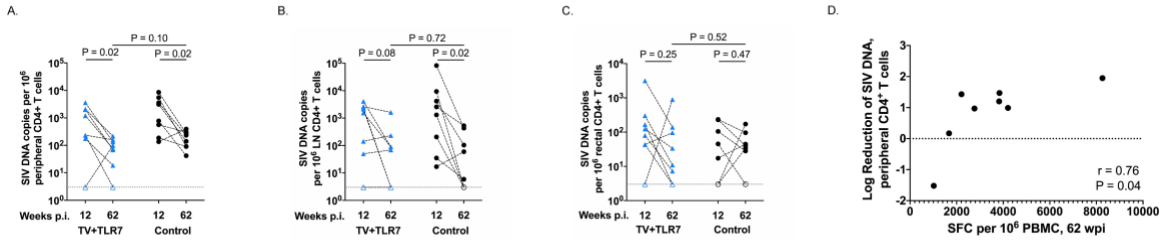

Fig 3.7. Impact of therapeutic vaccination and oral TLR-7 stimulation on SIV DNA persistence in CD4$^+$ T cells of SIV-infected, ART-treated infant RMs. Comparison of frequency of estimated SIV DNA levels in (A) peripheral, (B) LN, and (C) rectal CD4$^+$ T cells before (12 weeks post infection, wpi) and after (62 wpi) therapeutic vaccine regimen in TV+TLR7 and control RMs as determined by PCR. Dashed line represents the limit of detection and open symbols represent values below the limit of detection. Statistical analysis was performed using a two-sided Wilcoxon rank-sum tests ($P < 0.05$ was considered significant). (D) Association between log reduction of SIV DNA in peripheral CD4$^+$ and LN CD4$^+$ T cells from pre-vaccination to post-vaccination and magnitude of SIV-specific T cells at week 62 prior to ART interruption measured by IFN-γ ELISPOT in TV+TLR7 RMs. Two-sided Spearman rank correlation test was used to determine statistical significance. *R* value indicates correlation coefficient.

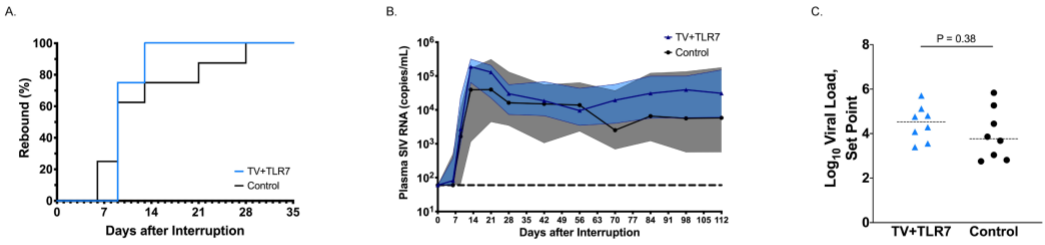

Fig 3.8. Influence of TV+TLR7 on time to rebound and post-rebound viremia following analytical treatment interruption (ATI) in SIV-infected, ART-treated infant RMs. (A) Comparison of time to viral rebound in TV+TLR7 and control RMs depicted by Kaplan-Meier curves. Survival curves for groups were compared through Log-rank (Mantel-Cox) test. (B) Median longitudinal plasma SIV RNA levels in TV+TLR7 and control RMs following ATI. The solid line represents the median, the shaded area represents interquartile range, and the horizontal dashed line represents the limit of detection of the assay. (C) Set point viremia following 16 weeks of ATI of TV+TLR7 and control RMs determined by the mean of the final three viral load measurements. Dashed bars represent median. Groups were compared using a two-sided Mann-Whitney test ($P < 0.05$ was considered significant).

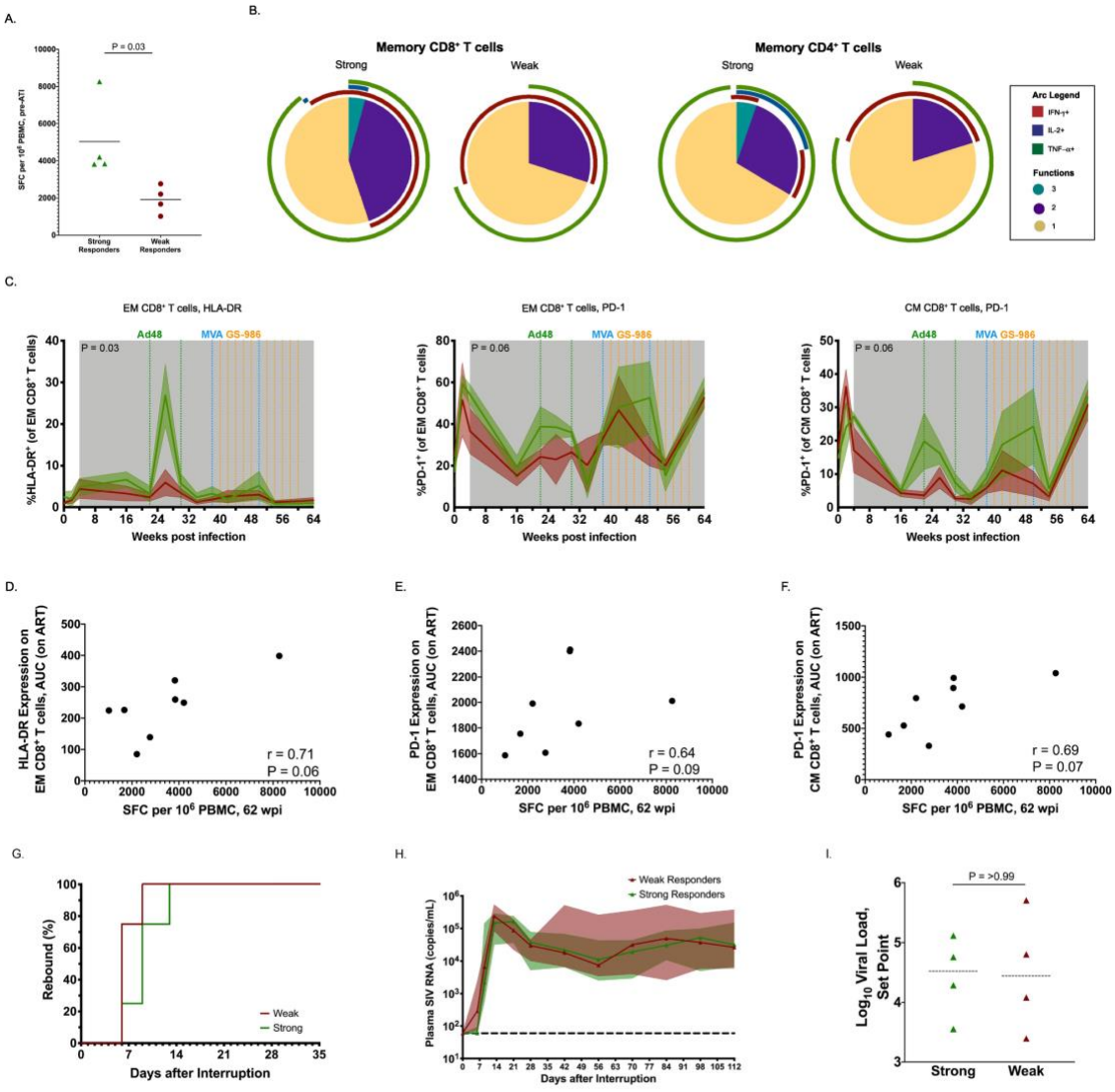

Fig 3.9. Comparison of strong and weak cellular vaccine response within TV+TLR7 infant RMs. (A) Magnitude of anti-SIV cellular immunity measured by IFN-γ ELISPOT prior to ATI at 62 weeks post infection of strong and weak responders. Dashed bars represent median. Groups were compared using a two-sided Mann-Whitney test ($P < 0.05$ was considered significant). (B) Pie charts depicting the ability of memory $CD8^+$ and $CD4^+$ T cells isolated from strong and weak TV+TLR7 responders to produce IFN-γ, IL-2 and/or TNF-α in response to stimulation with

SIVmac239 Gag peptide pool at 52 weeks post infection (n = 4). (C) Longitudinal analysis of HLA-DR and PD-1 expression on effector memory (EM) and central memory (CM) $CD8^+$ T cells in strong and weak responders within TV+TLR7 RMs (n = 8). The shaded area represents the period of ART treatment. AUC on ART was compared between groups using a two-sided Mann-Whitney test. ($P < 0.05$ was considered significant) Association between (D) HLA-DR expression on EM, (E) PD-1 expression on CM, and (F) PD-1 expression on EM $CD8^+$ T cells during ART represented by AUC and magnitude of SIV-specific T cells following end of vaccine regimen prior to ATI measured by ELISPOT in TV+TLR7 RMs. Two-sided Spearman rank correlation test was used to determine statistical significance. *R* value indicates correlation coefficient. (G) Comparison of time to viral rebound in strong and weak TV+TLR7 responder RMs depicted by Kaplan-Meier curves. (H) Median longitudinal plasma SIV RNA levels between strong and weak responders following ATI. The solid line represents the median, the shaded area represents interquartile range, and the horizontal dashed line represents the limit of detection of the assay. (I) Set point viremia following 16 weeks of ATI of strong and weak TV+TLR7 responders determined by the mean of the final three viral load measurements. Dashed bars represent median. Groups were compared using a two-sided Mann-Whitney test ($P < 0.05$ was considered significant).

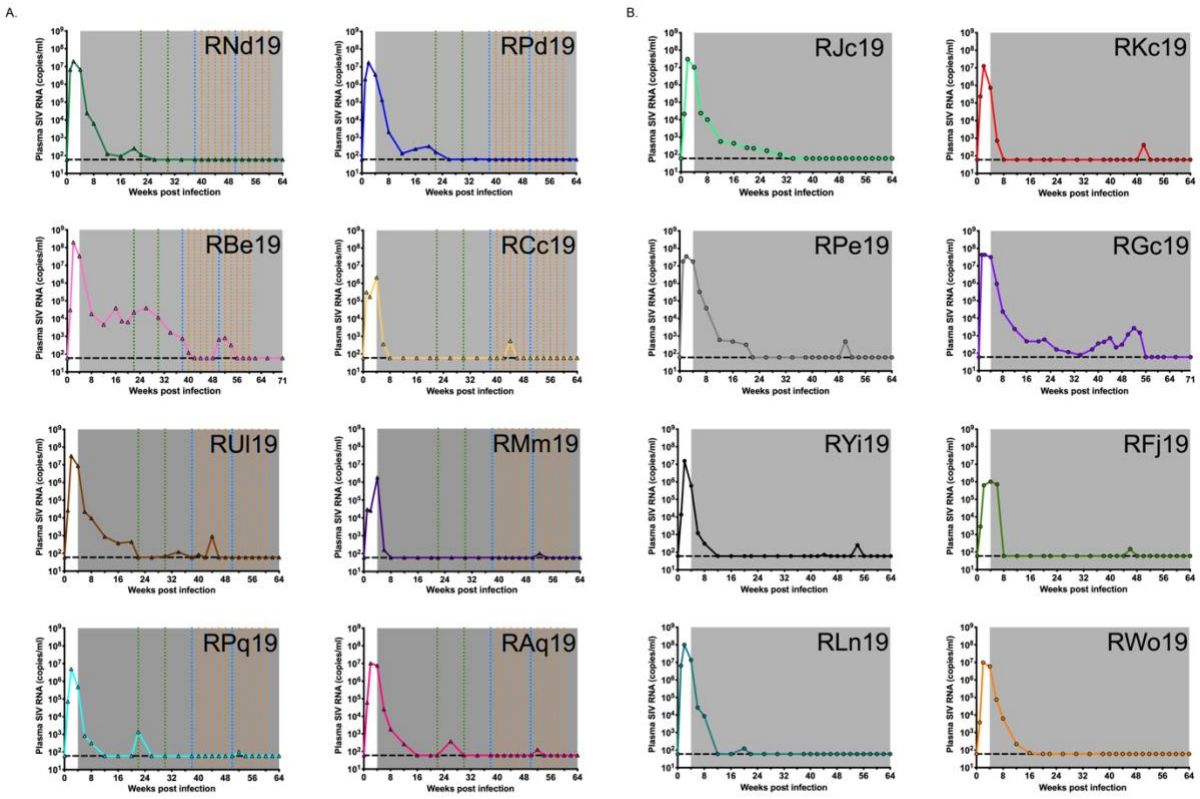

Supplemental Figure 3.1. On ART plasma viral loads of TV+TLR7 and control RMs. Longitudinal analysis of plasma SIV RNA levels in (A) TV+TLR7 and (B) control RMs. The shaded area represents the period of ART treatment. The colored dashed lines represent therapeutic intervention in TV+TLR7 RMs, Ad48 is in green, MVA is in blue, and GS-986 in orange. The horizontal dashed line represents the limit of detection of the assay.

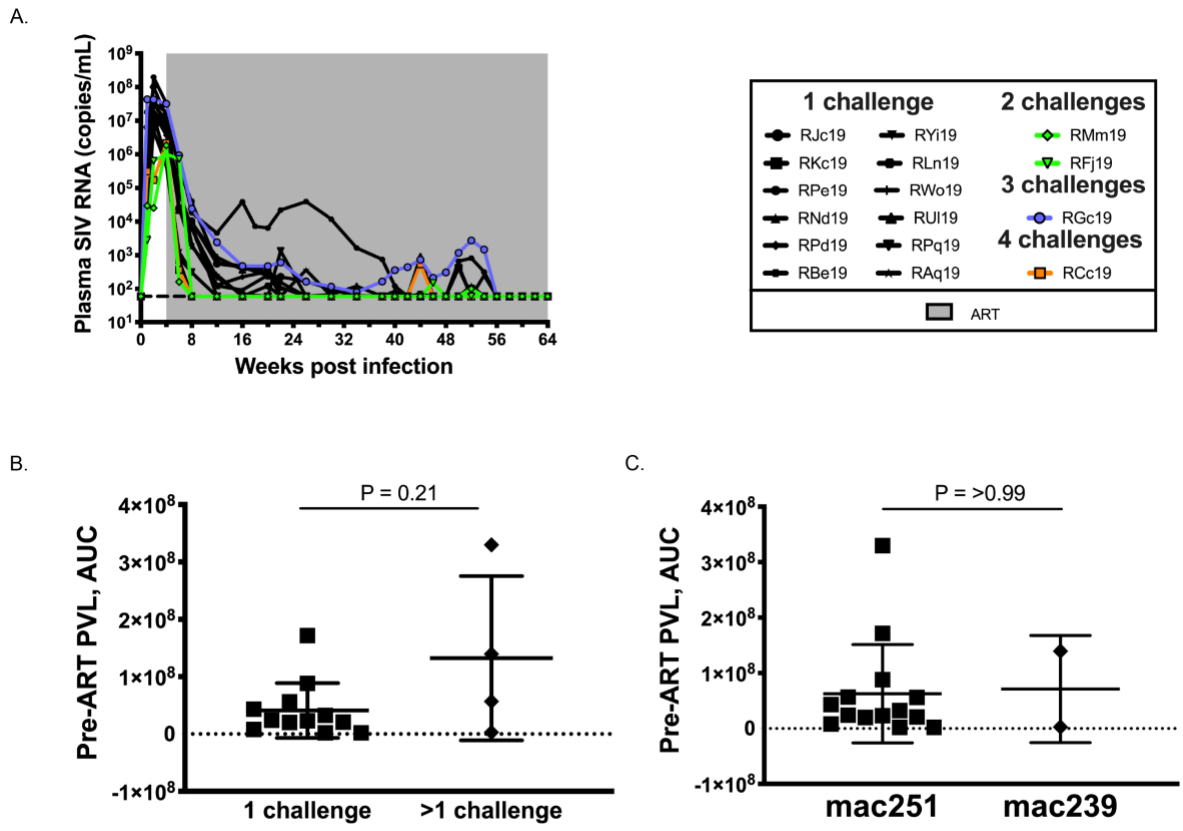

Supplemental Figure 3.2. Comparison of challenge variables on acute viral kinetics. (A) Longitudinal analysis of plasma SIV RNA levels by required number of challenges prior to successful infection. The shaded area represents the period of ART treatment. RMs that required one challenge, two challenges, three challenges, and four challenges are represented by black, green, purple, and orange lines, respectively. Pre-ART viral kinetics were not influenced by (B) required number of challenges or (C) challenge virus. Groups were compared using a two-sided Mann-Whitney test ($P < 0.05$ was considered significant). Bars represent mean ± SD.

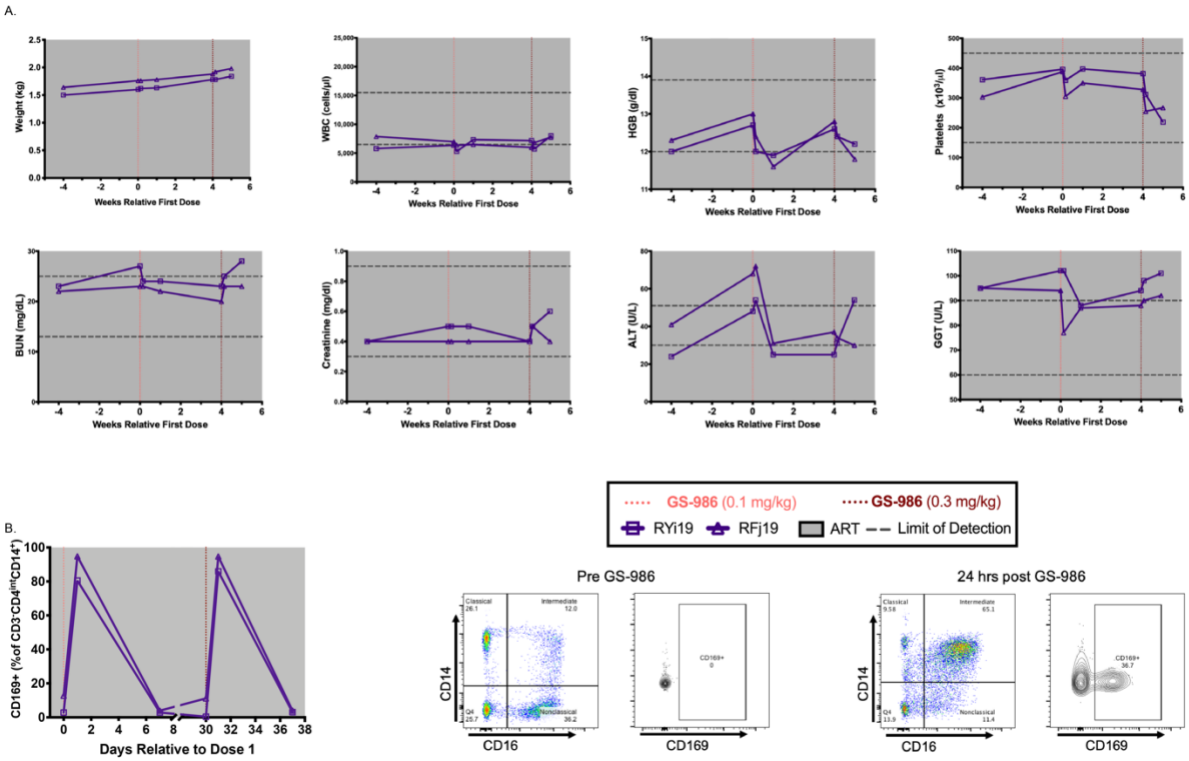

Supplemental Figure 3.3. Oral GS-986 is tolerable, safe, and induces anticipated immune stimulation at 0.1 and 0.3 mg/kg in SIV-infected, ART-treated infant RMs. (A) Longitudinal assessment of body weight, complete blood counts, and serum chemistries. The shaded areas represent the period of ART treatment. The dotted lines represent the normal range for each parameter. WBC, white blood cells; HGB, hemoglobin; BUN, blood urea nitrogen; ALT, alanine aminotransferase; GGT, gamma-glutamyltransferase. (B) Frequency of $CD169^{+}CD14^{+}$ monocytes before, 1 day after, and 7 days after oral GS-986. Representative staining for CD169 expression within $CD14^{+}$ monocytes is shown on the right.

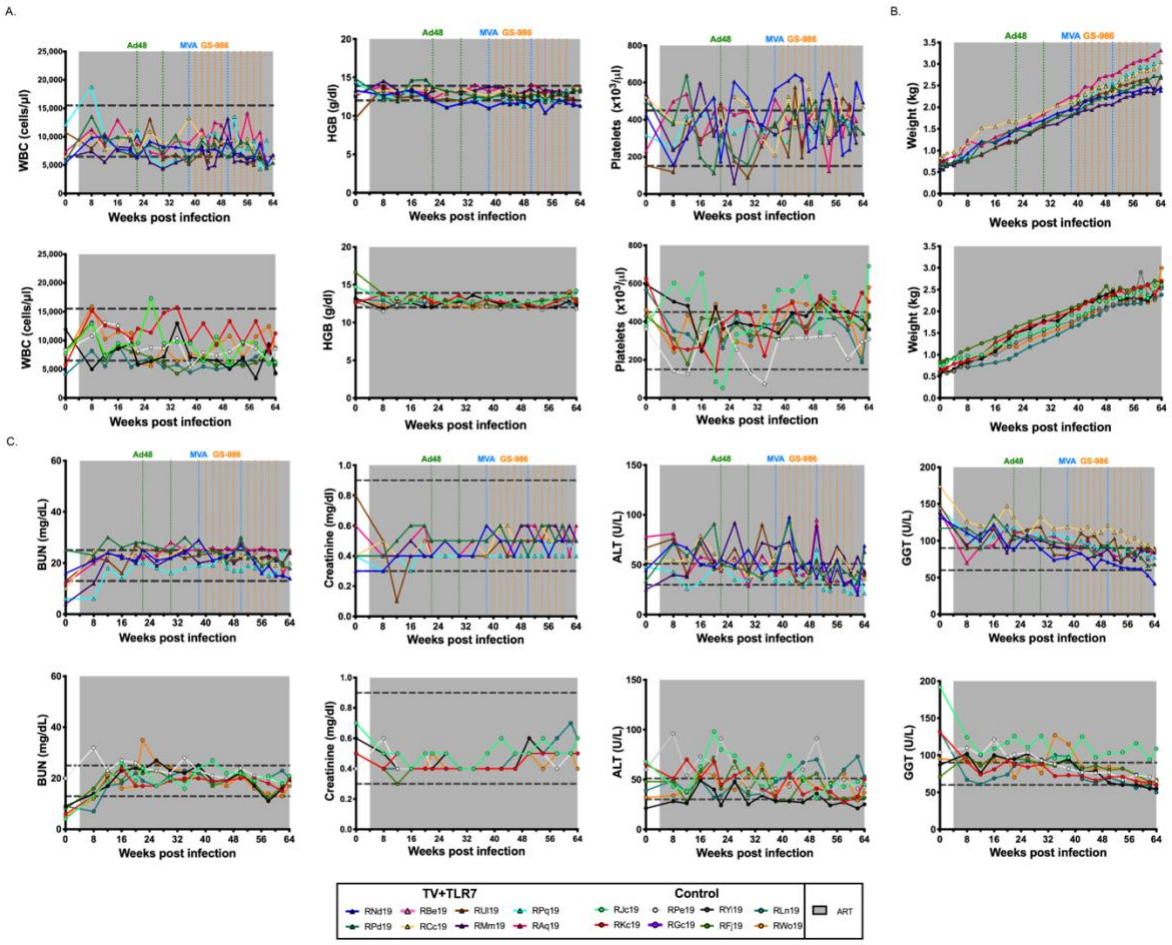

Supplemental Figure 3.4. Safety data in ART-treated SIV-infected RM infants. (A) Longitudinal assessment of complete blood counts (WBC, white blood cells; HGB, hemoglobin) (B) body weight, and (C) serum chemistries (BUN, blood urea nitrogen; ALT, alanine aminotransferase; GGT, gamma-glutamyltransferase). The shaded areas represent the period of ART treatment. The dotted lines represent the normal range for each parameter.

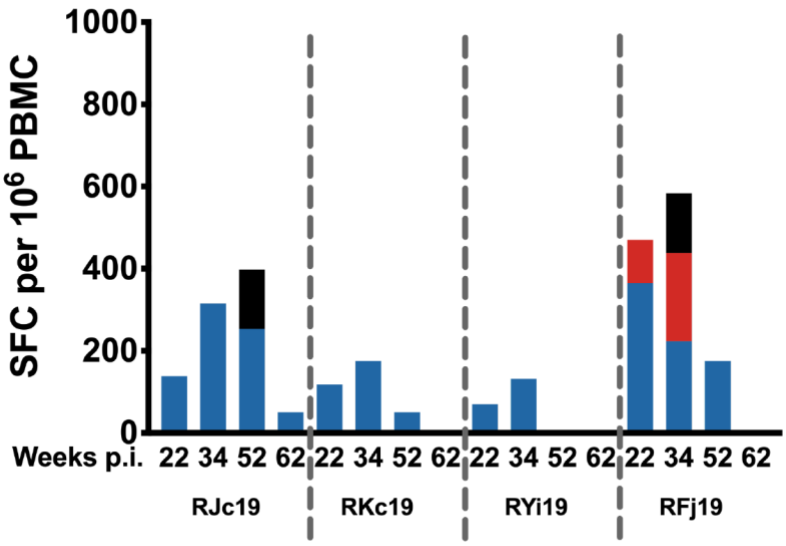

Supplemental Figure 3.5. Individual IFN-γ ELISPOT responses of control RMs. IFN-γ ELISPOT responses to Gag, Pol, and Env peptide pools from SIV_{mac239} were measured at 22, 34 52, and 62 weeks post infection (p.i.). SFC = spot forming cells.

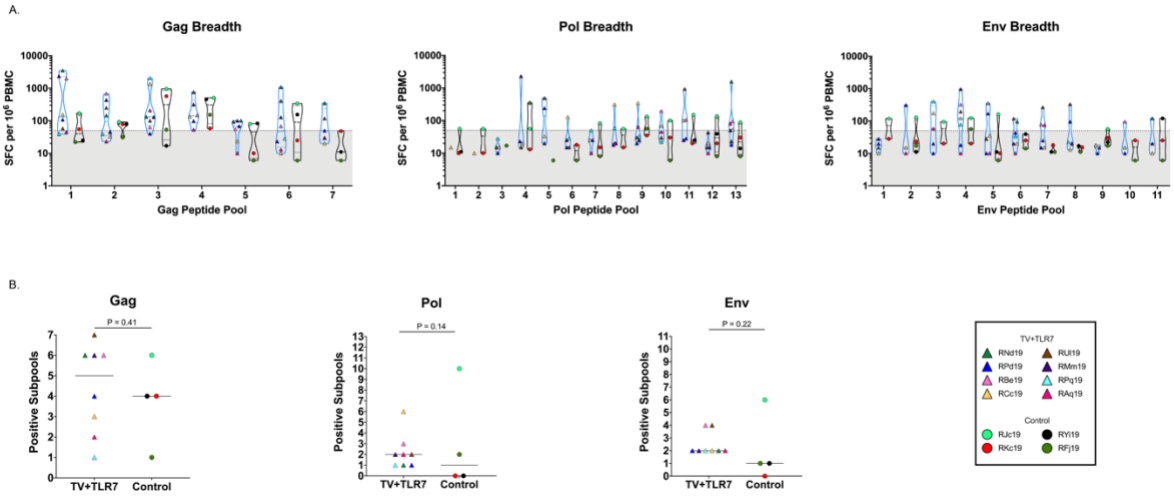

Supplemental Figure 3.6. Cellular breadth to individual peptide pools following analytical treatment interruption (ATI) measured by ELISPOT. (A) Individual IFN-γ ELISPOT responses to 10-mer peptide subpools spanning the Gag, Pol, and Env proteins from SIV_{mac239} following ATI in TV+TLR7 and control RMs. Bars represent median ± quartiles and the gray shading bordered by the horizontal dashed line represents the limit of detection. (B) Cellular immune breadth in TV+TLR7 RMs and control RMs as measured by positive subpools of 10 peptides spanning the SIV_{mac239} Gag, Pol, and Env proteins following ATI. Black bar represents median. Groups were compared using a two-sided Mann-Whitney test ($P < 0.05$ was considered significant).

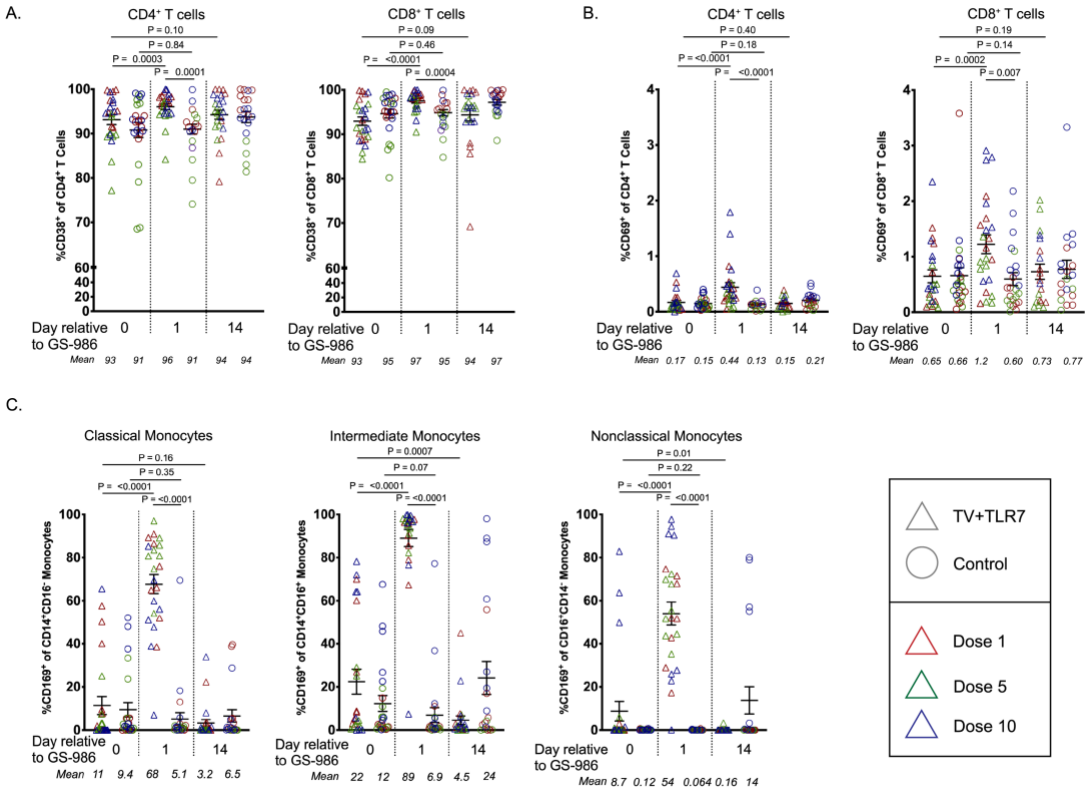

Supplemental Figure 3.7. Detailed immunological response to repeated oral GS-986 administration in SIV-infected, ART-treated infant RMs. Frequency of (A) $CD38^+$ and (B) $CD69^+$ peripheral $CD4^+$ and $CD8^+$ T cells immediately prior to, 1 day post, and 14 days post oral GS-986 doses 1, 5, and 10 in TV+TLR7 or equivalent sample day in control RMs, shown by individual animal. (C) Frequency of $CD169^+$ classical, intermediate, and nonclassical monocytes in TV+TLR7 and control RMs. Dose number is indicated by color. Bars represent mean ± SEM. Statistical analysis was performed using a Wilcoxon matched-pairs signed rank test.

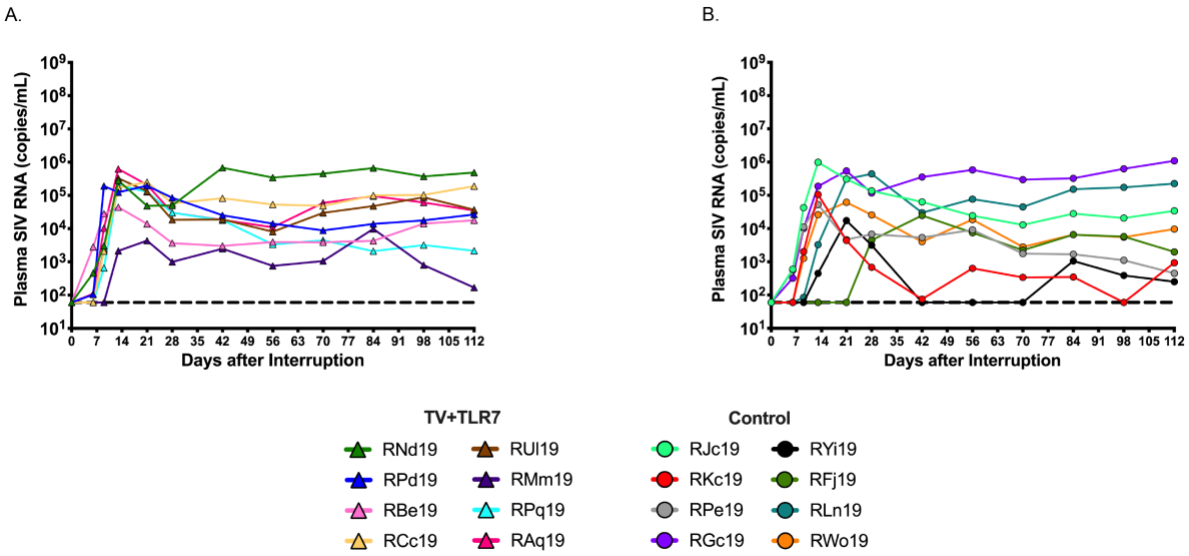

Supplemental Figure 3.8. Post analytical treatment interruption (ATI) plasma viral loads of TV+TLR7 and control RMs. Longitudinal analysis of plasma SIV RNA levels in (A) TV+TLR7 and (B) control RMs following ATI. The horizontal dashed line represents the limit of detection of the assay.

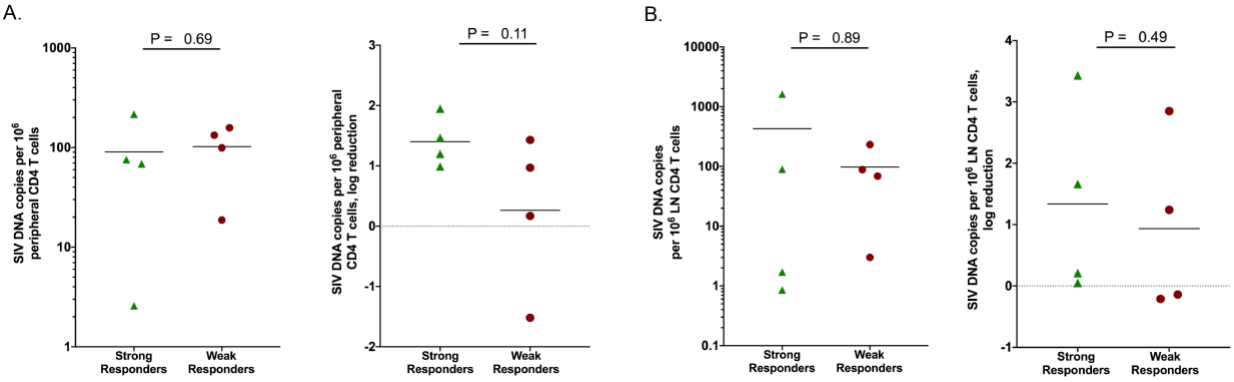

Supplemental Figure 3.9. Impact of therapeutic vaccination and oral TLR-7 stimulation on reservoir between good and poor vaccine responders within TV+TLR7 infant RMs. Comparison of frequency of estimated SIV DNA levels and log reduction from week 12 to week 62 in (A) peripheral and (B) LN $CD4^+$ T cell SIV DNA in strong and weak responders as determined by PCR.

Chapter Four: Altered response patterns following AZD5582 treatment of SIV-infected, ART-suppressed rhesus macaque infants

Katherine M. Bricker[1], Veronica Obregon-Perko[1], Brianna Williams[1], Danielle Oliver[1], Ferzan Uddin[1], Sherrie Jean[2,3], Jennifer S. Wood[2], Stephanie Ehnert[2], Shan Liang[2], Thomas Vanderford[2], Gregory K. Tharp[2], Steven E. Bosinger[2,3], Amanda P. Schauer[4], Maud Mavigner[1,5], Mackenzie L. Cottrell[4], David Margolis[6,7,8,9,10], Richard M. Dunham[6,8,11], and Ann Chahroudi[1,.2,5]

[1]Department of Pediatrics, Emory University School of Medicine, Atlanta, GA; [2]Yerkes National Primate Research Center, Emory University, Atlanta, GA; [3]Department of Pathology and Laboratory Medicine, Emory University School of Medicine, Atlanta, GA; [4]Division of Pharmacotherapy and Experimental Therapeutics, UNC Eshelman School of Pharmacy, University of North Carolina at Chapel Hill, Chapel Hill, NC; [5]Center for Childhood Infections and Vaccines of Children's Healthcare of Atlanta and Emory University, Atlanta, GA; [6]Division of Infectious Diseases, Department of Medicine, University of North Carolina at Chapel Hill, Chapel Hill, NC; [7]Center for AIDS Research, University of North Carolina at Chapel Hill, Chapel Hill, NC; [8]UNC HIV Cure Center, University of North Carolina at Chapel Hill, Chapel Hill, NC; [9]Department of Microbiology and Immunology, School of Medicine, University of North Carolina at Chapel Hill, Chapel Hill, NC; [10]Department of Epidemiology, Gillings School of Public Health, University of North Carolina at Chapel Hill, Chapel Hill, NC; [11]Qura Therapeutics, Chapel Hill, NC. HIV Drug Discovery, ViiV Healthcare, Research Triangle Park, NC

Submitted to Journal of Virology, In review.

Abstract

The “shock and kill” strategy for HIV-1 cure incorporates latency reversing agents (LRA) in combination with interventions that aid the host immune system in clearing virally reactivated cells. LRAs have not yet been investigated in pediatric clinical or preclinical studies. Here, we evaluated an inhibitor of apoptosis protein (IAP) inhibitor (IAPi), AZD5582, that activates the non-canonical NF-κB (ncNF-κB) signaling pathway to reverse latency. Ten weekly doses of AZD5582 were intravenously administered at 0.1 mg/kg to rhesus macaque (RM) infants orally infected with SIV_{mac251} at 4 weeks of age and treated with a triple ART regimen for over one year. During AZD5582 treatment, on-ART viremia above the limit of detection (LOD, 60 copies/ml) was seen in 5/8 infant RMs starting at 3 days post dose 4 and peaking at 771 copies/ml. Of the 135 measurements during AZD5582 treatment in these 5 RM infants, only 8 were above the LOD (6%), lower than the 46% we have previously reported in adult RMs. Pharmacokinetic analysis of plasma AZD5582 levels revealed a lower Cmax in treated infants compared to adults (294 ng/ml vs 802 ng/ml). RNA-Sequencing of CD4+ T cells comparing pre- and post-AZD5582 dosing showed many genes that were similarly upregulated in infants and adults, but through transcriptomics expression of key ncNF-κB genes, including *NFKB2* and *RELB*, was significantly higher in adult RMs. Our results suggest that dosing modifications for this latency reversal approach may be necessary to maximize virus reactivation in the pediatric setting for successful “shock and kill” strategies.

Author Summary

While antiretroviral therapy (ART) has improved HIV-1 disease outcome and reduced transmission, interruption of ART results in rapid viral rebound due to the persistent latent reservoir. Interventions to reduce the viral reservoir are of critical importance, especially for children who must adhere to lifelong ART to prevent disease progression. Here, we used a previously established pediatric nonhuman primate model of oral SIV infection to evaluate a potent latency reversing agent in the controlled setting of daily ART. We demonstrate the safety of the IAPi AZD5582 and evaluate the pharmacokinetics and pharmacodynamics of repeated dosing. The response to AZD5582 in macaque infants differed from what we have previously shown in adult macaques, with weaker latency reversal in infants likely due to altered pharmacokinetics. These data support the contention that HIV-1 cure strategies for children are best evaluated using pediatric model systems.

Introduction

Despite increased access to interventions to prevent mother-to-child transmission (MTCT) of HIV-1, pediatric HIV-1 continues to be a global health crisis with 1.7 million children infected worldwide and 150,000 new pediatric cases annually (189). The majority of new infections occur postnatally through the breastmilk transmission route (200). Antiretroviral therapy (ART) has dramatically improved disease outcome and reduced mortality but does not eliminate the long-lived viral reservoir established during acute infection (111, 117, 128, 281). Strategies to reduce or eliminate the viral reservoir to allow periods of ART-free remission towards a long-term functional or sterilizing cure would greatly benefit children who must adhere to lifelong ART to prevent progression to AIDS.

HIV-1 infection differs in children and adults, with children experiencing higher peak and set point viremia, slower decline to viral set point, and lower median survival in absence of ART (190). Additionally, the developing immune system yields a unique environment that may influence both the pediatric HIV-1 reservoir and the impact of HIV-1 cure strategies on this population. For these reasons, we advocate for HIV-1 cure strategies to be investigated specifically in children. The use of a relevant pediatric animal model can provide important safety and efficacy information necessary to bring experimental therapeutics to pediatric trials. Simian immunodeficiency virus (SIV) infection in the rhesus macaque (RM) has long been established as a robust animal model for HIV-1 and has been used extensively to inform HIV-1 cure strategies (111, 254, 255). Previous published work from our laboratory has demonstrated that oral SIV and

simian-human immunodeficiency virus (SHIV) infection of infant RMs can simulate postnatal HIV-1 infection through breastfeeding with ART-mediated suppression of viremia then permitting the study of virus persistence (149, 282). Through this model we have identified naïve CD4+ T cells as a significant contributor to the viral reservoir in both SIV and SHIV infection of infant RMs (149, 282) and tested therapeutic vaccination in combination with TLR-7 stimulation to promote anti-SIV immune responses (283). This preclinical model provides further opportunities to test important hypotheses regarding viral reservoirs, infant immunity, and remission/eradication strategies.

The "shock and kill" HIV-1 cure strategy aims to "shock" virally-infected cells out of a state of latency using a latency reversing agent (LRA) to induce production of viral RNA and proteins while introducing a "kill" therapeutic agent to aid the immune system in the clearance of infected, reactivated cells (177, 284-286). Performing such interventions in the controlled setting of ART prevents new rounds of infection in uninfected cells, while allowing intervention-mediated clearance of the existing reservoir. There has been extensive research into potential LRAs in preclinical and clinical trials; however, no LRA has yet been evaluated in infants or children. In recent work we identified an inhibitor of apoptosis protein (IAP) inhibitor (IAPi), AZD5582 (also called a SMAC mimetic), as an effective LRA that induced reactivation of the viral reservoir in SIV-infected adult RMs treated with ART (181). Importantly, AZD5582 reactivates cells by targeting the non-canonical NF-κB pathway (ncNF-κB), reducing off-target effects and improving safety over agents that activate canonical NF-κB cell signaling.

In the present study, we evaluated AZD5582 in a preclinical model of SIV-infected ART-suppressed RM infants. We report induction of on-ART viremia in 63% of AZD5582-treated infant RMs, but considerably reduced frequency of latency reversal compared to adult RMs. Transcriptomic analyses revealed significant differences in gene expression induced by AZD5582 in CD4+ T cells from infant and adult RMs. An altered pharmacokinetic profile of plasma AZD5582 in infant RMs was also observed, which may explain the dampened latency reversal. This study provides novel understanding of how an IAPi interacts with the pediatric viral reservoir and developing immune system and suggests that optimization of LRA dosing may be crucial for "shock and kill" strategies to be effective in pediatric patients.

Results

Ex vivo evaluation of AZD5582 on naïve and memory CD4+ T cells

We have previously shown that naïve CD4+ T cells are a major contributor to the viral reservoir in both SIV- and SHIV-infected infant macaques (149, 282). We were therefore first interested to determine whether AZD5582 would act similarly on both naïve and memory CD4+ T cells *ex vivo*, with the eventual goal of using this agent *in vivo* to reverse latency from multiple cell types in a pediatric macaque model. It is well documented that activation of naïve CD4+ T cells relies predominantly on cNF-κB and not the ncNF-κB pathway (287). However, AZD5582 targets intracellular components of the ncNF-κB pathway, including baculoviral inhibitor of apoptosis (IAP) repeat containing 2 (BIRC2) and 3 (BIRC3), which together with another key component of ncNF-kB signaling, the NFKB inducing kinase (NIK), are equally expressed between naïve and memory CD4+ T cells (288, 289). To confirm that the ncNF-κB pathway is activated following AZD5582 stimulation *ex vivo* in naïve and memory CD4+ T cells, we purified naïve (CD62L+CCR7+CD95-) and memory (CD95+) CD4+ T cells from the peripheral blood of eight SIV-infected, ART-suppressed infant macaques. Sorted cells were stimulated with 100 or 1,000 nM of AZD5582 for 24 hours and PCR was performed to evaluate the expression of the ncNF-κB pathway genes *BIRC3* and *NFkB2* (Fig. 4.1). No significant difference was observed in fold induction of *BIRC3* and *NFkB2* gene expression between naïve and memory CD4+ T cells at 1000 nM ($P = 0.88$ and >0.99, respectively, $n=4$) or 100 nM ($P = 0.88$ and

>0.99, respectively, n=4). These results indicate that both naïve and memory CD4+ T cells have the potential to utilize the ncNF-κB pathway following AZD5582 stimulation.

In vivo experimental design and treatments

Following confirmation of ncNF-kB activation in naïve CD4+ T cells *ex vivo*, we next sought to evaluate the impact of *in vivo* AZD5582 administration in SIV-infected, ART-suppressed infant rhesus macaques. Twelve Indian origin RMs (four males and eight females) were selected for this study. RMs were confirmed negative for the MHC haplotypes (Mamu-B*08 and -B*17) associated with natural control of SIV replication. The time course of the experimental design and interventions used are shown in Fig. 2A. All RMs were exposed to two consecutive doses of 10^5 50% tissue culture infective doses ($TCID_{50}$) SIV_{mac251} by oral administration at approximately 4 weeks of age (range: 3.1 w – 7.4 w, mean: 4.45 w). As breastmilk acquisition of HIV-1 is unlikely to be followed by very early ART initiation (i.e., within hours or days), here we started daily ART in all RMs at 4 weeks after SIV infection. The ART regimen (tenofovir, TDF; emtricitabine, FTC; dolutegravir, DTG) was administered as a single dose co-formulation once daily by subcutaneous injection, as described previously (149, 282, 283), throughout the experimental time course (indicated by gray shading in Fig. 4.2A). ART was effective at suppressing SIV RNA in plasma below the limit of detection (LOD, 60 copies/ml) in all RMs (Fig. 4.2B and 4.2C). As seen in HIV-1-infected children (258-260), time to suppression was variable, ranging from 4 to 26 weeks (median = 12 w) with some infants showing transient blips of viremia shortly following viral suppression.

Prior to the AZD5582 treatment phase of the experiment, two groups of RMs (control, n=4 and experimental ['AZD5582'], n=8) were balanced for sex, age at infection, $CD4^+$ T cell frequency at ART initiation, peak viral load, and area under the curve (AUC) of pre-ART viremia (Table 4.1). After over one year of daily ART (range: 66 w - 70 w), 8 RMs received ten weekly doses of AZD5582 at 0.1 mg/kg by intravenous (i.v.) infusion (Fig. 4.2A). This dose has been shown to be tolerated in adult RMs and effective in reversing latency (181). The remaining four RMs served as ART-treated controls. Peripheral blood (PB) and lymph node (LN) biopsies were collected longitudinally at the timepoints indicated in Fig. 4.2A. AZD5582 was well tolerated in infant macaques, without clinical adverse events throughout the intervention phase of the study.

Impact of AZD5582 on latency reversal in infant RMs

In this study, latency reversal was defined as a plasma SIV RNA level above 60 copies/ml during AZD5582 treatment in the presence of continued daily ART (or, "on-ART viremia"). The first instance of latency reversal was observed at 48 h after the 4^{th} dose (Fig. 4.3A). On-ART viremia peaked at 771 copies/ml in RVf20 2 days post-dose 9. In total, at least one episode of on-ART viremia was observed in 5/8 RMs (63%) over the course of treatment (Fig. 4.3A,C) in contrast with the durable viral suppression below 60 copies/ml observed in ART only controls (Fig. 3B). This is comparable to our previously published study in which 5/9 (56%) of AZD5582-treated SIV-infected adult RMs experienced on-ART viremia (Fig. 4.3C) (181). We note that 3/5 of the macaques that experienced latency reversal during AZD5582 treatment showed only a single

episode of low-level on-ART viremia (range: 62 – 110 copies/ml). This low level viremia contrasts, however, with the sustained suppression below 60 copies/ml in the 10 month period before AZD5582 treatment in these 3 infants (Fig. 4.2B).

Out of 135 total viral load measurements performed over the AZD5582 treatment course in the 5 RMs that showed on-ART viremia, 8 total measurements (6%) were above the limit of detection of 60 copies/ml. This frequency of on-ART viremia episodes was lower than that observed in RM adults treated with AZD5582 (46%) (181), despite similar overall percentages of responding animals (Fig. 4.3C).

SIV-infected adult RMs that exhibited on-ART viremia during AZD5582 treatment could be distinguished from those with stably suppressed viral loads during AZD5582 treatment by their significantly higher pre-ART viral loads (290). We investigated this association in the infants studied here but did not see a similar trend, although we were limited by small sample size (Fig. 4.3D). Although the pre-ART viral loads of infants and adults with on-ART viremia were similar ($p = 0.35$), there was no significant difference in pre-ART viral loads between infants that responded to AZD5582 and infants that remained stably suppressed ($p = 0.14$). Interestingly, the infant RM with the most pronounced latency reversal (RVf20) also had the lowest pre-ART viral load from the group with on-ART viremia (lower than two of the stably suppressed infants). Together, these data highlight distinct age-related responses to this dosing regimen of AZD5582.

Pharmacokinetics of AZD5582 is altered in infant RMs

As a potential explanation for the dampened virologic response to AZD5582 observed in infant RMs, we investigated AZD5582 pharmacokinetics (PK) following the third dose using a sparse sampling design. Blood samples were collected immediately following the infusion in 4 RMs and from 2 RMs per timepoint at 1h-, 2h-, 4h-, 8h-, and 24h-post infusion. Plasma concentrations of AZD5582 in infants exhibited biphasic elimination with a rapid distribution half-life followed by a slower terminal elimination half-life of 9.9 hours (Fig. 4.4A). Non compartmental analysis (NCA) was conducted to determine pharmacokinetic parameters in infants and compared with available PK data from adult historical controls of SIV-infected, ART-suppressed rhesus macaques (n=7) given matched doses of AZD5582 (Fig. 4.4B) (181). Infants exhibited a 2.5- and 2.3-fold lower Cmax and $AUC_{0\text{-}2h}$, respectively (Table 4.2). Although corresponding data were not collected from adult macaques, we note that in infants the $AUC_{0\text{-}24h}$ was calculated as 239 ng*hr/ml.

*Evaluation of ncNF-**κ**B gene expression following AZD5582 treatment*

Treatment with AZD5582 in SIV-infected, ART-suppressed adult RMs upregulates key genes associated with signaling through the ncNF-kB pathway, rather than the canonical NF-kB (cNF-kB) pathway in CD4+ T cells (181). Here we performed RNA-Seq in total CD4+ T cells

isolated from the peripheral blood of AZD5582-treated infant macaques at baseline (pre-dose 1) and at the end of the treatment period (post-dose 10). In total, 1,031 genes were identified as differentially expressed following AZD5582 treatment in infant RMs (855 up-regulated, 176 down-regulated) using a false discovery rate of 5% and a linear fold change of 50% (Fig. 4.5A). Principal component analysis revealed a distinct effect of AZD5582 on gene expression in CD4+ T cells isolated from infant RMs 2 days post dose 10 compared to peripheral CD4+ T cells from infants pre-AZD5582 (Fig. 4.5B).

Enrichment of NF-κB associated genes in AZD5582-treated infants was next compared to data generated from our prior adult macaque study, where RNA-Seq of peripheral CD4+ T cells was performed at the same time points (pre-AZD5582 and 2 days post-dose 10 of AZD5582) (181). The leading-edge genes in both groups of animals are shown in the heat maps in Fig. 5C-E, segregated by genes that were similarly changed in infants and adults (Fig. 5C), higher in infants compared to adults (Fig. 4.5D), and higher in adults compared to infants (Fig. 5E). *BIRC3* and *BIRC5* were both most significantly upregulated following AZD5582 in CD4+ T cells from AZD5582 treated infant and adult RMs (Fig. 4.5C). *BIRC3* encodes cellular inhibitor of apoptosis 2 (cIAP2) and *BIRC5* (encoding survivin) also belongs to the IAP gene family, with both genes involved in the regulation of the cNF-κB and ncNF-κB pathways (291, 292). Genes identified as most upregulated in infant RMs but not adults include *TNFRSF13B* and *TNFRSF17*, two TNF-receptor super family genes that encode proteins that can initiate activation of NF-κB signaling (Fig. 4.5D) (293). Interestingly, *RELB* and *NFKB2*, hallmark ncNF-κB signaling genes, as well as *NFKBIA*, an inhibitory gene of the cNF-κB signaling pathway, were identified as significantly

upregulated in CD4+ T cells isolated from adult RMs but not in infant RMs after AZD5582 treatment (Fig. 4.5E). While we showed that NFKB2 could be induced by AZD5582 *ex vivo* in infant CD4+ T cells with both a naïve and memory phenotype (Fig. 4.1), gene expression changes with *in vivo* treatment appeared more modest in infants compared to adults.

We did not identify a distinct gene expression profile that distinguished infants with on-ART viremia from those that did not show evidence of latency reversal during AZD5582 treatment. (Fig. 4.5C,D). This result is consistent with our previous observations in adult RMs treated with AZD5582 (181), and indicates that *in vivo* administration of this IAPi can impact CD4+ T cell gene expression whether or not our definition of latency reversal was achieved. Even so, it is clear from these data that adult macaques demonstrate greater upregulation of ncNF-kB signaling genes as well as a greater frequency of latency reversal events during treatment with AZD5582 when compared to infants, potentially due to the altered PK profile of AZD5582 in infants.

Immunologic and virologic impact of AZD5582 in infant RMs

The ncNF-κB pathway plays an important role in regulating T cell differentiation without causing broad systemic inflammation (287). We have previously observed a stimulatory effect on peripheral T cells following AZD5582 treatment specifically measurable through increased intracellular Ki67 expression (181). To further assess the effect of AZD5582 on infant RMs, flow

cytometry was performed longitudinally on whole blood on the day of doses 1, 3, 6 and 9 and both 48 – 72h and 7 days after each of these doses. These timepoints were selected to allow longitudinal evaluation while remaining within blood volume constraints. An increase in Ki67 expression in memory CD4+ and memory CD8+ T cells (identified as CD3+CD95+) was most prominent 7 days following dose 1 (Fig. 4.6A, 8.7% to 46.9% and 5.1% to 46.7%, respectively). When three baseline measurements were used to account for natural variation, Ki67 expression increased by an average of 24.3% and 23.3% after dose 1 on memory CD4+ and CD8+ T cells, respectively (Fig. 4.6A). To assess the response to all doses in tandem, the expression of Ki67 on peripheral memory CD4+ and memory CD8+ T cells averaged 21.0% and 18.2%, respectively, at baseline and significantly increased to a mean of 28.4% and 26.5%, respectively, at 3-days post AZD5582 (Fig. 4.6B, $p = 0.02$ and $p = 0.03$, respectively). We did not observe increases to other markers of activation, including HLA-DR and PD-1, following AZD5582 treatment. While we have previously shown that AZD5582 treatment alone did not consistently impact the size of the viral reservoir (181), we note that proliferation of CD4+ T cells (as suggested by increased Ki67 levels) may result in an expansion of infected cells. However, we found similar levels of cell-associated SIV DNA in CD4+ T cells isolated from the periphery and lymph nodes in AZD5582-treated infant RMs compared to ART-only controls (Fig. 4.6C).

Discussion

This study provides insight into the use of a latency reversing agents to reactivate the viral reservoir in a pediatric model of HIV-1 infection and ART suppression. We first sought to validate that AZD5582 activates the ncNF-κB pathway in both naïve and memory CD4+ T cells ex vivo. We next demonstrated safety of repeated AZD5582 infusions and evaluated pharmacokinetics and pharmacodynamics following AZD5582 treatment. The IAPi AZD5582 induced on-ART viremia in 63% of infants, a number similar to what has previously been reported in adult RMs. However, only 6% of assays of plasma viremia throughout AZD5582 treatment in the infants that experienced on-ART viremia were above the limit of detection, perhaps related to the altered pharmacokinetic profile compared to adult macaques and resultant differential gene expression patterns. Although pre-ART viral loads served as an efficient predictor of on-ART viremia following AZD5582 treatment in adults, in our infants, pre-ART viremia was not a predictor of the presence or absence of latency reversal during AZD5582 treatment. Finally, through flow cytometry, we identified an increase in Ki67 expression in peripheral memory CD4+ and memory CD8+ T cells at 3 days post-dose compared to the pre-dose timepoint. Despite this transient activation of memory CD4+ T cells we did not observe an expansion of infected cells in peripheral blood or lymph nodes.

Quantification of plasma AZD5582 concentrations revealed that weight-based dosing resulted in lower Cmax and AUC0-2h for infants when compared to adult RMs, which likely contributed to the altered response observed here compared to our previously published adult study

(181). Pharmacokinetic processes differ between children and adults and, therefore, the same dosage of many drugs may not correspond to the same pharmacological effect (294). Metabolism, body composition, and gastrointestinal absorption are just some factors that fluctuate during development and can influence pharmacokinetics and need to be considered when determining an optimal dosing strategy in pediatric populations (295). The dose we used (0.1 mg/kg) is the highest dose tested thus far in SIV-infected RMs to our knowledge and we found it to be well tolerated and safe in infants over 10 infusions. Thus, future efforts to maximize latency reversal in infants should involve testing a higher infusion dose or longer infusion duration to identify an optimal AZD5582 dosing strategy for this age group.

We found that the IAPi AZD5582 activates the NF-κB pathway in treated infant RMs as shown by transcriptomic analyses. IAP inhibitors target and activate the ncNF-κB pathway, which leads to activation of fewer host genes than the cNF-κB pathway, limiting systemic activation and likely increasing clinical tolerability (293). Through transcriptomic profiling, key ncNF-κB pathway genes, such as BIRC3 and BIRC5, were identified as significantly upregulated in both treated infant and adult RMs following AZD5582 treatment. However, we did not observe increased expression of hallmark ncNF-κB signaling genes RELB and NFKB2 nor the cNF-κB pathway inhibitor NFKBIA, unlike what we have previously reported in adult macaques. It is well established that naïve CD4+ T cells, the predominant subset in infants (149, 282), rely on the cNF-κB pathway for activation while the ncNF-κB pathway is more important in memory CD4+ T cells (293). However, we demonstrated that there is no significant difference between upregulation of both of the ncNF-κB genes BIRC3 and NFKB2 following ex vivo AZD5582 stimulation in naïve

and memory CD4+ T cells isolated from our SIV-infected, ART-suppressed infants. In the present study, we are unable to conclude if a lack of induction of these ncNF-κB genes in vivo is due to dampened pharmacokinetics or differences between naïve and memory CD4+ T cells because of cell availability limitations, but this is an area that should be further investigated in future work.

Previous data from our lab has demonstrated that naïve CD4+ T cells dominate the pediatric reservoir (149, 282) and it has also been shown that naïve cells are less inducible than more differentiated CD4+ T cells in vitro (296). Furthermore, naïve CD4+ T cells produce less infectious virus following multiple rounds of stimulation when compared to memory CD4+ T cells ex vivo (297). However, conflicting data on the inducibility of naïve CD4+ T cells exists with Zerbato et al. reporting similar levels of virus production in naïve and central memory CD4+ T cells following CD3/CD28 stimulation (298). In a study specifically investigating the reactivation potential of the pediatric reservoir, Dhummakupt et al. suggest that the reservoir from perinatally HIV-1 infected children is less inducible than the reservoir from HIV-1 infected adults ex vivo, but we note that this study did not distinguish differences between naïve and memory CD4+ T cells (272). While dampened pharmacokinetics of ADZ5582 in the infant RMs as compared to adult RMs was likely the major contributor towards our virologic findings, the results presented in this study compliment a growing body of evidence for lower inducibility potential of the pediatric viral reservoir.

This study has a number of limitations. The small size of infant RMs limits blood volume availability and biopsy frequency, reducing our ability to perform extensive evaluative assays.

Specifically, we were unable to perform ultrasensitive plasma viral load quantification, an assay with a much lower limit of detection compared to the 60 copies/ml limit used here. Although the ultrasensitive assay may have revealed a higher frequency of reactivation events under ART, it is expected that an effective LRA will induce high level on-ART viremia to permit clearance of virally infected cells and, as such, results from an ultrasensitive assay would likely not have altered our key findings. Additionally, through ex vivo stimulation with AZD5582 we demonstrated similar activation of the ncNF-κB pathway in naïve and memory CD4+ T cells, but we were unable to evaluate the effect of in vivo AZD5582 treatment on specific CD4+ T cell subsets. It is possible that latency reversal may differ between naïve and memory CD4+ T cells despite similar ncNF-κB activation levels. Additionally, infant macaques were infected with SIVmac251 while adult macaques were infected with SIVmac239, but both viral strains induce robust infection and reservoir formation so we do not believe this impacted our results. Finally, although not unexpected, AZD5582 alone did not impact the viral reservoir size estimated by CD4+ T cell-associated SIV DNA, but we acknowledge that we did not analyze the replication competent or rebound competent viral reservoir here. Despite these limitations, we believe studies such as this one demonstrate the importance of investigating HIV-1 in a pediatric model to provide key preclinical data of pediatric HIV-1 cure interventions.

In conclusion, we demonstrate that the IAPi AZD5582 is safe and can activate the T cell compartment in SIV-infected, ART-suppressed infant RMs. This activation differed from that seen in adult RMs in term of ncNF-kB gene expression and extent of latency reversal, which may be driven by altered drug metabolism and/or specific features of the pediatric viral reservoir. We hope

that future studies not only optimize LRA dosing in pediatric preclinical models but also incorporate the use of a “kill” agent to aid the immune system in clearing virally infected, reactivated cells to reduce the latent viral reservoir.

Materials and Methods

Cell sorting

For cell sorting, peripheral CD4+ T cells were first enriched by negative selection with the use of magnetic beads and column purification (nonhuman primate CD4+ T cell isolation kit; Miltenyi). Enriched CD4+ T cells were then stained with viability dye (Live/Dead Aqua) and previous determined volumes of the following fluorescently conjugated Mabs: CD3-AF700 (clone SP34-2), CD8-APC-Cy7 (clone SK1), CD95-PE-Cy5 (clone DX2), CD62L-PE (clone SK11), and CCR7-PE-Cy7 (clone 3D12) from BD Biosciences; CD4-BV650 from BioLegend. Sorted live CD3+CD8-CD4+ populations were defined as follows: naïve cells, CD62L+ CCR7+ CD95-; and memory, CD95+. Sorting was performed on a FACSAria LSR II (BD Biosciences) equipped with FACSDiva software.

Target gene RT-qPCR

Naïve and memory CD4+ T cells were treated with 100 or 1000 nM AZD5582 for 24 hours and then stored as a dry pellet until RNA extraction. Total RNA was isolated using the RNEasy Mini kit (Qiagen) according to the manufacturer's instructions. The following TaqMan primer probe sets were sourced from Applied Biosystems: Rh02837734_m1 (BIRC3), Rh01028900_m1 (NFKB2) and Rh00427620_m1 (TBP). TaqMan-based quantitative PCR with reverse transcription

(RT–qPCR; Fast Virus 1-Step Master Mix, Applied Biosystems) was used to amplify host genes of interest and acquire the signal on an Applied Biosystems 7500 Fast System (ThermoFisher). Gene expression was normalized to TATA-box binding protein (TBP) and the comparative threshold cycle (Ct) method (ΔΔCt) was used for relative quantification of gene expression. Relative quantification was analyzed by ABI 7500 Software (v.2.3, Life Technologies).

Animals and infection

Twelve infant Indian RMs (*Macaca mulatta*), with exclusion of Mamu B*08- and B*17-postive animals, were enrolled in this study. The animals were born at the Yerkes National Primate Research Center (YNPRC) to dams housed in indoor/outdoor group housing. The infants were removed from the dams when they were approximately 2 weeks old and transferred to an indoor nursery, where they were housed in social pairs with either full contact or protected contact for the duration of the study. The infants were fed in accordance with the YNPRC standard operating procedures (SOPs) for NHP feeding. After being removed from the dam, infants were fed center approved milk replacer (Similac Advance, OptiGro Infant Formula with Iron and/or Similac Soy Isomil OptiGro Infant Formula with Iron; Abbott Nutrition, Columbus, OH) until 14 weeks of age. Infants were provided softened standard primate jumbo chow biscuits (Jumbo Monkey Diet 5037; Purina Mills, St. Louis, MO) and a portion of orange starting between 2 – 4 weeks of age. As animals aged additional enrichment of various fresh produce items were provided daily. The animals were orally infected at 4 to 5 weeks of age with two consecutive doses of 10^5 $TCID_{50}$ (50% tissue culture infectious doses) of SIV_{mac251}. Three infants required multiple weekly 2-dose

challenges prior to successful infection (totaling up to three challenges). Eight historical controls that followed the same regimen were included in this study. Yerkes National Primate Research Center is accredited by both the U.S. Department of Agriculture (USDA) and by the Association for Assessment and Accreditation of Laboratory Animal Care (AAALAC). All animal procedures were performed in accordance with guidelines established by the Emory University Institutional Animal Care and Use Committee Guidelines and those set up by the NIH's Guide for the Care and Use of Laboratory Animals, 8th edition.

Antiretroviral therapy

The twelve RM infants were treated with a potent three-drug ART regimen initiated at 4 weeks postinfection. The preformulation ART cocktail contained two reverse transcriptase inhibitors, 5.1 mg/kg Tenofovir disoproxil fumarate (TDF) and 40 mg/kg Emtricitabine (FTC), plus 2.5 mg/kg of the integrase inhibitor Dolutegravir (DTG). This ART cocktail was administered once daily at 1 mg/kg via the subcutaneous route.

Administration of AZD5582

The IAPi AZD5582 was reconstituted to 0.4 mg/mL in 10% Captisol within one week of administration as previously described (181). Monkeys assigned to the experimental intervention

group received ten administrations of 0.1 mg/kg AZD5582 by intravenous (i.v.) infusion with an inline filter over a thirty-minute period every week for 10 weeks.

Sample collection and processing

EDTA-anticoagulated blood samples were collected regularly and used for a complete blood count, routine chemical analysis and immunostaining, with plasma separated by centrifugation within 1 h of phlebotomy. PBMCs were prepared by density gradient centrifugation. Lymph node biopsies were collected at indicated timepoints (Fig. 2A). Lymph nodes were ground using a 70-μm cell strainer. Cell suspensions were washed and immediately used for immunostaining or cryopreserved at -80 °C until use.

Immunophenotype by flow cytometry

Multicolor flow cytometric analysis was performed on whole blood (WB) or cell suspensions using predetermined optimal concentrations of the following fluorescently conjugated monoclonal antibodies (MAbs). For WB T cell analysis the following MAbs were used: CD3-allophycocyanin (APC)-Cy7 (clone SP34-2), CD95-phycoerythrin (PE)-Cy5 (clone DX2), Ki67-AF700 (clone B56), HLA-DR-peridinin chlorophyll protein (PerCP)-Cy5.5 (clone G46-6), CCR7-fluorescein isothiocyanate (FITC) (clone 150503), CCR5-APC (clone 3A9), CD62L (clone SK11), and CD45-RA-PE-Cy7 (clone L45) from BD Biosciences; CD8-BV711 (clone RPA-T8), CD4-BV650 (clone

OKT4), and PD-1-BV421 (clone EH12.2H7) from BioLegend; and CD28-ECD (clone CD28-2) from Beckman-Coulter. Flow cytometric acquisition and analysis of samples were performed on at least 100,000 events on an AURORA flow cytometer driven by the SpectroFlo software package (Cytek). Analyses of the acquired data were performed using FlowJo version 10.0.4 software (TreeStar).

Plasma RNA and cell-associated DNA lysate viral quantification

Plasma viral quantification was performed as described previously. Frozen cell pellet was lysed with proteinase K (100µg/ml in 10mM Tris-HCl pH 8) for 1h at 56ºC. Quantification of SIVmac *gag* DNA was performed by quantitative PCR using the 5' nuclease (TaqMan) assay with an ABI7500 system (PerkinElmer Life Sciences). The sequence of the forward primer for SIV_{mac} *gag* was 5′-GCAGAGGAGGAAATTACCCAGTAC-3′, the reverse primer sequence was 5′-CAATTTTACCCAGGCATTTAATGTT-3′, and the probe sequence was 5′-6-carboxyfluorescein (FAM)-TGTCCACCTGCCATTAAGCCCGA-6-carboxytetramethylrhodamine (TAMRA)-3′. 7.5µL of cell lysate were mixed in a 50µL reaction containing 1x Platinum Buffer, 3.5mM $MgCl_2$, 0.2mM dNTP, primers 200nM, probe 150nM, and 2U Platinum Taq. For cell number quantification, quantitative PCR was performed simultaneously for monkey albumin gene copy number. The sequence of the forward primer for albumin was F 5'-TGCATGAGAAAACGCCAGTAA-3'; the reverse primer sequence was 5'-ATGGTCGCCTGTTCACCAA-3' and the probe sequence was 5'-AGAAAGTCACCAAATGCTGCACGGAATC-3'(249). The reactions were performed on a 7500

real-time PCR system (Applied Biosystems) with the following thermal program: 10 min at 95ºC, followed by 40 cycles of denaturation at 95ºC for 15 s and annealing at 60ºC for 1min.

Pharmacokinetics of AZD5582

Plasma samples were collected from RMs over 24 hours following the start of a single 30 minute intravenous infusion of AZD5582 using a previously published (181). HPLC-MS/MS method with a dynamic range of 0.2 – 1000ng/ml. Non compartmental analysis (NCA) was performed using Phoenix64 WinNonlin v8.1 software using the sparse sampling function to derive mean PK parameters. The linear up-log down trapezoidal rule was used to calculate AUC. The terminal elimination rate constant (kel) was estimated by fitting a linear regression line on a semi-log plot to the individual concentration data constrained to observations from 4 to 24 hours post start of infusion and used to calculate terminal elimination half-life. One observation below the assay's limit of quantification was imputed at ½ the lower limit of quantification (299).

RNA-sequencing analysis

RNA-sequencing (RNA-seq) analysis was conducted at the Yerkes Nonhuman Primate Genomics Core Laboratory (http://www.yerkes.emory.edu/nhp_genomics_core/). RNA was purified from 50,000 peripheral-blood-derived $CD4^{+}$T cells purified by negative selection and lysed in 350 µL of RLT buffer at -80ºC, using Qiagen Micro RNEasy columns, and RNA quality was assessed

using an Agilent Bioanalyzer. Then, 2 ng of total RNA was used as input for mRNA amplification using 5' template switch PCR with the Clontech SMART-seq v4 Ultra Low Input RNA kit according to the manufacturer's instructions. Amplified mRNA was fragmented and appended with dual-index bar codes using Illumina NexteraXT DNA library preparation kits. Libraries were validated by capillary electrophoresis on an Agilent 4200 TapeStation, pooled and sequenced on an Illumina HiSeq 3000 using 100-bp single reads at an average depth of 25 million reads. Alignment was performed using STAR version 2.7.3a (300) and transcripts were annotated using a composite reference of rhesus macaque (Mmul10 Ensembl release 100).

Historical animal groups

Data from an additional group of SIV-infected, ART-suppressed adult RMs treated with AZD5582 were used for comparative analysis (181). Nine Indian rhesus macaques, with the exclusion of MamuB*08+ and MamuB*17+ animals, were infected i.v. with $3x10^3$ $TCID_{50}$ of SIV_{mac239} (*nef* open). Animals were treated with an identical ART regimen, as described above, initiated at 8 weeks postinfection. Animals remained suppressed for a similar timeframe, over one year, as the infant macaques prior to AZD5582 treatment.

Statistical Analyses

Statistical analyses were performed using GraphPad Prism Software (v.7 or v.8). $P \leq 0.05$ was considered statistically significant. To test the statistical significance observed in Ki67 expression on memory CD4+ and CD8+ T cells in Fig. 2 and BIRC3 and NFKB2 gene expression in Fig. 5, a Wilcoxon matched-pairs signed rank test was used. To compare differences in pre-ART viral loads between experimental groups in Fig. 3D and cell-associated SIV DNA between experimental groups in Sup. Fig. 2 a two-sided Mann-Whitney test was used. For RNA-seq analysis in Fig. 4, RNA-seq data were mapped to the NCBI Mmul10 assembly of the Indian rhesus macaque genome and alignment was performed with STAR (v.2.7.3a) using Ensemble release 100 annotation as a transcript annotation and splice junction reference. Transcript abundance estimates were calculated internal to the STAR aligner using the algorithm of htseq-count (301).(301). DESeq2 (302) was used for normalization and differential expression analysis. Gene set enrichment analysis(303) (GSEA), performed with the GSEA desktop module (available at https://www.broadinstitute.org/gsea/) and the Molecular Signatures Database (MSigDB), was used to determine pathway/geneset enrichment. Heat maps, volcano plots and principal component analysis plots were generated with the R (v 3.6.0) package ggplot2.

Acknowledgments

We would like to thank the Veterinary and Research Services Departments at the Yerkes NPRC for support of NHP research and Gilead and ViiV for provision of antiretroviral drugs. The authors also thank David Irlbeck for his expertise and feedback. This work was conducted with federal funds from the U.S. National Institutes of Health (R01 AI133706 and UM1 AI164566).

Research reported in this publication was also supported by the Emory CFAR Virology Core (P30 AI050409), the University of North Carolina at Chapel Hill CFAR (P30 AI050410), the Pediatrics/Winship Flow Cytometry Core of Winship Cancer Institute of Emory University, Children's Healthcare of Atlanta (P30 CA138292), and the Yerkes NPRC through the National Institutes of Health's Office of the Director, Office of Research Infrastructure Programs, P51 OD011132 and U42 OD011023

Chapter 4 Figures

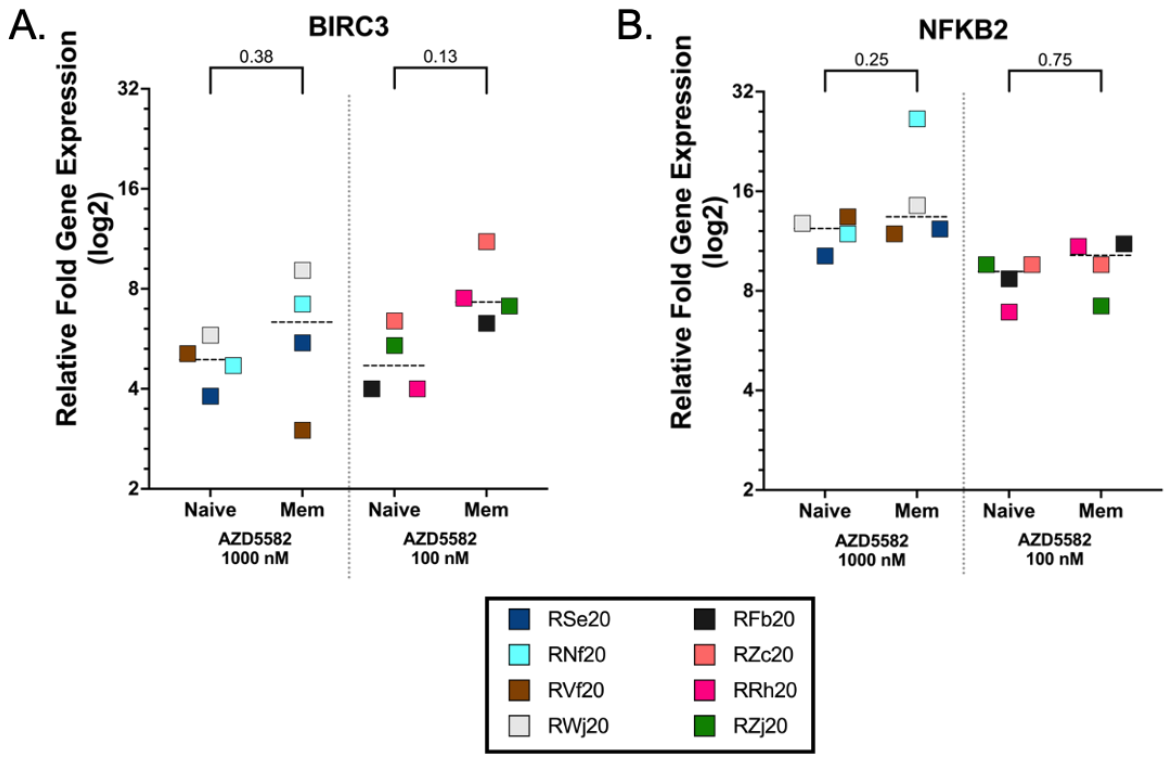

Figure 4.1. Induction of ncNF-kB genes following ex vivo AZD5582 treatment in naive and memory CD4+ T cells. Naïve and Memory CD4+ T cells were sorted and treated with 100 nM or 1000 nM of AZD5582 overnight. Cell lysates were analyzed by RT-PCR for (A) BIRC3 and (B) NFKB2, relative fold induction compared to housekeeping gene TATA-box binding protein (TBP) with average expression in DMSO controls subtracted is shown. Symbols represent three technical replicates from a single run. CD4+ subsets were compared using a Wilcoxon matched-pairs signed rank test ($P < 0.05$ was considered significant).

Group	ID	Sex	Age at infection, weeks	CD4 Freq, ART initiation	Peak PVL, pre-ART	AUC PVL, pre-ART
AZD5582	RVf20	F	3.1	47.9%	1.76E+07	3.34E+07
	RNf20	F	3.3	35.6%	7.13E+06	1.77E+07
	RSe20	F	3.9	25.5%	9.01E+06	2.05E+07
	RRh20	M	4	36.9%	9.53E+06	1.22E+07
	RWj20	M	4.4	n.d.	3.34E+07	9.59E+07
	RZj20	F	4.4	n.d.	1.61E+07	2.61E+07
	RZc20	F	7.1	25.0%	7.39E+06	1.18E+07
	RFb20	M	7.4	32.7%	3.40E+07	6.46E+07
Control	RQi20	M	3.7	34.9%	3.70E+07	1.00E+08
	RVb20	M	4	28.5%	3.77E+06	9.38E+06
	RQb20	F	4	23.3%	5.55E+05	9.89E+05
	RHb20	F	4.1	25.2%	1.99E+06	4.05E+06

Table 4.1. Parameters used to select experimental and control groups.

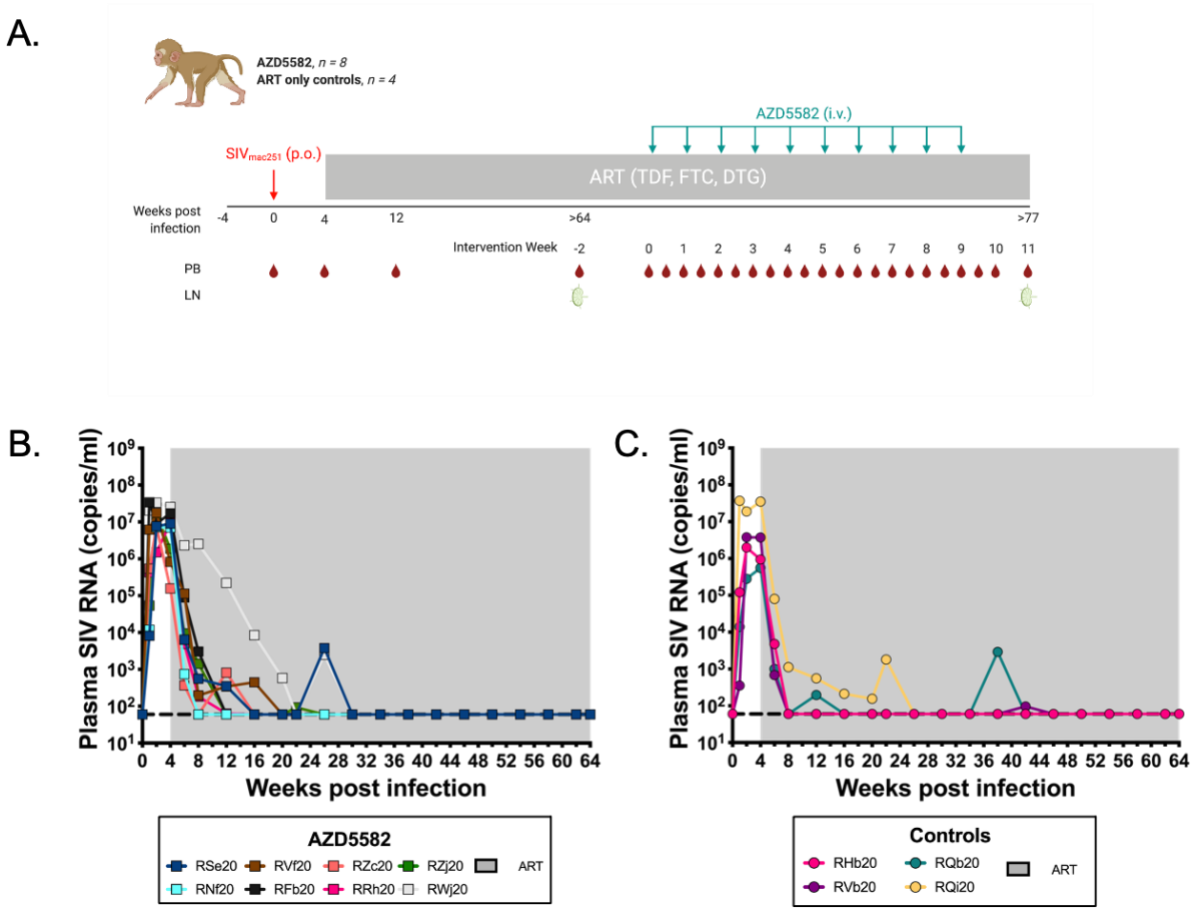

Figure 4.2. Experimental design and response to ART in SIV-infected infant RMs. (A) Schematic of the study design. Twelve infant RMs were infected orally with 10^5 TCID50 SIV_{mac251} (day 0), and starting at 4 weeks post infection were treated with combination ART (TDF, FTC, DTG) for greater than one year. Eight animals received 10 doses of AZD5582 (0.1 mg/kg, i.v. infusion) at the indicated time points. The remaining 4 animals served as ART-treated controls. Peripheral blood (PB), and lymph node (LN) biopsies were collected at the indicated time points. Longitudinal analysis of plasma SIV RNA levels pre-ART and during ART (but before AZD5582 treatment) in (B) AZD5582 and (C) control groups. The shaded area represents the period of ART treatment. The dashed line represents the limit of detection of the assay.

A.

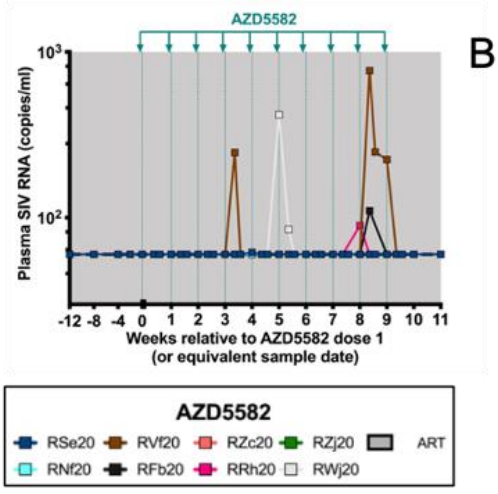

B.

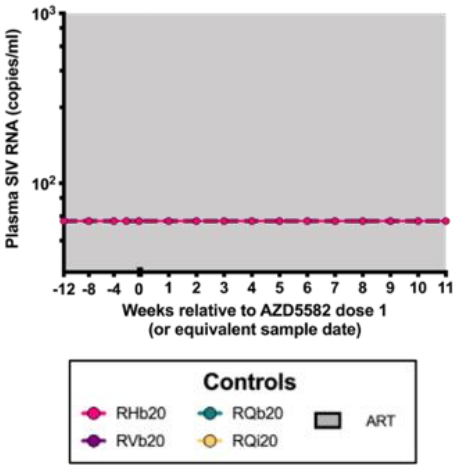

C.

SIV reactivation	Infant RMs	Adult RMs [17]
Per animal	5/8	5/9
	63%	*56%*
Events >60 copies/ml	8/135	64/140
	6%	*46%*
Peak on-ART viremia	771 copies/ml	1,390 copies/ml

D.

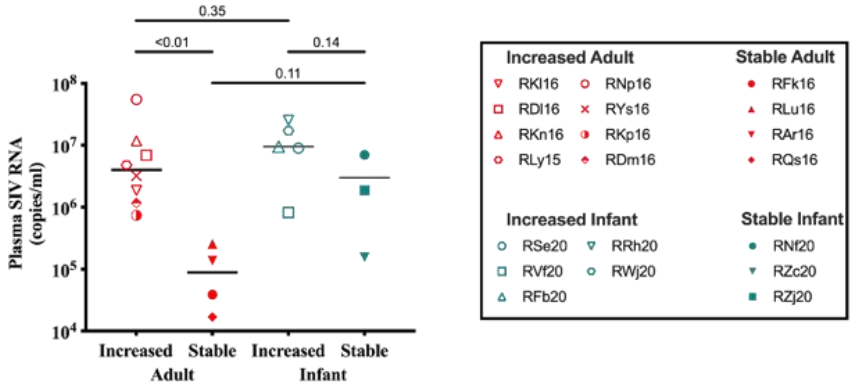

Figure 4.3. AZD5582 treatment and on-ART viremia in SIV-infected, ART-suppressed infant RMs. Longitudinal analysis of plasma SIV RNA levels during the intervention phase in (A) AZD5582 and (B) control groups. AZD5582 doses are indicated by green lines. The shaded

area represents ART treatment. The dashed line represents the limit of detection of the assay. (C) Comparison of on-ART viremia in SIV-infected, ART-treated infant macaques and SIV-infected, ART-treated adult macaques. (D) Comparison of pre-ART plasma viral loads in adult and infant RMs that experienced on-ART viremia during AZD5582 treatment (increased) or remained stably suppressed throughout AZD5582 treatment (stable). Solid line represents the median. Experimental groups were compared using a two-sided Mann-Whitney test.

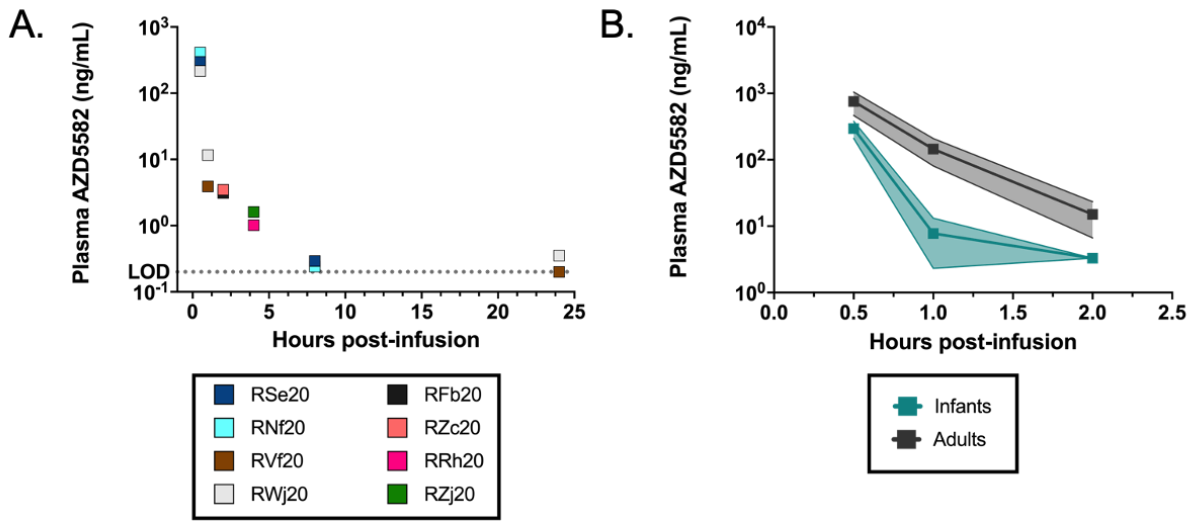

Figure 4.4. Pharmacokinetic assessment of AZD5582 in SIV-infected, ART-suppressed infant RMs. (A) AZD5582 (0.1 mg/kg) was administered by intravenous infusion and individual plasma concentrations are shown for the indicated time points (0.5h, n = 4; 1 - 24h, n = 2). (B) Plasma concentrations of AZD5582 in infant (teal) and adult (gray) SIV-infected, ART-suppressed RMs for indicated time points. Bars and shading represent mean ± SD.

Age Category	Cmax (ng/ml)	$AUC_{0\text{-}2h}$ (ng*hr/ml)	$AUC_{0\text{-}24h}$ (ng*hr/ml)	$T_{1/2}$ (hours)
Infant	294	223	239	9.9
Adult	802	512	n.d.	n.d.

Table 4.2. Pharmacokinetic properties of AZD5582 in infant compared to adult SIV-infected, ART-suppressed RMs. Cmax, maximum concentration; $T_{1/22}$, terminal elimination half-life; $AUC_{0\text{-}2h}$ and $AUC_{0\text{-}24h}$, area under the curve from time zero to 2 and 24 hours post infusion, respectively.

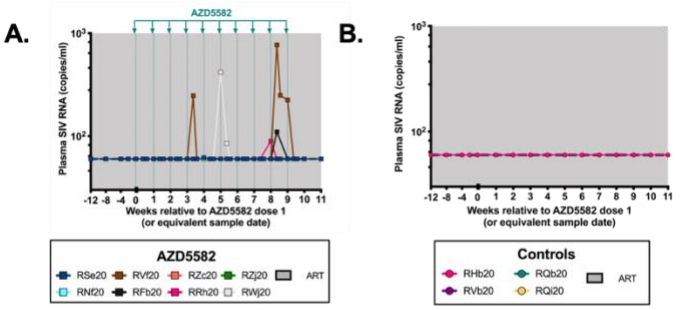

C.

SIV reactivation	Infant RMs	Adult RMs [17]
Per animal	5/8	5/9
	63%	*56%*
Events >60 copies/ml	8/135	64/140
	5.9%	*46%*
Peak on-ART viremia	771 copies/ml	1,390 copies/ml

D.

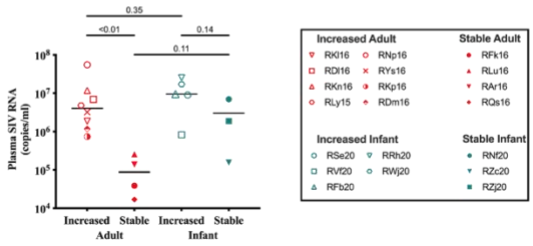

Figure 4.3. AZD5582 treatment result in reactivation of plasma viremia in SIV-infected, ART-suppressed infant RMs. Longitudinal analysis of plasma SIV RNA levels during intervention phase in (A) AZD5582 and (B) control RMs. The shaded area represents the period of ART treatment. (C) Table comparing on-ART viremia in SIV-infected, ART-treated infant macaques compared to SIV-infected, ART-treated adult macaques. (D) Comparison of pre-ART plasma viral loads in adult and infant RMs that experienced on-ART viremia during AZD5582 treatment (increased) or remained stably suppressed throughout treatment (stable). ($P < 0.05$ was considered significant).

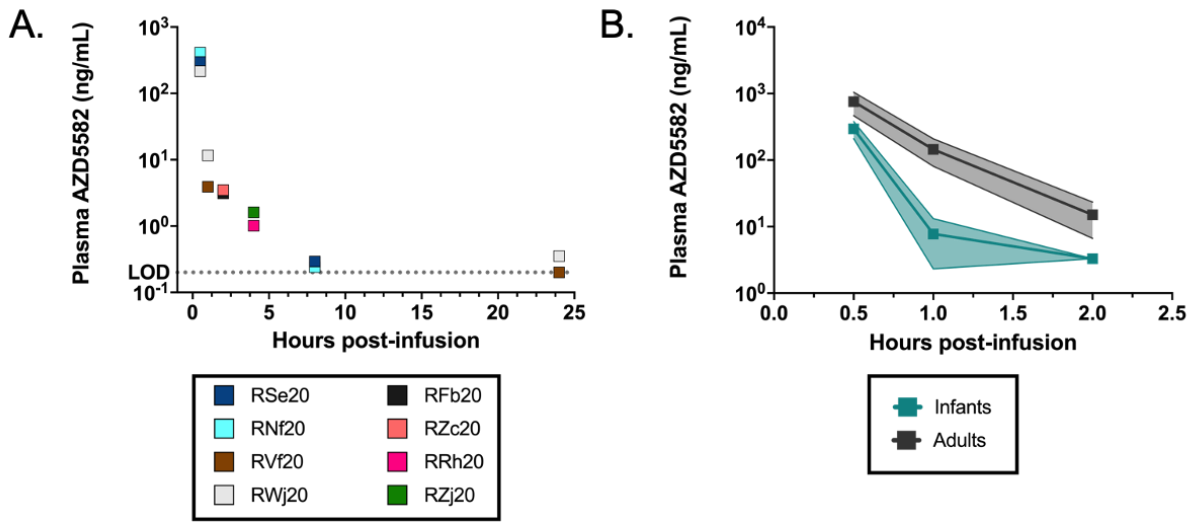

Figure 4.4. Pharmacokinetic assessment of AZD5582 in SIV-infected, ART-suppressed infant RMs. (A) AZD5582 (0.1 mg/kg) was administered by intravenous infusion and individual plasma concentrations are shown for the indicated time points.Bars represent mean ± SD.

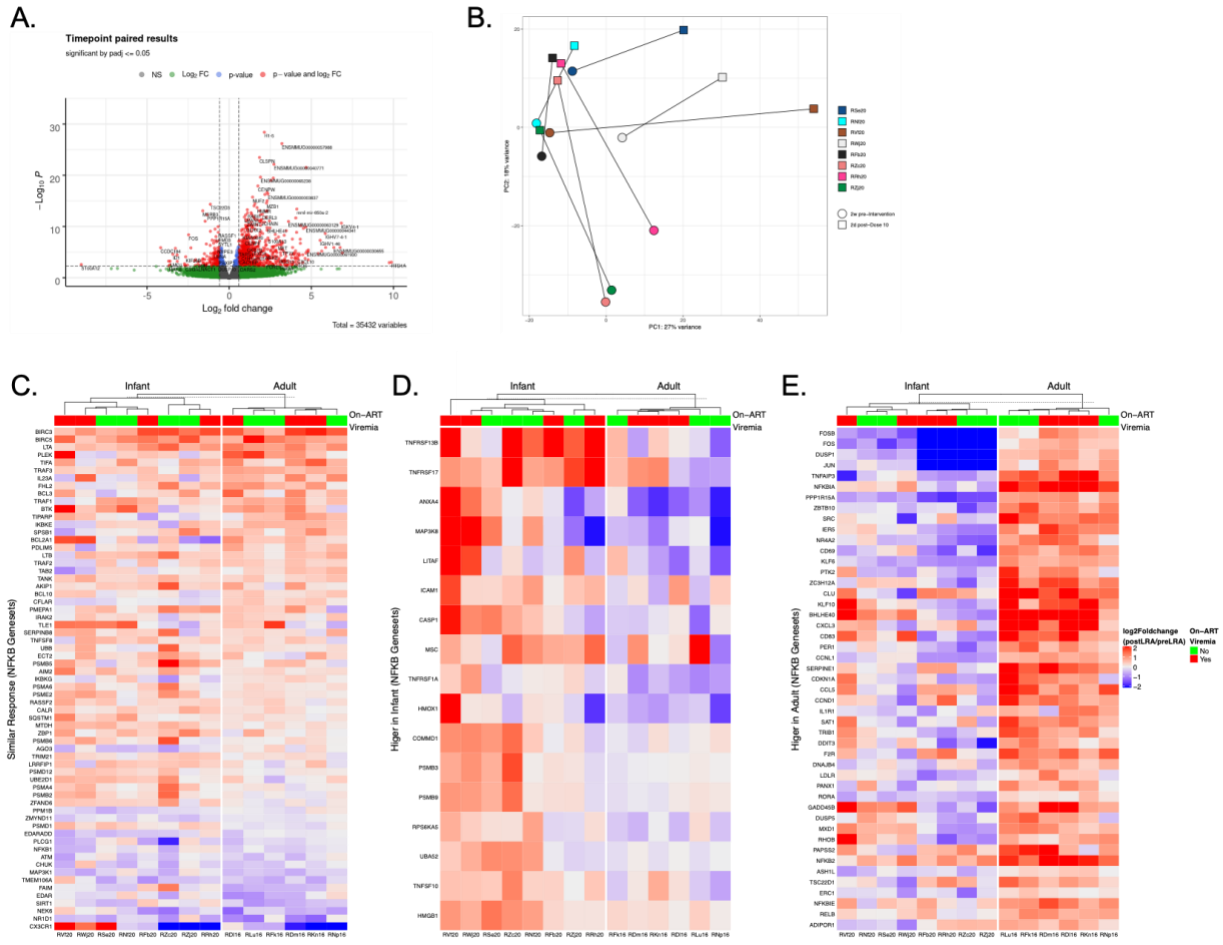

Figure 4.5. Gene expression changes in CD4+ T cells from peripheral blood of SIV-infected, ART-suppressed rhesus macaques before and after treatment with AZD5582. (A) Volcano plot showing genes up- or down-regulated in peripheral CD4+ T cells following AZD5582 treatment compared to pre-AZD5582 treatment of SIV-infected, ART-suppressed infant RMs. Log2-fold change is represented on x-axis and p-value is represented on y-axis. (B) Principal component (PC) analysis of the transcriptomes of CD4+ T cells from the peripheral blood before and after treatment with AZD5582. (C – E) Heat map of leading edge genes that were differentially expressed after AZD5582 treatment and were (C) similar between infant and adult SIV-infected, ART-suppressed RMs, (D) higher in SIV-infected, ART-suppressed infant RMs, or (E) higher in

SIV-infected, ART-suppressed adult RMs treated with AZD5582. Genes were identified in the leading edge of peripheral CD4+ T cell samples before and after treatment with AZD5582. The contrast depicted is the log2-fold change of each gene for each RM's post-treatment sample relative to the pre-treatment values for peripheral CD4+ T cells. Annotation indicates presence (red) or absence (green) of detectable on-ART viremia during AZD5582 treatment from pre-dose 1 to 3d post dose 10.

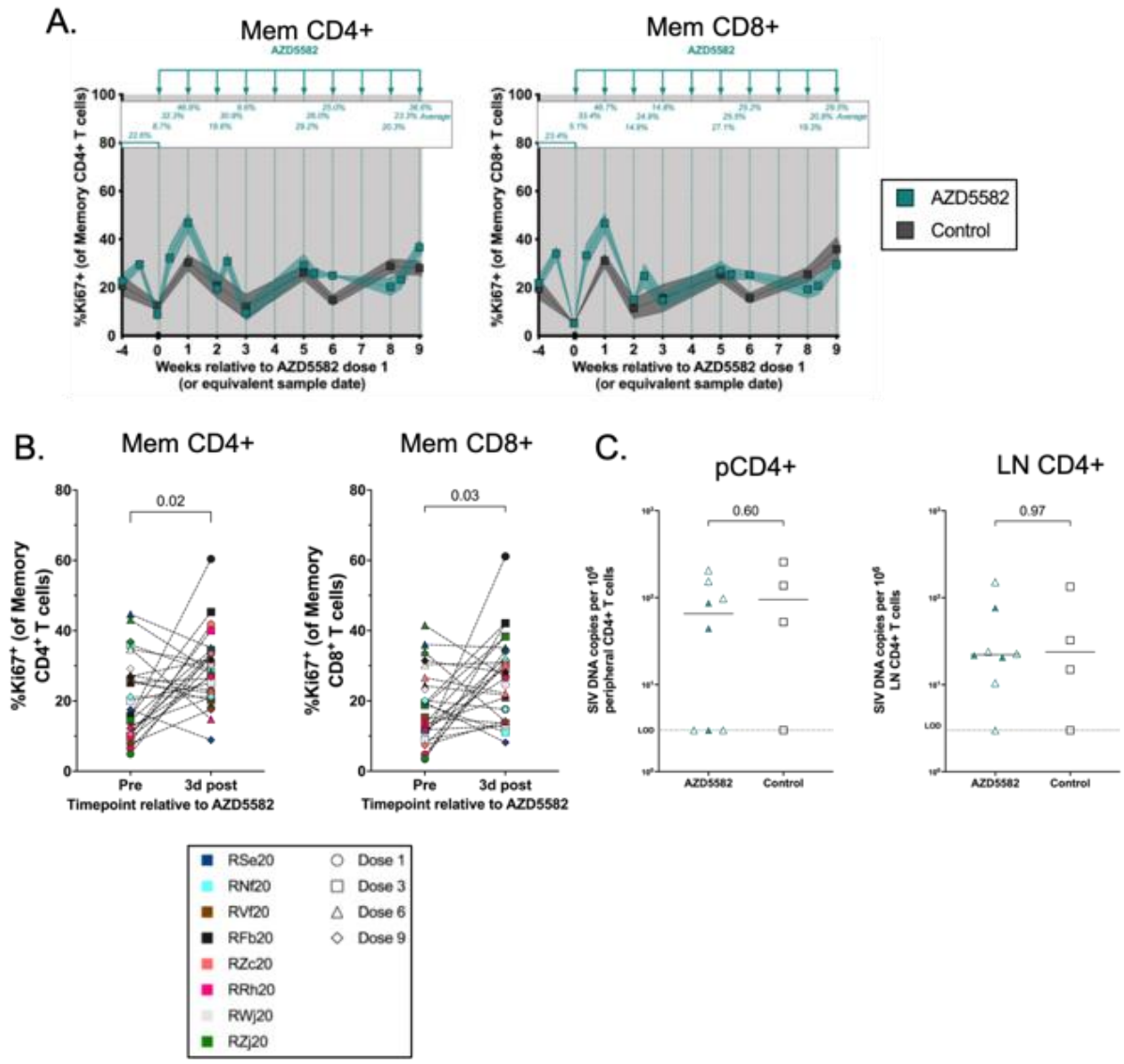

Figure 4.6. Immunologic and virologic response to repeated AZD5582 infusions in SIV-infected, ART-treated infant RMs. (A) Longitudinal analysis of Ki67 expression on memory CD4+ and memory CD8+ T cells in AZD5582-treated (teal, n = 8) and ART-only control (gray, n = 4) infant RMs. Mean of each timepoint is shown above except for baseline which is the mean of three timepoints. The shaded area represents the period of ART treatment and bars and shading represent mean ± SEM. (B) Frequency of Ki67+ peripheral memory CD4+ and memory CD8+ T

cells immediately prior to and 3 days post AZD5582 doses 1, 3, 6, and 9. Dose number is indicated by symbol shape and RM is indicated by symbol color. Statistical analysis was performed using a Wilcoxon matched-pairs signed rank test ($P < 0.05$ was considered significant). (C) Comparison of frequency of estimated SIV. (C) SIVgag DNA levels in peripheral and LN $CD4^+$ T cells post-after AZD5582 treatment (2 weeks post-dose 10) in AZD5582-treated and control RMs sampled after a similar time on ART as determined by PCR. Open symbols represent RMs that exhibited on-ART viremia and closed symbols represent animals that remained suppressed throughout treatment period. Dashed line represents the limit of detection (LOD) for the assay. Statistical analysis was performed using a two-sided Mann-Whitney test ($P < 0.05$ was considered significant).

Chapter Five: Discussion

Since the first described cases of unusual opportunistic infection and rare malignancies in five previously healthy, homosexual men in 1981 (1), later defined as AIDS, HIV-1 has claimed 36.3 million lives (5). While the field has come a long way with antiretroviral therapy dramatically improving the lives of individuals living with HIV-1; however, the latent viral reservoir persists despite suppression of viremia below detectable levels and therefore ART is not a cure. Not only are there comorbidities associated toHIV-1 and ART medications, there are also many limitations to ART. Approximately 16% of individuals living with HIV-1 do not know their status and are therefore not taking this life saving medication (5). Additionally, 70% of HIV-positive individuals reside in resource limited countries, such as Sub-Saharan Africa, where cost and availability influence adherence to ART. Finally, the stigma associated with HIV-1 can often prevent individuals from seeking out testing or medication even in high-resource areas. Identifying interventions for HIV-1 that reduce or eliminate the viral reservoir would be of great benefit.

Of those living with HIV-1, one of the arguably most at risk groups are children infected through the mother-to-child transmission route. Not only must children rely on a caretaker to receive proper medication and treatment, but disease progression to AIDS is much faster in children as approximately 50% of children not receiving ART die in their first two years of life (304). In 2020, only 54% of HIV-1infected children were accessing ART and 99,0000 of the estimated 680,000 AIDS related deaths were children under 15 years old (5).

Pediatric infection was brought to the spotlight in the mid-1980s when Ryan White, a young boy suffering from hemophilia, was diagnosed with AIDS on December 17, 1984 following a blood transfusion. Ryan White received national attention over his fight to attend school after his diagnosis and following his death, Congress enacted the Ryan White HIV/AIDS Program to improve the quality and availability of HIV care and treatment for low-income people living with HIV-1 (305).

Mother-to-child transmission in untreated HIV-1-infected woman not receiving ART ranges from 15% to 45%, but with proper screening and treatment transmission is highly preventable. Presently, the highest risk of transmission is in women that are acutely infected during pregnancy or through breastmilk transmission during infancy (200). Although pediatric infection has been on the decline since the turn of the century ultimately 150,000 new pediatric infections still occur annually (5). The developing pediatric immune system is dramatically different from that of an adult and as expected HIV-1 pathogenesis also differs in children when compared to adult infections. In addition to the altered transmission route, infants experience high peak viral acute loads, a slower decline to viral set point, and higher viral loads once set point is achieved. Finally, evidence from our lab indicates that in SIV- and SHIV-infected infant macaques the reservoir is dominated by naïve CD4+ T cells, a feature unique to pediatric infection that may influence pediatric cure strategies (149, 282). Despite these differences, pediatric HIV-1 cure clinical trials have been very limited with only 10 interventional trials initiated to date compared to over 200 adult HIV-1 cure related clinical trials (252). Of the trials to include infants and

children nearly half were focused on early ART intervention which is only feasible if infection is caught at birth and has demonstrated mixed results.

The work presented in this dissertation utilized a postnatal oral transmission route of SIV infection followed by ART suppression in infant rhesus macaques to evaluate promising cure interventions in a pediatric preclinical setting. Identifying strategies to reduce or eliminate the pediatric reservoir would be highly beneficial to the 1.8 million children living with HIV-1 globally. The work presented in this dissertation can be readily translated to inform future pediatric preclinical trials.

TLR agonists

TLR-7 agonists were selected as a strategy for SIV/HIV-1 cure given their ability to induce a potent immune response following activation of plasmacytoid dendritic cells. They have also demonstrated antiviral activity against hepatitis B virus (306-308). Lim *et al.* first reported that administration of the TLR-7 agonist, Vesatolimod, and its tool compound, GS-986, induced on-ART viremia and impacted the viral reservoir following removal of ART (245), but subsequent studies have failed to induce latency reversal with TLR-7 treatment either alone or in combination with additional therapeutic agents (169, 185, 246, 309). Despite lack of on-ART viremia reported in these later studies, the incorporation of a TLR-7 agonist to a combination strategy, either therapeutic vaccination or passive antibody administration, did improve viral rebound kinetics

after analytical treatment interruption. This finding suggests that even if TLR-7 does not serve as an effective LRA it still may have a purpose in HIV-1 combination cure. approaches perhaps by serving as an adjuvant that helps to activate the immune system and enhance the immunogenicity of additional therapeutic interventions. It is important to note that in both trials, ART was initiated early in infection which may have limited the size of the viral reservoir and influenced the positive outcome reported; however, animals that received a combination that included the TLR-7 agonist still fared better than animals that received early ART and were not treated with a TLR-7 agonist.

In this dissertation, we presented the results of the first *in vivo* evaluation of TLR-7 agonists in a pediatric setting (Chapter Two) and the results of that TLR-7 agonist in combination with a therapeutic vaccination (Chapter Three). We first performed a dose escalation evaluating oral administration of the TLR-7 agonist GS-986 at two dose concentrations in a small cohort of two macaques. In this dose escalation, we demonstrated that oral TLR-7 stimulation is well tolerated and induces expected pharmacodynamic immune responses at 24 hours post-dose with activation of monocytes and circulating macrophages and increased plasma concentrations of pro-inflammatory chemokines and cytokines. We next incorporated TLR-7 stimulation with a therapeutic vaccination in a larger cohort of SIV-infected, ART-treated infant macaques. The results of the therapeutic vaccination are discussed below. In addition to the anti-SIV immune response induced by vaccination, we did observe an increase in cellular activation of CD4+ T cells, CD8+ T cells, monocytes, and circulating macrophages following oral TLR-7 stimulation that was sustained through repeated dosing. A TLR-7 agonist has yet to be evaluated in a pediatric setting clinically, but these results indicate that should future clinical trials be conducted incorporation of

Vesatolimod is safe and immunogenic. However, as we did not observe a therapeutic benefit to GS-986 *in vivo* in the studies presented here, further NHP studies should confirm the efficacy of TLR-7 agonists, perhaps in an intervention that incorporates early ART, in a pediatric setting prior to transitioning to human clinical trials.

Therapeutic vaccination

A therapeutic vaccination administered to HIV-1 infected individuals during ART treatment may help the body's immune system to attack the infection allowing control or elimination of the virus following discontinuation of ART. There have been thirteen total adult HIV-1 clinical trials evaluating the impact of therapeutic vaccination, six ongoing and seven completed (252). The primary vaccine strategy utilized in HIV-1 cure is a heterologous prime-boost aimed at eliciting a potent humoral and cellular immunity through induction of an immune response to the antigen, which remains the same, and not the vector by which the antigen is delivered (310). These clinical trials have demonstrated that therapeutic vaccination is safe and generates varying degrees of immune responses, but thus far most have not shown an effect on rebound parameters, such as time to rebound or rebound set point viremia (311-313). These results imply that a therapeutic vaccination alone is unlikely to induce control necessary for a functional HIV-1 cure; however, the induction of anti-HIV-1 T cells following vaccination demonstrated in previous clinical trials implies that it may be effective in combination with other intervention strategies. Currently, a study is underway to evaluate therapeutic vaccination with the TLR-7

agonist vesatolimod in Spain, a similar study design to what we have presented in Chapter Three, but the results for that study are pending.

In infants, we demonstrated that therapeutic vaccination with an Ad48-prime and MVA-boost (both containing the same *Gag, Pol, Env* insert) in combination with repeated administration of an oral TLR-7 agonist resulted in a significant cellular and humoral anti-SIV immune response. Unlike what was previously reported in adults (169), in the infant macaques this immunogenic response did not correlate to a delay in time to rebound of a lower set point viremia once daily ART was removed. There were multiple variables in our study compared to the previous adult study that may have influenced the altered rebound kinetics including age of macaques, route and stock of viral challenge, and time to ART initiation. In our study, infant began ART at four weeks post infection compared to one week post infection in the adults which may have allowed more time for immune disruption and seeding of a larger viral reservoir. Many of the clinical trials that include a therapeutic vaccination have a selection criteria of early ART initiation and durable suppression prior to the interventional stage of the clinical trial with the idea that HIV-1 infected individuals that receive the vaccine will have a mostly intact immune response allowing them to form an optimal anti-HIV-1 immune response.

Currently there is one clinical trial underway (HVRICCANE) evaluating a DNA/MVA vaccination in with or without Cervarix, a TLR-4 agonist, in perinatally HIV-1-infected children and adolescents aged nine to twenty-one years (252). This is a Phase 1 proof of concept clinical trial aimed to evaluate the safety and efficacy of a therapeutic vaccination in HIV-1-infected youth

and although no analytic treatment interruption is planned for this clinical trial, it is a step in the right direction towards pediatric HIV-1 cure research.

"Shock" and "kill" HIV-1 cure strategies

The "shock" and "kill" approach to cure HIV-1 consists of combining an LRA to push the viral reservoir out of a state of latency, in the controlled setting of ART to prevent reservoir expansion, and a kill agent to aid the host immune system in clearing virally-infected, reactivated CD4+ T cells. Thirty-one clinical trials, ten ongoing and twenty-one completed, have included an LRA in their intervention strategy (252). All of these clinical trials to date have been restricted to HIV-1-infected adults over 18 years of age and thus far no LRA has been evaluated in a pediatric population. First generation LRAs, such as HDAC inhibitors, have not shown success in the clinic, (314), but so called recently identified second generation LRAs have shown strong, sustained on-ART viremia in adult rhesus macaques (286).

In this work, we demonstrate on-ART viremia up to 770 copies/ml in 63% of SIV-infected, ART-suppressed infant macaques following repeated administration of the SMAC mimetic AZD5582. Although on-ART viremia was low (60 – 110 copies/mL) in three AZD5582-treated infants, it was determined to be true reactivation of the latent viral reservoir as all treated animals were durably suppressed for over ten months prior to initiation of the experimental arm of this study. A major contrast between this study and a prior study following the same dose and regimen

of AZD5582 in SIV-infected, ART-suppressed adult macaques was a lower incidence of sustained viremia throughout the intervention phase with 6% of the total viral load measurements taken throughout the intervention in the five treated infants that had any on-ART viremia above the limit of detection of the assay compared to nearly 50% in adult macaques that had on-ART viremia.

We hypothesize that these results may be due to a number of factors. We first investigated if activation of the noncanonical NF-κB pathway was altered following AZD5582 stimulation *ex vivo* in naïve compared to memory CD4+ T cells. It is known that naïve CD4+ T cells predominately rely on canonical NF-κB signaling while memory CD4+ T cells rely on the noncanonical NF-κB pathway (293), but AZD5582 is a small molecule that acts upon proteins that are equally expressed between naïve and memory CD4+ T cells. In the present study, we saw similar expression of BIRC3 and NFKB2 following *ex vivo* stimulation with AZD5582 in naïve and memory CD4+ T cells indicating that CD4+ T cells have the potential to upregulate the noncanonical NF-κB pathway regardless of differentiation status. We did, however, demonstrate through transcriptomic profiling that some noncanonical NF-κB genes, such as RELB and NFKB2 were significantly upregulated in adult, but not infant CD4+ T cells following *in vivo* AZD5582 treatment. Finally, through quantification of plasma AZD5582 we demonstrate altered pharmacokinetics in infants compared to treated adult macaques.

Ultimately, the results presented in Chapter Four are likely due to a combination of the above factors. Future studies in this area should: 1) optimize the *in vivo* potential of AZD5582 in SIV-infected, ART-suppressed infant macaques by testing altered dose concentrations and infusion

times; 2) investigate the reactivation potential of the latent pediatric reservoir *in vitro*; and 3) evaluate LRAs targeted towards the unique features of the pediatric reservoir. such as therapeutics that specifically activate infected naïve CD4+ T cells. In the present study, we demonstrate through pharmacokinetic analysis of plasma AZD5582 that infants metabolize this drug faster than their adult counterparts. Through modeling, we predict that a longer infusion time of 45 minutes rather than the 30 minutes used in previous studies may create a Cmax closer to what was observed in SIV-infected, ART-suppressed adults treated with AZD5582. Additionally, as this drug was safe in the infants with no adverse clinical reactions, a dose escalation of the drug testing higher concentrations may reveal stronger virologic efficacy.

Ex vivo and *in vitro* investigation of LRAs on CD4+ T cells would help to fully understand the reactivation potential of the latent pediatric reservoir. On this avenue, Dhummakupt *et al.* using the Tat/Rev induced limited dilution assay have demonstrated that cells isolated from perinatally infected individuals are slower to reactivate and require more stimulation than cells isolated from individuals infected in adulthood (272). We have demonstrated that naïve CD4+ T cells are an important component of the pediatric reservoir of SIV- and SHIV-infected infant macaques (149, 282). Naïve CD4+ T cells have been shown to produce less infectious virus following *in vitro* and *ex vivo* stimulation compared to more differentiated memory CD4+ T cells (296, 297), but it is currently unclear if latency is deeper in the reservoir of HIV-1 infected children compared to memory CD4+ T cells that compose the traditional viral reservoir of adults *in vivo* or if other factors, such as the tolerogenic pediatric immune system, are the reason for these differences. As described above, we demonstrate that both naïve and memory CD4+ T cells from SIV-infected,

ART-suppressed infant macaques upregulate the noncanonical NF-κB genes BIRC3 and NFKB2; however, viral reactivation following stimulation with an LRA in these different subsets has yet to be explored and is an area of research that would be highly informative. Identification and optimization of an effective LRA strategy in perinatally infected individuals may require consideration of these factors that make pediatric infection unique. As we gain further understanding in this area, intervention strategies targeted towards the unique features may demonstrate optimal results.

Conclusion

Following the discovery of HIV-1 by Dr. Gallo at the National Cancer Institute and Dr. Montagnier at the Pasteur Institute in 1984, the then Health and Human Services Secretary, Margaret Heckler, expressed hope that we would have a vaccine within two years to help curb the epidemic (315). Nearly forty years later there have been promising steps in the HIV-1 cure field including achieving a functional cure in two HIV-1-positive individuals Timothy Ray Brown, the Berlin patient (154), and Adam Castillejo, the London patient (155). Additionally, there have been reports of sustained control of viremia following ART discontinuation in children who received early ART after birth (233, 316, 317). However, we still have a long way to go in terms of a realistic cure for the 37.7 million individuals living with HIV-1.

Cumulatively, the work presented in this thesis provides key pre-clinical data in a relevant pediatric model that can be used to inform future pediatric clinical trials. Importantly, we show that HIV-1/SIV cure interventions induce a different immunologic and virologic response in SIV-infected, ART-treated infants compared to SIV-infected, ART-treated adults, likely due to their developing immune system, altered pathogenesis, and differences in the viral reservoir. While these results are not surprising, testing and understanding them in a preclinical setting informs clinical trials saving time, money, and resources. Future studies must continue to test interventions in a pediatric setting to properly estimate how this unique population will respond and optimal cure strategies for children living with HIV-1 may need to target this unique system.

As there have been over 4.6 million COVID-19-related deaths as of September 2021 (318), it feels important to close with a note on how the current pandemic has affected other diseases that pose an enormous global health burden, such as HIV-1. Although COVID-19 does not seem to impact children as strongly as it is affecting adults (319), people living with HIV-1 are at higher risk for COVID-19 and the pandemic has slowed down access to HIV-1 testing and treatment (320).(320). Not only is the risk of dying from COVID-19 in HIV-1-infected individuals is twice that of the general population, but the majority of people living with HIV-1 are located in Sub-Saharan Africa where less than 3% of people have received at least one dose of a COVID-19 vaccine as of July 2021 (5).

During the first lockdown the Global Fund to Fight AIDS, Tuberculosis, and Malaria reported that HIV-1 testing declined by 41% and diagnosis and treatment referrals declined by

37% according to data collected in 32 African and Asian countries (5). Early modeling predicted that if services to prevent mother-to-child transmission of HIV-1 were disrupted for six months, the estimated increases in new pediatric HIV-1 infections for Malawi, Uganda, and Zimbabwe would be 162%, 139%, and 106%, respectively. Although the UNAIDS estimate for new pediatric infections in 2020 remained stable at 150,000 (5), this report is likely an underestimate due to the decline in testing caused by the pandemic. This global disruption is yet another reminder of why we need an HIV-1 cure.

Currently, HIV-1 cure clinical trials in children are very limited. Of the ten total clinical trials: three investigate the effect of early ART, three examine the impact of administration of antibodies such as VRC01, two focus on evaluating the impact of stem cell transplantation, and the final two use a combination strategy of early ART combined with VRC01 or a therapeutic vaccine with a TLR4 agonist (252). Gene therapies, immune checkpoint inhibitors, and LRAs are all among the HIV-1 cure clinical trial strategies that have yet to be evaluated in children.

List of Important Abbreviations

AIDS	Acquired Immune Deficiency Syndrome
ART	Antiretroviral Therapy
ATI	Analytical Treatment Interruption
bnAbs	Broadly Neutralizing Antibodies
HIV	Human Immunodeficiency Virus
HLA	Human Leukocyte Antigen
LN	Lymph Node
LRA	Latency Reversing Agent
MVA	Modified Vaccinia Ankara
MTCT	Mother-to-Child Transmission
NFkB	Nuclear Factor k-Light-Chain Enhancer of Activated B Cells
NHP	Non-Human Primate
PBMC	Peripheral Blood Mononuclear Cell
RM	Rhesus Macaque
SHIV	Simian-Human Immunodeficiency Virus
SIV	Simian Immunodeficiency Virus
TLR-7	Toll Like Receptor 7
WHO	World Health Organization

References

1. Centers for Disease C. Kaposi's sarcoma and Pneumocystis pneumonia among homosexual men--New York City and California. MMWR Morb Mortal Wkly Rep. 1981;30(25):305-8. Epub 1981/07/03. PubMed PMID: 6789108.
2. Haverkos HW, Curran JW. The current outbreak of Kaposi's sarcoma and opportunistic infections. CA Cancer J Clin. 1982;32(6):330-9. Epub 1982/11/01. PubMed PMID: 6812892.
3. Barre-Sinoussi F, Chermann JC, Rey F, Nugeyre MT, Chamaret S, Gruest J, Dauguet C, Axler-Blin C, Vezinet-Brun F, Rouzioux C, Rozenbaum W, Montagnier L. Isolation of a T-lymphotropic retrovirus from a patient at risk for acquired immune deficiency syndrome (AIDS). Science. 1983;220(4599):868-71. Epub 1983/05/20. PubMed PMID: 6189183.
4. [11/26/2018]. Available from: http://www.unaids.org/sites/default/files/media_asset/unaids-data-2018_en.pdf.
5. [06/11/2021]. Available from: https://www.unaids.org/en/resources/fact-sheet.
6. Sharp PM, Hahn BH. Origins of HIV and the AIDS pandemic. Cold Spring Harb Perspect Med. 2011;1(1):a006841. Epub 2012/01/10. doi: 10.1101/cshperspect.a006841. PubMed PMID: 22229120; PMCID: PMC3234451.
7. Gao F, Bailes E, Robertson DL, Chen Y, Rodenburg CM, Michael SF, Cummins LB, Arthur LO, Peeters M, Shaw GM, Sharp PM, Hahn BH. Origin of HIV-1 in the chimpanzee Pan troglodytes troglodytes. Nature. 1999;397(6718):436-41. Epub 1999/02/16. doi: 10.1038/17130. PubMed PMID: 9989410.
8. Huet T, Cheynier R, Meyerhans A, Roelants G, Wain-Hobson S. Genetic organization of a chimpanzee lentivirus related to HIV-1. Nature. 1990;345(6273):356-9. Epub 1990/05/24. doi: 10.1038/345356a0. PubMed PMID: 2188136.
9. Hahn BH, Shaw GM, De Cock KM, Sharp PM. AIDS as a zoonosis: scientific and public health implications. Science. 2000;287(5453):607-14. Epub 2000/01/29. PubMed PMID: 10649986.
10. Peeters M, Courgnaud V, Abela B, Auzel P, Pourrut X, Bibollet-Ruche F, Loul S, Liegeois F, Butel C, Koulagna D, Mpoudi-Ngole E, Shaw GM, Hahn BH, Delaporte E. Risk to human health from a plethora of simian immunodeficiency viruses in primate bushmeat. Emerg Infect Dis. 2002;8(5):451-7. Epub 2002/05/09. doi: 10.3201/eid0805.010522. PubMed PMID: 11996677; PMCID: PMC2732488.
11. De Leys R, Vanderborght B, Vanden Haesevelde M, Heyndrickx L, van Geel A, Wauters C, Bernaerts R, Saman E, Nijs P, Willems B, et al. Isolation and partial characterization of an unusual human immunodeficiency retrovirus from two persons of west-central African origin. J Virol. 1990;64(3):1207-16. Epub 1990/03/01. PubMed PMID: 2304140; PMCID: PMC249235.
12. Gurtler LG, Hauser PH, Eberle J, von Brunn A, Knapp S, Zekeng L, Tsague JM, Kaptue L. A new subtype of human immunodeficiency virus type 1 (MVP-5180) from Cameroon. J Virol. 1994;68(3):1581-5. Epub 1994/03/01. PubMed PMID: 8107219; PMCID: PMC236615.
13. Worobey M, Gemmel M, Teuwen DE, Haselkorn T, Kunstman K, Bunce M, Muyembe JJ, Kabongo JM, Kalengayi RM, Van Marck E, Gilbert MT, Wolinsky SM. Direct evidence of extensive diversity of HIV-1 in Kinshasa by 1960. Nature. 2008;455(7213):661-4. Epub 2008/10/04. doi: 10.1038/nature07390. PubMed PMID: 18833279; PMCID: PMC3682493.
14. Taylor BS, Hammer SM. The challenge of HIV-1 subtype diversity. N Engl J Med. 2008;359(18):1965-6. Epub 2008/10/31. doi: 10.1056/NEJMc086373. PubMed PMID: 18971501.
15. Gilbert MT, Rambaut A, Wlasiuk G, Spira TJ, Pitchenik AE, Worobey M. The emergence of HIV/AIDS in the Americas and beyond. Proc Natl Acad Sci U S A. 2007;104(47):18566-70. Epub 2007/11/06. doi: 10.1073/pnas.0705329104. PubMed PMID: 17978186; PMCID: PMC2141817.

16. Kiwanuka N, Robb M, Laeyendecker O, Kigozi G, Wabwire-Mangen F, Makumbi FE, Nalugoda F, Kagaayi J, Eller M, Eller LA, Serwadda D, Sewankambo NK, Reynolds SJ, Quinn TC, Gray RH, Wawer MJ, Whalen CC. HIV-1 viral subtype differences in the rate of CD4+ T-cell decline among HIV seroincident antiretroviral naive persons in Rakai district, Uganda. J Acquir Immune Defic Syndr. 2010;54(2):180-4. Epub 2009/12/17. doi: 10.1097/QAI.0b013e3181c98fc0. PubMed PMID: 20010433; PMCID: PMC2877752.
17. Baeten JM, Chohan B, Lavreys L, Chohan V, McClelland RS, Certain L, Mandaliya K, Jaoko W, Overbaugh J. HIV-1 subtype D infection is associated with faster disease progression than subtype A in spite of similar plasma HIV-1 loads. J Infect Dis. 2007;195(8):1177-80. Epub 2007/03/16. doi: 10.1086/512682. PubMed PMID: 17357054.
18. Hirsch VM, Olmsted RA, Murphey-Corb M, Purcell RH, Johnson PR. An African primate lentivirus (SIVsm) closely related to HIV-2. Nature. 1989;339(6223):389-92. Epub 1989/06/01. doi: 10.1038/339389a0. PubMed PMID: 2786147.
19. Berry N, Jaffar S, Schim van der Loeff M, Ariyoshi K, Harding E, N'Gom PT, Dias F, Wilkins A, Ricard D, Aaby P, Tedder R, Whittle H. Low level viremia and high CD4% predict normal survival in a cohort of HIV type-2-infected villagers. AIDS Res Hum Retroviruses. 2002;18(16):1167-73. Epub 2002/12/19. doi: 10.1089/08892220260387904. PubMed PMID: 12487822.
20. Popper SJ, Sarr AD, Gueye-Ndiaye A, Mboup S, Essex ME, Kanki PJ. Low plasma human immunodeficiency virus type 2 viral load is independent of proviral load: low virus production in vivo. J Virol. 2000;74(3):1554-7. Epub 2000/01/11. PubMed PMID: 10627569; PMCID: PMC111493.
21. Bhatia S, Patil SS, Sood R. Bovine immunodeficiency virus: a lentiviral infection. Indian J Virol. 2013;24(3):332-41. Epub 2014/01/16. doi: 10.1007/s13337-013-0165-9. PubMed PMID: 24426295; PMCID: PMC3832697.
22. Kanzaki LI, Looney DJ. Feline immunodeficiency virus: a concise review. Front Biosci. 2004;9:370-7. Epub 2004/02/10. PubMed PMID: 14766374.
23. Greenberg ME, Iafrate AJ, Skowronski J. The SH3 domain-binding surface and an acidic motif in HIV-1 Nef regulate trafficking of class I MHC complexes. EMBO J. 1998;17(10):2777-89. Epub 1998/06/10. doi: 10.1093/emboj/17.10.2777. PubMed PMID: 9582271; PMCID: PMC1170618.
24. Le Gall S, Buseyne F, Trocha A, Walker BD, Heard JM, Schwartz O. Distinct trafficking pathways mediate Nef-induced and clathrin-dependent major histocompatibility complex class I down-regulation. J Virol. 2000;74(19):9256-66. Epub 2000/09/12. PubMed PMID: 10982373; PMCID: PMC102125.
25. Piguet V, Wan L, Borel C, Mangasarian A, Demaurex N, Thomas G, Trono D. HIV-1 Nef protein binds to the cellular protein PACS-1 to downregulate class I major histocompatibility complexes. Nat Cell Biol. 2000;2(3):163-7. Epub 2000/03/09. doi: 10.1038/35004038. PubMed PMID: 10707087; PMCID: PMC1475706.
26. Wilen CB, Tilton JC, Doms RW. HIV: cell binding and entry. Cold Spring Harb Perspect Med. 2012;2(8). Epub 2012/08/22. doi: 10.1101/cshperspect.a006866. PubMed PMID: 22908191; PMCID: PMC3405824.
27. Feng Y, Broder CC, Kennedy PE, Berger EA. HIV-1 entry cofactor: functional cDNA cloning of a seven-transmembrane, G protein-coupled receptor. Science. 1996;272(5263):872-7. Epub 1996/05/10. PubMed PMID: 8629022.
28. Deng H, Liu R, Ellmeier W, Choe S, Unutmaz D, Burkhart M, Di Marzio P, Marmon S, Sutton RE, Hill CM, Davis CB, Peiper SC, Schall TJ, Littman DR, Landau NR. Identification of a major co-receptor for primary isolates of HIV-1. Nature. 1996;381(6584):661-6. Epub 1996/06/20. doi: 10.1038/381661a0. PubMed PMID: 8649511.

29. Dragic T, Litwin V, Allaway GP, Martin SR, Huang Y, Nagashima KA, Cayanan C, Maddon PJ, Koup RA, Moore JP, Paxton WA. HIV-1 entry into CD4+ cells is mediated by the chemokine receptor CC-CKR-5. Nature. 1996;381(6584):667-73. Epub 1996/06/20. doi: 10.1038/381667a0. PubMed PMID: 8649512.
30. Li WH, Tanimura M, Sharp PM. Rates and dates of divergence between AIDS virus nucleotide sequences. Mol Biol Evol. 1988;5(4):313-30. Epub 1988/07/01. doi: 10.1093/oxfordjournals.molbev.a040503. PubMed PMID: 3405075.
31. Mitchell RS, Beitzel BF, Schroder AR, Shinn P, Chen H, Berry CC, Ecker JR, Bushman FD. Retroviral DNA integration: ASLV, HIV, and MLV show distinct target site preferences. PLoS Biol. 2004;2(8):E234. Epub 2004/08/18. doi: 10.1371/journal.pbio.0020234. PubMed PMID: 15314653; PMCID: PMC509299.
32. Lusic M, Siliciano RF. Nuclear landscape of HIV-1 infection and integration. Nat Rev Microbiol. 2017;15(2):69-82. Epub 2016/12/13. doi: 10.1038/nrmicro.2016.162. PubMed PMID: 27941817.
33. Sundquist WI, Krausslich HG. HIV-1 assembly, budding, and maturation. Cold Spring Harb Perspect Med. 2012;2(7):a006924. Epub 2012/07/05. doi: 10.1101/cshperspect.a006924. PubMed PMID: 22762019; PMCID: PMC3385941.
34. Korber B, Gaschen B, Yusim K, Thakallapally R, Kesmir C, Detours V. Evolutionary and immunological implications of contemporary HIV-1 variation. Br Med Bull. 2001;58:19-42. Epub 2001/11/21. PubMed PMID: 11714622.
35. Ronen K, McCoy CO, Matsen FA, Boyd DF, Emery S, Odem-Davis K, Jaoko W, Mandaliya K, McClelland RS, Richardson BA, Overbaugh J. HIV-1 superinfection occurs less frequently than initial infection in a cohort of high-risk Kenyan women. PLoS Pathog. 2013;9(8):e1003593. Epub 2013/09/07. doi: 10.1371/journal.ppat.1003593. PubMed PMID: 24009513; PMCID: PMC3757054.
36. Shaw GM, Hunter E. HIV transmission. Cold Spring Harb Perspect Med. 2012;2(11). Epub 2012/10/09. doi: 10.1101/cshperspect.a006965. PubMed PMID: 23043157; PMCID: PMC3543106.
37. Dodd RY, Notari EP, Nelson D, Foster GA, Krysztof DE, Kaidarova Z, Milan-Benson L, Kessler DA, Shaz BH, Vahidnia F, Custer B, Stramer SL, Nhlbi Retrovirus Epidemiology Donor Study I. Development of a multisystem surveillance database for transfusion-transmitted infections among blood donors in the United States. Transfusion. 2016;56(11):2781-9. Epub 2016/08/26. doi: 10.1111/trf.13759. PubMed PMID: 27557553.
38. Milman G, Sharma O. Mechanisms of HIV/SIV mucosal transmission. AIDS Res Hum Retroviruses. 1994;10(10):1305-12. Epub 1994/10/01. doi: 10.1089/aid.1994.10.1305. PubMed PMID: 7848686.
39. Moutsopoulos NM, Greenwell-Wild T, Wahl SM. Differential mucosal susceptibility in HIV-1 transmission and infection. Adv Dent Res. 2006;19(1):52-6. Epub 2006/05/05. doi: 10.1177/154407370601900111. PubMed PMID: 16672550.
40. Derdeyn CA, Decker JM, Bibollet-Ruche F, Mokili JL, Muldoon M, Denham SA, Heil ML, Kasolo F, Musonda R, Hahn BH, Shaw GM, Korber BT, Allen S, Hunter E. Envelope-constrained neutralization-sensitive HIV-1 after heterosexual transmission. Science. 2004;303(5666):2019-22. Epub 2004/03/27. doi: 10.1126/science.1093137. PubMed PMID: 15044802.
41. Veazey RS, DeMaria M, Chalifoux LV, Shvetz DE, Pauley DR, Knight HL, Rosenzweig M, Johnson RP, Desrosiers RC, Lackner AA. Gastrointestinal tract as a major site of CD4+ T cell depletion and viral replication in SIV infection. Science. 1998;280(5362):427-31. Epub 1998/05/09. PubMed PMID: 9545219.
42. Miller CJ, Li Q, Abel K, Kim EY, Ma ZM, Wietgrefe S, La Franco-Scheuch L, Compton L, Duan L, Shore MD, Zupancic M, Busch M, Carlis J, Wolinsky S, Haase AT. Propagation and dissemination of infection after vaginal transmission of simian immunodeficiency virus. J Virol. 2005;79(14):9217-27. Epub 2005/07/05. doi: 10.1128/JVI.79.14.9217-9227.2005. PubMed PMID: 15994816; PMCID: PMC1168785.

43. Gartner S, Markovits P, Markovitz DM, Kaplan MH, Gallo RC, Popovic M. The role of mononuclear phagocytes in HTLV-III/LAV infection. Science. 1986;233(4760):215-9. Epub 1986/07/11. doi: 10.1126/science.3014648. PubMed PMID: 3014648.
44. Meltzer MS, Gendelman HE. Mononuclear phagocytes as targets, tissue reservoirs, and immunoregulatory cells in human immunodeficiency virus disease. Curr Top Microbiol Immunol. 1992;181:239-63. Epub 1992/01/01. doi: 10.1007/978-3-642-77377-8_9. PubMed PMID: 1424782.
45. Berger EA, Murphy PM, Farber JM. Chemokine receptors as HIV-1 coreceptors: roles in viral entry, tropism, and disease. Annu Rev Immunol. 1999;17:657-700. Epub 1999/06/08. doi: 10.1146/annurev.immunol.17.1.657. PubMed PMID: 10358771.
46. Connor RI, Sheridan KE, Ceradini D, Choe S, Landau NR. Change in coreceptor use correlates with disease progression in HIV-1--infected individuals. J Exp Med. 1997;185(4):621-8. Epub 1997/02/17. PubMed PMID: 9034141; PMCID: PMC2196142.
47. Schuitemaker H, Koot M, Kootstra NA, Dercksen MW, de Goede RE, van Steenwijk RP, Lange JM, Schattenkerk JK, Miedema F, Tersmette M. Biological phenotype of human immunodeficiency virus type 1 clones at different stages of infection: progression of disease is associated with a shift from monocytotropic to T-cell-tropic virus population. J Virol. 1992;66(3):1354-60. Epub 1992/03/01. PubMed PMID: 1738194; PMCID: PMC240857.
48. Tersmette M, Gruters RA, de Wolf F, de Goede RE, Lange JM, Schellekens PT, Goudsmit J, Huisman HG, Miedema F. Evidence for a role of virulent human immunodeficiency virus (HIV) variants in the pathogenesis of acquired immunodeficiency syndrome: studies on sequential HIV isolates. J Virol. 1989;63(5):2118-25. Epub 1989/05/01. doi: 10.1128/JVI.63.5.2118-2125.1989. PubMed PMID: 2564898; PMCID: PMC250628.
49. Liu R, Paxton WA, Choe S, Ceradini D, Martin SR, Horuk R, MacDonald ME, Stuhlmann H, Koup RA, Landau NR. Homozygous defect in HIV-1 coreceptor accounts for resistance of some multiply-exposed individuals to HIV-1 infection. Cell. 1996;86(3):367-77. Epub 1996/08/09. PubMed PMID: 8756719.
50. Trecarichi EM, Tumbarello M, de Gaetano Donati K, Tamburrini E, Cauda R, Brahe C, Tiziano FD. Partial protective effect of CCR5-Delta 32 heterozygosity in a cohort of heterosexual Italian HIV-1 exposed uninfected individuals. AIDS Res Ther. 2006;3:22. Epub 2006/09/27. doi: 10.1186/1742-6405-3-22. PubMed PMID: 16999868; PMCID: PMC1592103.
51. Migueles SA, Sabbaghian MS, Shupert WL, Bettinotti MP, Marincola FM, Martino L, Hallahan CW, Selig SM, Schwartz D, Sullivan J, Connors M. HLA B*5701 is highly associated with restriction of virus replication in a subgroup of HIV-infected long term nonprogressors. Proc Natl Acad Sci U S A. 2000;97(6):2709-14. Epub 2000/03/01. doi: 10.1073/pnas.050567397. PubMed PMID: 10694578; PMCID: PMC15994.
52. Mendoza D, Royce C, Ruff LE, Ambrozak DR, Quigley MF, Dang T, Venturi V, Price DA, Douek DC, Migueles SA, Connors M. HLA B*5701-positive long-term nonprogressors/elite controllers are not distinguished from progressors by the clonal composition of HIV-specific CD8+ T cells. J Virol. 2012;86(7):4014-8. Epub 2012/01/27. doi: 10.1128/JVI.06982-11. PubMed PMID: 22278241; PMCID: PMC3302536.
53. Miura T, Brockman MA, Schneidewind A, Lobritz M, Pereyra F, Rathod A, Block BL, Brumme ZL, Brumme CJ, Baker B, Rothchild AC, Li B, Trocha A, Cutrell E, Frahm N, Brander C, Toth I, Arts EJ, Allen TM, Walker BD. HLA-B57/B*5801 human immunodeficiency virus type 1 elite controllers select for rare gag variants associated with reduced viral replication capacity and strong cytotoxic T-lymphocyte [corrected] recognition. J Virol. 2009;83(6):2743-55. Epub 2009/01/01. doi: 10.1128/JVI.02265-08. PubMed PMID: 19116253; PMCID: PMC2648254.

54. Brenchley JM, Schacker TW, Ruff LE, Price DA, Taylor JH, Beilman GJ, Nguyen PL, Khoruts A, Larson M, Haase AT, Douek DC. CD4+ T cell depletion during all stages of HIV disease occurs predominantly in the gastrointestinal tract. J Exp Med. 2004;200(6):749-59. Epub 2004/09/15. doi: 10.1084/jem.20040874. PubMed PMID: 15365096; PMCID: PMC2211962.
55. Douek DC, Brenchley JM, Betts MR, Ambrozak DR, Hill BJ, Okamoto Y, Casazza JP, Kuruppu J, Kunstman K, Wolinsky S, Grossman Z, Dybul M, Oxenius A, Price DA, Connors M, Koup RA. HIV preferentially infects HIV-specific CD4+ T cells. Nature. 2002;417(6884):95-8. Epub 2002/05/03. doi: 10.1038/417095a. PubMed PMID: 11986671.
56. Borrow P, Lewicki H, Hahn BH, Shaw GM, Oldstone MB. Virus-specific CD8+ cytotoxic T-lymphocyte activity associated with control of viremia in primary human immunodeficiency virus type 1 infection. J Virol. 1994;68(9):6103-10. Epub 1994/09/01. PubMed PMID: 8057491; PMCID: PMC237022.
57. Koup RA, Safrit JT, Cao Y, Andrews CA, McLeod G, Borkowsky W, Farthing C, Ho DD. Temporal association of cellular immune responses with the initial control of viremia in primary human immunodeficiency virus type 1 syndrome. J Virol. 1994;68(7):4650-5. Epub 1994/07/01. PubMed PMID: 8207839; PMCID: PMC236393.
58. Time from HIV-1 seroconversion to AIDS and death before widespread use of highly-active antiretroviral therapy: a collaborative re-analysis. Collaborative Group on AIDS Incubation and HIV Survival including the CASCADE EU Concerted Action. Concerted Action on SeroConversion to AIDS and Death in Europe. Lancet. 2000;355(9210):1131-7. Epub 2000/05/03. PubMed PMID: 10791375.
59. Korn T, Bettelli E, Gao W, Awasthi A, Jager A, Strom TB, Oukka M, Kuchroo VK. IL-21 initiates an alternative pathway to induce proinflammatory T(H)17 cells. Nature. 2007;448(7152):484-7. Epub 2007/06/22. doi: 10.1038/nature05970. PubMed PMID: 17581588; PMCID: PMC3805028.
60. Lozupone CA, Li M, Campbell TB, Flores SC, Linderman D, Gebert MJ, Knight R, Fontenot AP, Palmer BE. Alterations in the gut microbiota associated with HIV-1 infection. Cell Host Microbe. 2013;14(3):329-39. Epub 2013/09/17. doi: 10.1016/j.chom.2013.08.006. PubMed PMID: 24034618; PMCID: PMC3864811.
61. Mutlu EA, Keshavarzian A, Losurdo J, Swanson G, Siewe B, Forsyth C, French A, Demarais P, Sun Y, Koenig L, Cox S, Engen P, Chakradeo P, Abbasi R, Gorenz A, Burns C, Landay A. A compositional look at the human gastrointestinal microbiome and immune activation parameters in HIV infected subjects. PLoS Pathog. 2014;10(2):e1003829. Epub 2014/03/04. doi: 10.1371/journal.ppat.1003829. PubMed PMID: 24586144; PMCID: PMC3930561.
62. Mazmanian SK, Round JL, Kasper DL. A microbial symbiosis factor prevents intestinal inflammatory disease. Nature. 2008;453(7195):620-5. Epub 2008/05/30. doi: 10.1038/nature07008. PubMed PMID: 18509436.
63. Dillon SM, Lee EJ, Kotter CV, Austin GL, Dong Z, Hecht DK, Gianella S, Siewe B, Smith DM, Landay AL, Robertson CE, Frank DN, Wilson CC. An altered intestinal mucosal microbiome in HIV-1 infection is associated with mucosal and systemic immune activation and endotoxemia. Mucosal Immunol. 2014;7(4):983-94. Epub 2014/01/09. doi: 10.1038/mi.2013.116. PubMed PMID: 24399150; PMCID: PMC4062575.
64. Hamer HM, Jonkers D, Venema K, Vanhoutvin S, Troost FJ, Brummer RJ. Review article: the role of butyrate on colonic function. Aliment Pharmacol Ther. 2008;27(2):104-19. Epub 2007/11/02. doi: 10.1111/j.1365-2036.2007.03562.x. PubMed PMID: 17973645.
65. Kelly CJ, Zheng L, Campbell EL, Saeedi B, Scholz CC, Bayless AJ, Wilson KE, Glover LE, Kominsky DJ, Magnuson A, Weir TL, Ehrentraut SF, Pickel C, Kuhn KA, Lanis JM, Nguyen V, Taylor CT, Colgan SP. Crosstalk between Microbiota-Derived Short-Chain Fatty Acids and Intestinal Epithelial HIF Augments Tissue Barrier

Function. Cell Host Microbe. 2015;17(5):662-71. Epub 2015/04/14. doi: 10.1016/j.chom.2015.03.005. PubMed PMID: 25865369; PMCID: PMC4433427.
66. Dillon SM, Kibbie J, Lee EJ, Guo K, Santiago ML, Austin GL, Gianella S, Landay AL, Donovan AM, Frank DN, Mc CM, Wilson CC. Low abundance of colonic butyrate-producing bacteria in HIV infection is associated with microbial translocation and immune activation. AIDS. 2017;31(4):511-21. Epub 2016/12/22. doi: 10.1097/QAD.0000000000001366. PubMed PMID: 28002063; PMCID: PMC5263163.
67. Vujkovic-Cvijin I, Dunham RM, Iwai S, Maher MC, Albright RG, Broadhurst MJ, Hernandez RD, Lederman MM, Huang Y, Somsouk M, Deeks SG, Hunt PW, Lynch SV, McCune JM. Dysbiosis of the gut microbiota is associated with HIV disease progression and tryptophan catabolism. Sci Transl Med. 2013;5(193):193ra91. Epub 2013/07/12. doi: 10.1126/scitranslmed.3006438. PubMed PMID: 23843452; PMCID: PMC4094294.
68. Estes JD, Harris LD, Klatt NR, Tabb B, Pittaluga S, Paiardini M, Barclay GR, Smedley J, Pung R, Oliveira KM, Hirsch VM, Silvestri G, Douek DC, Miller CJ, Haase AT, Lifson J, Brenchley JM. Damaged intestinal epithelial integrity linked to microbial translocation in pathogenic simian immunodeficiency virus infections. PLoS Pathog. 2010;6(8):e1001052. Epub 2010/09/03. doi: 10.1371/journal.ppat.1001052. PubMed PMID: 20808901; PMCID: PMC2924359.
69. Jiang W, Lederman MM, Hunt P, Sieg SF, Haley K, Rodriguez B, Landay A, Martin J, Sinclair E, Asher AI, Deeks SG, Douek DC, Brenchley JM. Plasma levels of bacterial DNA correlate with immune activation and the magnitude of immune restoration in persons with antiretroviral-treated HIV infection. J Infect Dis. 2009;199(8):1177-85. Epub 2009/03/07. doi: 10.1086/597476. PubMed PMID: 19265479; PMCID: PMC2728622.
70. Marchetti G, Bellistri GM, Borghi E, Tincati C, Ferramosca S, La Francesca M, Morace G, Gori A, Monforte AD. Microbial translocation is associated with sustained failure in CD4+ T-cell reconstitution in HIV-infected patients on long-term highly active antiretroviral therapy. AIDS. 2008;22(15):2035-8. Epub 2008/09/12. doi: 10.1097/QAD.0b013e3283112d29. PubMed PMID: 18784466.
71. Brenchley JM, Price DA, Schacker TW, Asher TE, Silvestri G, Rao S, Kazzaz Z, Bornstein E, Lambotte O, Altmann D, Blazar BR, Rodriguez B, Teixeira-Johnson L, Landay A, Martin JN, Hecht FM, Picker LJ, Lederman MM, Deeks SG, Douek DC. Microbial translocation is a cause of systemic immune activation in chronic HIV infection. Nat Med. 2006;12(12):1365-71. Epub 2006/11/23. doi: 10.1038/nm1511. PubMed PMID: 17115046.
72. Ferrari G, Korber B, Goonetilleke N, Liu MK, Turnbull EL, Salazar-Gonzalez JF, Hawkins N, Self S, Watson S, Betts MR, Gay C, McGhee K, Pellegrino P, Williams I, Tomaras GD, Haynes BF, Gray CM, Borrow P, Roederer M, McMichael AJ, Weinhold KJ. Relationship between functional profile of HIV-1 specific CD8 T cells and epitope variability with the selection of escape mutants in acute HIV-1 infection. PLoS Pathog. 2011;7(2):e1001273. Epub 2011/02/25. doi: 10.1371/journal.ppat.1001273. PubMed PMID: 21347345; PMCID: PMC3037354.
73. Sather DN, Armann J, Ching LK, Mavrantoni A, Sellhorn G, Caldwell Z, Yu X, Wood B, Self S, Kalams S, Stamatatos L. Factors associated with the development of cross-reactive neutralizing antibodies during human immunodeficiency virus type 1 infection. J Virol. 2009;83(2):757-69. Epub 2008/11/07. doi: 10.1128/JVI.02036-08. PubMed PMID: 18987148; PMCID: PMC2612355.
74. Rolland M, Tovanabutra S, deCamp AC, Frahm N, Gilbert PB, Sanders-Buell E, Heath L, Magaret CA, Bose M, Bradfield A, O'Sullivan A, Crossler J, Jones T, Nau M, Wong K, Zhao H, Raugi DN, Sorensen S, Stoddard JN, Maust BS, Deng W, Hural J, Dubey S, Michael NL, Shiver J, Corey L, Li F, Self SG, Kim J, Buchbinder S, Casimiro DR, Robertson MN, Duerr A, McElrath MJ, McCutchan FE, Mullins JI. Genetic impact of vaccination on breakthrough HIV-1 sequences from the STEP trial. Nat Med. 2011;17(3):366-71. Epub 2011/03/02. doi: 10.1038/nm.2316. PubMed PMID: 21358627; PMCID: PMC3053571.

75. Goonetilleke N, Liu MK, Salazar-Gonzalez JF, Ferrari G, Giorgi E, Ganusov VV, Keele BF, Learn GH, Turnbull EL, Salazar MG, Weinhold KJ, Moore S, B CCC, Letvin N, Haynes BF, Cohen MS, Hraber P, Bhattacharya T, Borrow P, Perelson AS, Hahn BH, Shaw GM, Korber BT, McMichael AJ. The first T cell response to transmitted/founder virus contributes to the control of acute viremia in HIV-1 infection. J Exp Med. 2009;206(6):1253-72. Epub 2009/06/03. doi: 10.1084/jem.20090365. PubMed PMID: 19487423; PMCID: PMC2715063.
76. HHS. Guidelines for Prevention and Treatment of Opportunistic Infections in HIV-Infected Adults and Adolescents. 2017 [11/29/2018]. Available from: https://aidsinfo.nih.gov/contentfiles/lvguidelines/AdultOITablesOnly.pdf.
77. Sepkowitz KA. Opportunistic infections in patients with and patients without Acquired Immunodeficiency Syndrome. Clin Infect Dis. 2002;34(8):1098-107. Epub 2002/03/27. doi: 10.1086/339548. PubMed PMID: 11914999.
78. Cooper DA, Gold J, Maclean P, Donovan B, Finlayson R, Barnes TG, Michelmore HM, Brooke P, Penny R. Acute AIDS retrovirus infection. Definition of a clinical illness associated with seroconversion. Lancet. 1985;1(8428):537-40. Epub 1985/03/09. PubMed PMID: 2857899.
79. Gaines H, von Sydow M, Pehrson PO, Lundbegh P. Clinical picture of primary HIV infection presenting as a glandular-fever-like illness. BMJ. 1988;297(6660):1363-8. Epub 1988/11/26. doi: 10.1136/bmj.297.6660.1363. PubMed PMID: 3146367; PMCID: PMC1835053.
80. Schacker T, Collier AC, Hughes J, Shea T, Corey L. Clinical and epidemiologic features of primary HIV infection. Ann Intern Med. 1996;125(4):257-64. Epub 1996/08/15. PubMed PMID: 8678387.
81. McBrien JB, Kumar NA, Silvestri G. Mechanisms of CD8(+) T cell-mediated suppression of HIV/SIV replication. Eur J Immunol. 2018;48(6):898-914. Epub 2018/02/11. doi: 10.1002/eji.201747172. PubMed PMID: 29427516; PMCID: PMC6531861.
82. Betts MR, Nason MC, West SM, De Rosa SC, Migueles SA, Abraham J, Lederman MM, Benito JM, Goepfert PA, Connors M, Roederer M, Koup RA. HIV nonprogressors preferentially maintain highly functional HIV-specific CD8+ T cells. Blood. 2006;107(12):4781-9. Epub 2006/02/10. doi: 10.1182/blood-2005-12-4818. PubMed PMID: 16467198; PMCID: PMC1895811.
83. Coffin J, Swanstrom R. HIV pathogenesis: dynamics and genetics of viral populations and infected cells. Cold Spring Harb Perspect Med. 2013;3(1):a012526. Epub 2013/01/04. doi: 10.1101/cshperspect.a012526. PubMed PMID: 23284080; PMCID: PMC3530041.
84. Pegu A, Hessell AJ, Mascola JR, Haigwood NL. Use of broadly neutralizing antibodies for HIV-1 prevention. Immunol Rev. 2017;275(1):296-312. Epub 2017/01/31. doi: 10.1111/imr.12511. PubMed PMID: 28133803; PMCID: PMC5314445.
85. Haynes BF, Gilbert PB, McElrath MJ, Zolla-Pazner S, Tomaras GD, Alam SM, Evans DT, Montefiori DC, Karnasuta C, Sutthent R, Liao HX, DeVico AL, Lewis GK, Williams C, Pinter A, Fong Y, Janes H, DeCamp A, Huang Y, Rao M, Billings E, Karasavvas N, Robb ML, Ngauy V, de Souza MS, Paris R, Ferrari G, Bailer RT, Soderberg KA, Andrews C, Berman PW, Frahm N, De Rosa SC, Alpert MD, Yates NL, Shen X, Koup RA, Pitisuttithum P, Kaewkungwal J, Nitayaphan S, Rerks-Ngarm S, Michael NL, Kim JH. Immune-correlates analysis of an HIV-1 vaccine efficacy trial. N Engl J Med. 2012;366(14):1275-86. Epub 2012/04/06. doi: 10.1056/NEJMoa1113425. PubMed PMID: 22475592; PMCID: PMC3371689.
86. Mouquet H, Scharf L, Euler Z, Liu Y, Eden C, Scheid JF, Halper-Stromberg A, Gnanapragasam PN, Spencer DI, Seaman MS, Schuitemaker H, Feizi T, Nussenzweig MC, Bjorkman PJ. Complex-type N-glycan recognition by potent broadly neutralizing HIV antibodies. Proc Natl Acad Sci U S A. 2012;109(47):E3268-77. Epub 2012/11/02. doi: 10.1073/pnas.1217207109. PubMed PMID: 23115339; PMCID: PMC3511153.

87. Klein F, Mouquet H, Dosenovic P, Scheid JF, Scharf L, Nussenzweig MC. Antibodies in HIV-1 vaccine development and therapy. Science. 2013;341(6151):1199-204. Epub 2013/09/14. doi: 10.1126/science.1241144. PubMed PMID: 24031012; PMCID: PMC3970325.
88. Haynes BF, Burton DR, Mascola JR. Multiple roles for HIV broadly neutralizing antibodies. Sci Transl Med. 2019;11(516). Epub 2019/11/02. doi: 10.1126/scitranslmed.aaz2686. PubMed PMID: 31666399; PMCID: PMC7171597.
89. Chintala K, Mohareer K, Banerjee S. Dodging the Host Interferon-Stimulated Gene Mediated Innate Immunity by HIV-1: A Brief Update on Intrinsic Mechanisms and Counter-Mechanisms. Front Immunol. 2021;12:716927. Epub 2021/08/17. doi: 10.3389/fimmu.2021.716927. PubMed PMID: 34394123; PMCID: PMC8358655.
90. Sheehy AM, Gaddis NC, Choi JD, Malim MH. Isolation of a human gene that inhibits HIV-1 infection and is suppressed by the viral Vif protein. Nature. 2002;418(6898):646-50. Epub 2002/08/09. doi: 10.1038/nature00939. PubMed PMID: 12167863.
91. Stremlau M, Owens CM, Perron MJ, Kiessling M, Autissier P, Sodroski J. The cytoplasmic body component TRIM5alpha restricts HIV-1 infection in Old World monkeys. Nature. 2004;427(6977):848-53. Epub 2004/02/27. doi: 10.1038/nature02343. PubMed PMID: 14985764.
92. Neil SJ, Zang T, Bieniasz PD. Tetherin inhibits retrovirus release and is antagonized by HIV-1 Vpu. Nature. 2008;451(7177):425-30. Epub 2008/01/18. doi: 10.1038/nature06553. PubMed PMID: 18200009.
93. McLane LM, Abdel-Hakeem MS, Wherry EJ. CD8 T Cell Exhaustion During Chronic Viral Infection and Cancer. Annu Rev Immunol. 2019;37:457-95. Epub 2019/01/25. doi: 10.1146/annurev-immunol-041015-055318. PubMed PMID: 30676822.
94. Wahren B, Morfeldt-Mansson L, Biberfeld G, Moberg L, Sonnerborg A, Ljungman P, Werner A, Kurth R, Gallo R, Bolognesi D. Characteristics of the specific cell-mediated immune response in human immunodeficiency virus infection. J Virol. 1987;61(6):2017-23. Epub 1987/06/01. PubMed PMID: 3033328; PMCID: PMC254211.
95. Day CL, Kaufmann DE, Kiepiela P, Brown JA, Moodley ES, Reddy S, Mackey EW, Miller JD, Leslie AJ, DePierres C, Mncube Z, Duraiswamy J, Zhu B, Eichbaum Q, Altfeld M, Wherry EJ, Coovadia HM, Goulder PJ, Klenerman P, Ahmed R, Freeman GJ, Walker BD. PD-1 expression on HIV-specific T cells is associated with T-cell exhaustion and disease progression. Nature. 2006;443(7109):350-4. Epub 2006/08/22. doi: 10.1038/nature05115. PubMed PMID: 16921384.
96. Petrovas C, Casazza JP, Brenchley JM, Price DA, Gostick E, Adams WC, Precopio ML, Schacker T, Roederer M, Douek DC, Koup RA. PD-1 is a regulator of virus-specific CD8+ T cell survival in HIV infection. J Exp Med. 2006;203(10):2281-92. Epub 2006/09/07. doi: 10.1084/jem.20061496. PubMed PMID: 16954372; PMCID: PMC2118095.
97. Trautmann L, Janbazian L, Chomont N, Said EA, Gimmig S, Bessette B, Boulassel MR, Delwart E, Sepulveda H, Balderas RS, Routy JP, Haddad EK, Sekaly RP. Upregulation of PD-1 expression on HIV-specific CD8+ T cells leads to reversible immune dysfunction. Nat Med. 2006;12(10):1198-202. Epub 2006/08/19. doi: 10.1038/nm1482. PubMed PMID: 16917489.
98. Etienne L, Nerrienet E, LeBreton M, Bibila GT, Foupouapouognigni Y, Rousset D, Nana A, Djoko CF, Tamoufe U, Aghokeng AF, Mpoudi-Ngole E, Delaporte E, Peeters M, Wolfe ND, Ayouba A. Characterization of a new simian immunodeficiency virus strain in a naturally infected Pan troglodytes troglodytes chimpanzee with AIDS related symptoms. Retrovirology. 2011;8:4. Epub 2011/01/15. doi: 10.1186/1742-4690-8-4. PubMed PMID: 21232091; PMCID: PMC3034674.
99. Keele BF, Jones JH, Terio KA, Estes JD, Rudicell RS, Wilson ML, Li Y, Learn GH, Beasley TM, Schumacher-Stankey J, Wroblewski E, Mosser A, Raphael J, Kamenya S, Lonsdorf EV, Travis DA, Mlengeya T, Kinsel MJ, Else JG, Silvestri G, Goodall J, Sharp PM, Shaw GM, Pusey AE, Hahn BH. Increased mortality

and AIDS-like immunopathology in wild chimpanzees infected with SIVcpz. Nature. 2009;460(7254):515-9. Epub 2009/07/25. doi: 10.1038/nature08200. PubMed PMID: 19626114; PMCID: PMC2872475.
100. Novembre FJ, Saucier M, Anderson DC, Klumpp SA, O'Neil SP, Brown CR, 2nd, Hart CE, Guenthner PC, Swenson RB, McClure HM. Development of AIDS in a chimpanzee infected with human immunodeficiency virus type 1. J Virol. 1997;71(5):4086-91. Epub 1997/05/01. PubMed PMID: 9094687; PMCID: PMC191562.
101. Gray RH, Wawer MJ, Brookmeyer R, Sewankambo NK, Serwadda D, Wabwire-Mangen F, Lutalo T, Li X, vanCott T, Quinn TC, Rakai Project T. Probability of HIV-1 transmission per coital act in monogamous, heterosexual, HIV-1-discordant couples in Rakai, Uganda. Lancet. 2001;357(9263):1149-53. Epub 2001/04/27. doi: 10.1016/S0140-6736(00)04331-2. PubMed PMID: 11323041.
102. Silvestri G. Naturally SIV-infected sooty mangabeys: are we closer to understanding why they do not develop AIDS? J Med Primatol. 2005;34(5-6):243-52. Epub 2005/09/01. doi: 10.1111/j.1600-0684.2005.00122.x. PubMed PMID: 16128919.
103. Paiardini M, Cervasi B, Reyes-Aviles E, Micci L, Ortiz AM, Chahroudi A, Vinton C, Gordon SN, Bosinger SE, Francella N, Hallberg PL, Cramer E, Schlub T, Chan ML, Riddick NE, Collman RG, Apetrei C, Pandrea I, Else J, Munch J, Kirchhoff F, Davenport MP, Brenchley JM, Silvestri G. Low levels of SIV infection in sooty mangabey central memory CD(4)(+) T cells are associated with limited CCR5 expression. Nat Med. 2011;17(7):830-6. Epub 2011/06/28. doi: 10.1038/nm.2395. PubMed PMID: 21706028; PMCID: PMC3253129.
104. Palesch D, Bosinger SE, Tharp GK, Vanderford TH, Paiardini M, Chahroudi A, Johnson ZP, Kirchhoff F, Hahn BH, Norgren RB, Patel NB, Sodora DL, Dawoud RA, Stewart CB, Seepo SM, Harris RA, Liu Y, Raveendran M, Han Y, English A, Thomas GWC, Hahn MW, Pipes L, Mason CE, Muzny DM, Gibbs RA, Sauter D, Worley K, Rogers J, Silvestri G. Sooty mangabey genome sequence provides insight into AIDS resistance in a natural SIV host. Nature. 2018;553(7686):77-81. Epub 2018/01/05. doi: 10.1038/nature25140. PubMed PMID: 29300007; PMCID: PMC5843367.
105. Hatziioannou T, Evans DT. Animal models for HIV/AIDS research. Nat Rev Microbiol. 2012;10(12):852-67. Epub 2012/11/17. doi: 10.1038/nrmicro2911. PubMed PMID: 23154262; PMCID: PMC4334372.
106. Kumar N, Chahroudi A, Silvestri G. Animal models to achieve an HIV cure. Curr Opin HIV AIDS. 2016;11(4):432-41. Epub 2016/05/07. doi: 10.1097/COH.0000000000000290. PubMed PMID: 27152962; PMCID: PMC4922307.
107. Micci L, Ryan ES, Fromentin R, Bosinger SE, Harper JL, He T, Paganini S, Easley KA, Chahroudi A, Benne C, Gumber S, McGary CS, Rogers KA, Deleage C, Lucero C, Byrareddy SN, Apetrei C, Estes JD, Lifson JD, Piatak M, Jr., Chomont N, Villinger F, Silvestri G, Brenchley JM, Paiardini M. Interleukin-21 combined with ART reduces inflammation and viral reservoir in SIV-infected macaques. J Clin Invest. 2015;125(12):4497-513. Epub 2015/11/10. doi: 10.1172/JCI81400. PubMed PMID: 26551680; PMCID: PMC4665780.
108. Cartwright EK, Spicer L, Smith SA, Lee D, Fast R, Paganini S, Lawson BO, Nega M, Easley K, Schmitz JE, Bosinger SE, Paiardini M, Chahroudi A, Vanderford TH, Estes JD, Lifson JD, Derdeyn CA, Silvestri G. CD8(+) Lymphocytes Are Required for Maintaining Viral Suppression in SIV-Infected Macaques Treated with Short-Term Antiretroviral Therapy. Immunity. 2016;45(3):656-68. Epub 2016/09/23. doi: 10.1016/j.immuni.2016.08.018. PubMed PMID: 27653601; PMCID: PMC5087330.
109. Byrareddy SN, Arthos J, Cicala C, Villinger F, Ortiz KT, Little D, Sidell N, Kane MA, Yu J, Jones JW, Santangelo PJ, Zurla C, McKinnon LR, Arnold KB, Woody CE, Walter L, Roos C, Noll A, Van Ryk D, Jelicic K, Cimbro R, Gumber S, Reid MD, Adsay V, Amancha PK, Mayne AE, Parslow TG, Fauci AS, Ansari AA. Sustained virologic control in SIV+ macaques after antiretroviral and alpha4beta7 antibody therapy.

Science. 2016;354(6309):197-202. Epub 2016/10/16. doi: 10.1126/science.aag1276. PubMed PMID: 27738167; PMCID: PMC5405455.
110. Del Prete GQ, Oswald K, Lara A, Shoemaker R, Smedley J, Macallister R, Coalter V, Wiles A, Wiles R, Li Y, Fast R, Kiser R, Lu B, Zheng J, Alvord WG, Trubey CM, Piatak M, Jr., Deleage C, Keele BF, Estes JD, Hesselgesser J, Geleziunas R, Lifson JD. Elevated Plasma Viral Loads in Romidepsin-Treated Simian Immunodeficiency Virus-Infected Rhesus Macaques on Suppressive Combination Antiretroviral Therapy. Antimicrob Agents Chemother. 2015;60(3):1560-72. Epub 2015/12/30. doi: 10.1128/AAC.02625-15. PubMed PMID: 26711758; PMCID: PMC4776002.
111. Whitney JB, Hill AL, Sanisetty S, Penaloza-MacMaster P, Liu J, Shetty M, Parenteau L, Cabral C, Shields J, Blackmore S, Smith JY, Brinkman AL, Peter LE, Mathew SI, Smith KM, Borducchi EN, Rosenbloom DI, Lewis MG, Hattersley J, Li B, Hesselgesser J, Geleziunas R, Robb ML, Kim JH, Michael NL, Barouch DH. Rapid seeding of the viral reservoir prior to SIV viraemia in rhesus monkeys. Nature. 2014;512(7512):74-7. Epub 2014/07/22. doi: 10.1038/nature13594. PubMed PMID: 25042999; PMCID: PMC4126858.
112. Li J, Lord CI, Haseltine W, Letvin NL, Sodroski J. Infection of cynomolgus monkeys with a chimeric HIV-1/SIVmac virus that expresses the HIV-1 envelope glycoproteins. J Acquir Immune Defic Syndr. 1992;5(7):639-46. Epub 1992/01/01. PubMed PMID: 1613662.
113. Bar KJ, Coronado E, Hensley-McBain T, O'Connor MA, Osborn JM, Miller C, Gott TM, Wangari S, Iwayama N, Ahrens CY, Smedley J, Moats C, Lynch RM, Haddad EK, Haigwood NL, Fuller DH, Shaw GM, Klatt NR, Manuzak JA. Simian-Human Immunodeficiency Virus SHIV.CH505 Infection of Rhesus Macaques Results in Persistent Viral Replication and Induces Intestinal Immunopathology. J Virol. 2019;93(18). Epub 2019/06/21. doi: 10.1128/JVI.00372-19. PubMed PMID: 31217249; PMCID: PMC6714786.
114. Obregon-Perko V, Bricker KM, Mensah G, Uddin F, Kumar MR, Fray EJ, Siliciano RF, Schoof N, Horner A, Mavigner M, Liang S, Vanderford T, Sass J, Chan C, Berendam SJ, Bar KJ, Shaw GM, Silvestri G, Fouda GG, Permar SR, Chahroudi A. Simian-Human Immunodeficiency Virus SHIV.C.CH505 Persistence in ART-Suppressed Infant Macaques Is Characterized by Elevated SHIV RNA in the Gut and a High Abundance of Intact SHIV DNA in Naive CD4(+) T Cells. J Virol. 2020;95(2). Epub 2020/10/23. doi: 10.1128/JVI.01669-20. PubMed PMID: 33087463; PMCID: PMC7944446.
115. Khanal S, Fennessey CM, O'Brien SP, Thorpe A, Reid C, Immonen TT, Smith R, Bess JW, Jr., Swanstrom AE, Del Prete GQ, Davenport MP, Okoye AA, Picker LJ, Lifson JD, Keele BF. In Vivo Validation of the Viral Barcoding of Simian Immunodeficiency Virus SIVmac239 and the Development of New Barcoded SIV and Subtype B and C Simian-Human Immunodeficiency Viruses. J Virol. 2019;94(1). Epub 2019/10/11. doi: 10.1128/JVI.01420-19. PubMed PMID: 31597757; PMCID: PMC6912102.
116. Crooks AM, Bateson R, Cope AB, Dahl NP, Griggs MK, Kuruc JD, Gay CL, Eron JJ, Margolis DM, Bosch RJ, Archin NM. Precise Quantitation of the Latent HIV-1 Reservoir: Implications for Eradication Strategies. J Infect Dis. 2015;212(9):1361-5. Epub 2015/04/17. doi: 10.1093/infdis/jiv218. PubMed PMID: 25877550; PMCID: PMC4601910.
117. Siliciano JD, Kajdas J, Finzi D, Quinn TC, Chadwick K, Margolick JB, Kovacs C, Gange SJ, Siliciano RF. Long-term follow-up studies confirm the stability of the latent reservoir for HIV-1 in resting CD4+ T cells. Nat Med. 2003;9(6):727-8. Epub 2003/05/20. doi: 10.1038/nm880. PubMed PMID: 12754504.
118. Deeks SG, Overbaugh J, Phillips A, Buchbinder S. HIV infection. Nat Rev Dis Primers. 2015;1:15035. Epub 2015/01/01. doi: 10.1038/nrdp.2015.35. PubMed PMID: 27188527.
119. Clotet B, Feinberg J, van Lunzen J, Khuong-Josses MA, Antinori A, Dumitru I, Pokrovskiy V, Fehr J, Ortiz R, Saag M, Harris J, Brennan C, Fujiwara T, Min S, Team INGS. Once-daily dolutegravir versus darunavir plus ritonavir in antiretroviral-naive adults with HIV-1 infection (FLAMINGO): 48 week results from the randomised open-label phase 3b study. Lancet. 2014;383(9936):2222-31. Epub 2014/04/05. doi: 10.1016/S0140-6736(14)60084-2. PubMed PMID: 24698485.

120. Walmsley SL, Antela A, Clumeck N, Duiculescu D, Eberhard A, Gutierrez F, Hocqueloux L, Maggiolo F, Sandkovsky U, Granier C, Pappa K, Wynne B, Min S, Nichols G, Investigators S. Dolutegravir plus abacavir-lamivudine for the treatment of HIV-1 infection. N Engl J Med. 2013;369(19):1807-18. Epub 2013/11/08. doi: 10.1056/NEJMoa1215541. PubMed PMID: 24195548.
121. Maeda K, Nakata H, Koh Y, Miyakawa T, Ogata H, Takaoka Y, Shibayama S, Sagawa K, Fukushima D, Moravek J, Koyanagi Y, Mitsuya H. Spirodiketopiperazine-based CCR5 inhibitor which preserves CC-chemokine/CCR5 interactions and exerts potent activity against R5 human immunodeficiency virus type 1 in vitro. J Virol. 2004;78(16):8654-62. Epub 2004/07/29. doi: 10.1128/JVI.78.16.8654-8662.2004. PubMed PMID: 15280474; PMCID: PMC479103.
122. St Clair MH, Richards CA, Spector T, Weinhold KJ, Miller WH, Langlois AJ, Furman PA. 3'-Azido-3'-deoxythymidine triphosphate as an inhibitor and substrate of purified human immunodeficiency virus reverse transcriptase. Antimicrob Agents Chemother. 1987;31(12):1972-7. Epub 1987/12/01. PubMed PMID: 2449866.
123. Vandormael A, Akullian A, Siedner M, de Oliveira T, Barnighausen T, Tanser F. Declines in HIV incidence among men and women in a South African population-based cohort. Nat Commun. 2019;10(1):5482. Epub 2019/12/04. doi: 10.1038/s41467-019-13473-y. PubMed PMID: 31792217; PMCID: PMC6889466.
124. Gunthard HF, Saag MS, Benson CA, del Rio C, Eron JJ, Gallant JE, Hoy JF, Mugavero MJ, Sax PE, Thompson MA, Gandhi RT, Landovitz RJ, Smith DM, Jacobsen DM, Volberding PA. Antiretroviral Drugs for Treatment and Prevention of HIV Infection in Adults: 2016 Recommendations of the International Antiviral Society-USA Panel. JAMA. 2016;316(2):191-210. Epub 2016/07/13. doi: 10.1001/jama.2016.8900. PubMed PMID: 27404187; PMCID: PMC5012643.
125. Cobb DA, Smith NA, Edagwa BJ, McMillan JM. Long-acting approaches for delivery of antiretroviral drugs for prevention and treatment of HIV: a review of recent research. Expert Opin Drug Deliv. 2020;17(9):1227-38. Epub 2020/06/20. doi: 10.1080/17425247.2020.1783233. PubMed PMID: 32552187; PMCID: PMC7442675.
126. Ambrosioni J, Petit E, Liegeon G, Laguno M, Miro JM. Primary HIV-1 infection in users of pre-exposure prophylaxis. Lancet HIV. 2021;8(3):e166-e74. Epub 2020/12/15. doi: 10.1016/S2352-3018(20)30271-X. PubMed PMID: 33316212.
127. Mouton JP, Cohen K, Maartens G. Key toxicity issues with the WHO-recommended first-line antiretroviral therapy regimen. Expert Rev Clin Pharmacol. 2016;9(11):1493-503. Epub 2016/08/09. doi: 10.1080/17512433.2016.1221760. PubMed PMID: 27498720.
128. Finzi D, Hermankova M, Pierson T, Carruth LM, Buck C, Chaisson RE, Quinn TC, Chadwick K, Margolick J, Brookmeyer R, Gallant J, Markowitz M, Ho DD, Richman DD, Siliciano RF. Identification of a reservoir for HIV-1 in patients on highly active antiretroviral therapy. Science. 1997;278(5341):1295-300. Epub 1997/11/21. PubMed PMID: 9360927.
129. Abreu C, Shirk EN, Queen SE, Beck SE, Mangus LM, Pate KAM, Mankowski JL, Gama L, Clements JE. Brain macrophages harbor latent, infectious simian immunodeficiency virus. AIDS. 2019;33 Suppl 2:S181-S8. Epub 2019/12/04. doi: 10.1097/QAD.0000000000002269. PubMed PMID: 31789817; PMCID: PMC7058191.
130. Pierson T, McArthur J, Siliciano RF. Reservoirs for HIV-1: mechanisms for viral persistence in the presence of antiviral immune responses and antiretroviral therapy. Annu Rev Immunol. 2000;18:665-708. Epub 2000/06/03. doi: 10.1146/annurev.immunol.18.1.665. PubMed PMID: 10837072.
131. Wang Z, Gurule EE, Brennan TP, Gerold JM, Kwon KJ, Hosmane NN, Kumar MR, Beg SA, Capoferri AA, Ray SC, Ho YC, Hill AL, Siliciano JD, Siliciano RF. Expanded cellular clones carrying replication-

competent HIV-1 persist, wax, and wane. Proc Natl Acad Sci U S A. 2018;115(11):E2575-E84. Epub 2018/02/28. doi: 10.1073/pnas.1720665115. PubMed PMID: 29483265; PMCID: PMC5856552.
132. Venanzi Rullo E, Pinzone MR, Cannon L, Weissman S, Ceccarelli M, Zurakowski R, Nunnari G, O'Doherty U. Persistence of an intact HIV reservoir in phenotypically naive T cells. JCI Insight. 2020;5(20). Epub 2020/10/16. doi: 10.1172/jci.insight.133157. PubMed PMID: 33055422; PMCID: PMC7605525.
133. Chun TW, Engel D, Berrey MM, Shea T, Corey L, Fauci AS. Early establishment of a pool of latently infected, resting CD4(+) T cells during primary HIV-1 infection. Proc Natl Acad Sci U S A. 1998;95(15):8869-73. Epub 1998/07/22. PubMed PMID: 9671771; PMCID: PMC21169.
134. Abrahams MR, Joseph SB, Garrett N, Tyers L, Moeser M, Archin N, Council OD, Matten D, Zhou S, Doolabh D, Anthony C, Goonetilleke N, Karim SA, Margolis DM, Pond SK, Williamson C, Swanstrom R. The replication-competent HIV-1 latent reservoir is primarily established near the time of therapy initiation. Sci Transl Med. 2019;11(513). Epub 2019/10/11. doi: 10.1126/scitranslmed.aaw5589. PubMed PMID: 31597754; PMCID: PMC7233356.
135. Brodin J, Zanini F, Thebo L, Lanz C, Bratt G, Neher RA, Albert J. Establishment and stability of the latent HIV-1 DNA reservoir. Elife. 2016;5. Epub 2016/11/18. doi: 10.7554/eLife.18889. PubMed PMID: 27855060; PMCID: PMC5201419.
136. Pankau MD, Reeves DB, Harkins E, Ronen K, Jaoko W, Mandaliya K, Graham SM, McClelland RS, Matsen Iv FA, Schiffer JT, Overbaugh J, Lehman DA. Dynamics of HIV DNA reservoir seeding in a cohort of superinfected Kenyan women. PLoS Pathog. 2020;16(2):e1008286. Epub 2020/02/06. doi: 10.1371/journal.ppat.1008286. PubMed PMID: 32023326; PMCID: PMC7028291.
137. North TW, Higgins J, Deere JD, Hayes TL, Villalobos A, Adamson L, Shacklett BL, Schinazi RF, Luciw PA. Viral sanctuaries during highly active antiretroviral therapy in a nonhuman primate model for AIDS. J Virol. 2010;84(6):2913-22. Epub 2009/12/25. doi: 10.1128/JVI.02356-09. PubMed PMID: 20032180; PMCID: PMC2826073.
138. Cadena AM, Ventura JD, Abbink P, Borducchi EN, Tuyishime H, Mercado NB, Walker-Sperling V, Siamatu M, Liu PT, Chandrashekar A, Nkolola JP, McMahan K, Kordana N, Hamza V, Bondzie EA, Fray E, Kumar M, Fischinger S, Shin SA, Lewis MG, Siliciano RF, Alter G, Barouch DH. Persistence of viral RNA in lymph nodes in ART-suppressed SIV/SHIV-infected Rhesus Macaques. Nat Commun. 2021;12(1):1474. Epub 2021/03/07. doi: 10.1038/s41467-021-21724-0. PubMed PMID: 33674572; PMCID: PMC7935896.
139. Siddiqui S, Perez S, Gao Y, Doyle-Meyers L, Foley BT, Li Q, Ling B. Persistent Viral Reservoirs in Lymphoid Tissues in SIV-Infected Rhesus Macaques of Chinese-Origin on Suppressive Antiretroviral Therapy. Viruses. 2019;11(2). Epub 2019/01/30. doi: 10.3390/v11020105. PubMed PMID: 30691203; PMCID: PMC6410399.
140. Clements JE, Li M, Gama L, Bullock B, Carruth LM, Mankowski JL, Zink MC. The central nervous system is a viral reservoir in simian immunodeficiency virus--infected macaques on combined antiretroviral therapy: a model for human immunodeficiency virus patients on highly active antiretroviral therapy. J Neurovirol. 2005;11(2):180-9. Epub 2005/07/23. doi: 10.1080/13550280590922748-1. PubMed PMID: 16036796.
141. Bruel T, Schwartz O. Markers of the HIV-1 reservoir: facts and controversies. Curr Opin HIV AIDS. 2018;13(5):383-8. Epub 2018/05/31. doi: 10.1097/COH.0000000000000482. PubMed PMID: 29846244.
142. Descours B, Petitjean G, Lopez-Zaragoza JL, Bruel T, Raffel R, Psomas C, Reynes J, Lacabaratz C, Levy Y, Schwartz O, Lelievre JD, Benkirane M. CD32a is a marker of a CD4 T-cell HIV reservoir harbouring replication-competent proviruses. Nature. 2017;543(7646):564-7. Epub 2017/03/16. doi: 10.1038/nature21710. PubMed PMID: 28297712.
143. Badia R, Ballana E, Castellvi M, Garcia-Vidal E, Pujantell M, Clotet B, Prado JG, Puig J, Martinez MA, Riveira-Munoz E, Este JA. CD32 expression is associated to T-cell activation and is not a marker of the HIV-

1 reservoir. Nat Commun. 2018;9(1):2739. Epub 2018/07/18. doi: 10.1038/s41467-018-05157-w. PubMed PMID: 30013105; PMCID: PMC6048139.
144. Cohn LB, Chomont N, Deeks SG. The Biology of the HIV-1 Latent Reservoir and Implications for Cure Strategies. Cell Host Microbe. 2020;27(4):519-30. Epub 2020/04/10. doi: 10.1016/j.chom.2020.03.014. PubMed PMID: 32272077; PMCID: PMC7219958.
145. von Stockenstrom S, Odevall L, Lee E, Sinclair E, Bacchetti P, Killian M, Epling L, Shao W, Hoh R, Ho T, Faria NR, Lemey P, Albert J, Hunt P, Loeb L, Pilcher C, Poole L, Hatano H, Somsouk M, Douek D, Boritz E, Deeks SG, Hecht FM, Palmer S. Longitudinal Genetic Characterization Reveals That Cell Proliferation Maintains a Persistent HIV Type 1 DNA Pool During Effective HIV Therapy. J Infect Dis. 2015;212(4):596-607. Epub 2015/02/26. doi: 10.1093/infdis/jiv092. PubMed PMID: 25712966; PMCID: PMC4539896.
146. Josefsson L, von Stockenstrom S, Faria NR, Sinclair E, Bacchetti P, Killian M, Epling L, Tan A, Ho T, Lemey P, Shao W, Hunt PW, Somsouk M, Wylie W, Douek DC, Loeb L, Custer J, Hoh R, Poole L, Deeks SG, Hecht F, Palmer S. The HIV-1 reservoir in eight patients on long-term suppressive antiretroviral therapy is stable with few genetic changes over time. Proc Natl Acad Sci U S A. 2013;110(51):E4987-96. Epub 2013/11/28. doi: 10.1073/pnas.1308313110. PubMed PMID: 24277811; PMCID: PMC3870728.
147. Reeves DB, Duke ER, Wagner TA, Palmer SE, Spivak AM, Schiffer JT. A majority of HIV persistence during antiretroviral therapy is due to infected cell proliferation. Nat Commun. 2018;9(1):4811. Epub 2018/11/18. doi: 10.1038/s41467-018-06843-5. PubMed PMID: 30446650; PMCID: PMC6240116.
148. Fletcher CV, Staskus K, Wietgrefe SW, Rothenberger M, Reilly C, Chipman JG, Beilman GJ, Khoruts A, Thorkelson A, Schmidt TE, Anderson J, Perkey K, Stevenson M, Perelson AS, Douek DC, Haase AT, Schacker TW. Persistent HIV-1 replication is associated with lower antiretroviral drug concentrations in lymphatic tissues. Proc Natl Acad Sci U S A. 2014;111(6):2307-12. Epub 2014/01/29. doi: 10.1073/pnas.1318249111. PubMed PMID: 24469825; PMCID: PMC3926074.
149. Mavigner M, Habib J, Deleage C, Rosen E, Mattingly C, Bricker K, Kashuba A, Amblard F, Schinazi RF, Jean S, Cohen J, McGary C, Paiardini M, Wood MP, Sodora DL, Silvestri G, Estes J, Chahroudi A. SIV persistence in cellular and anatomic reservoirs in ART-suppressed infant rhesus macaques. J Virol. 2018. Epub 2018/07/13. doi: 10.1128/JVI.00562-18. PubMed PMID: 29997216.
150. van Zyl G, Bale MJ, Kearney MF. HIV evolution and diversity in ART-treated patients. Retrovirology. 2018;15(1):14. Epub 2018/01/31. doi: 10.1186/s12977-018-0395-4. PubMed PMID: 29378595; PMCID: PMC5789667.
151. Deeks SG, Tracy R, Douek DC. Systemic effects of inflammation on health during chronic HIV infection. Immunity. 2013;39(4):633-45. Epub 2013/10/22. doi: 10.1016/j.immuni.2013.10.001. PubMed PMID: 24138880; PMCID: PMC4012895.
152. Katlama C, Deeks SG, Autran B, Martinez-Picado J, van Lunzen J, Rouzioux C, Miller M, Vella S, Schmitz JE, Ahlers J, Richman DD, Sekaly RP. Barriers to a cure for HIV: new ways to target and eradicate HIV-1 reservoirs. Lancet. 2013;381(9883):2109-17. Epub 2013/04/02. doi: 10.1016/S0140-6736(13)60104-X. PubMed PMID: 23541541; PMCID: PMC3815451.
153. Migueles SA, Connors M. Long-term nonprogressive disease among untreated HIV-infected individuals: clinical implications of understanding immune control of HIV. JAMA. 2010;304(2):194-201. Epub 2010/07/16. doi: 10.1001/jama.2010.925. PubMed PMID: 20628133.
154. Allers K, Hutter G, Hofmann J, Loddenkemper C, Rieger K, Thiel E, Schneider T. Evidence for the cure of HIV infection by CCR5Delta32/Delta32 stem cell transplantation. Blood. 2011;117(10):2791-9. Epub 2010/12/15. doi: 10.1182/blood-2010-09-309591. PubMed PMID: 21148083.
155. Gupta RK, Peppa D, Hill AL, Galvez C, Salgado M, Pace M, McCoy LE, Griffith SA, Thornhill J, Alrubayyi A, Huyveneers LEP, Nastouli E, Grant P, Edwards SG, Innes AJ, Frater J, Nijhuis M, Wensing AMJ, Martinez-Picado J, Olavarria E. Evidence for HIV-1 cure after CCR5Delta32/Delta32 allogeneic

haemopoietic stem-cell transplantation 30 months post analytical treatment interruption: a case report. Lancet HIV. 2020;7(5):e340-e7. Epub 2020/03/15. doi: 10.1016/S2352-3018(20)30069-2. PubMed PMID: 32169158; PMCID: PMC7606918.

156. Xu L, Yang H, Gao Y, Chen Z, Xie L, Liu Y, Liu Y, Wang X, Li H, Lai W, He Y, Yao A, Ma L, Shao Y, Zhang B, Wang C, Chen H, Deng H. CRISPR/Cas9-Mediated CCR5 Ablation in Human Hematopoietic Stem/Progenitor Cells Confers HIV-1 Resistance In Vivo. Mol Ther. 2017;25(8):1782-9. Epub 2017/05/22. doi: 10.1016/j.ymthe.2017.04.027. PubMed PMID: 28527722; PMCID: PMC5542791.

157. Rosenberg ES, Altfeld M, Poon SH, Phillips MN, Wilkes BM, Eldridge RL, Robbins GK, D'Aquila RT, Goulder PJ, Walker BD. Immune control of HIV-1 after early treatment of acute infection. Nature. 2000;407(6803):523-6. Epub 2000/10/12. doi: 10.1038/35035103. PubMed PMID: 11029005.

158. Buzon MJ, Martin-Gayo E, Pereyra F, Ouyang Z, Sun H, Li JZ, Piovoso M, Shaw A, Dalmau J, Zangger N, Martinez-Picado J, Zurakowski R, Yu XG, Telenti A, Walker BD, Rosenberg ES, Lichterfeld M. Long-term antiretroviral treatment initiated at primary HIV-1 infection affects the size, composition, and decay kinetics of the reservoir of HIV-1-infected CD4 T cells. J Virol. 2014;88(17):10056-65. Epub 2014/06/27. doi: 10.1128/JVI.01046-14. PubMed PMID: 24965451; PMCID: PMC4136362.

159. Schuetz A, Deleage C, Sereti I, Rerknimitr R, Phanuphak N, Phuang-Ngern Y, Estes JD, Sandler NG, Sukhumvittaya S, Marovich M, Jongrakthaitae S, Akapirat S, Fletscher JL, Kroon E, Dewar R, Trichavaroj R, Chomchey N, Douek DC, RJ OC, Ngauy V, Robb ML, Phanuphak P, Michael NL, Excler JL, Kim JH, de Souza MS, Ananworanich J, Rv254/Search, Groups RSS. Initiation of ART during early acute HIV infection preserves mucosal Th17 function and reverses HIV-related immune activation. PLoS Pathog. 2014;10(12):e1004543. Epub 2014/12/17. doi: 10.1371/journal.ppat.1004543. PubMed PMID: 25503054; PMCID: PMC4263756.

160. Ananworanich J, Schuetz A, Vandergeeten C, Sereti I, de Souza M, Rerknimitr R, Dewar R, Marovich M, van Griensven F, Sekaly R, Pinyakorn S, Phanuphak N, Trichavaroj R, Rutvisuttinunt W, Chomchey N, Paris R, Peel S, Valcour V, Maldarelli F, Chomont N, Michael N, Phanuphak P, Kim JH, Group RSS. Impact of multi-targeted antiretroviral treatment on gut T cell depletion and HIV reservoir seeding during acute HIV infection. PLoS One. 2012;7(3):e33948. Epub 2012/04/06. doi: 10.1371/journal.pone.0033948. PubMed PMID: 22479485; PMCID: PMC3316511.

161. Cheret A, Bacchus-Souffan C, Avettand-Fenoel V, Melard A, Nembot G, Blanc C, Samri A, Saez-Cirion A, Hocqueloux L, Lascoux-Combe C, Allavena C, Goujard C, Valantin MA, Leplatois A, Meyer L, Rouzioux C, Autran B, Group OA-S. Combined ART started during acute HIV infection protects central memory CD4+ T cells and can induce remission. J Antimicrob Chemother. 2015;70(7):2108-20. Epub 2015/04/23. doi: 10.1093/jac/dkv084. PubMed PMID: 25900157.

162. Whitney JB, Lim SY, Osuna CE, Kublin JL, Chen E, Yoon G, Liu PT, Abbink P, Borducci EN, Hill A, Lewis MG, Geleziunas R, Robb ML, Michael NL, Barouch DH. Prevention of SIVmac251 reservoir seeding in rhesus monkeys by early antiretroviral therapy. Nat Commun. 2018;9(1):5429. Epub 2018/12/24. doi: 10.1038/s41467-018-07881-9. PubMed PMID: 30575753; PMCID: PMC6303321.

163. Okoye AA, Hansen SG, Vaidya M, Fukazawa Y, Park H, Duell DM, Lum R, Hughes CM, Ventura AB, Ainslie E, Ford JC, Morrow D, Gilbride RM, Legasse AW, Hesselgesser J, Geleziunas R, Li Y, Oswald K, Shoemaker R, Fast R, Bosche WJ, Borate BR, Edlefsen PT, Axthelm MK, Picker LJ, Lifson JD. Early antiretroviral therapy limits SIV reservoir establishment to delay or prevent post-treatment viral rebound. Nat Med. 2018;24(9):1430-40. Epub 2018/08/08. doi: 10.1038/s41591-018-0130-7. PubMed PMID: 30082858; PMCID: PMC6389357.

164. Stohr W, Fidler S, McClure M, Weber J, Cooper D, Ramjee G, Kaleebu P, Tambussi G, Schechter M, Babiker A, Phillips RE, Porter K, Frater J. Duration of HIV-1 viral suppression on cessation of antiretroviral

therapy in primary infection correlates with time on therapy. PLoS One. 2013;8(10):e78287. Epub 2013/11/10. doi: 10.1371/journal.pone.0078287. PubMed PMID: 24205183; PMCID: PMC3808338.

165. Hogan CM, Degruttola V, Sun X, Fiscus SA, Del Rio C, Hare CB, Markowitz M, Connick E, Macatangay B, Tashima KT, Kallungal B, Camp R, Morton T, Daar ES, Little S, Team AS. The setpoint study (ACTG A5217): effect of immediate versus deferred antiretroviral therapy on virologic set point in recently HIV-1-infected individuals. J Infect Dis. 2012;205(1):87-96. Epub 2011/12/20. doi: 10.1093/infdis/jir699. PubMed PMID: 22180621; PMCID: PMC3242744.

166. Saez-Cirion A, Bacchus C, Hocqueloux L, Avettand-Fenoel V, Girault I, Lecuroux C, Potard V, Versmisse P, Melard A, Prazuck T, Descours B, Guergnon J, Viard JP, Boufassa F, Lambotte O, Goujard C, Meyer L, Costagliola D, Venet A, Pancino G, Autran B, Rouzioux C, Group AVS. Post-treatment HIV-1 controllers with a long-term virological remission after the interruption of early initiated antiretroviral therapy ANRS VISCONTI Study. PLoS Pathog. 2013;9(3):e1003211. Epub 2013/03/22. doi: 10.1371/journal.ppat.1003211. PubMed PMID: 23516360; PMCID: PMC3597518.

167. Investigators ST, Fidler S, Porter K, Ewings F, Frater J, Ramjee G, Cooper D, Rees H, Fisher M, Schechter M, Kaleebu P, Tambussi G, Kinloch S, Miro JM, Kelleher A, McClure M, Kaye S, Gabriel M, Phillips R, Weber J, Babiker A. Short-course antiretroviral therapy in primary HIV infection. N Engl J Med. 2013;368(3):207-17. Epub 2013/01/18. doi: 10.1056/NEJMoa1110039. PubMed PMID: 23323897; PMCID: PMC4131004.

168. Deng K, Pertea M, Rongvaux A, Wang L, Durand CM, Ghiaur G, Lai J, McHugh HL, Hao H, Zhang H, Margolick JB, Gurer C, Murphy AJ, Valenzuela DM, Yancopoulos GD, Deeks SG, Strowig T, Kumar P, Siliciano JD, Salzberg SL, Flavell RA, Shan L, Siliciano RF. Broad CTL response is required to clear latent HIV-1 due to dominance of escape mutations. Nature. 2015;517(7534):381-5. Epub 2015/01/07. doi: 10.1038/nature14053. PubMed PMID: 25561180; PMCID: PMC4406054.

169. Borducchi EN, Cabral C, Stephenson KE, Liu J, Abbink P, Ng'ang'a D, Nkolola JP, Brinkman AL, Peter L, Lee BC, Jimenez J, Jetton D, Mondesir J, Mojta S, Chandrashekar A, Molloy K, Alter G, Gerold JM, Hill AL, Lewis MG, Pau MG, Schuitemaker H, Hesselgesser J, Geleziunas R, Kim JH, Robb ML, Michael NL, Barouch DH. Ad26/MVA therapeutic vaccination with TLR7 stimulation in SIV-infected rhesus monkeys. Nature. 2016;540(7632):284-7. Epub 2016/11/15. doi: 10.1038/nature20583. PubMed PMID: 27841870; PMCID: PMC5145754.

170. Pan Y, Wang R, Hu D, Xie W, Fu Y, Hou J, Xu L, Zhang Y, Chen M, Zhou Z. Comparative safety and efficacy of molecular-targeted drugs, immune checkpoint inhibitors, hepatic arterial infusion chemotherapy and their combinations in advanced hepatocellular carcinoma: findings from advances in landmark trials. Front Biosci (Landmark Ed). 2021;26(10):873-81. Epub 2021/11/02. doi: 10.52586/4994. PubMed PMID: 34719212.

171. Velu V, Titanji K, Zhu B, Husain S, Pladevega A, Lai L, Vanderford TH, Chennareddi L, Silvestri G, Freeman GJ, Ahmed R, Amara RR. Enhancing SIV-specific immunity in vivo by PD-1 blockade. Nature. 2009;458(7235):206-10. Epub 2008/12/17. doi: 10.1038/nature07662. PubMed PMID: 19078956; PMCID: PMC2753387.

172. Barouch DH, Whitney JB, Moldt B, Klein F, Oliveira TY, Liu J, Stephenson KE, Chang HW, Shekhar K, Gupta S, Nkolola JP, Seaman MS, Smith KM, Borducchi EN, Cabral C, Smith JY, Blackmore S, Sanisetty S, Perry JR, Beck M, Lewis MG, Rinaldi W, Chakraborty AK, Poignard P, Nussenzweig MC, Burton DR. Therapeutic efficacy of potent neutralizing HIV-1-specific monoclonal antibodies in SHIV-infected rhesus monkeys. Nature. 2013;503(7475):224-8. Epub 2013/11/01. doi: 10.1038/nature12744. PubMed PMID: 24172905; PMCID: PMC4017780.

173. Horwitz JA, Halper-Stromberg A, Mouquet H, Gitlin AD, Tretiakova A, Eisenreich TR, Malbec M, Gravemann S, Billerbeck E, Dorner M, Buning H, Schwartz O, Knops E, Kaiser R, Seaman MS, Wilson JM,

Rice CM, Ploss A, Bjorkman PJ, Klein F, Nussenzweig MC. HIV-1 suppression and durable control by combining single broadly neutralizing antibodies and antiretroviral drugs in humanized mice. Proc Natl Acad Sci U S A. 2013;110(41):16538-43. Epub 2013/09/18. doi: 10.1073/pnas.1315295110. PubMed PMID: 24043801; PMCID: PMC3799352.

174. Klein F, Halper-Stromberg A, Horwitz JA, Gruell H, Scheid JF, Bournazos S, Mouquet H, Spatz LA, Diskin R, Abadir A, Zang T, Dorner M, Billerbeck E, Labitt RN, Gaebler C, Marcovecchio P, Incesu RB, Eisenreich TR, Bieniasz PD, Seaman MS, Bjorkman PJ, Ravetch JV, Ploss A, Nussenzweig MC. HIV therapy by a combination of broadly neutralizing antibodies in humanized mice. Nature. 2012;492(7427):118-22. Epub 2012/10/30. doi: 10.1038/nature11604. PubMed PMID: 23103874; PMCID: PMC3809838.

175. Halper-Stromberg A, Lu CL, Klein F, Horwitz JA, Bournazos S, Nogueira L, Eisenreich TR, Liu C, Gazumyan A, Schaefer U, Furze RC, Seaman MS, Prinjha R, Tarakhovsky A, Ravetch JV, Nussenzweig MC. Broadly neutralizing antibodies and viral inducers decrease rebound from HIV-1 latent reservoirs in humanized mice. Cell. 2014;158(5):989-99. Epub 2014/08/19. doi: 10.1016/j.cell.2014.07.043. PubMed PMID: 25131989; PMCID: PMC4163911.

176. Murray AJ, Kwon KJ, Farber DL, Siliciano RF. The Latent Reservoir for HIV-1: How Immunologic Memory and Clonal Expansion Contribute to HIV-1 Persistence. J Immunol. 2016;197(2):407-17. Epub 2016/07/07. doi: 10.4049/jimmunol.1600343. PubMed PMID: 27382129; PMCID: PMC4936486.

177. Rasmussen TA, Lewin SR. Shocking HIV out of hiding: where are we with clinical trials of latency reversing agents? Curr Opin HIV AIDS. 2016;11(4):394-401. Epub 2016/03/15. doi: 10.1097/COH.0000000000000279. PubMed PMID: 26974532.

178. Riddler SA, Para M, Benson CA, Mills A, Ramgopal M, DeJesus E, Brinson C, Cyktor J, Jacobs J, Koontz D, Mellors JW, Laird GM, Wrin T, Patel H, Guo S, Wallin J, Boice J, Zhang L, Humeniuk R, Begley R, German P, Graham H, Geleziunas R, Brainard DM, SenGupta D. Vesatolimod, a Toll-like Receptor 7 Agonist, Induces Immune Activation in Virally Suppressed Adults Living With Human Immunodeficiency Virus-1. Clin Infect Dis. 2021;72(11):e815-e24. Epub 2020/10/13. doi: 10.1093/cid/ciaa1534. PubMed PMID: 33043969.

179. Wykes MN, Lewin SR. Immune checkpoint blockade in infectious diseases. Nat Rev Immunol. 2018;18(2):91-104. Epub 2017/10/11. doi: 10.1038/nri.2017.112. PubMed PMID: 28990586; PMCID: PMC5991909.

180. Harper J, Gordon S, Chan CN, Wang H, Lindemuth E, Galardi C, Falcinelli SD, Raines SLM, Read JL, Nguyen K, McGary CS, Nekorchuk M, Busman-Sahay K, Schawalder J, King C, Pino M, Micci L, Cervasi B, Jean S, Sanderson A, Johns B, Koblansky AA, Amrine-Madsen H, Lifson J, Margolis DM, Silvestri G, Bar KJ, Favre D, Estes JD, Paiardini M. CTLA-4 and PD-1 dual blockade induces SIV reactivation without control of rebound after antiretroviral therapy interruption. Nat Med. 2020;26(4):519-28. Epub 2020/04/15. doi: 10.1038/s41591-020-0782-y. PubMed PMID: 32284611; PMCID: PMC7790171.

181. Nixon CC, Mavigner M, Sampey GC, Brooks AD, Spagnuolo RA, Irlbeck DM, Mattingly C, Ho PT, Schoof N, Cammon CG, Tharp GK, Kanke M, Wang Z, Cleary RA, Upadhyay AA, De C, Wills SR, Falcinelli SD, Galardi C, Walum H, Schramm NJ, Deutsch J, Lifson JD, Fennessey CM, Keele BF, Jean S, Maguire S, Liao B, Browne EP, Ferris RG, Brehm JH, Favre D, Vanderford TH, Bosinger SE, Jones CD, Routy JP, Archin NM, Margolis DM, Wahl A, Dunham RM, Silvestri G, Chahroudi A, Garcia JV. Systemic HIV and SIV latency reversal via non-canonical NF-kappaB signalling in vivo. Nature. 2020;578(7793):160-5. Epub 2020/01/24. doi: 10.1038/s41586-020-1951-3. PubMed PMID: 31969707; PMCID: PMC7111210.

182. McBrien JB, Mavigner M, Franchitti L, Smith SA, White E, Tharp GK, Walum H, Busman-Sahay K, Aguilera-Sandoval CR, Thayer WO, Spagnuolo RA, Kovarova M, Wahl A, Cervasi B, Margolis DM, Vanderford TH, Carnathan DG, Paiardini M, Lifson JD, Lee JH, Safrit JT, Bosinger SE, Estes JD, Derdeyn CA, Garcia JV, Kulpa DA, Chahroudi A, Silvestri G. Robust and persistent reactivation of SIV and HIV by N-803

and depletion of CD8(+) cells. Nature. 2020;578(7793):154-9. Epub 2020/01/24. doi: 10.1038/s41586-020-1946-0. PubMed PMID: 31969705; PMCID: PMC7580846.
183. McBrien JB, Wong AKH, White E, Carnathan DG, Lee JH, Safrit JT, Vanderford TH, Paiardini M, Chahroudi A, Silvestri G. Combination of CD8beta Depletion and Interleukin-15 Superagonist N-803 Induces Virus Reactivation in Simian-Human Immunodeficiency Virus-Infected, Long-Term ART-Treated Rhesus Macaques. J Virol. 2020;94(19). Epub 2020/07/17. doi: 10.1128/JVI.00755-20. PubMed PMID: 32669328; PMCID: PMC7495383.
184. Mavigner M, Liao LE, Brooks AD, Ke R, Mattingly C, Schoof N, McBrien J, Carnathan D, Liang S, Vanderford TH, Paiardini M, Kulpa D, Lifson JD, Dunham RM, Easley KA, Margolis DM, Perelson AS, Silvestri G, Chahroudi A. CD8 lymphocyte depletion enhances the latency reversal activity of the SMAC mimetic AZD5582 in ART-suppressed SIV-infected rhesus macaques. J Virol. 2021. Epub 2021/02/12. doi: 10.1128/JVI.01429-20. PubMed PMID: 33568515; PMCID: PMC8103677.
185. Bekerman E, Hesselgesser J, Carr B, Nagel M, Hung M, Wang A, Stapleton L, von Gegerfelt A, Elyard HA, Lifson JD, Geleziunas R. PD-1 Blockade and TLR7 Activation Lack Therapeutic Benefit in Chronic Simian Immunodeficiency Virus-Infected Macaques on Antiretroviral Therapy. Antimicrob Agents Chemother. 2019;63(11). Epub 2019/09/11. doi: 10.1128/AAC.01163-19. PubMed PMID: 31501143; PMCID: PMC6811450.
186. Mylvaganam GH, Chea LS, Tharp GK, Hicks S, Velu V, Iyer SS, Deleage C, Estes JD, Bosinger SE, Freeman GJ, Ahmed R, Amara RR. Combination anti-PD-1 and antiretroviral therapy provides therapeutic benefit against SIV. JCI Insight. 2018;3(18). Epub 2018/09/21. doi: 10.1172/jci.insight.122940. PubMed PMID: 30232277; PMCID: PMC6237231.
187. Ananworanich J, McSteen B, Robb ML. Broadly neutralizing antibody and the HIV reservoir in acute HIV infection: a strategy toward HIV remission? Curr Opin HIV AIDS. 2015;10(3):198-206. Epub 2015/02/24. doi: 10.1097/COH.0000000000000144. PubMed PMID: 25700203; PMCID: PMC4428158.
188. Centers for Disease C. Unexplained immunodeficiency and opportunistic infections in infants--New York, New Jersey, California. MMWR Morb Mortal Wkly Rep. 1982;31(49):665-7. Epub 1982/12/17. PubMed PMID: 6819445.
189. [10/06/2020]. Available from: https://www.unaids.org/en/resources/fact-sheet.
190. Goulder PJ, Lewin SR, Leitman EM. Paediatric HIV infection: the potential for cure. Nat Rev Immunol. 2016;16(4):259-71. Epub 2016/03/15. doi: 10.1038/nri.2016.19. PubMed PMID: 26972723; PMCID: PMC5694689.
191. [01/04/2018]. Available from: http://www.unaids.org/en/resources/fact-sheet.
192. De Cock KM, Fowler MG, Mercier E, de Vincenzi I, Saba J, Hoff E, Alnwick DJ, Rogers M, Shaffer N. Prevention of mother-to-child HIV transmission in resource-poor countries: translating research into policy and practice. JAMA. 2000;283(9):1175-82. Epub 2000/03/07. PubMed PMID: 10703780.
193. Iliff PJ, Piwoz EG, Tavengwa NV, Zunguza CD, Marinda ET, Nathoo KJ, Moulton LH, Ward BJ, Humphrey JH, group Zs. Early exclusive breastfeeding reduces the risk of postnatal HIV-1 transmission and increases HIV-free survival. AIDS. 2005;19(7):699-708. Epub 2005/04/12. PubMed PMID: 15821396.
194. Coovadia HM, Rollins NC, Bland RM, Little K, Coutsoudis A, Bennish ML, Newell ML. Mother-to-child transmission of HIV-1 infection during exclusive breastfeeding in the first 6 months of life: an intervention cohort study. Lancet. 2007;369(9567):1107-16. Epub 2007/04/03. doi: 10.1016/S0140-6736(07)60283-9. PubMed PMID: 17398310.
195. Connor EM, Sperling RS, Gelber R, Kiselev P, Scott G, O'Sullivan MJ, VanDyke R, Bey M, Shearer W, Jacobson RL, et al. Reduction of maternal-infant transmission of human immunodeficiency virus type 1 with zidovudine treatment. Pediatric AIDS Clinical Trials Group Protocol 076 Study Group. N Engl J Med.

1994;331(18):1173-80. Epub 1994/11/03. doi: 10.1056/NEJM199411033311801. PubMed PMID: 7935654.
196. Cooper ER, Charurat M, Mofenson L, Hanson IC, Pitt J, Diaz C, Hayani K, Handelsman E, Smeriglio V, Hoff R, Blattner W, Women, Infants' Transmission Study G. Combination antiretroviral strategies for the treatment of pregnant HIV-1-infected women and prevention of perinatal HIV-1 transmission. J Acquir Immune Defic Syndr. 2002;29(5):484-94. Epub 2002/05/01. PubMed PMID: 11981365.
197. Organization GWH. WHO. Programmatic Update Guidelines Use of Antiretroviral Drugs for Treating Pregnant Women and Preventing HIV Infection in Infants. Executive Summary 2012 [11/28/2018]. Available from: http://www.who.int/hiv/PMTCT_update.pdf.
198. Townsend CL, Byrne L, Cortina-Borja M, Thorne C, de Ruiter A, Lyall H, Taylor GP, Peckham CS, Tookey PA. Earlier initiation of ART and further decline in mother-to-child HIV transmission rates, 2000-2011. AIDS. 2014;28(7):1049-57. Epub 2014/02/26. doi: 10.1097/QAD.0000000000000212. PubMed PMID: 24566097.
199. Lim ES, Wang D, Holtz LR. The Bacterial Microbiome and Virome Milestones of Infant Development. Trends Microbiol. 2016;24(10):801-10. Epub 2016/06/30. doi: 10.1016/j.tim.2016.06.001. PubMed PMID: 27353648.
200. Luzuriaga K, Mofenson LM. Challenges in the Elimination of Pediatric HIV-1 Infection. N Engl J Med. 2016;374(8):761-70. Epub 2016/03/05. doi: 10.1056/NEJMra1505256. PubMed PMID: 26933850.
201. Jani IV, Meggi B, Mabunda N, Vubil A, Sitoe NE, Tobaiwa O, Quevedo JI, Lehe JD, Loquiha O, Vojnov L, Peter TF. Accurate early infant HIV diagnosis in primary health clinics using a point-of-care nucleic acid test. J Acquir Immune Defic Syndr. 2014;67(1):e1-4. Epub 2014/06/17. doi: 10.1097/QAI.0000000000000250. PubMed PMID: 24933096.
202. The Use of Antiretroviral Drugs for Treating and Preventing HIV Infection [11/23/2018]. Available from: http://apps.who.int/iris/bitstream/handle/10665/85321/9789241505727_eng.pdf?sequence=1.
203. Organization GWH. WHO recommendations on the diagnosis of HIV infection in infants and children. 2010 [11/26/2018]. Available from: http://whqlibdoc.who.int/publications/2010/9789241599085_eng.pdf?ua=1.
204. UNAIDS. The Gap Report [11/26/2018]. Available from: http://www.unaids.org/sites/default/files/media_asset/UNAIDS_Gap_report_en.pdf.
205. Creek TL, Sherman GG, Nkengasong J, Lu L, Finkbeiner T, Fowler MG, Rivadeneira E, Shaffer N. Infant human immunodeficiency virus diagnosis in resource-limited settings: issues, technologies, and country experiences. Am J Obstet Gynecol. 2007;197(3 Suppl):S64-71. Epub 2007/09/14. doi: 10.1016/j.ajog.2007.03.002. PubMed PMID: 17825652.
206. Seidenberg P, Nicholson S, Schaefer M, Semrau K, Bweupe M, Masese N, Bonawitz R, Chitembo L, Goggin C, Thea DM. Early infant diagnosis of HIV infection in Zambia through mobile phone texting of blood test results. Bull World Health Organ. 2012;90(5):348-56. Epub 2012/05/17. doi: 10.2471/BLT.11.100032. PubMed PMID: 22589568; PMCID: PMC3341697.
207. Essajee S, Bhairavabhotla R, Penazzato M, Kiragu K, Jani I, Carmona S, Rewari B, Kiyaga C, Nkengasong J, Peter T. Scale-up of Early Infant HIV Diagnosis and Improving Access to Pediatric HIV Care in Global Plan Countries: Past and Future Perspectives. J Acquir Immune Defic Syndr. 2017;75 Suppl 1:S51-S8. Epub 2017/04/12. doi: 10.1097/QAI.0000000000001319. PubMed PMID: 28398997.
208. Goulder PJ, Brander C, Tang Y, Tremblay C, Colbert RA, Addo MM, Rosenberg ES, Nguyen T, Allen R, Trocha A, Altfeld M, He S, Bunce M, Funkhouser R, Pelton SI, Burchett SK, McIntosh K, Korber BT, Walker BD. Evolution and transmission of stable CTL escape mutations in HIV infection. Nature. 2001;412(6844):334-8. Epub 2001/07/19. doi: 10.1038/35085576. PubMed PMID: 11460164.

209. Wilson CC, Brown RC, Korber BT, Wilkes BM, Ruhl DJ, Sakamoto D, Kunstman K, Luzuriaga K, Hanson IC, Widmayer SM, Wiznia A, Clapp S, Ammann AJ, Koup RA, Wolinsky SM, Walker BD. Frequent detection of escape from cytotoxic T-lymphocyte recognition in perinatal human immunodeficiency virus (HIV) type 1 transmission: the ariel project for the prevention of transmission of HIV from mother to infant. J Virol. 1999;73(5):3975-85. Epub 1999/04/10. PubMed PMID: 10196293; PMCID: PMC104176.
210. Bunders MJ, van der Loos CM, Klarenbeek PL, van Hamme JL, Boer K, Wilde JC, de Vries N, van Lier RA, Kootstra N, Pals ST, Kuijpers TW. Memory CD4(+)CCR5(+) T cells are abundantly present in the gut of newborn infants to facilitate mother-to-child transmission of HIV-1. Blood. 2012;120(22):4383-90. Epub 2012/10/04. doi: 10.1182/blood-2012-06-437566. PubMed PMID: 23033270.
211. Wang X, Xu H, Pahar B, Alvarez X, Green LC, Dufour J, Moroney-Rasmussen T, Lackner AA, Veazey RS. Simian immunodeficiency virus selectively infects proliferating CD4+ T cells in neonatal rhesus macaques. Blood. 2010;116(20):4168-74. Epub 2010/08/19. doi: 10.1182/blood-2010-03-273482. PubMed PMID: 20716768; PMCID: PMC2993622.
212. Veazey RS, Lifson JD, Pandrea I, Purcell J, Piatak M, Jr., Lackner AA. Simian immunodeficiency virus infection in neonatal macaques. J Virol. 2003;77(16):8783-92. Epub 2003/07/30. PubMed PMID: 12885897; PMCID: PMC167220.
213. Mor G, Aldo P, Alvero AB. The unique immunological and microbial aspects of pregnancy. Nat Rev Immunol. 2017;17(8):469-82. Epub 2017/06/20. doi: 10.1038/nri.2017.64. PubMed PMID: 28627518.
214. Mold JE, Michaelsson J, Burt TD, Muench MO, Beckerman KP, Busch MP, Lee TH, Nixon DF, McCune JM. Maternal alloantigens promote the development of tolerogenic fetal regulatory T cells in utero. Science. 2008;322(5907):1562-5. Epub 2008/12/06. doi: 10.1126/science.1164511. PubMed PMID: 19056990; PMCID: PMC2648820.
215. Takahata Y, Nomura A, Takada H, Ohga S, Furuno K, Hikino S, Nakayama H, Sakaguchi S, Hara T. CD25+CD4+ T cells in human cord blood: an immunoregulatory subset with naive phenotype and specific expression of forkhead box p3 (Foxp3) gene. Exp Hematol. 2004;32(7):622-9. Epub 2004/07/13. doi: 10.1016/j.exphem.2004.03.012. PubMed PMID: 15246158.
216. Wang X, Xu H, Shen C, Alvarez X, Liu D, Pahar B, Ratterree MS, Doyle-Meyers LA, Lackner AA, Veazey RS. Profound loss of intestinal Tregs in acutely SIV-infected neonatal macaques. J Leukoc Biol. 2015;97(2):391-400. Epub 2014/12/11. doi: 10.1189/jlb.4A0514-266RR. PubMed PMID: 25492938; PMCID: PMC4304427.
217. Hebel K, Weinert S, Kuropka B, Knolle J, Kosak B, Jorch G, Arens C, Krause E, Braun-Dullaeus RC, Brunner-Weinzierl MC. CD4+ T cells from human neonates and infants are poised spontaneously to run a nonclassical IL-4 program. J Immunol. 2014;192(11):5160-70. Epub 2014/04/30. doi: 10.4049/jimmunol.1302539. PubMed PMID: 24778440.
218. Siegrist CA. Neonatal and early life vaccinology. Vaccine. 2001;19(25-26):3331-46. Epub 2001/05/12. PubMed PMID: 11348697.
219. Reikie BA, Adams RCM, Leligdowicz A, Ho K, Naidoo S, Rusk CE, de Beer C, Preiser W, Cotton MF, Speert DP, Esser M, Kollmann TR. Altered innate immune development in HIV-exposed uninfected infants. J Acquir Immune Defic Syndr. 2014;66(3):245-55. Epub 2014/04/16. doi: 10.1097/QAI.0000000000000161. PubMed PMID: 24732876; PMCID: PMC4146715.
220. Sugimoto C, Merino KM, Hasegawa A, Wang X, Alvarez XA, Wakao H, Mori K, Kim WK, Veazey RS, Didier ES, Kuroda MJ. Critical Role for Monocytes/Macrophages in Rapid Progression to AIDS in Pediatric Simian Immunodeficiency Virus-Infected Rhesus Macaques. J Virol. 2017;91(17). Epub 2017/06/02. doi: 10.1128/JVI.00379-17. PubMed PMID: 28566378; PMCID: PMC5553179.
221. Luzuriaga K, McManus M, Catalina M, Mayack S, Sharkey M, Stevenson M, Sullivan JL. Early therapy of vertical human immunodeficiency virus type 1 (HIV-1) infection: control of viral replication and

absence of persistent HIV-1-specific immune responses. J Virol. 2000;74(15):6984-91. Epub 2000/07/11. doi: 10.1128/jvi.74.15.6984-6991.2000. PubMed PMID: 10888637; PMCID: PMC112215.
222. Slyker JA, John-Stewart GC, Dong T, Lohman-Payne B, Reilly M, Atzberger A, Taylor S, Maleche-Obimbo E, Mbori-Ngacha D, Rowland-Jones SL. Phenotypic characterization of HIV-specific CD8+ T cells during early and chronic infant HIV-1 infection. PLoS One. 2011;6(5):e20375. Epub 2011/06/10. doi: 10.1371/journal.pone.0020375. PubMed PMID: 21655252; PMCID: PMC3105047.
223. Xu H, Ziani W, Shao J, Doyle-Meyers LA, Russell-Lodrigue KE, Ratterree MS, Veazey RS, Wang X. Impaired Development and Expansion of Germinal Center Follicular Th Cells in Simian Immunodeficiency Virus-Infected Neonatal Macaques. J Immunol. 2018;201(7):1994-2003. Epub 2018/08/15. doi: 10.4049/jimmunol.1800235. PubMed PMID: 30104244; PMCID: PMC6245642.
224. Muema DM, Macharia GN, Olusola BA, Hassan AS, Fegan GW, Berkley JA, Urban BC, Nduati EW. Proportions of circulating follicular helper T cells are reduced and correlate with memory B cells in HIV-infected children. PLoS One. 2017;12(4):e0175570. Epub 2017/04/27. doi: 10.1371/journal.pone.0175570. PubMed PMID: 28445512; PMCID: PMC5405965.
225. Simonich CA, Williams KL, Verkerke HP, Williams JA, Nduati R, Lee KK, Overbaugh J. HIV-1 Neutralizing Antibodies with Limited Hypermutation from an Infant. Cell. 2016;166(1):77-87. Epub 2016/06/28. doi: 10.1016/j.cell.2016.05.055. PubMed PMID: 27345369; PMCID: PMC4930401.
226. Goo L, Chohan V, Nduati R, Overbaugh J. Early development of broadly neutralizing antibodies in HIV-1-infected infants. Nat Med. 2014;20(6):655-8. Epub 2014/05/27. doi: 10.1038/nm.3565. PubMed PMID: 24859529; PMCID: PMC4060046.
227. Eckard AR, Fowler SL, Haston JC, Dixon TC. Complications of Treatment in Youth with HIV. Curr HIV/AIDS Rep. 2016;13(4):226-33. Epub 2016/05/29. doi: 10.1007/s11904-016-0320-1. PubMed PMID: 27234970; PMCID: PMC4977197.
228. Kaslow RA, Carrington M, Apple R, Park L, Munoz A, Saah AJ, Goedert JJ, Winkler C, O'Brien SJ, Rinaldo C, Detels R, Blattner W, Phair J, Erlich H, Mann DL. Influence of combinations of human major histocompatibility complex genes on the course of HIV-1 infection. Nat Med. 1996;2(4):405-11. Epub 1996/04/01. PubMed PMID: 8597949.
229. International HIVCS, Pereyra F, Jia X, McLaren PJ, Telenti A, de Bakker PI, Walker BD, Ripke S, Brumme CJ, Pulit SL, Carrington M, Kadie CM, Carlson JM, Heckerman D, Graham RR, Plenge RM, Deeks SG, Gianniny L, Crawford G, Sullivan J, Gonzalez E, Davies L, Camargo A, Moore JM, Beattie N, Gupta S, Crenshaw A, Burtt NP, Guiducci C, Gupta N, Gao X, Qi Y, Yuki Y, Piechocka-Trocha A, Cutrell E, Rosenberg R, Moss KL, Lemay P, O'Leary J, Schaefer T, Verma P, Toth I, Block B, Baker B, Rothchild A, Lian J, Proudfoot J, Alvino DM, Vine S, Addo MM, Allen TM, Altfeld M, Henn MR, Le Gall S, Streeck H, Haas DW, Kuritzkes DR, Robbins GK, Shafer RW, Gulick RM, Shikuma CM, Haubrich R, Riddler S, Sax PE, Daar ES, Ribaudo HJ, Agan B, Agarwal S, Ahern RL, Allen BL, Altidor S, Altschuler EL, Ambardar S, Anastos K, Anderson B, Anderson V, Andrady U, Antoniskis D, Bangsberg D, Barbaro D, Barrie W, Bartczak J, Barton S, Basden P, Basgoz N, Bazner S, Bellos NC, Benson AM, Berger J, Bernard NF, Bernard AM, Birch C, Bodner SJ, Bolan RK, Boudreaux ET, Bradley M, Braun JF, Brndjar JE, Brown SJ, Brown K, Brown ST, Burack J, Bush LM, Cafaro V, Campbell O, Campbell J, Carlson RH, Carmichael JK, Casey KK, Cavacuiti C, Celestin G, Chambers ST, Chez N, Chirch LM, Cimoch PJ, Cohen D, Cohn LE, Conway B, Cooper DA, Cornelson B, Cox DT, Cristofano MV, Cuchural G, Jr., Czartoski JL, Dahman JM, Daly JS, Davis BT, Davis K, Davod SM, DeJesus E, Dietz CA, Dunham E, Dunn ME, Ellerin TB, Eron JJ, Fangman JJ, Farel CE, Ferlazzo H, Fidler S, Fleenor-Ford A, Frankel R, Freedberg KA, French NK, Fuchs JD, Fuller JD, Gaberman J, Gallant JE, Gandhi RT, Garcia E, Garmon D, Gathe JC, Jr., Gaultier CR, Gebre W, Gilman FD, Gilson I, Goepfert PA, Gottlieb MS, Goulston C, Groger RK, Gurley TD, Haber S, Hardwicke R, Hardy WD, Harrigan PR, Hawkins TN, Heath S, Hecht FM, Henry WK, Hladek M, Hoffman RP, Horton JM, Hsu RK, Huhn GD, Hunt P, Hupert MJ, Illeman ML, Jaeger H, Jellinger

RM, John M, Johnson JA, Johnson KL, Johnson H, Johnson K, Joly J, Jordan WC, Kauffman CA, Khanlou H, Killian RK, Kim AY, Kim DD, Kinder CA, Kirchner JT, Kogelman L, Kojic EM, Korthuis PT, Kurisu W, Kwon DS, LaMar M, Lampiris H, Lanzafame M, Lederman MM, Lee DM, Lee JM, Lee MJ, Lee ET, Lemoine J, Levy JA, Llibre JM, Liguori MA, Little SJ, Liu AY, Lopez AJ, Loutfy MR, Loy D, Mohammed DY, Man A, Mansour MK, Marconi VC, Markowitz M, Marques R, Martin JN, Martin HL, Jr., Mayer KH, McElrath MJ, McGhee TA, McGovern BH, McGowan K, McIntyre D, McLeod GX, Menezes P, Mesa G, Metroka CE, Meyer-Olson D, Miller AO, Montgomery K, Mounzer KC, Nagami EH, Nagin I, Nahass RG, Nelson MO, Nielsen C, Norene DL, O'Connor DH, Ojikutu BO, Okulicz J, Oladehin OO, Oldfield EC, 3rd, Olender SA, Ostrowski M, Owen WF, Jr., Pae E, Parsonnet J, Pavlatos AM, Perlmutter AM, Pierce MN, Pincus JM, Pisani L, Price LJ, Proia L, Prokesch RC, Pujet HC, Ramgopal M, Rathod A, Rausch M, Ravishankar J, Rhame FS, Richards CS, Richman DD, Rodes B, Rodriguez M, Rose RC, 3rd, Rosenberg ES, Rosenthal D, Ross PE, Rubin DS, Rumbaugh E, Saenz L, Salvaggio MR, Sanchez WC, Sanjana VM, Santiago S, Schmidt W, Schuitemaker H, Sestak PM, Shalit P, Shay W, Shirvani VN, Silebi VI, Sizemore JM, Jr., Skolnik PR, Sokol-Anderson M, Sosman JM, Stabile P, Stapleton JT, Starrett S, Stein F, Stellbrink HJ, Sterman FL, Stone VE, Stone DR, Tambussi G, Taplitz RA, Tedaldi EM, Telenti A, Theisen W, Torres R, Tosiello L, Tremblay C, Tribble MA, Trinh PD, Tsao A, Ueda P, Vaccaro A, Valadas E, Vanig TJ, Vecino I, Vega VM, Veikley W, Wade BH, Walworth C, Wanidworanun C, Ward DJ, Warner DA, Weber RD, Webster D, Weis S, Wheeler DA, White DJ, Wilkins E, Winston A, Wlodaver CG, van't Wout A, Wright DP, Yang OO, Yurdin DL, Zabukovic BW, Zachary KC, Zeeman B, Zhao M. The major genetic determinants of HIV-1 control affect HLA class I peptide presentation. Science. 2010;330(6010):1551-7. Epub 2010/11/06. doi: 10.1126/science.1195271. PubMed PMID: 21051598; PMCID: PMC3235490.

230. Kiepiela P, Ngumbela K, Thobakgale C, Ramduth D, Honeyborne I, Moodley E, Reddy S, de Pierres C, Mncube Z, Mkhwanazi N, Bishop K, van der Stok M, Nair K, Khan N, Crawford H, Payne R, Leslie A, Prado J, Prendergast A, Frater J, McCarthy N, Brander C, Learn GH, Nickle D, Rousseau C, Coovadia H, Mullins JI, Heckerman D, Walker BD, Goulder P. CD8+ T-cell responses to different HIV proteins have discordant associations with viral load. Nat Med. 2007;13(1):46-53. Epub 2006/12/19. doi: 10.1038/nm1520. PubMed PMID: 17173051.

231. Shearer WT, Rosenblatt HM, Gelman RS, Oyomopito R, Plaeger S, Stiehm ER, Wara DW, Douglas SD, Luzuriaga K, McFarland EJ, Yogev R, Rathore MH, Levy W, Graham BL, Spector SA, Pediatric ACTG. Lymphocyte subsets in healthy children from birth through 18 years of age: the Pediatric AIDS Clinical Trials Group P1009 study. J Allergy Clin Immunol. 2003;112(5):973-80. Epub 2003/11/12. doi: 10.1016/j.jaci.2003.07.003. PubMed PMID: 14610491.

232. Silvestri G, Sodora DL, Koup RA, Paiardini M, O'Neil SP, McClure HM, Staprans SI, Feinberg MB. Nonpathogenic SIV infection of sooty mangabeys is characterized by limited bystander immunopathology despite chronic high-level viremia. Immunity. 2003;18(3):441-52. Epub 2003/03/22. PubMed PMID: 12648460.

233. Persaud D, Gay H, Ziemniak C, Chen YH, Piatak M, Jr., Chun TW, Strain M, Richman D, Luzuriaga K. Absence of detectable HIV-1 viremia after treatment cessation in an infant. N Engl J Med. 2013;369(19):1828-35. Epub 2013/10/25. doi: 10.1056/NEJMoa1302976. PubMed PMID: 24152233; PMCID: PMC3954754.

234. Butler KM, Gavin P, Coughlan S, Rochford A, Mc Donagh S, Cunningham O, Poulsom H, Watters SA, Klein N. Rapid viral rebound after 4 years of suppressive therapy in a seronegative HIV-1 infected infant treated from birth. Pediatr Infect Dis J. 2015;34(3):e48-51. Epub 2015/03/06. doi: 10.1097/INF.0000000000000570. PubMed PMID: 25742088.

235. Cotton MF, Violari A, Otwombe K, Panchia R, Dobbels E, Rabie H, Josipovic D, Liberty A, Lazarus E, Innes S, van Rensburg AJ, Pelser W, Truter H, Madhi SA, Handelsman E, Jean-Philippe P, McIntyre JA, Gibb

DM, Babiker AG, Team CS. Early time-limited antiretroviral therapy versus deferred therapy in South African infants infected with HIV: results from the children with HIV early antiretroviral (CHER) randomised trial. Lancet. 2013;382(9904):1555-63. Epub 2013/11/12. doi: 10.1016/S0140-6736(13)61409-9. PubMed PMID: 24209829; PMCID: PMC4104982.

236. Giacomet V, Trabattoni D, Zanchetta N, Biasin M, Gismondo M, Clerici M, Zuccotti G. No cure of HIV infection in a child despite early treatment and apparent viral clearance. Lancet. 2014;384(9950):1320. Epub 2014/10/07. doi: 10.1016/S0140-6736(14)61405-7. PubMed PMID: 25283573.

237. [02/21/2017]. Available from: http://www.clinicaltrials.gov.

238. Abel K, Pahar B, Van Rompay KK, Fritts L, Sin C, Schmidt K, Colon R, McChesney M, Marthas ML. Rapid virus dissemination in infant macaques after oral simian immunodeficiency virus exposure in the presence of local innate immune responses. J Virol. 2006;80(13):6357-67. Epub 2006/06/16. doi: 10.1128/JVI.02240-05. PubMed PMID: 16775324; PMCID: PMC1488945.

239. Milush JM, Kosub D, Marthas M, Schmidt K, Scott F, Wozniakowski A, Brown C, Westmoreland S, Sodora DL. Rapid dissemination of SIV following oral inoculation. AIDS. 2004;18(18):2371-80. Epub 2004/12/29. PubMed PMID: 15622313.

240. Liu J, Li H, Iampietro MJ, Barouch DH. Accelerated heterologous adenovirus prime-boost SIV vaccine in neonatal rhesus monkeys. J Virol. 2012;86(15):7829-35. Epub 2012/05/18. doi: 10.1128/JVI.00512-12. PubMed PMID: 22593160; PMCID: PMC3421666.

241. Jensen K, Pena MG, Wilson RL, Ranganathan UD, Jacobs WR, Jr., Fennelly G, Larsen M, Van Rompay KK, Kozlowski PA, Abel K. A neonatal oral Mycobacterium tuberculosis-SIV prime / intramuscular MVA-SIV boost combination vaccine induces both SIV and Mtb-specific immune responses in infant macaques. Trials Vaccinol. 2013;2:53-63. Epub 2014/01/24. doi: 10.1016/j.trivac.2013.09.005. PubMed PMID: 24454591; PMCID: PMC3894789.

242. Persaud D, Palumbo PE, Ziemniak C, Hughes MD, Alvero CG, Luzuriaga K, Yogev R, Capparelli EV, Chadwick EG. Dynamics of the resting CD4(+) T-cell latent HIV reservoir in infants initiating HAART less than 6 months of age. AIDS. 2012;26(12):1483-90. Epub 2012/05/05. doi: 10.1097/QAD.0b013e3283553638. PubMed PMID: 22555165; PMCID: PMC3495308.

243. Roethle PA, McFadden RM, Yang H, Hrvatin P, Hui H, Graupe M, Gallagher B, Chao J, Hesselgesser J, Duatschek P, Zheng J, Lu B, Tumas DB, Perry J, Halcomb RL. Identification and optimization of pteridinone Toll-like receptor 7 (TLR7) agonists for the oral treatment of viral hepatitis. J Med Chem. 2013;56(18):7324-33. Epub 2013/08/22. doi: 10.1021/jm400815m. PubMed PMID: 23961878.

244. Macedo AB, Novis CL, Bosque A. Targeting Cellular and Tissue HIV Reservoirs With Toll-Like Receptor Agonists. Front Immunol. 2019;10:2450. Epub 2019/11/05. doi: 10.3389/fimmu.2019.02450. PubMed PMID: 31681325; PMCID: PMC6804373.

245. Lim SY, Osuna CE, Hraber PT, Hesselgesser J, Gerold JM, Barnes TL, Sanisetty S, Seaman MS, Lewis MG, Geleziunas R, Miller MD, Cihlar T, Lee WA, Hill AL, Whitney JB. TLR7 agonists induce transient viremia and reduce the viral reservoir in SIV-infected rhesus macaques on antiretroviral therapy. Sci Transl Med. 2018;10(439). Epub 2018/05/04. doi: 10.1126/scitranslmed.aao4521. PubMed PMID: 29720451; PMCID: PMC5973480.

246. Borducchi EN, Liu J, Nkolola JP, Cadena AM, Yu WH, Fischinger S, Broge T, Abbink P, Mercado NB, Chandrashekar A, Jetton D, Peter L, McMahan K, Moseley ET, Bekerman E, Hesselgesser J, Li W, Lewis MG, Alter G, Geleziunas R, Barouch DH. Antibody and TLR7 agonist delay viral rebound in SHIV-infected monkeys. Nature. 2018;563(7731):360-4. Epub 2018/10/05. doi: 10.1038/s41586-018-0600-6. PubMed PMID: 30283138; PMCID: PMC6237629.

247. Liu M, Guo S, Hibbert JM, Jain V, Singh N, Wilson NO, Stiles JK. CXCL10/IP-10 in infectious diseases pathogenesis and potential therapeutic implications. Cytokine Growth Factor Rev. 2011;22(3):121-30. Epub 2011/08/02. doi: 10.1016/j.cytogfr.2011.06.001. PubMed PMID: 21802343; PMCID: PMC3203691.
248. Grabowska J, Lopez-Venegas MA, Affandi AJ, den Haan JMM. CD169(+) Macrophages Capture and Dendritic Cells Instruct: The Interplay of the Gatekeeper and the General of the Immune System. Front Immunol. 2018;9:2472. Epub 2018/11/13. doi: 10.3389/fimmu.2018.02472. PubMed PMID: 30416504; PMCID: PMC6212557.
249. Bolton DL, Minang JT, Trivett MT, Song K, Tuscher JJ, Li Y, Piatak M, Jr., O'Connor D, Lifson JD, Roederer M, Ohlen C. Trafficking, persistence, and activation state of adoptively transferred allogeneic and autologous Simian Immunodeficiency Virus-specific CD8(+) T cell clones during acute and chronic infection of rhesus macaques. J Immunol. 2010;184(1):303-14. Epub 2009/12/02. doi: 10.4049/jimmunol.0902413. PubMed PMID: 19949089; PMCID: PMC2797565.
250. Chun TW, Stuyver L, Mizell SB, Ehler LA, Mican JA, Baseler M, Lloyd AL, Nowak MA, Fauci AS. Presence of an inducible HIV-1 latent reservoir during highly active antiretroviral therapy. Proc Natl Acad Sci U S A. 1997;94(24):13193-7. Epub 1997/12/16. doi: 10.1073/pnas.94.24.13193. PubMed PMID: 9371822; PMCID: PMC24285.
251. Ho YC, Shan L, Hosmane NN, Wang J, Laskey SB, Rosenbloom DI, Lai J, Blankson JN, Siliciano JD, Siliciano RF. Replication-competent noninduced proviruses in the latent reservoir increase barrier to HIV-1 cure. Cell. 2013;155(3):540-51. Epub 2013/11/19. doi: 10.1016/j.cell.2013.09.020. PubMed PMID: 24243014; PMCID: PMC3896327.
252. ClinicalTrials.gov [05/17/2020]. Available from: http://www.clinicaltrials.gov.
253. Palma P, Romiti ML, Montesano C, Santilli V, Mora N, Aquilani A, Dispinseri S, Tchidjou HK, Montano M, Eriksson LE, Baldassari S, Bernardi S, Scarlatti G, Wahren B, Rossi P. Therapeutic DNA vaccination of vertically HIV-infected children: report of the first pediatric randomised trial (PEDVAC). PLoS One. 2013;8(11):e79957. Epub 2013/12/07. doi: 10.1371/journal.pone.0079957. PubMed PMID: 24312194; PMCID: PMC3842924.
254. Del Prete GQ, Smedley J, Macallister R, Jones GS, Li B, Hattersley J, Zheng J, Piatak M, Jr., Keele BF, Hesselgesser J, Geleziunas R, Lifson JD. Short Communication: Comparative Evaluation of Coformulated Injectable Combination Antiretroviral Therapy Regimens in Simian Immunodeficiency Virus-Infected Rhesus Macaques. AIDS Res Hum Retroviruses. 2016;32(2):163-8. Epub 2015/07/08. doi: 10.1089/AID.2015.0130. PubMed PMID: 26150024; PMCID: PMC4761795.
255. Shytaj IL, Norelli S, Chirullo B, Della Corte A, Collins M, Yalley-Ogunro J, Greenhouse J, Iraci N, Acosta EP, Barreca ML, Lewis MG, Savarino A. A highly intensified ART regimen induces long-term viral suppression and restriction of the viral reservoir in a simian AIDS model. PLoS Pathog. 2012;8(6):e1002774. Epub 2012/06/28. doi: 10.1371/journal.ppat.1002774. PubMed PMID: 22737073; PMCID: PMC3380955.
256. Nixon CC, Mavigner M, Silvestri G, Garcia JV. In Vivo Models of Human Immunodeficiency Virus Persistence and Cure Strategies. J Infect Dis. 2017;215(suppl_3):S142-S51. Epub 2017/05/19. doi: 10.1093/infdis/jiw637. PubMed PMID: 28520967; PMCID: PMC5410984.
257. Policicchio BB, Pandrea I, Apetrei C. Animal Models for HIV Cure Research. Front Immunol. 2016;7:12. Epub 2016/02/10. doi: 10.3389/fimmu.2016.00012. PubMed PMID: 26858716; PMCID: PMC4729870.
258. Meyers TM, Yotebieng M, Kuhn L, Moultrie H. Antiretroviral therapy responses among children attending a large public clinic in Soweto, South Africa. Pediatr Infect Dis J. 2011;30(11):974-9. Epub 2011/07/08. doi: 10.1097/INF.0b013e31822539f6. PubMed PMID: 21734620; PMCID: PMC3193588.

259. Teasdale CA, Abrams EJ, Coovadia A, Strehlau R, Martens L, Kuhn L. Adherence and viral suppression among infants and young children initiating protease inhibitor-based antiretroviral therapy. Pediatr Infect Dis J. 2013;32(5):489-94. Epub 2012/12/20. doi: 10.1097/INF.0b013e31827e84ba. PubMed PMID: 23249913; PMCID: PMC3624073.
260. van Dijk JH, Sutcliffe CG, Munsanje B, Sinywimaanzi P, Hamangaba F, Thuma PE, Moss WJ. HIV-infected children in rural Zambia achieve good immunologic and virologic outcomes two years after initiating antiretroviral therapy. PLoS One. 2011;6(4):e19006. Epub 2011/05/10. doi: 10.1371/journal.pone.0019006. PubMed PMID: 21552521; PMCID: PMC3084269.
261. Abbink P, Lemckert AA, Ewald BA, Lynch DM, Denholtz M, Smits S, Holterman L, Damen I, Vogels R, Thorner AR, O'Brien KL, Carville A, Mansfield KG, Goudsmit J, Havenga MJ, Barouch DH. Comparative seroprevalence and immunogenicity of six rare serotype recombinant adenovirus vaccine vectors from subgroups B and D. J Virol. 2007;81(9):4654-63. Epub 2007/03/03. doi: 10.1128/JVI.02696-06. PubMed PMID: 17329340; PMCID: PMC1900173.
262. Liu J, Ewald BA, Lynch DM, Denholtz M, Abbink P, Lemckert AA, Carville A, Mansfield KG, Havenga MJ, Goudsmit J, Barouch DH. Magnitude and phenotype of cellular immune responses elicited by recombinant adenovirus vectors and heterologous prime-boost regimens in rhesus monkeys. J Virol. 2008;82(10):4844-52. Epub 2008/03/14. doi: 10.1128/JVI.02616-07. PubMed PMID: 18337575; PMCID: PMC2346755.
263. Teigler JE, Iampietro MJ, Barouch DH. Vaccination with adenovirus serotypes 35, 26, and 48 elicits higher levels of innate cytokine responses than adenovirus serotype 5 in rhesus monkeys. J Virol. 2012;86(18):9590-8. Epub 2012/07/13. doi: 10.1128/JVI.00740-12. PubMed PMID: 22787208; PMCID: PMC3446581.
264. Almeida JR, Price DA, Papagno L, Arkoub ZA, Sauce D, Bornstein E, Asher TE, Samri A, Schnuriger A, Theodorou I, Costagliola D, Rouzioux C, Agut H, Marcelin AG, Douek D, Autran B, Appay V. Superior control of HIV-1 replication by CD8+ T cells is reflected by their avidity, polyfunctionality, and clonal turnover. J Exp Med. 2007;204(10):2473-85. Epub 2007/09/26. doi: 10.1084/jem.20070784. PubMed PMID: 17893201; PMCID: PMC2118466.
265. Scott ZA, Chadwick EG, Gibson LL, Catalina MD, McManus MM, Yogev R, Palumbo P, Sullivan JL, Britto P, Gay H, Luzuriaga K, Investigators P. Infrequent detection of HIV-1-specific, but not cytomegalovirus-specific, CD8(+) T cell responses in young HIV-1-infected infants. J Immunol. 2001;167(12):7134-40. Epub 2001/12/12. doi: 10.4049/jimmunol.167.12.7134. PubMed PMID: 11739536.
266. Del Prete GQ, Alvord WG, Li Y, Deleage C, Nag M, Oswald K, Thomas JA, Pyle C, Bosche WJ, Coalter V, Wiles A, Wiles R, Berkemeier B, Hull M, Chipriano E, Silipino L, Fast R, Kiser J, Kiser R, Malys T, Kramer J, Breed MW, Trubey CM, Estes JD, Barnes TL, Hesselgesser J, Geleziunas R, Lifson JD. TLR7 agonist administration to SIV-infected macaques receiving early initiated cART does not induce plasma viremia. JCI Insight. 2019;4(11). Epub 2019/06/07. doi: 10.1172/jci.insight.127717. PubMed PMID: 31167974; PMCID: PMC6629134.
267. Siliciano JD, Siliciano RF. Assays to Measure Latency, Reservoirs, and Reactivation. In: Silvestri G, Lichterfeld M, editors. HIV-1 Latency. Cham: Springer International Publishing; 2018. p. 23-41.
268. Bender AM, Simonetti FR, Kumar MR, Fray EJ, Bruner KM, Timmons AE, Tai KY, Jenike KM, Antar AAR, Liu PT, Ho YC, Raugi DN, Seydi M, Gottlieb GS, Okoye AA, Del Prete GQ, Picker LJ, Mankowski JL, Lifson JD, Siliciano JD, Laird GM, Barouch DH, Clements JE, Siliciano RF. The Landscape of Persistent Viral Genomes in ART-Treated SIV, SHIV, and HIV-2 Infections. Cell Host Microbe. 2019;26(1):73-85 e4. Epub 2019/07/12. doi: 10.1016/j.chom.2019.06.005. PubMed PMID: 31295427; PMCID: PMC6724192.

269. Long S, Fennessey CM, Newman L, Reid C, O'Brien SP, Li Y, Del Prete GQ, Lifson JD, Gorelick RJ, Keele BF. Evaluating the Intactness of Persistent Viral Genomes in Simian Immunodeficiency Virus-Infected Rhesus Macaques after Initiating Antiretroviral Therapy within One Year of Infection. J Virol. 2019;94(1). Epub 2019/10/11. doi: 10.1128/JVI.01308-19. PubMed PMID: 31597776; PMCID: PMC6912123.
270. Garcia-Broncano P, Maddali S, Einkauf KB, Jiang C, Gao C, Chevalier J, Chowdhury FZ, Maswabi K, Ajibola G, Moyo S, Mohammed T, Ncube T, Makhema J, Jean-Philippe P, Yu XG, Powis KM, Lockman S, Kuritzkes DR, Shapiro R, Lichterfeld M. Early antiretroviral therapy in neonates with HIV-1 infection restricts viral reservoir size and induces a distinct innate immune profile. Sci Transl Med. 2019;11(520). Epub 2019/11/30. doi: 10.1126/scitranslmed.aax7350. PubMed PMID: 31776292.
271. Muenchhoff M, Prendergast AJ, Goulder PJ. Immunity to HIV in Early Life. Front Immunol. 2014;5:391. Epub 2014/08/28. doi: 10.3389/fimmu.2014.00391. PubMed PMID: 25161656; PMCID: PMC4130105.
272. Dhummakupt A, Rubens JH, Anderson T, Powell L, Nonyane BA, Siems LV, Collinson-Streng A, Nilles T, Jones RB, Tepper V, Agwu A, Persaud D. Differences in inducibility of the latent HIV reservoir in perinatal and adult infection. JCI Insight. 2020;5(4). Epub 2020/01/31. doi: 10.1172/jci.insight.134105. PubMed PMID: 31999647; PMCID: PMC7101150.
273. Obregon-Perko V, Bricker K, Chahroudi A. The Brain Retains: Nonhuman Primate Models for Pediatric HIV-1 in the CNS. Curr HIV/AIDS Rep. 2020;17(4):343-53. Epub 2020/05/11. doi: 10.1007/s11904-020-00503-4. PubMed PMID: 32388691; PMCID: PMC7355271.
274. Goswami R, Nelson AN, Tu JJ, Dennis M, Feng L, Kumar A, Mangold J, Mangan RJ, Mattingly C, Curtis AD, 2nd, Obregon-Perko V, Mavigner M, Pollara J, Shaw GM, Bar KJ, Chahroudi A, De Paris K, Chan C, Van Rompay KKA, Permar SR. Analytical Treatment Interruption after Short-Term Antiretroviral Therapy in a Postnatally Simian-Human Immunodeficiency Virus-Infected Infant Rhesus Macaque Model. mBio. 2019;10(5). Epub 2019/09/07. doi: 10.1128/mBio.01971-19. PubMed PMID: 31488511; PMCID: PMC6945967.
275. Berendam SJ, Nelson AN, Goswami R, Persaud D, Haigwood NL, Chahroudi A, Fouda GG, Permar SR. Pediatric HIV: the Potential of Immune Therapeutics to Achieve Viral Remission and Functional Cure. Curr HIV/AIDS Rep. 2020;17(3):237-48. Epub 2020/05/02. doi: 10.1007/s11904-020-00495-1. PubMed PMID: 32356090; PMCID: PMC7296986.
276. Ourmanov I, Brown CR, Moss B, Carroll M, Wyatt L, Pletneva L, Goldstein S, Venzon D, Hirsch VM. Comparative efficacy of recombinant modified vaccinia virus Ankara expressing simian immunodeficiency virus (SIV) Gag-Pol and/or Env in macaques challenged with pathogenic SIV. J Virol. 2000;74(6):2740-51. Epub 2000/02/23. doi: 10.1128/jvi.74.6.2740-2751.2000. PubMed PMID: 10684290; PMCID: PMC111764.
277. Zhang Z, Schwartz S, Wagner L, Miller W. A greedy algorithm for aligning DNA sequences. J Comput Biol. 2000;7(1-2):203-14. Epub 2000/07/13. doi: 10.1089/10665270050081478. PubMed PMID: 10890397.
278. Altschul SF, Madden TL, Schaffer AA, Zhang J, Zhang Z, Miller W, Lipman DJ. Gapped BLAST and PSI-BLAST: a new generation of protein database search programs. Nucleic Acids Res. 1997;25(17):3389-402. Epub 1997/09/01. doi: 10.1093/nar/25.17.3389. PubMed PMID: 9254694; PMCID: PMC146917.
279. Altschul SF, Wootton JC, Gertz EM, Agarwala R, Morgulis A, Schaffer AA, Yu YK. Protein database searches using compositionally adjusted substitution matrices. FEBS J. 2005;272(20):5101-9. Epub 2005/10/13. doi: 10.1111/j.1742-4658.2005.04945.x. PubMed PMID: 16218944; PMCID: PMC1343503.
280. Tomaras GD, Yates NL, Liu P, Qin L, Fouda GG, Chavez LL, Decamp AC, Parks RJ, Ashley VC, Lucas JT, Cohen M, Eron J, Hicks CB, Liao HX, Self SG, Landucci G, Forthal DN, Weinhold KJ, Keele BF, Hahn BH, Greenberg ML, Morris L, Karim SS, Blattner WA, Montefiori DC, Shaw GM, Perelson AS, Haynes BF. Initial

B-cell responses to transmitted human immunodeficiency virus type 1: virion-binding immunoglobulin M (IgM) and IgG antibodies followed by plasma anti-gp41 antibodies with ineffective control of initial viremia. J Virol. 2008;82(24):12449-63. Epub 2008/10/10. doi: 10.1128/JVI.01708-08. PubMed PMID: 18842730; PMCID: PMC2593361.

281. Finzi D, Blankson J, Siliciano JD, Margolick JB, Chadwick K, Pierson T, Smith K, Lisziewicz J, Lori F, Flexner C, Quinn TC, Chaisson RE, Rosenberg E, Walker B, Gange S, Gallant J, Siliciano RF. Latent infection of CD4+ T cells provides a mechanism for lifelong persistence of HIV-1, even in patients on effective combination therapy. Nat Med. 1999;5(5):512-7. Epub 1999/05/06. doi: 10.1038/8394. PubMed PMID: 10229227.

282. Obregon-Perko V, Bricker K, Mensah G, Uddin F, Kumar M, Fray E, Siliciano RF, Schoof N, Horner A, Mavigner M, Liang S, Vanderford T, Sass J, Chan C, Berendam SJ, Bar K, Shaw GM, Silvestri G, Fouda G, Permar S, Chahroudi A. SHIV.C.CH505 Persistence in ART-Suppressed Infant Macaques is Characterized by Elevated SHIV RNA in the Gut and High Abundance of Intact SHIV DNA in Naive CD4+ T cells. J Virol. 2020. Epub 2020/10/23. doi: 10.1128/JVI.01669-20. PubMed PMID: 33087463.

283. Bricker KM, Obregon-Perko V, Uddin F, Williams B, Uffman EA, Garrido C, Fouda GG, Geleziunas R, Robb M, Michael N, Barouch DH, Chahroudi A. Therapeutic vaccination of SIV-infected, ART-treated infant rhesus macaques using Ad48/MVA in combination with TLR-7 stimulation. PLoS Pathog. 2020;16(10):e1008954. Epub 2020/10/27. doi: 10.1371/journal.ppat.1008954. PubMed PMID: 33104758; PMCID: PMC7644092 Sciences. AC is a spouse of a member of the editorial board of a PLoS journal (Guido Silvestri, Associate Editor PLoS Pathogens).

284. Margolis DM, Archin NM, Cohen MS, Eron JJ, Ferrari G, Garcia JV, Gay CL, Goonetilleke N, Joseph SB, Swanstrom R, Turner AW, Wahl A. Curing HIV: Seeking to Target and Clear Persistent Infection. Cell. 2020;181(1):189-206. Epub 2020/03/30. doi: 10.1016/j.cell.2020.03.005. PubMed PMID: 32220311; PMCID: PMC7896558.

285. Zerbato JM, Purves HV, Lewin SR, Rasmussen TA. Between a shock and a hard place: challenges and developments in HIV latency reversal. Curr Opin Virol. 2019;38:1-9. Epub 2019/05/03. doi: 10.1016/j.coviro.2019.03.004. PubMed PMID: 31048093; PMCID: PMC6819240.

286. Bricker KM, Chahroudi A, Mavigner M. New Latency Reversing Agents for HIV-1 Cure: Insights from Nonhuman Primate Models. Viruses. 2021;13(8). Epub 2021/08/29. doi: 10.3390/v13081560. PubMed PMID: 34452425; PMCID: PMC8402914.

287. Sun SC. The non-canonical NF-kappaB pathway in immunity and inflammation. Nat Rev Immunol. 2017;17(9):545-58. Epub 2017/06/06. doi: 10.1038/nri.2017.52. PubMed PMID: 28580957; PMCID: PMC5753586.

288. Uhlen M, Fagerberg L, Hallstrom BM, Lindskog C, Oksvold P, Mardinoglu A, Sivertsson A, Kampf C, Sjostedt E, Asplund A, Olsson I, Edlund K, Lundberg E, Navani S, Szigyarto CA, Odeberg J, Djureinovic D, Takanen JO, Hober S, Alm T, Edqvist PH, Berling H, Tegel H, Mulder J, Rockberg J, Nilsson P, Schwenk JM, Hamsten M, von Feilitzen K, Forsberg M, Persson L, Johansson F, Zwahlen M, von Heijne G, Nielsen J, Ponten F. Proteomics. Tissue-based map of the human proteome. Science. 2015;347(6220):1260419. Epub 2015/01/24. doi: 10.1126/science.1260419. PubMed PMID: 25613900.

289. Human Protein Atlas [09/15/2021]. Available from: http://www.proteinatlas.org/.

290. Dashti A, Waller C, Mavigner M, Schoof N, Bar KJ, Shaw GM, Vanderford TH, Liang S, Lifson JD, Dunham RM, Ferrari G, Tuyishime M, Lam CK, Nordstrom JL, Margolis DM, Silvestri G, Chahroudi A. SMAC Mimetic Plus Triple-Combination Bispecific HIVxCD3 Retargeting Molecules in SHIV.C.CH505-Infected, Antiretroviral Therapy-Suppressed Rhesus Macaques. J Virol. 2020;94(21). Epub 2020/08/21. doi: 10.1128/JVI.00793-20. PubMed PMID: 32817214; PMCID: PMC7565632.

291. Mahoney DJ, Cheung HH, Mrad RL, Plenchette S, Simard C, Enwere E, Arora V, Mak TW, Lacasse EC, Waring J, Korneluk RG. Both cIAP1 and cIAP2 regulate TNFalpha-mediated NF-kappaB activation. Proc Natl Acad Sci U S A. 2008;105(33):11778-83. Epub 2008/08/14. doi: 10.1073/pnas.0711122105. PubMed PMID: 18697935; PMCID: PMC2575330.
292. Mohamed MS, Bishr MK, Almutairi FM, Ali AG. Inhibitors of apoptosis: clinical implications in cancer. Apoptosis. 2017;22(12):1487-509. Epub 2017/10/27. doi: 10.1007/s10495-017-1429-4. PubMed PMID: 29067538.
293. Sun SC. The noncanonical NF-kappaB pathway. Immunol Rev. 2012;246(1):125-40. Epub 2012/03/23. doi: 10.1111/j.1600-065X.2011.01088.x. PubMed PMID: 22435551; PMCID: PMC3313452.
294. Fernandez E, Perez R, Hernandez A, Tejada P, Arteta M, Ramos JT. Factors and Mechanisms for Pharmacokinetic Differences between Pediatric Population and Adults. Pharmaceutics. 2011;3(1):53-72. Epub 2011/01/01. doi: 10.3390/pharmaceutics3010053. PubMed PMID: 24310425; PMCID: PMC3857037.
295. Shi R, Derendorf H. Pediatric Dosing and Body Size in Biotherapeutics. Pharmaceutics. 2010;2(4):389-418. Epub 2010/12/16. doi: 10.3390/pharmaceutics2040389. PubMed PMID: 27721364; PMCID: PMC3967145.
296. Kulpa DA, Talla A, Brehm JH, Ribeiro SP, Yuan S, Bebin-Blackwell AG, Miller M, Barnard R, Deeks SG, Hazuda D, Chomont N, Sekaly RP. Differentiation into an Effector Memory Phenotype Potentiates HIV-1 Latency Reversal in CD4(+) T Cells. J Virol. 2019;93(24). Epub 2019/10/04. doi: 10.1128/JVI.00969-19. PubMed PMID: 31578289; PMCID: PMC6880164.
297. Kwon KJ, Timmons AE, Sengupta S, Simonetti FR, Zhang H, Hoh R, Deeks SG, Siliciano JD, Siliciano RF. Different human resting memory CD4(+) T cell subsets show similar low inducibility of latent HIV-1 proviruses. Sci Transl Med. 2020;12(528). Epub 2020/01/31. doi: 10.1126/scitranslmed.aax6795. PubMed PMID: 31996465; PMCID: PMC7875249.
298. Zerbato JM, McMahon DK, Sobolewski MD, Mellors JW, Sluis-Cremer N. Naive CD4+ T Cells Harbor a Large Inducible Reservoir of Latent, Replication-competent Human Immunodeficiency Virus Type 1. Clin Infect Dis. 2019;69(11):1919-25. Epub 2019/02/13. doi: 10.1093/cid/ciz108. PubMed PMID: 30753360; PMCID: PMC6853701.
299. Beal SL. Ways to fit a PK model with some data below the quantification limit. J Pharmacokinet Pharmacodyn. 2001;28(5):481-504. Epub 2002/01/05. doi: 10.1023/a:1012299115260. PubMed PMID: 11768292.
300. Dobin A, Davis CA, Schlesinger F, Drenkow J, Zaleski C, Jha S, Batut P, Chaisson M, Gingeras TR. STAR: ultrafast universal RNA-seq aligner. Bioinformatics. 2013;29(1):15-21. Epub 2012/10/30. doi: 10.1093/bioinformatics/bts635. PubMed PMID: 23104886; PMCID: PMC3530905.
301. Anders S, Pyl PT, Huber W. HTSeq--a Python framework to work with high-throughput sequencing data. Bioinformatics. 2015;31(2):166-9. Epub 2014/09/28. doi: 10.1093/bioinformatics/btu638. PubMed PMID: 25260700; PMCID: PMC4287950.
302. Love MI, Huber W, Anders S. Moderated estimation of fold change and dispersion for RNA-seq data with DESeq2. Genome Biol. 2014;15(12):550. Epub 2014/12/18. doi: 10.1186/s13059-014-0550-8. PubMed PMID: 25516281; PMCID: PMC4302049.
303. Subramanian A, Tamayo P, Mootha VK, Mukherjee S, Ebert BL, Gillette MA, Paulovich A, Pomeroy SL, Golub TR, Lander ES, Mesirov JP. Gene set enrichment analysis: a knowledge-based approach for interpreting genome-wide expression profiles. Proc Natl Acad Sci U S A. 2005;102(43):15545-50. Epub 2005/10/04. doi: 10.1073/pnas.0506580102. PubMed PMID: 16199517; PMCID: PMC1239896.
304. Newell ML, Coovadia H, Cortina-Borja M, Rollins N, Gaillard P, Dabis F, Ghent International ASWGoHIVIiW, Children. Mortality of infected and uninfected infants born to HIV-infected mothers in

Africa: a pooled analysis. Lancet. 2004;364(9441):1236-43. Epub 2004/10/07. doi: 10.1016/S0140-6736(04)17140-7. PubMed PMID: 15464184.
305. HRSA's Ryan White HIV/AIDS Program Fact Sheet 2020 [09/13/2021]. Available from: https://hab.hrsa.gov/sites/default/files/hab/Publications/factsheets/program-factsheet-program-overview.pdf.
306. Menne S, Tumas DB, Liu KH, Thampi L, AlDeghaither D, Baldwin BH, Bellezza CA, Cote PJ, Zheng J, Halcomb R, Fosdick A, Fletcher SP, Daffis S, Li L, Yue P, Wolfgang GH, Tennant BC. Sustained efficacy and seroconversion with the Toll-like receptor 7 agonist GS-9620 in the Woodchuck model of chronic hepatitis B. J Hepatol. 2015;62(6):1237-45. Epub 2015/01/07. doi: 10.1016/j.jhep.2014.12.026. PubMed PMID: 25559326; PMCID: PMC4439359.
307. Lanford RE, Guerra B, Chavez D, Giavedoni L, Hodara VL, Brasky KM, Fosdick A, Frey CR, Zheng J, Wolfgang G, Halcomb RL, Tumas DB. GS-9620, an oral agonist of Toll-like receptor-7, induces prolonged suppression of hepatitis B virus in chronically infected chimpanzees. Gastroenterology. 2013;144(7):1508-17, 17 e1-10. Epub 2013/02/19. doi: 10.1053/j.gastro.2013.02.003. PubMed PMID: 23415804; PMCID: PMC3691056.
308. Lopatin U, Wolfgang G, Tumas D, Frey CR, Ohmstede C, Hesselgesser J, Kearney B, Moorehead L, Subramanian GM, McHutchison JG. Safety, pharmacokinetics and pharmacodynamics of GS-9620, an oral Toll-like receptor 7 agonist. Antivir Ther. 2013;18(3):409-18. Epub 2013/02/19. doi: 10.3851/IMP2548. PubMed PMID: 23416308.
309. SenGupta D, Brinson C, DeJesus E, Mills A, Shalit P, Guo S, Cai Y, Wallin JJ, Zhang L, Humeniuk R, Begley R, Geleziunas R, Mellors J, Wrin T, Jones N, Milush J, Ferre AL, Shacklett BL, Laird GM, Moldt B, Vendrame E, Brainard DM, Ramgopal M, Deeks SG. The TLR7 agonist vesatolimod induced a modest delay in viral rebound in HIV controllers after cessation of antiretroviral therapy. Sci Transl Med. 2021;13(599). Epub 2021/06/25. doi: 10.1126/scitranslmed.abg3071. PubMed PMID: 34162752.
310. Hargrave A, Mustafa AS, Hanif A, Tunio JH, Hanif SNM. Current Status of HIV-1 Vaccines. Vaccines (Basel). 2021;9(9). Epub 2021/09/29. doi: 10.3390/vaccines9091026. PubMed PMID: 34579263; PMCID: PMC8471857.
311. Sneller MC, Justement JS, Gittens KR, Petrone ME, Clarridge KE, Proschan MA, Kwan R, Shi V, Blazkova J, Refsland EW, Morris DE, Cohen KW, McElrath MJ, Xu R, Egan MA, Eldridge JH, Benko E, Kovacs C, Moir S, Chun TW, Fauci AS. A randomized controlled safety/efficacy trial of therapeutic vaccination in HIV-infected individuals who initiated antiretroviral therapy early in infection. Sci Transl Med. 2017;9(419). Epub 2017/12/08. doi: 10.1126/scitranslmed.aan8848. PubMed PMID: 29212716.
312. Colby DJ, Sarnecki M, Barouch DH, Tipsuk S, Stieh DJ, Kroon E, Schuetz A, Intasan J, Sacdalan C, Pinyakorn S, Grandin P, Song H, Tovanabutra S, Shubin Z, Kim D, Paquin-Proulx D, Eller MA, Thomas R, de Souza M, Wieczorek L, Polonis VR, Pagliuzza A, Chomont N, Peter L, Nkolola JP, Vingerhoets J, Truyers C, Pau MG, Schuitemaker H, Phanuphak N, Michael N, Robb ML, Tomaka FL, Ananworanich J. Safety and immunogenicity of Ad26 and MVA vaccines in acutely treated HIV and effect on viral rebound after antiretroviral therapy interruption. Nat Med. 2020;26(4):498-501. Epub 2020/04/03. doi: 10.1038/s41591-020-0774-y. PubMed PMID: 32235883.
313. Mothe B, editor. A placebo-controlled ATI trial of HIT vaccines in early treated HIV infection. Conference on Retroviruses and Opportunistic Infections; 2021; Virtual.
314. Shang HT, Ding JW, Yu SY, Wu T, Zhang QL, Liang FJ. Progress and challenges in the use of latent HIV-1 reactivating agents. Acta Pharmacol Sin. 2015;36(8):908-16. Epub 2015/06/02. doi: 10.1038/aps.2015.22. PubMed PMID: 26027656; PMCID: PMC4564876.
315. Heckler SM. Executive Court Reporters. 1984.

316. Frange P, Faye A, Avettand-Fenoel V, Bellaton E, Descamps D, Angin M, David A, Caillat-Zucman S, Peytavin G, Dollfus C, Le Chenadec J, Warszawski J, Rouzioux C, Saez-Cirion A, Cohort AE-CP, the AEPVsg. HIV-1 virological remission lasting more than 12 years after interruption of early antiretroviral therapy in a perinatally infected teenager enrolled in the French ANRS EPF-CO10 paediatric cohort: a case report. Lancet HIV. 2016;3(1):e49-54. Epub 2016/01/15. doi: 10.1016/S2352-3018(15)00232-5. PubMed PMID: 26762993.

317. Violari A, Cotton MF, Kuhn L, Schramm DB, Paximadis M, Loubser S, Shalekoff S, Da Costa Dias B, Otwombe K, Liberty A, McIntyre J, Babiker A, Gibb D, Tiemessen CT. A child with perinatal HIV infection and long-term sustained virological control following antiretroviral treatment cessation. Nat Commun. 2019;10(1):412. Epub 2019/01/27. doi: 10.1038/s41467-019-08311-0. PubMed PMID: 30679439; PMCID: PMC6345921.

318. Dong E, Du H, Gardner L. An interactive web-based dashboard to track COVID-19 in real time. Lancet Infect Dis. 2020;20(5):533-4. Epub 2020/02/23. doi: 10.1016/S1473-3099(20)30120-1. PubMed PMID: 32087114; PMCID: PMC7159018.

319. Howard LM, Garguilo K, Gillon J, LeBlanc K, Seegmiller AC, Schmitz JE, Byrne DW, Domenico HJ, Moore RP, Webber SA, Halasa NB, Banerjee R. The first 1000 symptomatic pediatric SARS-CoV-2 infections in an integrated health care system: a prospective cohort study. BMC Pediatr. 2021;21(1):403. Epub 2021/09/15. doi: 10.1186/s12887-021-02863-1. PubMed PMID: 34517879.

320. UNAIDS. The effects of the COVID-19 pandemic on the HIV response 2021 [09/13/2021]. Available from: https://www.unaids.org/sites/default/files/media_asset/effects-of-covid19-pandemic-on-hiv-response_en.pdf.